UNIVERSITAT DE BARCELONA

Design, Development, and Validation of Medical Wearable Devices: Challenges and Solutions for Technology Integration, Industrialization and Certification

Javier Aguilar Torán

PhD Thesis

Design, Development, and Validation of Medical Wearable Devices: Challenges and Solutions for Technology Integration, Industrialization and Certification

Javier Aguilar Torán

UNIVERSITAT DE BARCELONA

Design, Development, and Validation of Medical Wearable Devices: Challenges and Solutions for Technology Integration, Industrialization and Certification

Programa de doctorat en

Enginyeria i Ciències Aplicades

Autor/a: Javier Aguilar Torán

Director/a: Dr. Jaime Punter Villagrasa

Dr. Pere Lluís Miribel Català

Tutor/a: Dr. Pere Lluís Miribel Català

UNIVERSITAT DE BARCELONA

Agradecimientos / Acknowledgements

Esta tesis doctoral no la hubiese acabado sin la ayuda de varias personas e instituciones que siempre me han apoyado y ayudado en este proceso. Sin todos vosotros esta tesis nunca se hubiera hecho realidad.

En primer lugar, quiero agradecer al Dr. Jaime Punter Villagrasa por toda su dedicación, su esfuerzo y sus buenos consejos. Estos últimos años han sido muy locos, incluso parecía que se acababa el mundo por momentos, pero siempre ha seguido ahí dando lo mejor de sí mismo. No tengo más que palabras de agradecimiento por su incansable trabajo y por ayudarme a ser una mejor versión de mí mismo.

También quiero agradecer a mi codirector Dr. Pere Lluís Miribel Català que siempre me ha brindado su ayuda y aconsejado sabiamente. Siendo la voz de la razón en multitud de ocasiones, ha hecho que esta tesis sea posible gracias a su esfuerzo.

Gracias a la empresa Onalabs por confiar en mí y brindarme la oportunidad de hacer un doctorado industrial. También agradecer a la Agencia de Gestión de Ayudas Universitarias y de Investigación (AGAUR) por su apoyo económico.

No puedo seguir sin agradecer al Dr. Francesc Xavier Muñoz Pascual, el cual inició hace unos años la aventura conocida como Onalabs y me ha dado la oportunidad de crecer junto a la empresa desde sus inicios. Tampoco puedo seguir sin dar las gracias al Dr. Oscar Castillo Fernández que desde que hice mi trabajo final de grado siempre ha estado presente y me ha brindado todo su apoyo.

Gracias también a mis compañeros y amigos Genis y Valeria. Desde el inicio de Onalabs han estado presentes compartiendo victorias y derrotas, miserias y alegrías. Cada uno a su manera, siempre han estado ahí en mi día a día y ayudado a dar lo mejor de mí mismo.

A todos los miembros de la empresa Onalabs desde Andrea, por todos los cafés compartidos y por formar un gran equipo a diario, hasta Elisabet, por darme la confianza para liderar un proyecto y mostrar todo mi potencial. En especial quiero agradecer a Albert que llegó de forma inesperada a mitad de mi tesis y que me ha ayudado tanto a nivel técnico como humano haciendo que este trabajo se convierta en una realidad.

Agradecer a mi familia. A mi madre Rosa María por su preocupación y su cariño. A mi padre Rafael por sus consejos y apoyo incluso en los momentos más bajos e inculcarme los valores del esfuerzo y del trabajo. A mi hermana Marta por su alegría y por su afecto. Y a mis dos abuelos que ya no están aquí y que les hubiera encantado verme como doctor.

A todos mis amigos por alegrarme cada fin de semana y escuchar mis quejas. Gracias (Sergi, Guille, Pablo, Marta, James, Oscar e Irene) por estar ahí y hacer de este mundo un lugar mejor.

Por último, quiero agradecer a Sam todo su apoyo, su comprensión y su paciencia. No tengo palabras para darte las gracias. Decir que hubiera sido imposible acabar la tesis sin ti sería quedarse corto. Únicamente puedo darte las gracias de todo corazón.

Abbreviations

HAH – Hospital at Home

EU – European Union

ICU – Intensive Care Unit

MDR – Medical Device Regulation

IC – Integrated Circuit

PR – Pulse Rate

HR – Heart Rate

SpO_2 – Peripheral Oxygen Saturation

ABP – Arterial Blood Pressure

SABP – Systolic Blood Pressure

DABP – Diastolic Blood Pressure

RR – Respiratory Rate

STEMP – Skin Temperature

BTEMP – Body Temperature

API – Application Programming Interface

PPG – Photoplethysmogram

IR – Infrared

ECG – Electrocardiogram

IMU – Inertial Measurement Unit

PCB – Printed Circuit Board

MCU – Microcontroller

LDO – Low-Dropout Regulator

BLE – Bluetooth Low Energy

ADC – Analog to Digital Converter

DAC – Digital to Analog Converter

OPAMP – Operational Amplifier

WE – Working Electrode

RE – Reference Electrode

CE – Counter Electrode

CA – Chronoamperometry

CV – Cyclic Voltammetry

LiPo – Lithium Polymer

SQI – Signal Quality Index

STD – Standard Deviation

MAE – Mean Absolute Error

RMSE – Root Mean Square Error

UPIC – Polyvalent Clinical Research Unit

UCO – Coronary Care Unit

UCRI – Intermittent Respiratory Care Unit

EMC – Electromagnetic Compatibility

ESD – Electrostatic Discharge

IP – Ingress Protection

UDI – Unique Device Identifier

AI – Artificial Intelligence

Contents

List of Figures

List of Tables

1. Introduction

Onalabs Inno-Hub SL [1] (henceforth Onalabs) is a company that develops non-invasive wearable devices which measure, digitalize, and transmit health-related biomarkers. The thesis presented here is an industrial PhD [2] jointly conducted between Onalabs and the research group D2In-SIC-BIO from the University of Barcelona [3], [4]. As an industrial PhD, this thesis does not only focus on scientific advances and new technologies, but also on product development, validation, industrialization, and certification.

1.1. Wearable devices in the healthcare landscape

Due to the advances in the field of medical care, worldwide life span has increased over the past decades (see Figure 1.1a). According to the 2019 revision of world population prospects, elderly people will represent 16 % of the population by 2050 [5]. The percentage of elderly will be larger in developed countries, such as the state members of the European Union (EU) or the United States. For instance, individuals over the age of 65 will represent 30.4 % and 30.0 % of the population of Spain and Germany in 2050, respectively [6], [7].

This rise in longevity comes hand in hand with an increase in health expenditure as aging-associated diseases are becoming more prevalent. Aging associated diseases are normally chronic illnesses that need constant attention. Public health expenditures in the EU member states have grown during the last decades (5.9 % of GDP in 1995 to 8.1 % in 2021) [8] and it is expected to rise even more in the following years due to the population aging. Therefore, structural reforms must be carried out in order to maintain the sustainability of healthcare systems, while at the same time guaranteeing access to services for all citizens.

Most of the population over 65 years exhibits chronic diseases, with at least one affecting 80 %, while two or more afflict 68 % [9]. The most common chronic illnesses are heart failure, chronic obstructive pulmonary disease, diabetes, and hypertension, among others (see Figure 1.1b). These account for a significant percentage of DALYs (disability-adjusted life years), which is a measurement that reflects premature deaths and years lived without health [10].

One of the major risk factors of most chronic diseases is a sedentary lifestyle. For instance, there is a strong correlation between obesity and the risk of suffering diabetes. Diabetes is an illness that occurs either when the pancreas does not produce enough insulin (a hormone that regulates blood glucose), or when the body cannot effectively use this hormone [11]. The major consequences of diabetes are cardiovascular diseases, such as ischemic heart disease and stroke, which are leading causes of death and a major contributor to disability in developed countries [12].

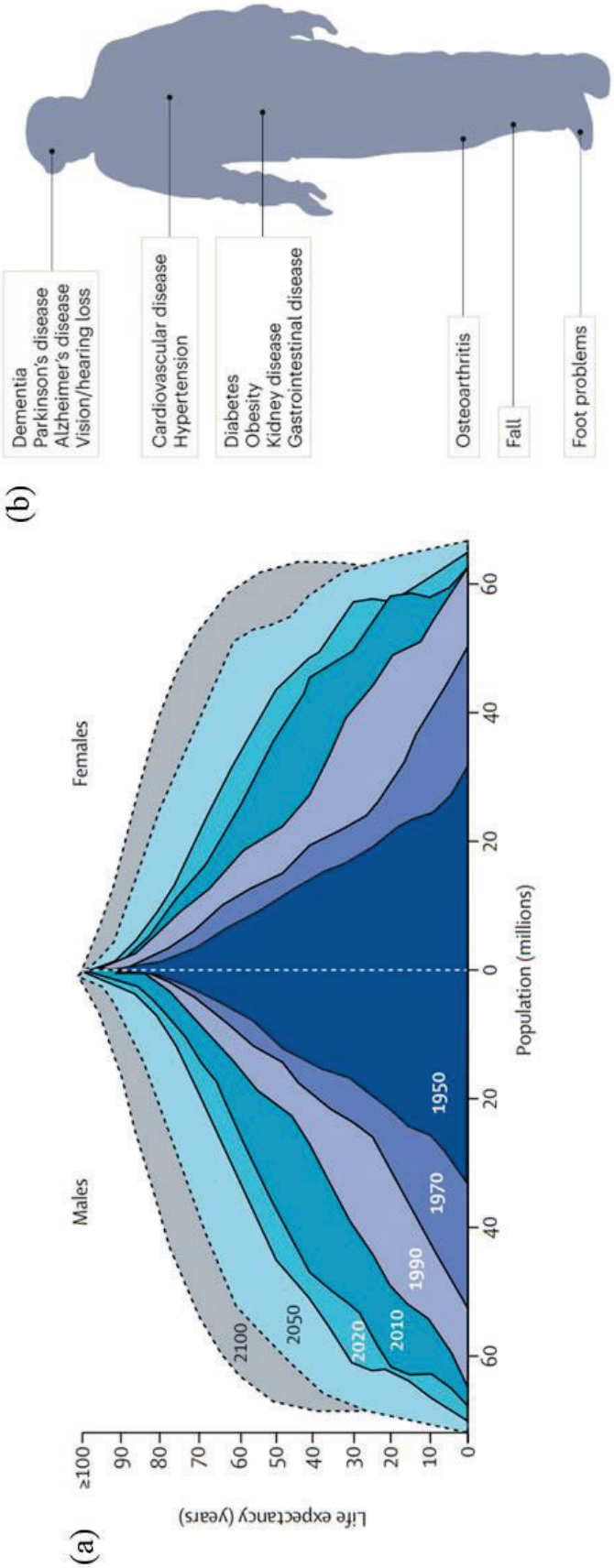

Figure 1.1. Evolution of population life expectancy and chronic diseases related to the longevity rise. (a) Longevity worldwide rise in function of time. Courtesy of Scott (2021) [13], used with permission. (b) Most prevalent aging associated diseases. Courtesy of Chen (2023) [14], used with permission.

Apart from the increase of chronic diseases, the COVID-19 pandemic demonstrated that the healthcare system is not ready for an exponential growth of patients in a short period of time. During a health crisis, such as a pandemic, reorganization and prioritization of scarce resources are necessary to avoid the collapse of this system. A resilient and adaptive response is necessary to ensure a balanced response in a fast-changing scenario.

Pandemics have been present in every period of history. During the last century, the influenza A/H1N1 pandemic of 1918-1919 (Spanish Flu) claimed an estimated 50 million lives worldwide and the influenza A/H2N2 pandemic of 1957 caused the death of one million individuals [15]. The recent COVID-19 pandemic has killed nearly seven million people during the past four years (see Figure 1.2) [16]. It is impossible to predict the next pandemic, but certainly another one will appear, and the society must be prepared to confront it.

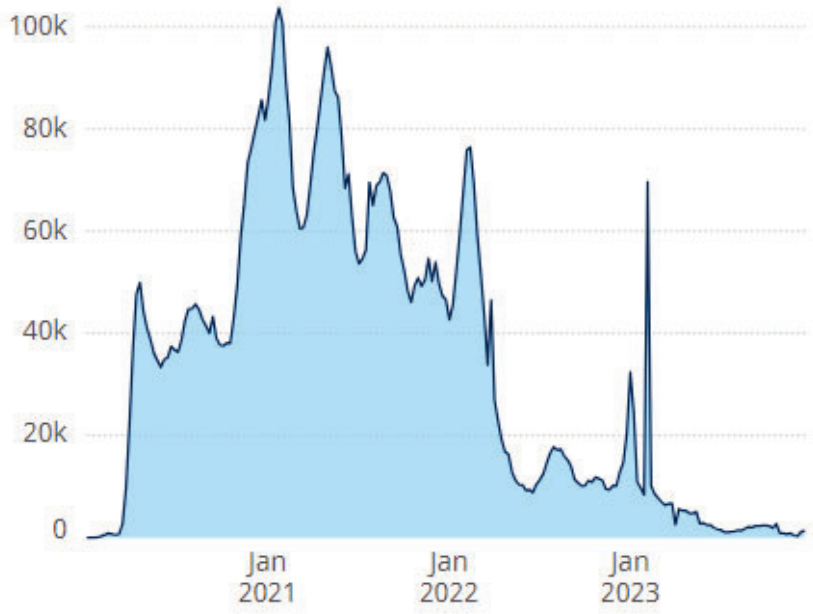

Figure 1.2. COVID-19 deaths reported worldwide (weekly) [16].

Given this scenario, there is a growing need to reduce the impact on the healthcare system of aging associated diseases and future pandemics. To increase the sustainability of this system, Hospital at Home (HAH) units have been created. HAH units offer to patients the alternative of receiving treatment and hospital care at home, under conditions comparable to those provided by conventional hospitalization [17], [18]. This model provides better outcomes of health recovery [19] along with reduced costs up to 38 % in comparison to traditional hospital methodology [20].

Most HAH nurses' and doctors' visits are focused on the acquisition of biometric data related to patient physiological status, such as oxygen saturation or arterial blood pressure. These personnel can be better used in more critical scenarios where their expertise and skills are urgently required. Digital or electronic health (eHealth) is defined as the organization and provision of health services using information and communication technologies. The term involves technological development but also a new way of working, aimed at improving health care at local, regional, and worldwide levels through the use of technological devices, information, and communication [21], [22], [23], [24].

A complementary concept is telemedicine, defined as remotely performing medical activity using technological resources.

The aim of telemedicine is to be able to improve healthcare processes, communication and monitoring mechanisms, speed up red tape, and reduce costs. Thanks to technological advances and increased availability of easy-to-use equipment, eHealth is increasingly accepted by both health services and patients. The COVID-19 pandemic situation has made clear that telemedicine is a necessary component of clinical practice as it provides safer care during and after this health crisis [25]. Using technological resources as a basic tool in the management of healthcare processes ensures greater traceability of information and helps to standardize work systems [26].

To regularize the application of new technologies in the medical field, the Action Plan on Electronic Health 2012-2020 was drafted [27]. The first eHealth action plan was drawn up in 2004 and since then the European Commission has been formulating specific policy initiatives to encourage widespread adoption of electronic health throughout the EU.

If applied effectively, eHealth provides personalized and citizen-centered healthcare. It also provides more specific and effective attention, reduces medical errors and hospitalization duration. The European Society of Cardiology mentions that eHealth can complement conventional cardiac rehabilitation, for instance to increase patient participation and long-term adherence to healthy behaviors [28]. Furthermore, the standards of the Spanish Society of Arteriosclerosis indicate that telemedicine facilitate access to clinical patient information and better control of cardiovascular risk factors [29].

A wearable device is any system designed to be worn on the user's body, such as a bracelet or a patch (see Figure 1.3) [30], [31]. This characteristic enables continuous and remote monitoring of the patient removing the need to use trained personnel to perform this task [32]. The measurements performed by these systems are not always accurate [33], [34] since most wearable devices on the market are envisaged as consumer electronics that do not have the medical certification required to be used in a clinical environment [35].

Despite the lack of reliable commercial wearable devices, these systems have been increasingly used in clinical settings. The primary emphasis on the inclusion of wearable devices in the healthcare system is checking the patient’s health status on a frequent basis while ensuring the patient’s comfort [36]. Periodically monitoring individuals generates huge amounts of data that can be used to develop specialized algorithms utilizing big data techniques [37]. These algorithms can be extremely useful for disease prediction, prevention, and intervention [38], [39], permitting an improved attention. Thus, one of the main data groups to be considered when thinking of wearable medical devices are vital signs, as they provide a lot of information about the patient’s health status. These parameters reflect the essential body functions, allowing healthcare providers to estimate the progression of a disease and determine if any kind of attention is required, or the treatment must be adjusted. Wearable medical devices have been present on a wide variety of studies, such as a study that shows the benefits of continuous monitoring to improve patient safety on surgical ward [40] or another one that associates the continuous monitoring of patient vital signs using wearable monitoring technology with the reduction in unplanned Intensive Care Unit (ICU) admissions [41].

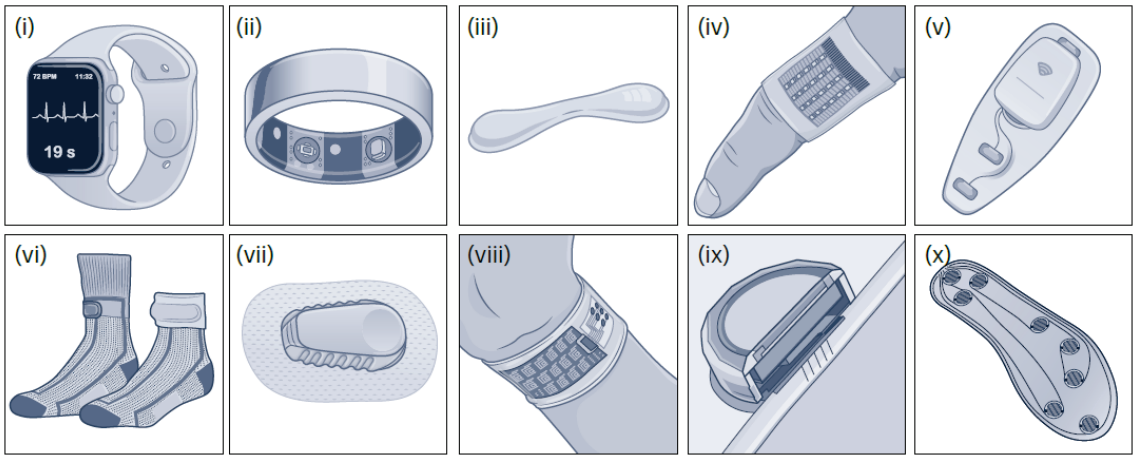

Figure 1.3. Common wearable devices. (i), Apple watch, (ii), Oura ring (iii), Philips VitalPatch (iv), Wearable ultrasound patch (v), Mobile Cardiac Outpatient Telemetry ECG sensor (vi), Sensoria Fitness Smart Socks (vii), Dexcom CGM (viii), Integrated wearable sensor (ix), Wearable microneedle array (x), and Orpyx Insoles plantar pressure sensor. Courtesy of Chen (2023) [14], used with permission.

Vital sign monitoring allows doctors and nurses to know the state of health of a patient, but they do not show the complete picture. To complement the information provided by these parameters, the biochemical data, such as the level of glucose in blood, must be collected and analyzed. Blood tests are the gold standard method (reference technique) [42] for biochemical analysis, but it has several drawbacks that limit its use. These tests are invasive, require trained personnel, and only allows to know the state of the patient at the moment of the extraction. An alternative analysis that has gained a lot of interest during the past few years is based on the use of sweat as the sample to be analyzed [43], [44].

Sweat is a biofluid composed mainly of water, but it contains various electrolytes, ions, amino acids, proteins, and other small molecules. Due to its rich content, this fluid has become a great candidate for analysis. Sweat analysis is non-invasive, does not require a professional to collect the sample, and can be carried out continuously, since this biofluid is always present on the skin due to the body's thermoregulation [45]. Despite these advantages, nowadays, sweat is barely used and only some clinical trials, such as the cystic fibrosis test, utilize this biofluid [46]. The lack of tests that utilize sweat as a sample is because a standardized method to extract sweat from skin does not exist. This fact, along with the low sample volume available (range of nanoliters) and liquid evaporation, turns sweat into a biofluid difficult to be measured [47].

Tracking simultaneously the vital signs and chemical biomarkers of individuals gives a large amount of information to nurses and doctors that can be used to provide an improved service to the users of the healthcare system [14]. The new generation of wearable devices will give this rich longitudinal information in order to offer continuous monitoring of chronic diseases, ranging from diabetes and cardiovascular diseases to dementia and arthritis.

1.2. Medical wearable devices

The global wearable market was valued at USD 61.30 billion in 2022. An important percentage of this market are wearable medical devices, which were valued at USD 23.10 billion in 2021 and it is projected to reach USD 81.30 billion by 2030 [48], [49]. A wearable medical device is any portable device used to track the user's state of health.

Wearable devices, such as smart watches or finger rings, have been around for a while, but the COVID-19 pandemic increased the interest in these devices. This pandemic made the population more concerned about their health and part of the society focused their attention on this novel technology.

Despite the increase of the wearable medical device market, most of the available systems are consumer electronic devices that do not provide reliable data [50]. These devices are intended to be used for fitness and they cannot be utilized in healthcare systems. The medical devices used by doctors and nurses must be approved by the health national authorities of each country where they are commercialized.

The certification process of a medical device is time-consuming (from a few months to several years depending on the device's characteristics) and very expensive. To obtain the approval of the authorities, several requirements must be fulfilled: the trustworthiness of the data must be demonstrated in a clinical trial, the patient information security must be verified to the authorities, and the device must be demonstrated to be safe, among others. This hard process reduces the number of new medical devices available on the market, but it ensures that the equipment that obtains the approval of the authorities is reliable.

Medical devices in the EU are regulated by the Medical Device Regulation (MDR) [51]. The MDR is a set of norms and regulations that every medical device must comply with to be distributed in the European Economic Area, which includes EU members as well as some non-EU countries. Notified bodies are the organizations designated by EU countries to assess the conformity of medical products before being placed on the market [52].

The MDR classifies medical devices into four categories: I, IIa, IIb, and III [53]. This classification is a system based on risk, considering the inherent risks associated with the design or manufacturing of medical devices and their potential impact on patients. To classify a medical device in one or another category, not only the technical aspects or the fabrication process are taken into account, but also its intended use is. The intended use of a device refers to the purpose for which it is designed and produced. Depending on the intended use of a medical device, it can be classified in different categories. For instance, the difference between class IIa and IIb is a thin line that mainly depends on its purpose:

- **Class IIa:** "Active devices intended for diagnosis or monitoring of vital physiological processes".
- **Class IIb:** "Active devices monitoring of vital physiological parameters and the nature of variations of those parameters is such that it could result in immediate danger to the patient". For instance, variations on the central nervous system or cardiac performance.

Once the medical device is classified, several requirements must be fulfilled and specific tests must be carried out. Then, the obtained evidence is presented to a notified body, which evaluates this data. If the presented evidence demonstrates that all the requirements are fulfilled, the notified body grants the CE mark to the product (see Figure 1.4). The CE mark is a certification mark that indicates a device complies with EU safety, health, and environmental requirements. This mark is mandatory for certain products, such as medical devices or consumer electronics, to be commercialized in the European Economic Area [54]. The requirements vary depending on the device, so the trials that must be performed in medical devices are not the same for consumer electronics.

To design, implement, evaluate, and manufacture a medical device, organizations must follow a quality system standard. This standard is regulated by the norm ISO 13485 [55], which ensures that an organization adheres to the procedures for fabricating and distributing medical products. While this quality standard is not mandatory for obtaining the CE mark of a medical device, the organization must comply with this norm for manufacturing the medical product once certification is granted.

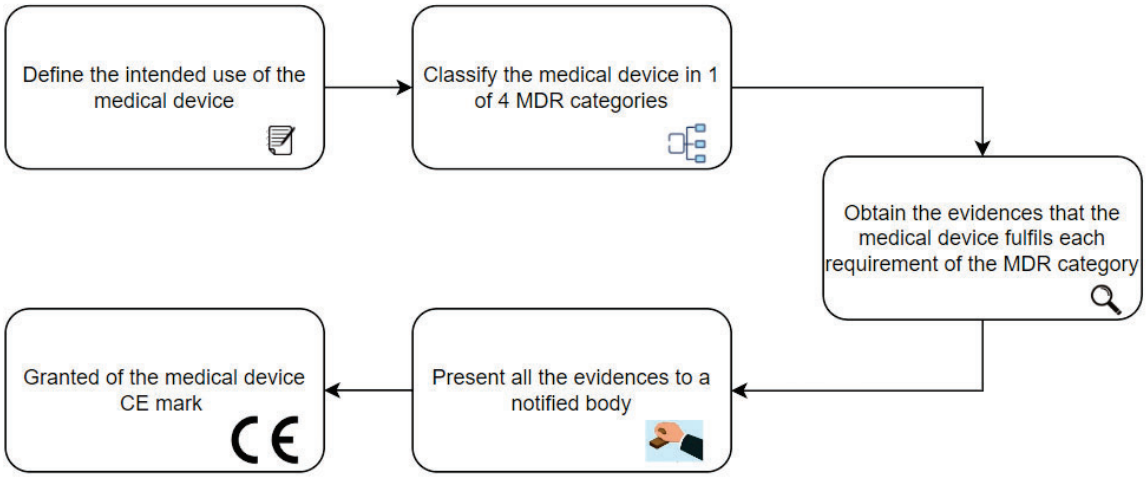

Figure 1.4. Certification process of a medical device in the EU.

1.3. Vital signs as a patient monitoring tool

Vitals signs are a set of physiological parameters that reflects the essential functions of a living organism [56]. All these parameters tend to be within a well-defined range to maintain the homeostasis, which it is the body state of equilibrium. Homeostasis is a dynamic condition as the body responds to the changing environment conditions using several internal regulation mechanisms. When the body is not capable of maintaining the homeostasis, an illness appears [57].

The five vital signs (see Figure 1.5) [58] that are typically measured by healthcare providers are:

- Pulse rate (PR) and/or Heart rate (HR)
- Peripheral oxygen saturation (SpO_2)
- Blood pressure (ABP)
- Respiratory rate (RR)
- Body temperature (BTEMP)

Each vital sign is related to the others, so it is important to measure every parameter in order to assess the health status of a patient. For instance, if the SpO_2 decreases due to a sleep apnea, the body will increase the PR to ensure that the oxygen arrives to every tissue and organ [59].

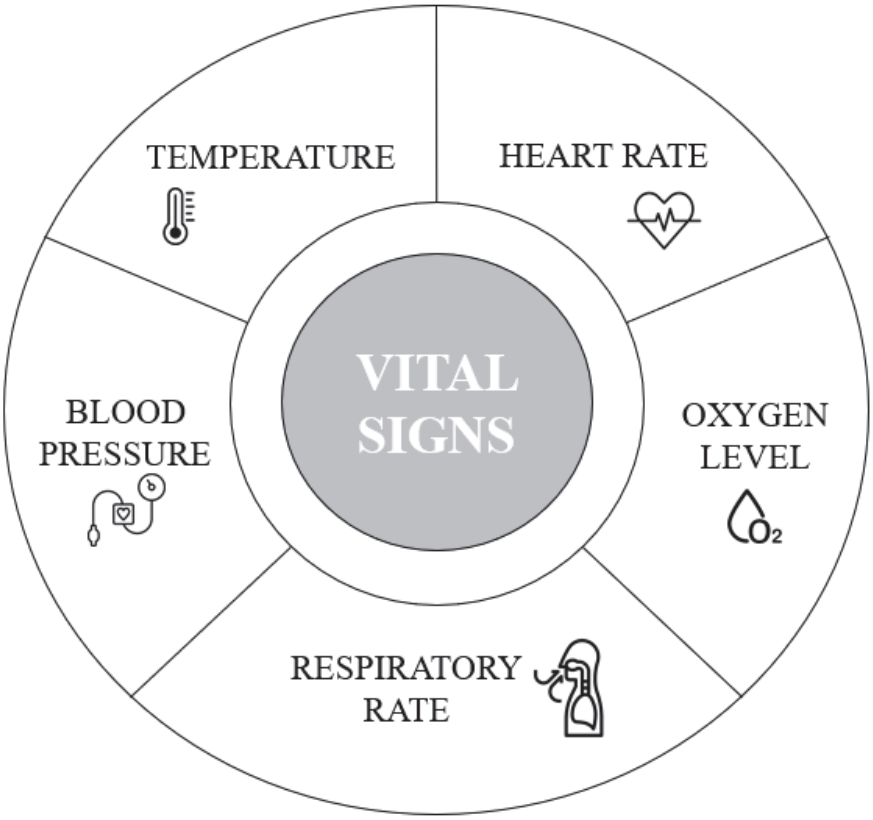

Figure 1.5. Traditional vital signs measured to assess the health state of a patient.

1.3.1. Pulse rate and heart rate

The PR and HR are the number of times that the heart beats per minute (bpm) and the only difference between them is how they are measured. The PR is estimated from the flow of the blood in the arteries and the HR from the heart's electrical activity. To measure the PR, a pulse oximeter is typically used, and to extract the HR, an electrocardiogram is utilized.

The PR normally ranges between 60 to 100 bpm at rest for an adult. There are several factors that affect this parameter, such as age, sex, fitness level, stress level, or overall health, among others. For instance, newborn resting PR ranges from 100 to 175 bpm, and then it gradually decreases until young adulthood (see Table 1.1) [60], [61].

Age	PR (bpm)
Newborn to 1 month	100-175
1 month to 2 years	90-160
2 to 6 years	70-150
7 to 11 years	60-130
12 to 18 years	50-110
Adults	60-100

Table 1.1. Pulse rate by age.

By the monitoring of the PR two different conditions can be detected:

- **Tachycardia:** Tachycardia refers to a condition where the heart beats too fast. In adults, a resting PR over 100 bpm is considered tachycardia. There are several types of tachycardia, including atrial fibrillation which is an irregular and rapid heartbeat, supraventricular tachycardia that consist of a fast heartbeat originating above the heart's ventricles, and ventricular tachycardia which is a rapid heartbeat originating in the heart's lower chambers. Tachycardia can be caused by various factors such as stress, fever, anemia, some cardiomyopathies, or certain medications [62].
- **Bradycardia:** It refers to a slow PR, typically less than 60 bpm in adults. Athletes and certain individuals, such as those who are very physically active, may have a resting PR below 60 bpm, which is normal for them. However, in some cases, bradycardia can indicate a problem of the heart's electrical system. It can be caused by aging, heart damage from heart attack, infections that affect the circulatory system, certain medications, or an inherent problem with the heart's structure [63].

The normal PR is regular, but sinus arrhythmia is a common condition in children, adolescents, and young adults. Sinus arrhythmia involves an irregular pulse rhythm in which the PR varies with the respiratory cycle: the heart rate increases at inspiration and decreases back to normal upon expiration. The underlying physiology of this condition is that the pumping frequency increases to compensate for the decreased stroke volume from the heart’s left side upon inspiration [64].

1.3.2. Oxygen saturation

Oxygen saturation is the percentage of oxygenated hemoglobin compared to the total amount of hemoglobin in blood. The hemoglobin is a protein present in blood that binds up to four oxygen molecules and it carries them to the body's tissues and organs. Therefore, oxygen saturation is an indicator of the respiratory function and overall oxygen levels in the body [56].

The acceptable oxygen saturation ranges between 95 and 100%. Saturations below 90% are considered hypoxemia, which is a condition characterized by insufficient oxygen in the blood and requires the immediate attention of healthcare providers. Some illnesses like chronic obstructive pulmonary disease cause low levels of oxygen saturation that must be controlled regularly to ensure the well-being of the patient and avoid risky situations [65].

The oxygen saturation is generally measured at the extremities of the body, such as fingers or ear, using a pulse oximeter. This instrument gives the peripheral oxygen saturation (SpO_2) value, which is the level of oxygenation at the boundaries of the body. To know the level of oxygenation of the whole body, a catheter must be inserted into an artery to analyze the arterial blood composition (SaO_2). Exists a strong correlation between the SpO_2 and the SaO_2, so it is no significant difference to measure one or another parameter. To avoid of using a catheter, the instrument typically utilized is a pulse oximeter [66].

1.3.3. Blood pressure

Blood pressure is the force of blood against artery walls. This pressure changes depending on whether the heart is contracting and pushing blood out in the arteries or whether the heart is in a resting phase and filling with blood [56]:

- **Systolic blood pressure (SABP):** Maximum pressure on the arteries during left ventricular contraction, which is responsible for pumping blood (systole).
- **Diastolic blood pressure (DABP):** Pressure on the arteries between each cardiac contraction when the heart's chambers are filled with blood (diastole).

The blood pressure is usually reported in millimeters of mercury (mmHg), in which the SABP is the numerator and DABP is the denominator. A normal blood pressure reading is around 120/80 mmHg, but this can vary depending on factors such as age, sex, and overall health. ABP too high or too low can be classified in the following way (see Table 1.2):

- **Hypertension:** It is defined as chronic blood pressure measurements of 140/90 mmHg or above in the adult. Hypertension is a silent disorder, so hypertensive patients may not recognize their condition and not adhere to their treatment plan. The result is often a heart attack or stroke. Hypertension may also lead to peripheral arterial chronic kidney disease, or heart failure.
- **Hypotension:** Hypotension is considered less than 95/60 mmHg in an adult. However, low ABP measurements are always interpreted in the context of a patient's baseline and past readings, as well as their health state. Common symptoms associated with hypotension are lightheadedness, loss of consciousness, blurry vision, clammy skin, and fatigue.

Category	SABP (mmHg)	and/or	DABP (mmHg)
Low	Less than 90	and	Less than 60
Normal	Less than 120	and	Less than 80
Elevated	120-129	and	Less than 80
Hypertension stage 1	130-139	or	80-89
Hypertension stage 2	140 or higher	or	90 or higher
Hypertension crisis	Higher than 180	or	90 or higher

Table 1.2. Blood pressure ranges [67].

ABP is generally taken in a sitting or supine position to not disturb the measurement. There are different instruments used to measure this vital sign, but the most common is the automatic sphygmomanometer.

1.3.4. Respiratory rate

Respiratory rate refers to the number of breaths taken in one minute. The respiratory system provides oxygen to the tissues and organs of the body, removes the carbon dioxide, which is the waste product of cellular respiration, and helps to maintain the acid-base balance. Inspiration is the process that causes air to enter the lungs, and expiration is the process that causes air to leave the lungs. A respiratory cycle is one sequence of inspiration and expiration [68].

Normal RR has a regular rhythm and varies depending on age, activity level, and overall health. The normal RR rate for adults is 10 to 20 breaths per minute. Children younger than one year normally have a RR of 30 to 60 breaths per minute, but by the age of ten, the normal rate is usually 18 to 30 [56].

Several illnesses can be detected by the measurement of the RR:

- **Pneumonia:** An unusually high RR can be an early sign of pneumonia, especially in children and the elderly.
- **Asthma:** Rapid breathing or shortness of breath is a common symptom during asthma attacks.
- **Anxiety:** Emotional states, such as anxiety or panic, can cause an increase in respiratory rate.

1.3.5. Body temperature

Body temperature refers to the average internal body temperature. This parameter is regulated by the hypothalamus, which ensures that the body maintains a stable temperature, even when external conditions change. For instance, the hypothalamus can activate peripheral vasoconstriction to prevent a decrease in BTEMP [56].

The normal core BTEMP is 36.5-37.5ºC. A wider range from 35.5 to 37.7ºC is acceptable in infants since heat control mechanisms are less effective. There are different factors that influence the temperature of the body such as the diurnal rhythm, exercise, stress, menstrual cycle, and pregnancy. The diurnal cycle (circadian rhythm) causes a fluctuation of one degree Celsius, with temperatures lowest in the early morning and highest in the late afternoon [69].

Accurate measurement of core temperature allows to identify hyperthermia and hypothermia conditions:

- **Hyperthermia:** It refers to an elevated body temperature and it can be related to an internal or external source. On one hand, external sources include exposure to excessive heat on a hot day or being in a sauna or hot tub. On the other hand, internal sources include fever caused by an infection or tissue breakdown associated with physical trauma or some neurological conditions.
- **Hypothermia:** Hypothermia refers to a lowered body temperature. It is usually related to an external source such as being exposed to the cold for an extended period.

There are multiple methods to measure the BTEMP based on age, cognitive functioning, state of health, and safety. The most accurate method is an invasive technique through a pulmonary artery catheter, but it is only performed in ICUs when constant measurements are required. Other methods include oral, axillary, tympanic, rectal, and dermal routes, although they do not provide core temperature. It is important to consider the body position where the temperature is taken since this parameter changes in every position (see Figure 1.6) [70].

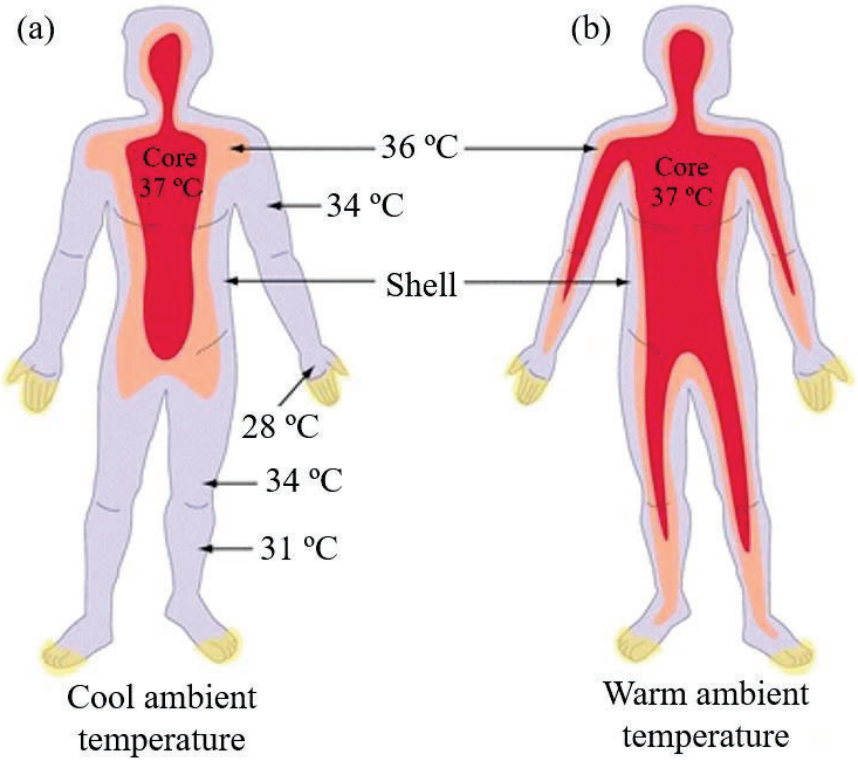

Figure 1.6. Body temperature in the human body. (a) Temperature in cold and (b) in warm environments. Courtesy of White (2011) [71], used with permission.

1.4. Sweat as an alternative biofluid for non-invasive biomarker measurement

Sweat is a mixture of secretions from millions of eccrine, apocrine, apoeccrine, and sebaceous glands as well as bacteria, yeast, fungi, other microbiota, and cellular debris that reside on the skin. It is mainly composed of water (~99 %) with large numbers of different small molecules, such as sodium, chloride, lactate, or glucose [45]. Several research have studied the sweat composition and have quantified every component present in this biofluid (see Table 1.3) [72].

It has multiple functions on the operation of the organism:

- **Thermoregulation:** The main function is to regulate the body temperature. When the body overheats due to physical activity, high temperature, or fever, this biofluid is produced in order to cool down the internal temperature of the organism.
- **Excretion:** Sweat contains small amounts of waste products, such as urea or ammonium. Sweating allows the body to eliminate these substances.
- **Protection:** A protective barrier is created by sweat, which prevents some bacterial and fungal infections. The acidic nature of this biofluid can inhibit the growth of certain microbes on the skin surface.

Sweat is excreted from the body by the sweat glands. The process of sweating is regulated by the autonomic nervous system and can be triggered by various factors, including temperature, physical activity, and emotional stress.

Constituents	Median concentration (M)	Min. concentration (M)	Max. concentration (M)
Primary electrolytes			
Sodium	3.1×10^{-2}	1.1×10^{-4}	3.9×10^{-1}
Chloride	2.3×10^{-2}	1.7×10^{-5}	2.8×10^{-1}
Calcium	5.2×10^{-3}	4.7×10^{-6}	1.5×10^{-2}
Potassium	6.1×10^{-3}	6.7×10^{-6}	3.8×10^{-2}
Magnesium	8.2×10^{-5}	7.4×10^{-8}	3.8×10^{-3}
Phosphate	3.1×10^{-4}	2.3×10^{-5}	1.1×10^{-3}
Ionic constituents			
Sulfate	4.2×10^{-4}	7.0×10^{-5}	2.0×10^{-3}
Copper	9.4×10^{-7}	1.3×10^{-8}	1.2×10^{-3}
Iron	9.8×10^{-6}	1.5×10^{-8}	1.1×10^{-3}
Manganese	1.1×10^{-6}	1.1×10^{-9}	1.3×10^{-3}
Lactic acid	1.4×10^{-2}	3.7×10^{-3}	5.0×10^{-2}
Glucose	1.7×10^{-4}	5.6×10^{-6}	2.2×10^{-3}
Amino acids			
Isoleucine	1.7×10^{-4}	7.6 x 10-5	2.8×10^{-4}
Ammonia	5.2×10^{-3}	4.7×10^{-4}	2.5×10^{-2}
Uric acid	5.9×10^{-5}	4.2×10^{-6}	4.8×10^{-3}
Urea	1.0×10^{-2}	1.8×10^{-3}	4.6×10^{-2}
Creatinine	8.4×10^{-5}	8.8×10^{-6}	2.0×10^{-3}
Vitamins			
Thiamine	5.0×10^{-3}	4.5×10^{-9}	5.0×10^{0}
Folic acid	1.6×10^{-8}	1.2×10^{-8}	2.0×10^{-8}
Ascorbic acid	1.0×10^{-5}	1.1×10^{-7}	3.6×10^{-4}
Inositol	1.6×10^{-6}	8.3×10^{-7}	1.2×10^{0}
Choline	2.6×10^{-5}	6.8×10^{-7}	1.5×10^{-4}

Table 1.3. Estimated content of sweat. Adapted with permission from Harvey (2010) [72].

1.5. State of the art of biometric devices

There are several wearable devices that are capable of recoding physiological data of a patient. They can be split between devices that monitor the vital signs and systems that analyze the sweat content.

1.5.1. Vital sign monitoring wearable devices

The market is plenty of wearable devices capable of monitoring the vital signs of an individual (see Table 1.4). Despite the number of devices available, most of these systems cannot be used by healthcare providers since they are consumer electronics and not have been granted with medical certification. There are a few wearable devices that have been approved by health national authorities. In almost every case, the information provided by the approved medical devices is incomplete because these systems do not monitor all the vital signs. Furthermore, most wearable devices cannot be connected to third-party programs and must be utilized in the applications/programs of the distribution companies,

which can be a problem for institutions that possess their own digital systems, such as hospitals or insurance companies.

Company	Device	Clinical trials performed	Medical certification
Samsung Electronics	Samsung Galaxy Watch 6	NO	NO
Apple Inc.	Apple Watch 9	YES	NO
Corsano Health	Cardio Watch 287	YES	NO
Masimo corporation	Masimo W1	YES	NO
Biosency	Bora-Band BB-100	YES	Europe
Bio-Beat	Wrist Monitor	YES	Europe and EEUU

Table 1.4. Sample of wearable devices available on the market that measure the vital signs [73], [74], [75], [76], [77], [78].

Apart from the certification, there are other barriers that prevent potential users to utilize medical wearable devices in their daily lives. Older adults typically have high adherence to using a wearable watch, and most are willing to contribute with home monitoring [79]. Nevertheless, age remains a major barrier to the acceptability of digital services [80], [81]. Those with digital literacy and visual impairments may have trouble using smartphones with numerous buttons and tiny text. Expanding digital health services to the geriatric population requires simpler and user-tailored devices. Wearables need to be centered on individuals with a range of other pre-existing health conditions, such as fragile skin or reduced vision. The lifetime, size, and weight of the developed devices should also be taken into consideration. Overall, a better understanding of the barriers that older adults face will enable designers to tailor future devices to their needs [14].

To facilitate the adoption of medical wearable technologies to the elderly and disabled population, novel functional approaches must be developed. An approach that seems easy but requires a lot of work to be implemented involves the creation of smart systems capable of monitoring the individual without user interaction. These devices are placed on the patient and start taking measurements continuously. The main issue with these systems is that they must be able to distinguish certain situations in order to record a measurement only when the result can be accurate.

1.5.2. Sweat analyzers

Sweat is barely utilized by the medical community. The lack of trials that use sweat as a sample is due to the non-existence of a standardized method to collect this biofluid, the low volume of the sample (range of nanoliters), and the liquid evaporation. These issues can be solved by attaching sensors to the skin, but this methodology produces a major issue: contamination of the sample due to the accumulation of sweat on the sensor's surface. To avoid this unwanted situation, a microfluidic system can be used to renew the sample and expel the generated waste [82].

Several research groups have developed systems capable of collecting sweat from the skin, processing it, and analyzing its content using different sensors. Liang et al. developed a paper-based microfluidic device for the real-time monitoring of sweat potassium [83]. Martín et al. presented a microfluidic detection platform for the monitoring of glucose and lactate levels [84]. Kim et al. developed a microfluidic patch

that allowed for rapid colorimetric assessments of the concentrations of multiple essential nutrients in sweat [85]. Feng et al. presented a patch capable to monitor the lactate, glucose, potassium, and sodium sweat concentrations in real-time [86].

Apart from the devices developed by researchers, there are several commercial products capable of analyzing sweat content. These devices are focused on diagnosis of conditions such as cystic fibrosis or peripheral neuropathies (see Table 1.5).

Cystic fibrosis is a genetic disease that causes persistent lung infections and limits the ability to breathe over time. Early diagnosis and treatment can significantly improve the quality of life and lifespan of patients. The gold standard to detect cystic fibrosis consists in the conductivity analysis of sweat due to the fact that chloride content in this biofluid is altered, increasing exponentially the medium's impedance [87], [88].

Peripheral neuropathy is a common complication of diabetes and leads to an increase in morbidity. It is crucial in the pathogenesis of foot ulcers. 15 % of diabetics develop a foot ulcer that can progress to severe injury and even amputation. A neglected component of peripheral neuropathy is sudomotor neuropathy, which results in reduced sweating, dry, and sensitive skin with a propensity towards callus and fissure formation. A reliable method to detect this condition consists of using a colorimetric patch that changes its color by the presence of chloride ions in sweat. This presence is related to an abnormal perspiration, so the neuropathy can be diagnosed utilizing this system [89], [90].

During the past few years, novel devices capable of performing more complex analysis have appeared on the market, such as the Gx Sweat Patch (Epicore Biosystems; Cambridge, MA, USA) [91]. This device is a colorimetric patch that enables sweating rate analysis and sweat chloride concentration estimation, which can be used to know the user's dehydration. It is typically utilized by athletes to monitor their health status during a training or competition. To use this device a smartphone is required because to extract the data from this patch, a photograph of the device must be taken [92]. This requirement reduces the usefulness of this system since continuous monitoring cannot be carried out.

All the sweat analyzers available on the market have the same limitation: there are single-use devices. Single-use systems help the healthcare providers to assess the state of an individual at a specific moment although it does not allow to see the user's evolution. So, a new generation of devices capable of analyzing the sweat in a continuous manner are necessary.

Manufacturer	Research/Industrial	Parameters monitored
Liang et al	Research	Potassium
Martín et al	Research	Glucose and lactate
Kim et al	Research	Vitamin C, calcium, zinc, and iron
Feng et al	Research	Lactate, glucose, potassium, and sodium
ELITechGroup	Industrial	Sweat conductivity
Neuropad	Industrial	Chloride
Epicore Biosystems	Industrial	Sweating rate and chloride

Table 1.5. Sweat analyzers (research and industrial) [83], [84], [85], [86], [91], [93], [94].

1.6. New generation of hospital at home units

As discussed earlier, the rising life expectancy directly impacts on the sustainability of healthcare systems. There is a growing need for new methods and tools to reduce this impact and improve the attention provided to patients. In response to these challenges, Onalabs developed a monitoring medical system for HAH units (see Figure 1.7). This system is composed of three key elements:

- **Biometric devices:** These elements are wearable devices that collect physiological data from the users and send this information to a cloud by means of a gateway.
- **Gateway:** This component can be a specific hardware or a mobile phone. It acts as a repeater: it receives the data from the mentioned wearables and send the information to a digital platform.
- **Digital platform:** This element receives the data sent by the gateway and analyzes the information, so rapid deterioration can be identified, and medical personnel efficiently assigned. The system is a cloud platform with capabilities of data storage and data management along with the digital security required in the healthcare field.

The digital platform is the central module of the system. It collects the acquired data and analyzes the obtained information. Users, healthcare providers, and institutions can access to the data by means of an Application Programming Interface (API). An API is a software interface that allows two or more programs to communicate to each other [95]. This system based on APIs enables the integration of the platform on third-party software, such as that used by doctors and nurses at hospitals. The adoption of this kind of digital platforms is not always easy because the healthcare providers need rapid solutions to a changing and stressful environment, so the integrating new solutions in the actual systems ease their adoption.

The Onalabs system was designed and developed to be scalable. Scalability refers to the ability to handle increasing amounts of work without compromising performance or efficiency of the system. It is a big issue that usually is overshadowed by other aspects of the technological development. A system must be capable of handling workloads that vary constantly depending on the number of devices connected to the network. The system also must be responsive to these changes and manage the data provided by the biometric devices without losing valuable information in the process.

Another important aspect of the Onalabs system is the use of gateways to transmit the data from the biometric devices to the cloud. One of the most common approaches consist of transmitting the gathered data directly from the device to the cloud utilizing powerful communication systems, such as WiFi or 3G/4G/5G. These communication systems send the information at high speed, but require a lot of energy, which significantly reduces the autonomy of portable devices. A gateway solves this problem since it collects the information and transmits this data to the digital platform. To establish the communication between wearables and gateways, less power consuming communication systems can be used, like Bluetooth or NFC [96]. There are multiple devices that can be utilized as gateways and the most common one is the smartphone. A smartphone has the capabilities to be a gateway and permits to display the gathered data. A drawback of these

devices is that the user does not always possess a smartphone. In these cases, a specific hardware which acts as a gateway can be installed on the settings where they are utilized, such as hospitals or homes.

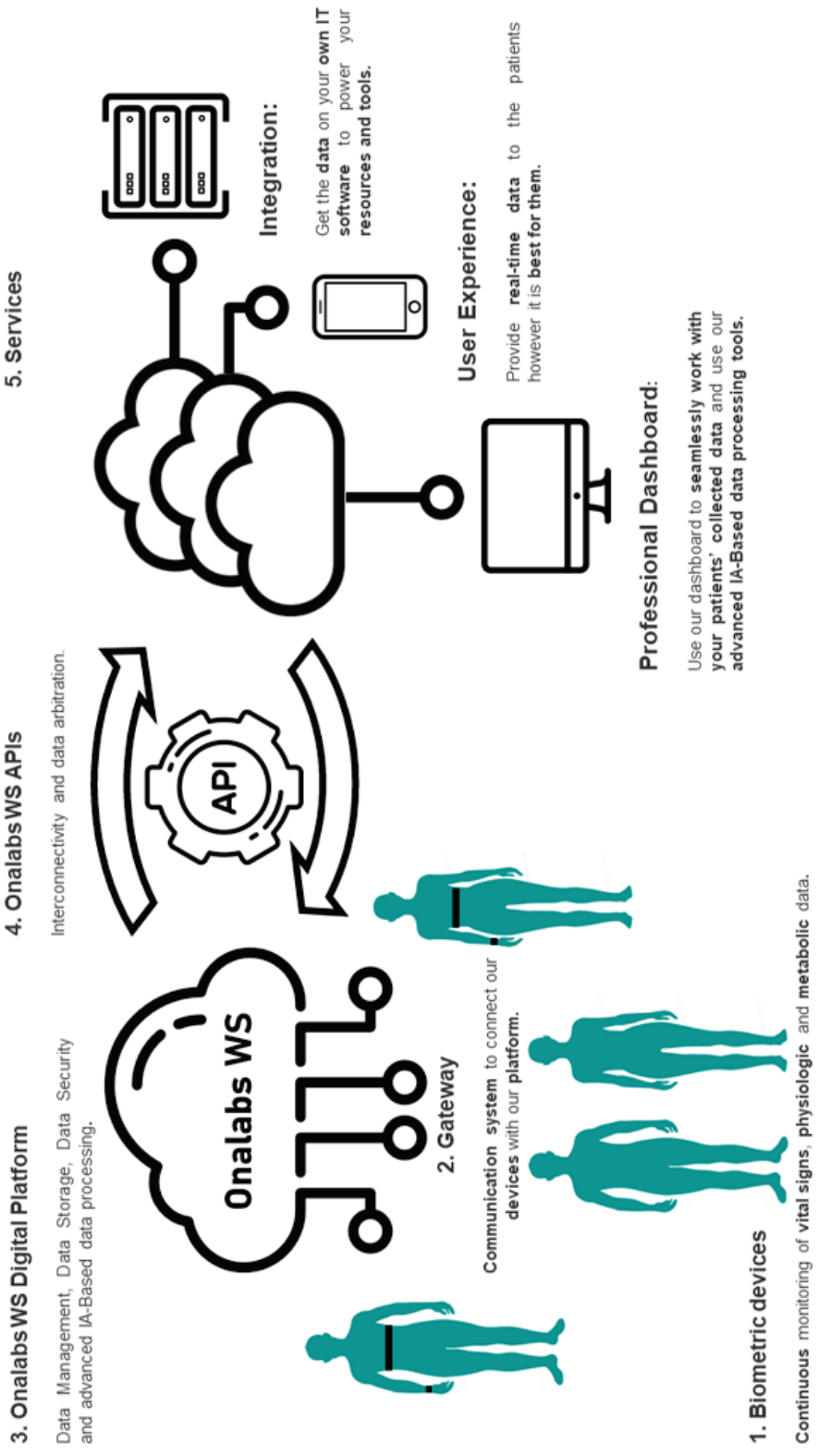

Figure 1.7. Structure of the Onalabs' HAH system. The biometric devices (wearables) collect physiological data of the patients and send this information to a digital platform by means of a gateway. All the data acquired is stored and analyzed by this platform. To access the information of the cloud, an API is used. This API allows to easily integrate the system to third-party platforms.

1.7. Contribution of this thesis

The aim of this thesis is developing wearable devices for the Onalabs' biometric monitoring system. These devices must be able to track the patient's health status by measuring their vital signs and analyzing their sweat content. Tracking both vital signs and sweat biomarkers provides an accurate and comprehensive assessment of an individual state.

On one hand, a medical wearable device capable of measuring the patient's vital signs is implemented. This monitoring tool allows healthcare providers to assess the patients' health status continuously and remotely in a non-invasive manner. Not only this device is developed, but the certification and industrialization of this system are carried out, giving as outcome a robust product ready to be used by the medical personnel.

Medical certification is mandatory for using a device in a clinical setting, such as hospitals or clinics. This certification is granted by the regulatory authorities of the country where the system is utilized. The medical certification process involves several steps ranging from assessing device security to demonstrating data accuracy, which must be conducted meticulously to ensure the wearable device receives the medical device label.

Industrialization refers to the process of transitioning a product from its initial design to mass production. This process involves setting-up the manufacturing processes, systems, and infrastructure to produce the device efficiently, cost-effectively, and in large quantities. Industrialization must be carried out properly to ensure that every manufactured system has the same characteristics.

On the other hand, a novel wearable device able to capture sweat from the skin and analyze its content is developed. Sweat is a biofluid with a rich content that provides a huge amount of data about the individual in a non-invasive and continuous way. A system capable of analyzing this biofluid can be an invaluable tool for the medical personnel because it provides clinical information only available by means of blood testing.

These two wearable devices are connected to the same digital platform, so the gathered data from both systems can be used to assess the individuals' state. The biometric monitoring system developed has the potential to revolutionize the healthcare field because a remotely, non-invasive, and continuous monitorization of individuals can be carried out.

This work is focused on the wearables developed and the electronics involved. The other parts of the system are described, but the insights of these elements are not presented here since they are out of the work's scope.

The thesis is structured in the following way:

- **Chapter 1:** In this section, the aging population problem and diseases related to age have been described. Wearable technology has been presented as a solution to mitigate this problem because it allows continuous and non-invasive monitorization of healthcare system users. The data gathered by these devices improves the resource management of healthcare institutions being more efficient.

- **Chapter 2:** A description about the functional and operational capabilities of the system developed by Onalabs is presented. Here, the capabilities of the system and the technologies involved are described. Furthermore, the process followed to develop the wearable devices described in this thesis is presented.
- **Chapter 3:** In this chapter, the device able to monitor the patients' vital signs is described. This system is a bracelet that is worn on the user's wrist. It was conceived taking in mind the target user (patients) and it was created in a close relation with healthcare providers to satisfy their necessities.
- **Chapter 4:** The clinical evaluations carried out using the vital signs monitoring device are presented. Every phase of the evaluation is described, and the obtained results are discussed.
- **Chapter 5:** Any device used in a clinical setting must be approved by the regulatory authorities. This process is costly and time consuming, but it ensures that every system granted with medical certification is safe and provides accurate data. Apart from the certification process, the industrialization of the device must be handled properly to produce devices with the same performance and characteristics. Here, both processes (medical certification and industrialization) are described.
- **Chapter 6:** In this section, the novel wearable device capable of collecting sweat from the skin and analyzing its content is presented. This device is applied to the sports medicine field due the fact that it is easier to obtain larger volumes of this biofluid passively during a physical activity.
- **Chapter 7:** Eventually, the thesis conclusions are presented, and the future work is described.

1.8. References

[1] "Onalabs Inno-Hub SL." Accessed: Jul. 09, 2023. [Online]. Available: https://onalabs.com/en/

[2] "Industrial Doctorates – Industrial Doctorates Plan of the Generalitat." Accessed: Jul. 09, 2023. [Online]. Available: https://doctoratsindustrials.gencat.cat/en/

[3] "Discrete-to-Integrated Systems Lab (D2In)." Accessed: Jul. 09, 2023. [Online]. Available: https://d2in.org/

[4] "Nanobioengineering and Bioelectrònics (SIC-BIO)." Accessed: Jul. 09, 2023. [Online]. Available: https://webgrec.ub.edu/cgi-bin/3DADREC/crfitgrup.cgi?PAR=SICBIOIN

[5] U. N. Department of Economic and Social Affairs, "World Population Prospects 2019 Highlights," 2019. Accessed: Apr. 02, 2024. [Online]. Available: https://population.un.org/wpp/Publications/Files/WPP2019_Highlights.pdf

[6] Instituto Nacional de Estadística (INE), "Projection of the resident population in Spain (2022-2072)," Oct. 2022. Accessed: Apr. 02, 2024. [Online]. Available: https://www.ine.es/en/prensa/pp_2022_2072_en.pdf

[7] Statistisches Bundesamt, "Germany´s Population by 2050," Nov. 2006. Accessed: Apr. 02, 2024. [Online]. Available: https://www.destatis.de/EN/Themes/Society-Environment/Population/Population-Projection/Publications/Downloads-Population-

Projection/germany-population-2050.pdf?__blob=publicationFile#:~:text=As%20a%20consequence%2C%20Germany's%20population,nearly%2069%20million%20in%202050.

[8] "Government expenditure on health EU." Accessed: Sep. 03, 2023. [Online]. Available: https://ec.europa.eu/eurostat/statistics-explained/index.php?title=Government_expenditure_on_health

[9] "The Inequities in the Cost of Chronic Disease for Older Adults." Accessed: Dec. 27, 2023. [Online]. Available: https://www.ncoa.org/article/the-inequities-in-the-cost-of-chronic-disease-why-it-matters-for-older-adults

[10] A. D. Lopez, C. D. Mathers, M. Ezzati, D. T. Jamison, and C. J. L. Murray, "Global and regional burden of disease and risk factors, 2001: systematic analysis of population health data," *The Lancet*, vol. 367, no. 9524, pp. 1747–1757, 2006, doi: https://doi.org/10.1016/S0140-6736(06)68770-9.

[11] World Health Organization, "Global report on diabetes," 2016. Accessed: Apr. 03, 2024. [Online]. Available: https://www.who.int/publications/i/item/9789241565257

[12] G. A. Roth *et al.*, "Global Burden of Cardiovascular Diseases and Risk Factors, 1990-2019: Update From the GBD 2019 Study," *Journal of the American College of Cardiology*, vol. 76, no. 25. Elsevier Inc., pp. 2982–3021, Dec. 22, 2020. doi: 10.1016/j.jacc.2020.11.010.

[13] A. J. Scott, "The longevity society," *The Lancet Healthy Longevity*, vol. 2, no. 12. Elsevier Ltd, pp. e820–e827, Dec. 01, 2021. doi: 10.1016/S2666-7568(21)00247-6.

[14] C. Chen, S. Ding, and J. Wang, "Digital health for aging populations," *Nat Med*, vol. 29, no. 7, pp. 1623–1630, Jul. 2023, doi: 10.1038/s41591-023-02391-8.

[15] G. Neumann and Y. Kawaoka, "Which Virus Will Cause the Next Pandemic?," *Viruses*, vol. 15, no. 1, Jan. 2023, doi: 10.3390/v15010199.

[16] "COVID-19 deaths." Accessed: Dec. 27, 2023. [Online]. Available: https://data.who.int/dashboards/covid19/deaths?n=c

[17] J. M. Pericàs *et al.*, "Hospital at home for the management of COVID-19: preliminary experience with 63 patients," *Infection*, vol. 49, no. 2, pp. 327–332, Apr. 2021, doi: 10.1007/s15010-020-01527-z.

[18] E. Coloma and D. Nicolás, "Hospital at Home units in the post-COVID 19 era," *European Journal of Clinical Investigation*, vol. 50, no. 11. Blackwell Publishing Ltd, Nov. 01, 2020. doi: 10.1111/eci.13390.

[19] B. Leff *et al.*, "Comparison of functional outcomes associated with hospital at home care and traditional acute hospital care," *J Am Geriatr Soc*, vol. 57, no. 2, pp. 273–278, Feb. 2009, doi: 10.1111/j.1532-5415.2008.02103.x.

[20] D. M. Levine *et al.*, "Hospital-level care at home for acutely ill adults a randomized controlled trial," *Ann Intern Med*, vol. 172, no. 2, pp. 77–85, Jan. 2020, doi: 10.7326/M19-0600.

[21] E. A. Boogerd, T. Arts, L. J. Engelen, and T. H. van de Belt, "'What Is eHealth': Time for An Update?," *JMIR Res Protoc*, vol. 4, no. 1, p. e29, Mar. 2015, doi: 10.2196/resprot.4065.

[22] C. Pagliari *et al.*, "What is eHealth (4): A scoping exercise to map the field," *Journal of Medical Internet Research*, vol. 7, no. 1. JMIR Publications Inc., 2005. doi: 10.2196/jmir.7.1.e9.

[23] M. H. da Fonseca, F. Kovaleski, C. T. Picinin, B. Pedroso, and P. Rubbo, "E-health practices and technologies: A systematic review from 2014 to 2019," *Healthcare (Switzerland)*, vol. 9, no. 9. MDPI, Sep. 01, 2021. doi: 10.3390/healthcare9091192.

[24] C. A. Meier, M. C. Fitzgerald, and J. M. Smith, "EHealth: Extending, enhancing, and evolving health care," *Annual Review of Biomedical Engineering*, vol. 15. pp. 359–382, Jul. 2013. doi: 10.1146/annurev-bioeng-071812-152350.

[25] F. Saigí-Rubió *et al.*, "Determinants of Catalan public primary care Professionals' intention to use digital clinical consultations (eConsulta) in the post-COVID-19 context: Mixed methods study," *J Med Internet Res*, vol. 23, no. 6, Jun. 2021, doi: 10.2196/28944.

[26] C. E. Grau, J. C. Colet, and J. M. V. Rotellar, "Applications of telemedicine in monitoring heart failure: Experience in an integral unit," *FMC*, vol. 22, no. 4, pp. 188–195, 2015, doi: 10.1016/j.fmc.2015.01.002.

[27] European Comission, "eHealth Action Plan 2012-2020," Dec. 2012. Accessed: Jul. 23, 2023. [Online]. Available: https://health.ec.europa.eu/document/download/39c9a1ee-6afa-4ab9-a472-ddeac925d14f_en?filename=com_2012_736_en.pdf

[28] F. Visseren *et al.*, "2021 ESC Guidelines on cardiovascular disease prevention in clinical practice," *European Heart Journal*, vol. 42, no. 34. Oxford University Press, pp. 3227–3337, Sep. 07, 2021. doi: 10.1093/eurheartj/ehab484.

[29] J. M. Mostaza *et al.*, "SEA 2022 Standards for Global Control of Cardiovascular Risk," *Clinica e Investigacion en Arteriosclerosis*, vol. 34, no. 3, pp. 130–179, May 2022, doi: 10.1016/j.arteri.2021.11.003.

[30] H. K. Thakkar, S. R. Chowdhury, A. K. Bhoi, and P. Barsocchi, "Applications of wearable technologies in healthcare: an analytical study," in *5G IoT and Edge Computing for Smart Healthcare*, Elsevier, 2022, pp. 279–299. doi: 10.1016/B978-0-323-90548-0.00001-2.

[31] M. A. Chopra and M. A. Singhal, "Understanding the Wearable Technology," in *International Conference on Innovative Computing & Communication (ICICC)*, Apr. 2021. doi: http://dx.doi.org/10.2139/ssrn.3833316.

[32] M. Jacobsen, T. A. Dembek, G. Kobbe, P. W. Gaidzik, and L. Heinemann, "Noninvasive Continuous Monitoring of Vital Signs With Wearables: Fit for Medical Use?," *Journal of Diabetes Science and Technology*, vol. 15, no. 1. SAGE Publications Inc., pp. 34–43, 2020. doi: 10.1177/1932296820904947.

[33] M. Etiwy *et al.*, "Accuracy of wearable heart rate monitors in cardiac rehabilitation," *Cardiovasc Diagn Ther*, vol. 9, no. 3, pp. 262–271, 2019, doi: 10.21037/cdt.2019.04.08.

[34] A. Shcherbina *et al.*, “Accuracy in wrist-worn, sensor-based measurements of heart rate and energy expenditure in a diverse cohort,” *J Pers Med*, vol. 7, no. 2, Jun. 2017, doi: 10.3390/jpm7020003.

[35] J. K. Devine, L. P. Schwartz, and S. R. Hursh, “Technical, Regulatory, Economic, and Trust Issues Preventing Successful Integration of Sensors into the Mainstream Consumer Wearables Market,” *Sensors*, vol. 22, no. 7, Apr. 2022, doi: 10.3390/s22072731.

[36] S. Soon, H. Svavarsdottir, C. Downey, and D. G. Jayne, “Wearable devices for remote vital signs monitoring in the outpatient setting: An overview of the field,” *BMJ Innovations*, vol. 6, no. 2. BMJ Publishing Group, p. 55, Apr. 01, 2020. doi: 10.1136/bmjinnov-2019-000354.

[37] M. Haghi, S. Danyali, S. Ayasseh, J. Wang, R. Aazami, and T. M. Deserno, “Wearable devices in health monitoring from the environmental towards multiple domains: A survey,” *Sensors*, vol. 21, no. 6. MDPI AG, pp. 1–24, Mar. 02, 2021. doi: 10.3390/s21062130.

[38] P. Amin, N. R. Anikireddypally, S. Khurana, S. Vadakkemadathil, and W. Wu, “Personalized health monitoring using predictive analytics,” in *Proceedings - 5th IEEE International Conference on Big Data Service and Applications, BigDataService 2019, Workshop on Big Data in Water Resources, Environment, and Hydraulic Engineering and Workshop on Medical, Healthcare, Using Big Data Technologies*, Institute of Electrical and Electronics Engineers Inc., Apr. 2019, pp. 271–278. doi: 10.1109/BigDataService.2019.00048.

[39] I. J. Brekke, L. H. Puntervoll, P. B. Pedersen, J. Kellett, and M. Brabrand, “The value of vital sign trends in predicting and monitoring clinical deterioration: A systematic review,” *PLoS One*, vol. 14, no. 1, Jan. 2019, doi: 10.1371/journal.pone.0210875.

[40] C. Areia *et al.*, “Experiences of current vital signs monitoring practices and views of wearable monitoring: A qualitative study in patients and nurses,” *J Adv Nurs*, vol. 78, no. 3, pp. 810–822, Mar. 2022, doi: 10.1111/jan.15055.

[41] C. S. Webster, T. W. L. Scheeren, and Y. I. Wan, “Patient monitoring, wearable devices, and the healthcare information ecosystem,” *British Journal of Anaesthesia*, vol. 128, no. 5. Elsevier Ltd, pp. 756–758, May 01, 2022. doi: 10.1016/j.bja.2022.02.034.

[42] J. R. Cardoso, L. M. Pereira, M. D. Iversen, and A. L. Ramos, “What is gold standard and what is ground truth?,” *Dental Press J Orthod*, vol. 19, no. 5, pp. 27–30, Sep. 2014, doi: 10.1590/2176-9451.19.5.027-030.ebo.

[43] P. Yang, G. Wei, A. Liu, F. Huo, and Z. Zhang, “A review of sampling, energy supply and intelligent monitoring for long-term sweat sensors,” *npj Flexible Electronics*, vol. 6, no. 1. Nature Research, Dec. 01, 2022. doi: 10.1038/s41528-022-00165-9.

[44] D. S. Yang, R. Ghaffari, and J. A. Rogers, “Sweat as a diagnostic biofluid,” *Science (1979)*, vol. 379, no. 6634, pp. 760–761, Feb. 2023, doi: 10.1126/science.abq5916.

[45] J. N. Hussain, N. Mantri, M. M. Cohen, and J. Hussain, “Working Up a Good Sweat-The Challenges of Standardising Sweat Collection for Metabolomics Analysis,” *Clin Biochem Rev*, vol. 38, no. 1, pp. 13–34, Feb. 2017.

[46] Y. Gokdemir and B. T. Karadag, “Sweat Testing and Recent Advances,” *Frontiers in Pediatrics*, vol. 9. Frontiers Media S.A., May 04, 2021. doi: 10.3389/fped.2021.649904.

[47] Z. Sonner *et al.*, “The microfluidics of the eccrine sweat gland, including biomarker partitioning, transport, and biosensing implications,” *Biomicrofluidics*, vol. 9, no. 3, May 2015, doi: 10.1063/1.4921039.

[48] “Wearable Medical Devices Market Size, Share, Trends & Forecast.” Accessed: Dec. 27, 2023. [Online]. Available: https://www.verifiedmarketresearch.com/product/wearable-medical-devices-market/

[49] “Wearable Technology Market Share & Trends Report, 2030.” Accessed: Dec. 27, 2023. [Online]. Available: https://www.grandviewresearch.com/industry-analysis/wearable-technology-market

[50] D. Fuller *et al.*, “Reliability and Validity of Commercially Available Wearable Devices for Measuring Steps, Energy Expenditure, and Heart Rate: Systematic Review,” *JMIR mHealth and uHealth*, vol. 8, no. 9. JMIR Publications Inc., Sep. 01, 2020. doi: 10.2196/18694.

[51] “2017/745 - Medical Device Regulation.” Accessed: Jan. 20, 2024. [Online]. Available: https://eur-lex.europa.eu/legal-content/EN/TXT/HTML/?uri=CELEX:32017R0745

[52] “Notified bodies.” Accessed: Jan. 20, 2024. [Online]. Available: https://single-market-economy.ec.europa.eu/single-market/goods/building-blocks/notified-bodies_en

[53] “ANNEX VIII - Medical Device Regulation.” Accessed: Jan. 20, 2024. [Online]. Available: https://www.medical-device-regulation.eu/2019/08/08/annex-viii/

[54] “CE marking.” Accessed: Jan. 20, 2024. [Online]. Available: https://single-market-economy.ec.europa.eu/single-market/ce-marking_en

[55] “ISO 13485.” Accessed: Jan. 28, 2024. [Online]. Available: https://www.iso.org/standard/59752.html

[56] J. L. Lapum, M. Verkuyl, O. St-Amant, W. Garcia, and A. Tan, *Vital sign measurement across the lifespan (2nd ed.)*. BCcampus, 2021. [Online]. Available: https://opentextbc.ca/vitalsignmeasurement/

[57] G. J. Tortora and B. Derrickson, “An introduction to the human body,” in *Principles of anatomy and physiology*, Wiley, 2016, pp. 1–26.

[58] D. Dias and J. P. S. Cunha, “Wearable health devices—vital sign monitoring, systems and technologies,” *Sensors (Switzerland)*, vol. 18, no. 8. MDPI AG, Aug. 01, 2018. doi: 10.3390/s18082414.

[59] T. Penzel, “Is heart rate variability the simple solution to diagnose sleep apnoea?,” *European Respiratory Journal*, vol. 22, no. 6. European Respiratory Society, pp. 870–871, 2003. doi: 10.1183/09031936.03.00102003.

[60] D. Zhang, X. Shen, and X. Qi, “Resting heart rate and all-cause and cardiovascular mortality in the general population: A meta-analysis,” *CMAJ*, vol. 188, no. 3, pp. E53–E63, Feb. 2016, doi: 10.1503/cmaj.150535.

[61] Y. Ostchega, K. S. Porter, J. Hughes, M. P. H. ; Charles, F. Dillon, and T. Nwankwo, “Resting Pulse Rate Reference Data for Children, Adolescents, and Adults: United States, 1999-2008,” 2011.

[62] R. Gopinathannair and B. Olshansky, “Management of tachycardia,” *F1000Prime Rep*, vol. 7, May 2015, doi: 10.12703/P7-60.

[63] S. Sidhu and J. E. Marine, “Evaluating and managing bradycardia,” *Trends in Cardiovascular Medicine*, vol. 30, no. 5. Elsevier Inc., pp. 265–272, Jul. 01, 2020. doi: 10.1016/j.tcm.2019.07.001.

[64] B. Rassler, K. Blinowska, M. Kaminski, and G. Pfurtscheller, “Analysis of Respiratory Sinus Arrhythmia and Directed Information Flow between Brain and Body Indicate Different Management Strategies of fMRI-Related Anxiety,” *Biomedicines*, vol. 11, no. 4, Apr. 2023, doi: 10.3390/biomedicines11041028.

[65] P. J. Barnes *et al.*, “Chronic obstructive pulmonary disease,” *Nat Rev Dis Primers*, vol. 1, Dec. 2015, doi: 10.1038/nrdp.2015.76.

[66] E. D. Chan, M. M. Chan, and M. M. Chan, “Pulse oximetry: Understanding its basic principles facilitates appreciation of its limitations,” *Respiratory Medicine*, vol. 107, no. 6. pp. 789–799, Jun. 2013. doi: 10.1016/j.rmed.2013.02.004.

[67] “Understanding Blood Pressure Readings.” Accessed: Feb. 10, 2024. [Online]. Available: https://www.heart.org/en/health-topics/high-blood-pressure/understanding-blood-pressure-readings

[68] A. Nicolò, C. Massaroni, E. Schena, and M. Sacchetti, “The importance of respiratory rate monitoring: From healthcare to sport and exercise,” *Sensors (Switzerland)*, vol. 20, no. 21. MDPI AG, pp. 1–45, Nov. 01, 2020. doi: 10.3390/s20216396.

[69] B. Coiffard, A. B. Diallo, S. Mezouar, M. Leone, and J. L. Mege, “A tangled threesome: Circadian rhythm, body temperature variations, and the immune system,” *Biology*, vol. 10, no. 1. MDPI AG, pp. 1–16, Jan. 01, 2021. doi: 10.3390/biology10010065.

[70] C. M. Lee, S. P. Jin, E. J. Doh, D. H. Lee, and J. H. Chung, “Regional variation of human skin surface temperature,” *Ann Dermatol*, vol. 31, no. 3, pp. 349–352, 2019, doi: 10.5021/ad.2019.31.3.349.

[71] M. D. White, C. M. Bosio, B. N. Duplantis, and F. E. Nano, “Human body temperature and new approaches to constructing temperature-sensitive bacterial vaccines,” *Cellular and Molecular Life Sciences*, vol. 68, no. 18. pp. 3019–3031, Sep. 2011. doi: 10.1007/s00018-011-0734-2.

[72] C. J. Harvey, R. F. LeBouf, and A. B. Stefaniak, “Formulation and stability of a novel artificial human sweat under conditions of storage and use,” *Toxicology in Vitro*, vol. 24, no. 6, pp. 1790–1796, Sep. 2010, doi: 10.1016/j.tiv.2010.06.016.

[73] “Galaxy Watch6 Smartwatch.” Accessed: Feb. 10, 2024. [Online]. Available: https://www.samsung.com/us/watches/galaxy-watch6/

[74] “Apple Watch Series 9.” Accessed: Feb. 10, 2024. [Online]. Available: https://www.apple.com/apple-watch-series-9/

[75] “Corsano Health.” Accessed: Feb. 10, 2024. [Online]. Available: https://corsano.com/products/bracelet-2/

[76] “Masimo W1.” Accessed: Feb. 10, 2024. [Online]. Available: https://professional.masimo.com/products/monitors/masimo-w1-medical-watch/

[77] “Bora band.” Accessed: Feb. 10, 2024. [Online]. Available: https://doc.bora-connect.com/en/manuals/bora-band-model-bb100/

[78] “Biobeat Medical.” Accessed: Feb. 10, 2024. [Online]. Available: https://www.bio-beat.com/

[79] T. J. Schaffner *et al.*, “Remote patient monitoring to facilitate same-day discharge after laparoscopic sleeve gastrectomy: a pilot evaluation,” *Surgery for Obesity and Related Diseases*, vol. 19, no. 9, pp. 1067–1074, Sep. 2023, doi: 10.1016/j.soard.2023.02.028.

[80] A. V. Kalicki, K. A. Moody, E. Franzosa, P. M. Gliatto, and K. A. Ornstein, “Barriers to telehealth access among homebound older adults,” *J Am Geriatr Soc*, vol. 69, no. 9, pp. 2404–2411, Sep. 2021, doi: 10.1111/jgs.17163.

[81] M. M. Baig, S. Afifi, H. GholamHosseini, and F. Mirza, “A Systematic Review of Wearable Sensors and IoT-Based Monitoring Applications for Older Adults – a Focus on Ageing Population and Independent Living,” *Journal of Medical Systems*, vol. 43, no. 8. Springer New York LLC, Aug. 01, 2019. doi: 10.1007/s10916-019-1365-7.

[82] Z. Sonner *et al.*, “The microfluidics of the eccrine sweat gland, including biomarker partitioning, transport, and biosensing implications,” *Biomicrofluidics*, vol. 9, no. 3, May 2015, doi: 10.1063/1.4921039.

[83] B. Liang *et al.*, “An Integrated Paper-Based Microfluidic Device for Real-Time Sweat Potassium Monitoring,” *IEEE Sens J*, vol. 21, no. 8, pp. 9642–9648, Apr. 2021, doi: 10.1109/JSEN.2020.3009327.

[84] A. Martín *et al.*, “Epidermal Microfluidic Electrochemical Detection System: Enhanced Sweat Sampling and Metabolite Detection,” *ACS Sens*, vol. 2, no. 12, pp. 1860–1868, Dec. 2017, doi: 10.1021/acssensors.7b00729.

[85] J. Kim *et al.*, “A Skin-Interfaced, Miniaturized Microfluidic Analysis and Delivery System for Colorimetric Measurements of Nutrients in Sweat and Supply of Vitamins Through the Skin,” *Advanced Science*, vol. 9, no. 2, Jan. 2022, doi: 10.1002/advs.202103331.

[86] J. Feng *et al.*, “An Energy-Efficient Flexible Multi-Modal Wireless Sweat Sensing System Based on Laser Induced Graphene,” *Sensors*, vol. 23, no. 10, May 2023, doi: 10.3390/s23104818.

[87] Y. Gokdemir and B. T. Karadag, “Sweat Testing and Recent Advances,” *Frontiers in Pediatrics*, vol. 9. Frontiers Media S.A., May 04, 2021. doi: 10.3389/fped.2021.649904.

[88] M. F. Servidoni *et al.*, “Teste do suor e fibrose cística: Panorama da realização do teste em centros públicos e privados do estado de São Paulo,” *Jornal Brasileiro de Pneumologia*, vol. 43, no. 2, pp. 121–128, 2017, doi: 10.1590/S1806-37562016000000076.

[89] G. Ponirakis *et al.*, “The diagnostic accuracy of Neuropad® for assessing large and small fibre diabetic neuropathy,” *Diabetic Medicine*, vol. 31, no. 12, pp. 1673–1680, Dec. 2014, doi: 10.1111/dme.12536.

[90] G. Ponirakis *et al.*, “Automated quantification of neuropad improves its diagnostic ability in patients with diabetic neuropathy,” *J Diabetes Res*, vol. 2015, 2015, doi: 10.1155/2015/847854.

[91] “Gx Sweat Patch.” Accessed: Aug. 08, 2023. [Online]. Available: https://www.epicorebiosystems.com/gx-sweat-patch/

[92] L. B. Baker *et al.*, “Skin-interfaced microfluidic system with personalized sweating rate and sweat chloride analytics for sports science applications,” *Sci Adv*, vol. 6, no. 50, p. eabe3929, 2020, doi: 10.1126/sciadv.abe3929.

[93] “Neuropad.” Accessed: Feb. 24, 2024. [Online]. Available: https://neuropad.co.uk/

[94] “Nanoduct.” Accessed: Feb. 24, 2024. [Online]. Available: https://macroductadvanced.com/nanoduct.html

[95] “What is an Application Programming Interface (API)?” Accessed: Mar. 14, 2024. [Online]. Available: https://www.ibm.com/topics/api

[96] A.-M. Rahmani *et al.*, “Smart e-Health Gateway: Bringing intelligence to Internet-of-Things based ubiquitous healthcare systems,” in *12th Annual IEEE Consumer Communications and Networking Conference (CCNC)*, IEEE, 2015.

2. System Architecture

The previous section introduced the Onalabs' monitoring system alongside the wearable devices developed in this thesis. While a general description of each element has been provided, specific details regarding the system and devices have not been included.

In this chapter, a description of functional and operational capabilities of the whole system is provided. On one hand, functional characteristics encompass the features provided to users whether they are patients, doctors, or healthcare organizations. On the other hand, operational characteristics refer to how these features are delivered, i.e. the technologies involved. Furthermore, the process followed to develop the system and the associated management risk plan are described.

2.1. Functional characteristics

The accuracy and robustness of the system rely on three key components: wearable devices, gateway, and digital platform (see Figure 2.1). First, the wearable device sensors obtain raw physiological data from the user and the health features are extracted from this raw data using an embedded processing algorithm. These features are sent to the gateway which resends this information to the digital platform. Finally, the information is received by the digital platform, which stores every health feature and analyzes this data. After this analysis, the cloud platform delivers medical relevant information, such as recommendations, to the healthcare professionals, caretakers, and patients. All the data is displayed in a web dashboard, or it can be integrated into third-party programs using an Application Programming Interface (API).

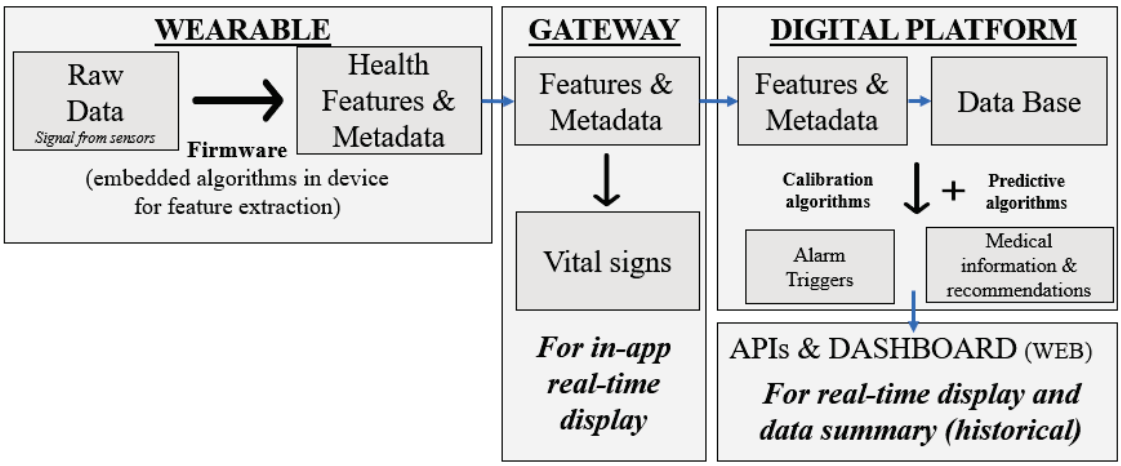

Figure 2.1. Process followed to estimate the user's health features.

One of technological trends is to create networks of interconnected devices and sensors that send the information acquired to the cloud. This is the concept of the well-known Internet-of-Things (IoT) [1], which has been extensively implemented in different areas, such as home automatization. During the past few years, this trend has expanded to the medical world, and it receives the name of Internet-of-Medical-Things (IoMT) [2]. The architecture defined in this work is an IoMT system that has the goal to enhance the healthcare system.

The cloud of an IoMT system is the central module. All the information is stored in the cloud, and it can be accessed anywhere and anytime giving a lot of flexibility to individuals and healthcare providers. The Onalabs platform (see Figure 2.2a) is a complete tool that allows nurses, doctors, and medical institutions to assess the health state of a patient. To perform this task, a modular platform that allows customization of the web dashboard using the API was created. The healthcare providers can display the historical evolution of each physiological parameter of every patient (see Figure 2.2b).

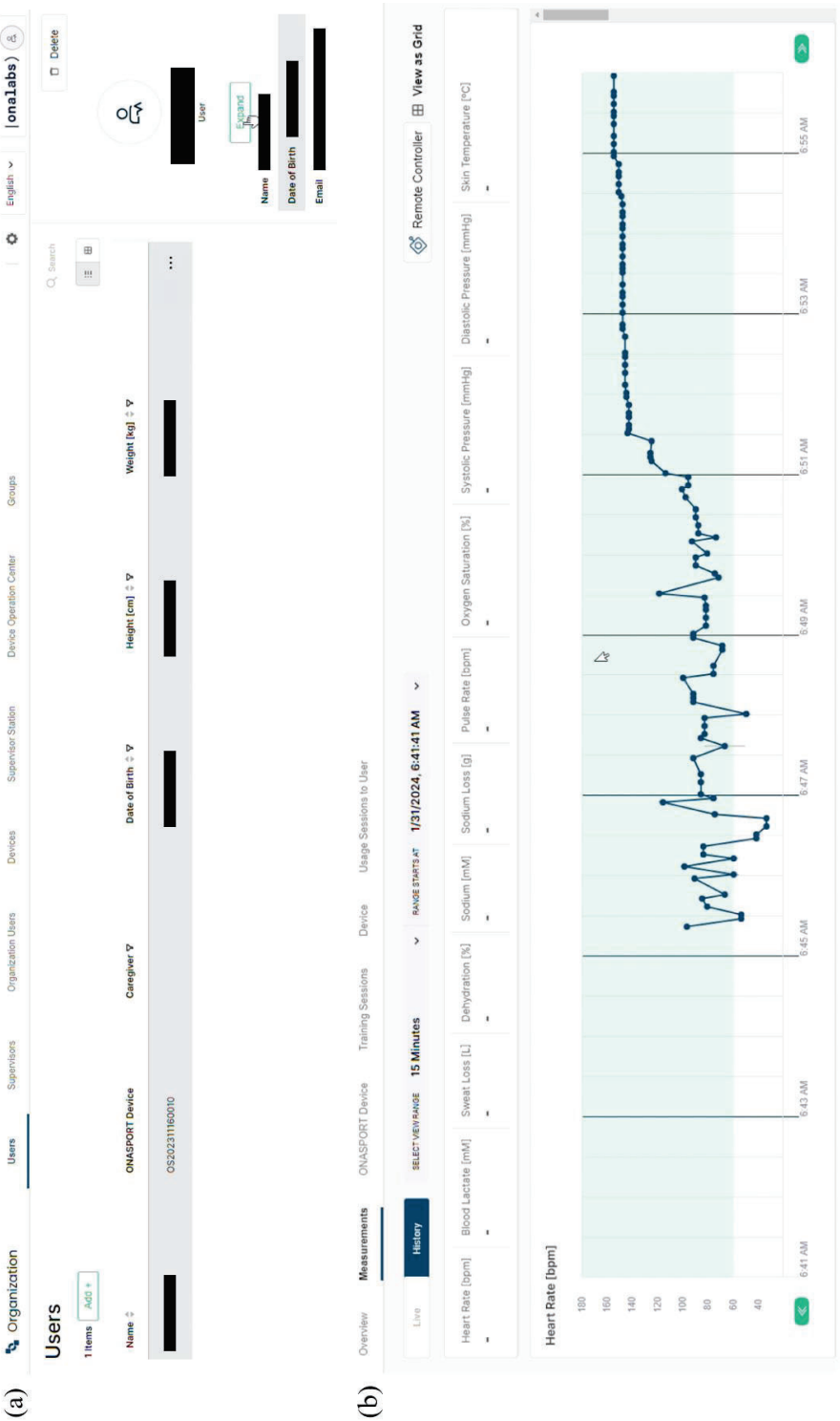

Figure 2.2. Digital platform of the system. (a) Dashboard of the platform, and (b) sample of the historical evolution of a single patient.

IoMT systems gather and store huge amounts of sensitive data that must be protected against attacks or unauthorized access. Cyber security is the practice of protecting digital systems from malicious activities [3]. Multiple cyber security standards must be followed by IoMT platforms, such as the General Data Protection Regulation (GDPR) [4] or the ISO 27001 [5], to protect the users and their information.

Not every digital platform user can display the data of each patient. A hierarchical system has been implemented to secure the information and avoid privacy issues. There are different user's profiles inside the platform that allows to manage the data and avoid uncertain situations:

- **Manufacturer admin:** Main administrator of the digital platform. It manages the system and creates the other profiles. The administrator does not have access to the patients' information. This role is done by Onalabs.
- **Organization admin:** It manages the entities of the system, e.g., caregivers, patients, etc. This role is performed by the healthcare institutions and has access to the patients' information.
- **Caregiver:** A physician or nurse who can observe patients' data remotely. They have access to the data of their patients.
- **Patient:** The individual who uses the device. This user has access to their own data which is the same as caregivers view. Patients have the inherent right to access to their medical records/profile.

There are multiple applications to the IoMT technology developed. This system can be applied to the telemedicine to provide medical attention to the patients at their homes. The remote and continuous monitoring of patients allows to know the state of health of individuals and act accordingly. This system can be also used in hospitals both at care units and hospital emergency departments. Most of the hospitals do not have continuous monitoring equipment and only have this kind of instruments at the Intensive Care Unit (ICUs), so a biometric device that gives physiological information about the patients can be a powerful tool that facilitates the job of the healthcare providers and improves the attention provided.

2.2. Operational characteristics

To provide the mentioned functionalities, multiple technologies are involved. These technologies encompass sensors, electronic instrumentation, and cloud services, among others. This thesis makes emphasis on the development and implementation of wearable devices, so only the related parts to the device are described.

A wearable device can take multiple forms and have diverse functionalities, but normally has the same structure/architecture (see Figure 2.3):

- **Control unit:** The control unit is composed by a microprocessor or a microcontroller (MCU) and their peripherals, such as buttons and/or LEDs. This component runs the system firmware. The firmware is the embedded program inside the MCU that controls every action performed by the wearable device. It also realizes the analysis of the results obtained from the sensors.
- **Sensors and instrumentation module:** This module contains the sensors and the electronic instrumentation used to measure the parameters of interest.

- **Power supply module:** This module extracts energy from a battery or other power source and uses this energy to power all the elements of the wearable device.
- **Communication module:** The communication module sends/receives information to/from the gateway.
- **External memory:** The external memory is an optional module that is used to store the data processed by the control unit.

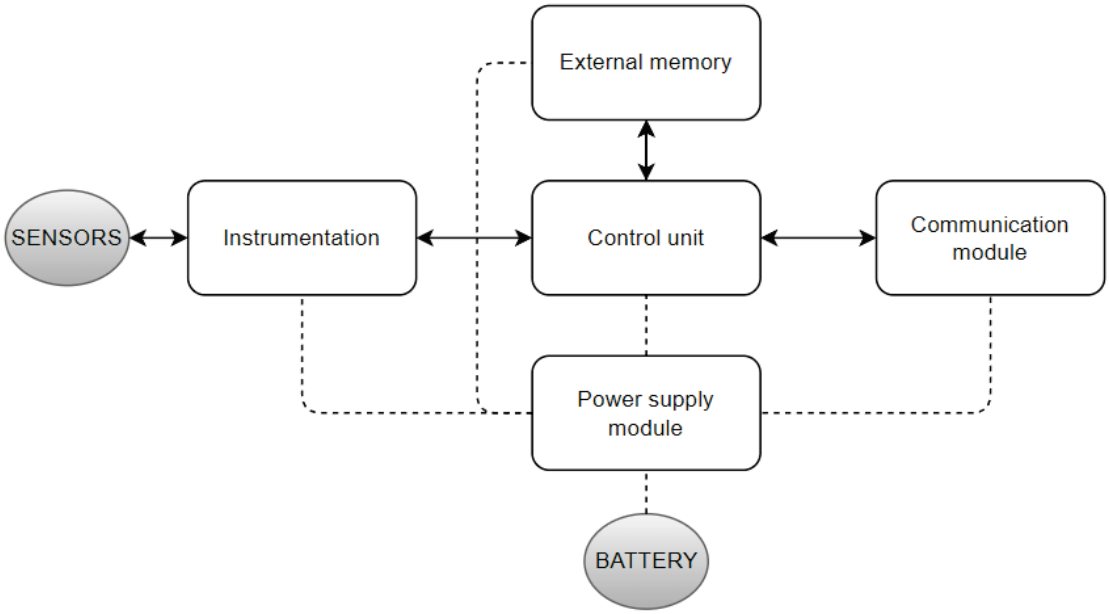

Figure 2.3. General architecture of a wearable device.

Each module, except both the sensors and the batteries, is integrated in a single printed circuit board (PCB). The PCB serves as mechanical support for every component and provides electrical connection between them.

2.2.1. Control unit

The control unit is formed by a microprocessor or MCU, and their peripherals. This unit is the brain of the system, since it manages all the operations performed by the system and analyzes the generated information.

Normally, a MCU is the central component of a control unit. This component performs specific tasks and is commonly used in dedicated systems rather than general-purpose computing. The key elements of a MCU include:

- **Central Processing Unit (CPU):** It is the core of this integrated circuit (IC) which executes the firmware instructions and performs every necessary calculation.
- **Memory:** A MCU normally has program memory to store the firmware and intermediate results.
- **Peripherals:** MCUs have pins that allow it to interface with its environment. These connections can include digital and analog input/output pins, communication ports, timers, counters, and other specialized peripherals.
- **Clock circuit:** MCUs require a clock signal to synchronize their operations. The clock circuit provides the timing reference for the IC.

MCUs are chosen for their compact size, low power consumption, and the ability to provide a cost-effective solution. Common microcontroller families include PIC, AVR, ARM, among others.

2.2.2. Sensors and their electronic instrumentation

To quantify a magnitude, a sensor is used. A sensor is a device that measures the parameters of interest from the environment and gives a response proportional this magnitude. The sensor's input can be practically anything, such as light, heat, or electricity, and it usually has as output an electrical signal. This signal is processed by an electronic instrumentation and the response of this instrumentation is recorded by an MCU [6], [7].

Sensors and their related instrumentation are one of the main points of this thesis. Here, an introduction about these elements is provided and the information is extended in each chapter along with the obtained results.

There are multiple ways to classify sensors. The two most common classifications include:

- **Based on the measured magnitude:** One of the most common ways to cluster sensors is by the magnitude to quantify. For instance, there are optical sensors that measure the light and chemical sensors which quantify a chemical reaction.
- **Based on the sensor technology:** Another method to classify sensors is by the sensing technology utilized. For example, a resistive sensor uses changes in electrical resistance to measure a variable and a piezoelectric sensor converts changes in pressure or force into an electrical signal.

Depending on the application, one type of sensor or other is used. To ensure that fits the requirement of the project involved it is important to review the main characteristics of the sensor [8]:

- **Dynamic range:** Ratio between the minimum and maximum value that the sensor can measure.
- **Accuracy:** Similarity (correlation) between the measured and the true (reference) values.
- **Precision:** Capacity of a sensor to give the same reading when repetitively measuring the same quantity under the same prescribed conditions.
- **Linearity:** Maximum deviation between the measured values of a sensor from ideal calibration curve.
- **Noise:** Random fluctuation of the output's sensor independent of the input parameter.
- **Reproducibility:** Ability of a sensor to produce the same output when the same input is applied.
- **Repeatability:** Ability of a sensor to produce the same output when the same input is applied, and all the physical and measurement conditions kept the same.
- **Response time:** Time at which the output of the sensor reaches a certain percentage of its final value.

An electronic instrumentation is required to acquire the response of every sensor. The instrumentation (front-end) adapts the sensor output to the levels of the Analog to Digital Converter (ADC) of a MCU (back-end), which acquires this signal. It is crucial to design and develop the instrumentation according to the sensor used, due to the system performance relies on all the system elements. Nowadays, there are countless ICs that integrate in a single package both the sensors and the electronic instrumentation. These chips allow to speed up development, so developers mainly focus on the overall system.

Either a sensor along with a custom electronic instrumentation or simply an IC is used, the sensor response must be processed by an MCU. An MCU performs diverse mathematical operations to extract relevant information from the acquired signals. This set of instructions is known as an algorithm. An algorithm generally has several well-defined steps. The first step is the pre-processing of the signal which consists in reducing the noise from the signal by means of several filters. Then, the relevant features are extracted from this signal. Eventually, the analysis of these features is carried out [9]. This process is described in more detail in the third chapter, where the algorithms related to the vital signs monitoring device are presented.

To estimate the vital signs of a patient and analyze his sweat content, it is necessary to use different types of sensors. These sensors have diverse characteristics and modes of function.

2.2.2.1. *V*ital signs monitoring sensors

There are multitude sensing technologies that can be used to monitor a patient's vital signs. Only the most common techniques are described here.

A. Pulse oximetry

Pulse oximetry (PPG) is a technique that allows caregivers to assess both the pulse rate (PR) and peripheral oxygen saturation (SpO_2) in a simple and non-invasive manner. It is regularly used in hospitals and ambulatories for patient screening, and it has been demonstrated to be very helpful in emergency scenarios, such as the recent COVID-19 pandemic [10].

Oxygen is transported from the lungs to the body tissues by means of hemoglobin. The hemoglobin that carries oxygen is called oxyhemoglobin (O_2Hb), and the one that does not is named reduced hemoglobin (HHb). O_2Hb and HHb have different light absorption properties (see Figure 2.4a). O_2Hb absorbs greater amounts of infrared (IR) light and lower amounts of red light than does reduced hemoglobin. On the other hand, HHb absorbs more red light. This difference is used to estimate the percentage of O_2Hb respect to the total amount of hemoglobin in blood and hence to determine the SpO_2 value [11].

The PPG signal (see Figure 2.4b) reflects the changes of blood volume at the capillaries and hence reflects the cardiac cycle. During the systole, the blood volume increases, and it decreases at the diastole. This difference can be observed in the PPG signal since there is a constant baseline at the diastole and at the systole appears a pulsatile component corresponding to each heartbeat. Measuring the time elapsed between the heartbeats, the PR can be calculated.

Another application of this technology consists of assessing the cardiovascular state of a patient by means of the PPG signals. The PPG signal reflects the state of the circulatory system since the fluctuations of the blood vessels are acquired. Studying the shape of these signals, several conditions can be assessed. For instance, the stiffness of blood vessels can be determined by the PPG signals form [12].

Although pulse oximetry is very useful, it has several drawbacks that limit its use. On one hand, there are multiple health conditions that cause poor perfusion, making impossible to the system to estimate the PR and SpO_2 [13]. On the other hand, several artifacts appear on the PPG signals due to the movement, hindering the calculation of any parameter [14].

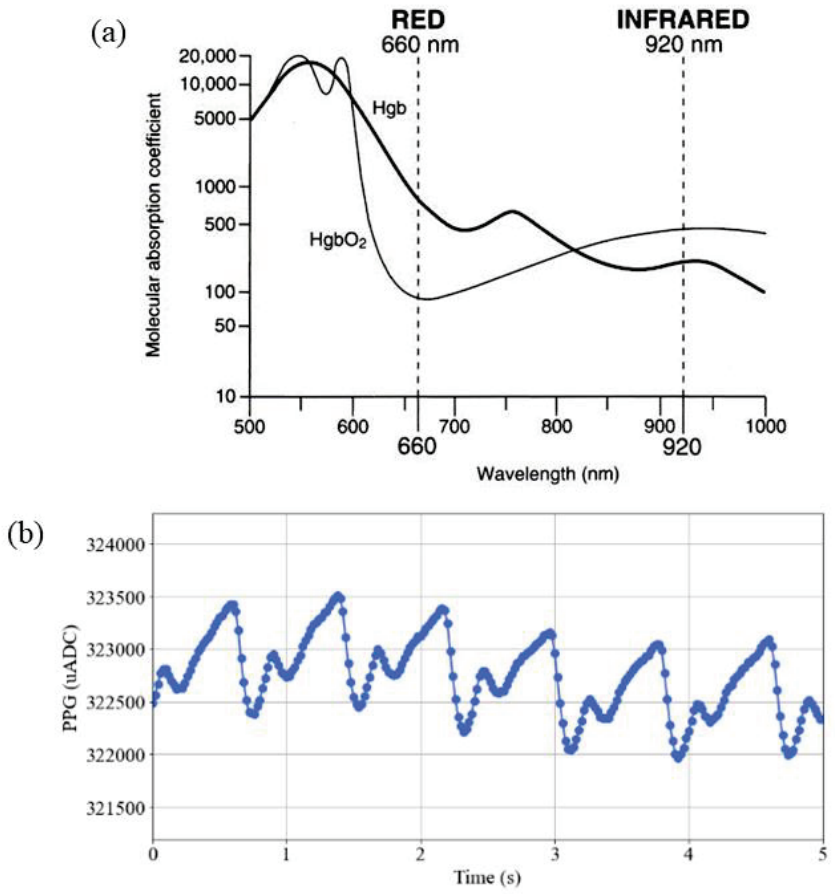

Figure 2.4. Basic concepts about pulse oximetry. (a) Absorption spectra of the hemoglobin. Courtesy of Dildy (1996) [15], used with permission. (b) Sample of a PPG waveform.

The pulse oximeter operation is very simple: it emits light directly to the skin and measures the light that is not absorbed. LEDs are used to emit the light and photodiodes (PD) are utilized to capture the response. There are two configurations of pulse oximeters depending on the position of the transmitter and the receiver [16]:

- **Transmissive PPG:** The light source is placed on one side of the body, and a PD is placed on the opposite side (see Figure 2.5a). The light from the source passes through the tissue and the PD detects the transmitted light. This is the technique used when the measurement side is an extremity of the body, such as a finger or an earlobe.

- **Reflective PPG:** Both the light source and the PD are placed on the same side of the body part (see Figure 2.5b). The light is emitted into the tissue and then reflected to the PD. This is the method utilized when the measurement position is not an extremity of the body, such as the wrist.

The PPG instrumentation operates the LEDs and captures the PD response. To do that, the common approach is developing a circuit that biases the light emitter and measures the current produced by the PD. This approach is used less and less because a lot of commercial chips with these capabilities have appeared on the market. Chips like that integrate in the same package all the elements required to perform the measurement and transmit the data directly to a MCU using a digital interphase.

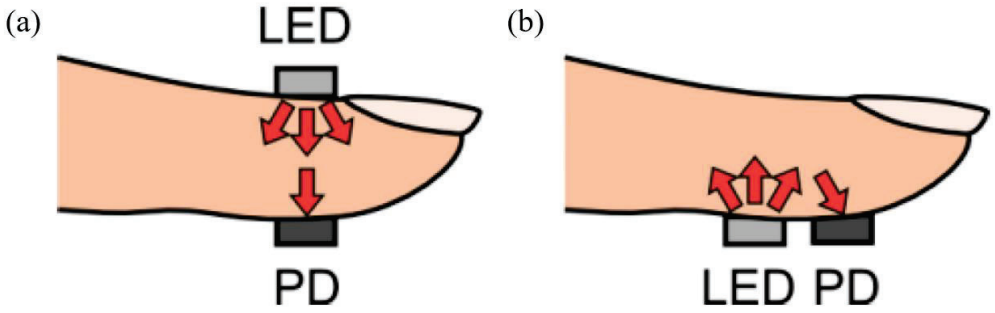

Figure 2.5. Configurations of PPG. (a) Transmissive and (b) reflective PPG. Courtesy of Tamura (2014) [16], used with permission.

B. Electrocardiography

Electrocardiography is the gold standard technique in cardiology. It consists of recording the heart's electrical activity over a certain period of time, which gives as a result an electrocardiogram (ECG) [17]. An ECG is the plot of the electrical activity of this organ, and it is interpreted by cardiologists that assess the heart state. Every wave of the ECG reflects a function of this muscle (see Figure 2.6a):

- **P Wave:** Represents the depolarization of the atria (the upper chambers of the heart).
- **QRS Complex:** Represents the depolarization of the ventricles (the lower chambers of the heart).
- **T Wave:** Represents the repolarization of the ventricles.

The heart's electrical activity is produced by action potentials. An action potential is a brief change in the voltage across cell membranes. The cardiac action potentials are originated in specialized cells at the right atrium which they are called the sinoatrial node, the natural pacemaker of the heart. This voltage passes along the cells of this organ causing the contraction of the heart. To record this process to obtain an ECG, a set of electrodes are used. There are different types of electrodes and using one or other only depends on the application. For instance, single-use pre-gelled electrodes are regularly utilized to obtain medical grade ECGs. These electrodes are adhered on the patient's skin and the conductive gel allows to record a clear and accurate ECG since the resistance between the skin and the electrode is reduced by this gel. The reduced resistance improves the electrical signal transmission [18].

The minimum number of electrodes required to record an ECG is two. However, an ECG recorded by two electrodes is poor and only allows to identify the QRS complex. A great number of electrodes must be used to obtain a medical grade ECG. Normally 10 electrodes are utilized for this purpose and the difference of potential between each electrode is recorded. This system is named 12 derivation ECG, since 12 electrical signals from various perspectives around the heart are recorded to create a comprehensive view of this organ electrical activity (see Figure 2.6b) [19].

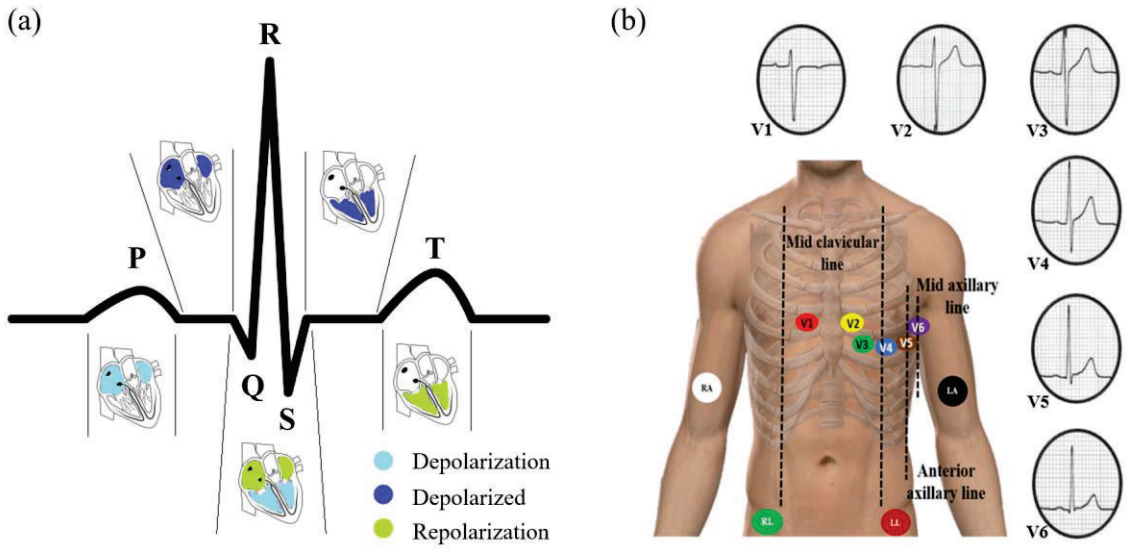

Figure 2.6. Basic concepts about electrocardiography. (a) Origin of every wave of an ECG. Adapted with permission from Pereira (2022) [20]. (b) Derivations of a complete ECG. Courtesy of Romero (2023) [21], used with permission.

An electronic instrumentation is essential to record an ECG. This circuit captures the potential difference between the electrodes using an instrumentation amplifier. Following this amplifier, an amplification stage adapts the signal amplitude, and several filters reduce the noise from this signal [22]. An ECG instrumentation can be implemented using analog components, but nowadays, there are several analog front-ends available on the market that integrate in a single package all the necessary elements to perform an ECG (see Figure 2.7).

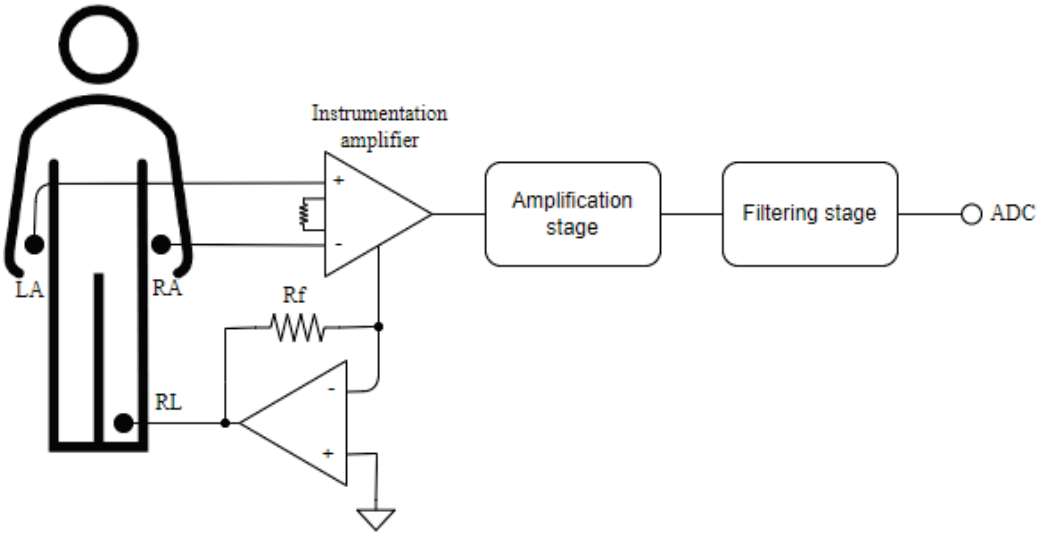

Figure 2.7. Basic configuration of an ECG instrumentation.

C. Temperature estimation

There are two types of thermometers (sensor that measures the temperature): contact and non-contact sensors. Contact sensors measure the temperature by coming into direct contact with the object of interest and non-contact sensors do not require this interaction [23].

On one hand, the most common contact thermometer are the following ones:

- **Thermocouples:** A thermocouple consists of two dissimilar metals that generate a voltage proportional to the temperature difference between the two ends.
- **Thermistors:** A thermistor is a resistor whose electrical resistance changes with temperature.

On the other hand, the most popular non-contact temperature sensors are the infrared sensors. These sensors detect the infrared radiation emitted by the eardrum and convert it into a temperature reading.

The utilization of one type of sensor or another depends on the system requirements. For instance, the oral and rectal thermometers are thermocouples or thermistors, meanwhile tympanic thermometers are infrared sensors. In general, contact sensors are cheaper because they are composed by materials whose electrical properties change in function of temperature, whereas non-contact sensors rely on an optical system composed by lenses, light sources, and detectors that are very expensive.

As every sensor, an instrumentation that acquires its response is required. In the case of contact sensors, the front-end is an analog circuit, such as a Wheatstone bridge or a circuit composed of several operational amplifiers (OPAMPs). Meanwhile, most non-contact thermometers are sold in an IC with a digital interphase to extract the data.

D. Other relevant parameters

Other relevant parameters apart from the vital signs can be recorded and used to assess the status of an individual. Normally, these parameters are complementary to vital signs monitoring and provide information about non-critical functions of the body. For instance, a parameter of great interest for healthcare providers is the number of steps that a patient does during a day [24]. This parameter indicates the patient lifestyle, which is relevant to monitor diseases related with sedentary habits, such as diabetes. Another parameter of interest is the gait of a patient. Multiple biomechanical studies have demonstrated that the analysis of gait can reveal the presence of certain diseases, such as Alzheimer or Parkinson disease [25].

These parameters are related to body movement. The movement of the body can be monitored using accelerometers, gyroscopes, and magnetometers. All these elements are sensors that provide information about the position of a body in the space:

- **Accelerometer:** This sensor measures linear acceleration along the 3-dimensional axes. It is used to determine the direction and intensity of the acceleration forces acting on an object or person.

- **Gyroscopes:** The gyroscope measures angular velocity or the rate of rotation around the same axes. It helps to track the object's orientation and angular movement.
- **Magnetometer:** A magnetometer measures the strength and direction of the magnetic field around the sensor. It is used to determine the object's orientation relative to the Earth's magnetic field.

The combination of these sensors in the same package receives the name of Inertial Measurement Unit (IMU). By combining the data from these sensors, an IMU can provide information about an object's position, velocity, and orientation in real-time.

Aside from estimating relevant parameters, these elements can be utilized to complement the information provided by other sensors. For instance, a PPG has a lot of artifacts caused by the user movement, so an accelerometer can help to discriminate when a section of a signal presents motion artifacts or not [26].

The electronic instrumentation of an IMU is minimal due to most of these sensors are commercial chips with a digital interphase to extract the data. So, to use an IMU, only it is necessary this component and a MCU to acquire the recorded information.

2.2.2.2. Sweat biomarkers estimation sensors

Biosensors are used to analyze the sweat content. A biosensor is a type of sensor that converts a biological response to a quantifiable and processable signal [27]. Chemical sensors are a subfamily of biosensors utilized in multiple industries. This kind of sensors use molecules named bioreceptors to recognize the analyte (chemical component under test) specifically. Bioreceptors are immobilized on a transducer element and produce a chemical reaction when interacts with the analyte. This reaction is converted to a measurable signal by a transducer [28].

Electrochemical sensors are the largest group of biosensors. These sensors convert the biological recognition event into an electrical signal proportional to the analyte concentration. An electrochemical sensor is formed by a bioreceptor and an electrode that acts as a transducer. The bioreceptor is immobilized on the electrode and when the chemical reaction takes place, an electric signal can be recorded on the transducer [29].

An electrochemical cell is formed not only by a single electrode. This cell normally has three electrodes: a working electrode (WE), that it is the surface where the electrochemical reaction takes place; a counter or auxiliary electrode (CE), which tracks the potential solution; and a reference electrode (RE), which supplies the current required for the electrochemical reaction at WE. Depending on the technique utilized and the application, the materials and the operation mode of these electrodes vary [30].

Electrochemical sensors have several advantages in front of other detection techniques like high speed, high specificity, easy mineralization, or low cost of manufacturing, among others. There are three main families of electrochemical sensors depending on the operating principle:

- **Amperometric:** Measure the current resulting from oxidation or reduction (redox) of an electroactive species. A great number of electrochemical sensors developed nowadays are amperometric sensors. The most famous amperometric

sensor is the glucose sensor, which it is used to quantify the sugar level in diabetic patients' blood.

- **Conductimetric**: Measure the medium conductivity. A subset of this family is impedimetric sensors which estimate the impedance of the system under study. An application of this technique that has gained a lot of interest in the past few years is the quantification of bacteria in water.
- **Potentiometric:** Measure the potential when zero or no significant current flows between the electrodes. They are usually utilized to quantify the concentration of ions. One of the most popular sensors of this kind is pH sensor, which are extensively utilized at chemical laboratories.

There are multiple electrochemical techniques, but the most popular are cyclic voltammetry (CV), chronoamperometry (CA), and electrochemical impedance spectroscopy (EIS) [31]:

- **Cyclic voltammetry:** A variable potential is applied to the electrochemical cell while the current that provides this electrochemical cell is measured (see Figure 2.8a). The voltage varies until it reaches an established potential value, then it changes direction (triangular waveform). This process is repeated an established number of cycles depending on the sensor. The result is plotted in a cyclic voltammogram, which represents the current through the WE against the voltage applied to the electrochemical cell. This technique gives a lot of information about the chemical and physical behavior of a system by simply observing the shape of the cyclic voltammogram.
- **Chronoamperometry:** This technique consists of the application of a constant potential at the WE and the current produced is measured as a function of time (see Figure 2.8b). The current varies according to the diffusion of an analyte from the bulk solution to the sensor surface. Chronoamperometry measures the dependence between the current and time of a diffusion-controlled process that changes with the analyte concentration.
- **Electrochemical Impedance Spectroscopy:** Resistance is a measure of the ability of a system to resist the flow of electrical current and it is defined by the Ohm's law (see Equation 2.1):

$$R = \frac{V}{I} \tag{2.1}$$

where R is the resistance, V is the voltage, and I is the current.

This well-known relationship is limited to the ideal resistor. In the real-world other phenomena, such as capacity or inductance, must be considered, so the concept of resistance is extended to impedance. Impedance is frequency-dependent, so it is necessary to apply an AC potential to the electrochemical cell and then measure the current through the cell. In EIS multiple signals at different frequencies are applied and the response is captured. There are different ways to represent the impedance, but the most common way to do it is by means a Nyquist plot (see Figure 2.8c). The study of this plot provides a large amount of information about the system composition.

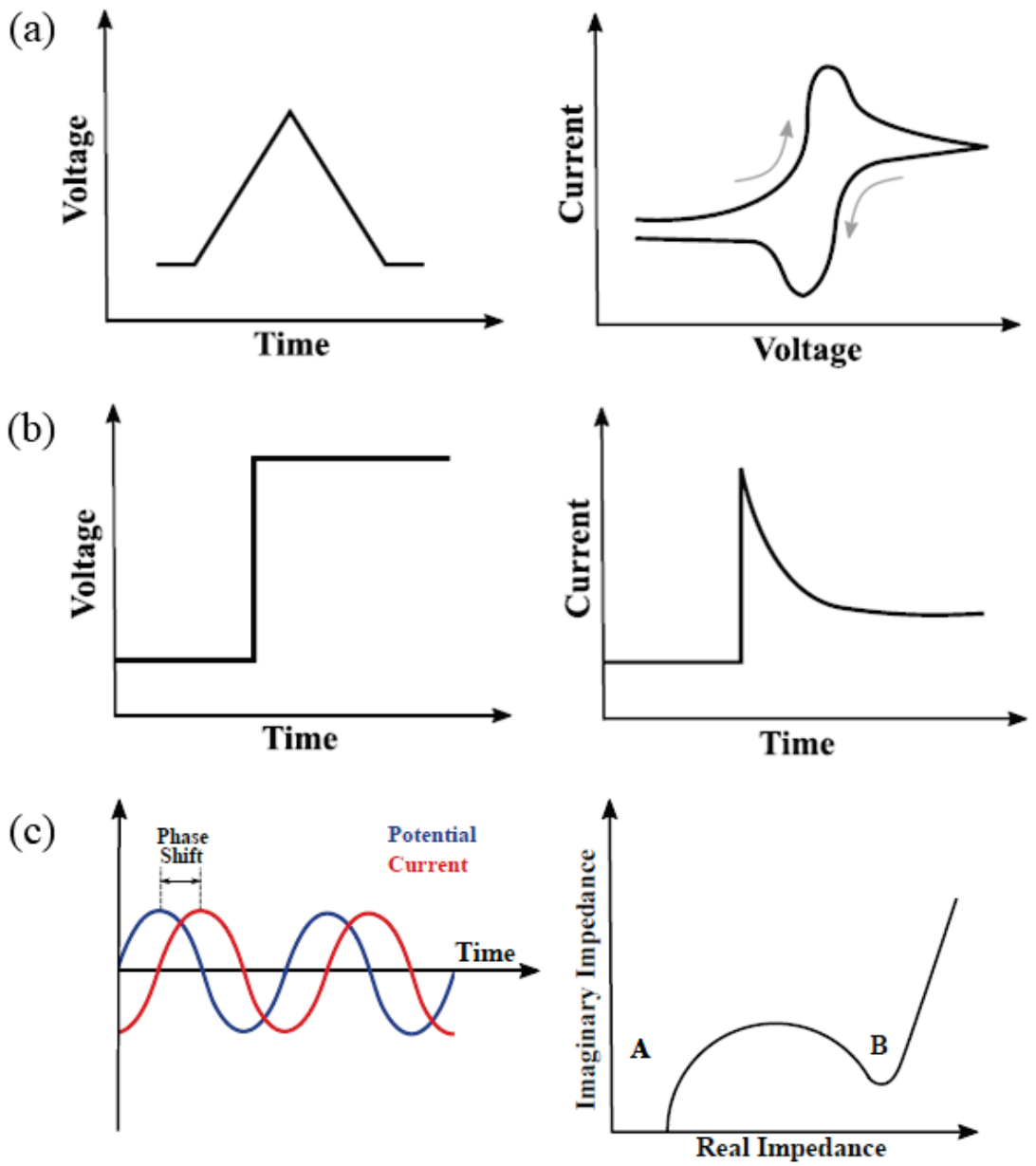

Figure 2.8. Electrochemical techniques. (a) Cyclic voltammetry input and output waveforms, (b) chronoamperometry input and output waveforms, and (c) electrochemical impedance spectroscopy (an oscillating perturbation produces an oscillating current response which is typically represented using a Nyquist plot). Courtesy of Montes Cebrián [31], used with permission.

A lot of biological samples are liquids, such as blood or saliva, that are difficult to handle. These samples normally require a pre-treatment before an electrochemical sensor quantifies their content. To perform this treatment in a controlled and automatic way, microfluidic systems are used. A microfluidic device is a miniaturized system designed to manipulate and control small volumes of fluid (nanoliter to microliter scale). These systems simplify the measurement process and allow a continuous monitorization of the analyte.

An electronic instrumentation is necessary to acquire a biosensor response. The potentiostat is the instrumentation of most electrochemical sensors. A potentiostat is a circuit that biases the cell under study and captures its response. Depending on the technique utilized, its mode of operation changes. In the case of an amperometric sensor,

the potentiostat fixes a constant potential between the RE and the WE injects current to the CE to balance the system. This instrumentation also captures the current produced on the WE when the chemical reaction is produced [32].

Despite many electrochemical sensors have been developed during the last decades, only a few are regularly used outside laboratories [33]. The glucose sensor is the most well-known sensor, but other ones such as amperometric lactate sensors can be found on the market. The lack of electrochemical sensors in the market is due to the difficulty to maintain the reproducibility and stability of the sensor in complex real environments, the inability to identify suitable niche applications, the elevated cost of production, and the problems related to the industrialization of the product.

2.2.3. Power supply module

A system requires a power source to operate. In the case of a wearable device, this power source is typically a battery. A battery is an electrochemical cell that stores electrical energy in the form of chemical energy and releases this energy as electrical power by means of a redox reaction when it is connected to a circuit. There are multiple types of batteries and the selection of one or another depends on the characteristics and needs of the system (see Table 2.1) [34]. Batteries can be classified by different criteria:

- **Type of chemistry:** This classification refers to the chemical materials used to generate energy. It is important to know the chemistry of a power source since the characteristics of the battery differ depending on the materials utilized to manufacture it. Some of the most popular batteries are the lithium-ion batteries (Li-ion), nickel-metal hydride batteries (MiMH), and nickel-cadmium batteries (NiCd), among others.
- **Rechargeability:** A battery can be rechargeable or not. Rechargeable batteries (primary cells) have the capability of being charged and used multiple times, while non-rechargeable batteries (secondary cells) are used once lifecycle and then discharged.
- **Energy density:** The energy density is the amount of energy that can store a battery relative to its size and weight. High-energy density batteries, like lithium batteries, are smaller and lighter compared to the quantity of energy that they can provide. It is normally expressed in watts-hour per kilogram (Wh/Kg).

Before selecting a battery, it is crucial to study the characteristics of this cell [35]:

- **Nominal voltage:** It is the average voltage between the battery terminals when it is fully charged. Batteries have different voltage ratings, with common nominal values such as 1.5 V (alkaline AA batteries) and 3.7 V (lithium-ion batteries).
- **Capacity:** The capacity is the amount of electrical charge that a battery can store, and it indicates how long a battery can supply current before becoming depleted. Higher capacity batteries can provide power for longer durations. It is normally expressed in ampere-hours (Ah) or milliampere-hours (mAh).
- **Peak current:** Maximum current that a battery can deliver. It is directly dependent on the internal equivalent series resistance of the power source.
- **Self-discharge rate:** All batteries gradually lose their stored energy over time, even when they are not used. This parameter refers to how quickly a battery loses

its charge when idle. Low self-discharge batteries retain their energy for longer periods of time.

- **Cycle life:** For rechargeable batteries, cycle life is the number of charge and discharge cycles that a battery can endure before its capacity significantly degrades. A longer cycle life is desirable for rechargeable batteries.
- **Temperature dependence:** Temperature is an important parameter for the batteries because they have a high dependency with this parameter. Extreme temperatures can affect a battery's capacity and overall performance.

The most common power sources for wearable devices are coin cells, alkaline batteries, and lithium-ion/lithium polymer batteries. On one hand, coin cells and alkaline batteries are regularly used in multiple devices, but only on low-power systems that do not require frequent charge. These electrochemical cells are cheap and available in any store. On the other hand, the lithium-ion/lithium polymer batteries are extensively utilized in portable systems that must be charged periodically. They are rechargeable and the energy density is very high compared to its weight. Their main drawbacks are the elevated production cost and its flammability.

Battery	Energy density	Price	Rechargeable
Lithium-ion	High (250 Wh/kg)	High (15 to 30 €/Wh)	Yes
Alkaline	Medium (100 Wh/kg)	Low (0.5 to 2 €/battery)	No
Lead-acid	High (30-40 Wh/kg)	Low (10 to 20 €/Wh)	Yes

Table 2.1. Popular batteries and their characteristics.

Despite the market is full of batteries, this technology must improve to satisfy the increasing demand of new wearable devices. On one hand, the current batteries have a limited capacity which does not allow to use a system for more than a few hours or days. Since the volume and weight of wearable devices is limited, batteries with higher energy densities are required. On the other hand, some batteries, such as lithium batteries, must be handled in a proper way because they are very fragile, and explosions can occur. The battery-explosion accidents are originated from the thermal runaway caused by mechanical abuse (crash, penetration, etc.), electrochemical abuse (short circuit, over-charge/discharge, etc.) and thermal abuse (overheat, thermal shock, fire, etc.). A new generation of batteries that are safer than the current ones are necessary to ensure the users safety [36].

Battery technology is in continuous development and new technologies appears every year. These new solutions are led using novel materials and configurations, but despite the progress made, there are no batteries capable to solve the aforementioned problems.

An alternative to the conventional systems is the energy harvesting. Energy harvesting represents the energy derived from the ambient sources and directly converted into electrical energy [37]. This approach prevents the utilization of batteries and avoids unwanted situations, such as the amount of waste generated by the discarded batteries. Despite this field has evolved a lot, more investigation is required and, nowadays, a wearable device cannot rely on this power source to operate.

Regardless of the power source used to supply wearable devices, the energy must be adapted to power the system. Power management circuitry is used to efficient distribution and regulation of power through the device. There are multiple power management ICs, such as Linear-Dropout Regulators (LDOs) or BOOST and BUCK converters. These circuits perform the following tasks:

- **Voltage regulation:** Every circuit requires stable voltage to operate correctly. This tension is within a fixed range, and the voltage must be adapted from the power source to supply the system. Specialized ICs regulate the tension for the correct operation of the device.
- **Current regulation:** Circuits not only require tension, but also current. This magnitude is not fixed and varies depending on the action performed by the multiple ICs involved. Power management circuits must provide the amount of current required at every moment.
- **Power monitoring:** Another feature related to these circuits is measuring the amount of energy remaining inside the battery. This function is not essential for the operation of the device, but it is highly recommended for correct power source management.
- **Battery management:** There are specialized ICs used to charge the battery and assess its state. These circuits help to correctly manage the power source and avoid unwanted situations, such as overheating or aging.

Correctly dimensioning of the required power source and designing an efficient power management system is essential to optimize the wearable device autonomy. Each circuit consumes different amounts of current which are provided by both mentioned elements (power source and power management circuity). More functionalities mean more circuits, and therefore more current consumption, which reduces the system autonomy. There is a tradeoff between the functions performed by the equipment and the consumption. The autonomy of a wearable device is given by the following expression (see Equation 2.2):

$$Autonomy\ (hours) = \frac{Capacity\ (Ah)}{Current\ consumption\ (A)} \tag{2.2}$$

For instance, if the rated capacity of a battery is 100 mAh and the system consumes an average of 100 mA, the autonomy of this device is one hour.

2.2.4. Wireless communication module

The data collected by a biometric device must be transmitted to a gateway. To do that, a wireless communication module is used. A wireless communication system is a technology that allows the transmission and reception of information without the need of a physical connection [38].

The main characteristics of a wireless communication system are the following ones:

- **Range:** Refers to the maximum distance over which the system can transmit and receive data effectively. It is measured in meters or kilometers.
- **Communication rate:** Indicates the amount of data that can be transmitted per unit of time. It is expressed in bits per second (bps) or its multiples, such as kilobits per second (Kbps) or megabits per second (Mbps).

- **Frequency band:** Wireless communication systems operate within specific frequency bands. Different frequency bands have different propagation characteristics.
- **Bandwidth:** Range of frequencies within the frequency band that the wireless communication module can use for transmission.
- **Latency:** Delay between the moment of sending and receiving data. Low latency is critical for real-time applications.
- **Power consumption:** It refers to the amount of electrical power that the system requires to operate. Low power consumption is essential for devices that run on batteries.

There are dozens of wireless communication protocols (see Table 2.2), but some of the most popular are the following ones [39]:

- **Bluetooth and Bluetooth Low-Energy (BLE):** Bluetooth is a short-range, high data rate, and low-power wireless technology that operates in the 2.4 GHz industrial, scientific, and medical (ISM) band. The low-power version of this protocol is BLE, which provides considerably reduced power consumption and cost while maintaining a comparable range. Bluetooth is one of the most popular communication systems and it can be found on any portable device.
- **Near Field Communication (NFC):** NFC is a short-range, low data range, and ultra-low-power communication system. It operates at 13.56 MHz, and it is designed for exchange of data between two devices that are brought into close proximity, typically a few centimeters. This characteristic makes it suitable for secure transactions, such as payments.
- **WiFi:** WiFi is a medium-range, high data rate, and high-power wireless communication protocol. It operates at 2.4 or 5 GHz and WiFi is normally used to establish a wireless connection between devices and a router.
- **LoRa:** LoRa is a long-range, low data rate, and low-power wireless communication protocol. It uses license-free sub gigahertz bands like 433, 915, and 923 MHz. LoRa is a type of network that serves the needs of applications requiring long-distance communications, but also with limited power budget.
- **Cellular networks (3/4/5G)**: Cellular networks are long-range, high data rate, and high-power communication systems. Depending on the technology, the frequency band changes, and velocity of the transmission varies. This type of protocols are mainly used by smartphones that exchange information at high speed.

The election of a communication system or another depends mainly on the intended use of the device. For instance, a medical wearable device powered by a battery requires a communication system that enlarges the life of this battery, so a module of low power consumption, such as BLE or NFC, are normally used.

Protocol	Range	Data rate	Power consumption
Bluetooth and BLE	Short (up to 10 meters)	High (up to 2 Mbps)	Low (few milliwatts)
NFC	Short (up to 10 cm)	Low (424 Kbps)	Low (few milliwatts)
WiFi	Medium (up to 35 meters)	High (several Gbps)	High (hundred milliwatts)
LoRa	Long (several kilometers)	Low (tens of Kbps)	Low (few milliwatts)
Cellular networks	Medium (hundred meters)	High (several Gbps)	High (hundred milliwatts)

Table 2.2. Popular wireless communication protocols.

2.3. Development procedure

The international standard ISO 13485 establishes the procedure to develop a medical device. This procedure ensures that medical devices comply with the regulatory standards for safety and effectiveness. To create the wearable devices described in this thesis, this development procedure was followed.

Based on the ISO 13485 standard, the development procedure can be divided into the following steps (see Figure 2.9):

- **Early Design:** The first step consists of creating an initial concept of the system based on the user needs and market requirements. Preliminary designs and feasibility studies are conducted in this phase.
- **Planning:** After the early design phase, a plan outlining tasks, milestones, resources, and timelines for the development process is created. Regulatory requirements, risk management strategies, and quality assurance measures are also established during this stage.
- **Development:** Once the planning is ready, the actual design and engineering of the medical device take place. Prototypes are built, refined, and tested iteratively to ensure functionality, safety, and reliability.
- **Implementation:** Upon the validation of the design, manufacturing process is established to mass-production of the device. Quality control procedures are also implemented to maintain consistency and adherence to specifications during production.
- **Test and Validation:** Rigorous testing and validation are conducted to verify the performance, safety, and efficacy of the system. Results are analyzed, and necessary adjustments are made based on the observations.
- **Certify and Release:** Eventually, the information related to tests and validation is gathered and submitted to the notified body for approval. Regulatory organisms review the documentation to ensure compliance with applicable standards and regulations. Once regulatory clearance or approval is obtained, the medical device is certified for commercial release.

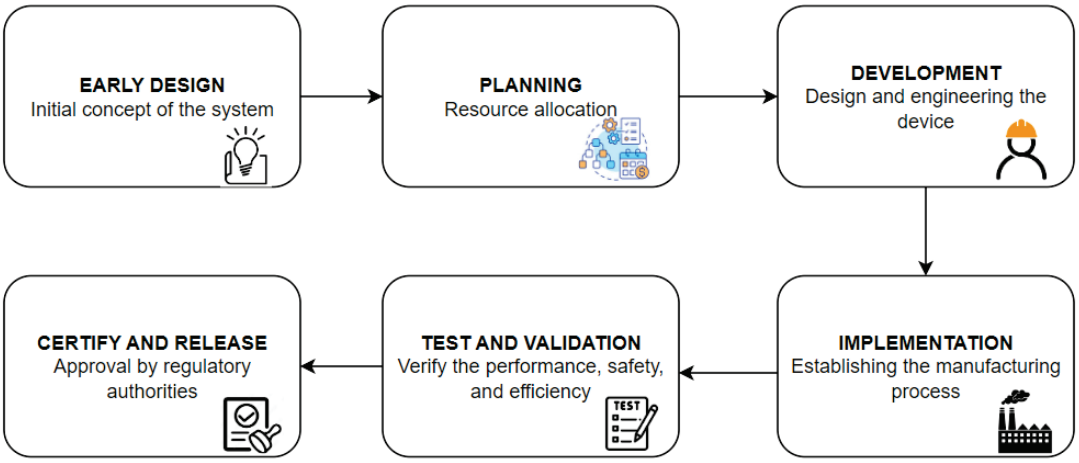

Figure 2.9. Development procedure of a medical device.

2.4. Risk management plan

Apart from the development procedure described in the previous section, a risk management plan is required to design, implement, and validate a medical device. This plan is a document which describes the process for identifying, assessing, and mitigating potential risks associated with the design, development, manufacture, and use of the device. It includes risk assessment methodologies, mitigation strategies, and monitoring measures to ensure the system's safety and effectiveness throughout its lifecycle. To develop the wearable devices described in this thesis, risk management plans for both products were implemented.

The risk management plan is based on risk levels, so the first step is defining the risk tolerance levels for every part of the development procedure. Five different levels can be set based on the norm ISO 14971 [40]:

- **Critical:** The system provokes an injury to the user.
- **Major:** A long-term malfunction of the device occurs.
- **Serious:** A short-term malfunction of the system occurs.
- **Minor:** Slight user inconvenience occurs.
- **Negligible:** Any or negligible risk to the user or the device.

Depending on the probability occurrence, the risk is classified as acceptable or unacceptable (see Table 2.3).

	Negligible	Minor	Serious	Major	Critical
Frequent (1 in 100)	UNACCEPTABLE	UNACCEPTABLE	UNACCEPTABLE	UNACCEPTABLE	UNACCEPTABLE
Probable (1 in 1000)	ACCEPTABLE	UNACCEPTABLE	UNACCEPTABLE	UNACCEPTABLE	UNACCEPTABLE
Occasional (1 in 10000)	ACCEPTABLE	ACCEPTABLE	UNACCEPTABLE	UNACCEPTABLE	UNACCEPTABLE
Remote (1 in 100000)	ACCEPTABLE	ACCEPTABLE	ACCEPTABLE	UNACCEPTABLE	UNACCEPTABLE
Improbable (1 in 1000000)	ACCEPTABLE	ACCEPTABLE	ACCEPTABLE	ACCEPTABLE	UNACCEPTABLE

Table 2.3. Risk acceptability criteria.

Then, the initial hazard analysis documents the preliminary risk analysis for the device under development. This analysis is an essential activity to control and/or reduce residual risk from intolerable to acceptable based upon previously defined risk tolerance levels. The identified hazards are transferred onto the failure mode effects analysis (FMEA) report and evaluated to determine whether the benefit outweighs the risk.

Next, the development requirements along with the associated acceptance criteria are extracted from the risk assessment. These risk assessments and analysis in conjunction with the established procedures related to the standard ISO 13485 provide the tools for the development of a medical device that ensures the following:

- **Good performance:** Medical devices must provide accurate and precise measurements relevant to their intended claims (i.e. measurement of pulse rate).
- **Device safety:** The device must be safe for the user and other stakeholders in the framework established by its intended use, precautions, and warnings (i.e. adult patients in a homecare scenario).

Upon establishing the development requirements, the specific technical requirements must be subservient to accomplish the claims and intended use of the medical device with the technologies best suited and clearly marked acceptance criteria for the technical development validation.

Eventually, once the development has been completed, an evaluation plan must be carried out to verify the medical device is ready for certification as it performs as intended, accomplishes the claims, and it is safe to use.

2.5. Conclusions

In this chapter, the functional characteristics of the HAH system developed have been presented and described. This system uses biometric devices (wearable devices) to collect the physiological information of the patients and send this data to a digital platform by means of a gateway. The information gathered can be consulted anywhere and anytime by the system users, either healthcare providers or patients. This system flexibility allows doctors and healthcare organizations to monitor the evolution of each patient and use the resources efficiently.

Apart from presenting the functions of the system, the operational characteristics have been described. The operational characteristics refer to the technologies involved in the operation of the HAH system, focusing on the wearable devices. Each element that usually forms a wearable device has been presented and described. Especial emphasis has been made in the sensing technologies used to estimate the vital signs and analysis the sweat content.

Finally, the development procedure and the risk management plan have been described. Following these steps are fundamental to develop, implement, and validate a medical device, so must be handled correctly to obtain a robust product.

Both the functional and operational characteristics along with the development procedure are described deeply in the following chapters. In these sections, the wearable devices developed are presented and characterized giving a better understanding of the HAH system.

2.6. References

[1] R. Chataut, A. Phoummalayvane, and R. Akl, "Unleashing the Power of IoT: A Comprehensive Review of IoT Applications and Future Prospects in Healthcare, Agriculture, Smart Homes, Smart Cities, and Industry 4.0," *Sensors*, vol. 23, no. 16. Multidisciplinary Digital Publishing Institute (MDPI), Aug. 01, 2023. doi: 10.3390/s23167194.

[2] C. Huang, J. Wang, S. Wang, and Y. Zhang, "Internet of medical things: A systematic review," *Neurocomputing*, vol. 557, Nov. 2023, doi: 10.1016/j.neucom.2023.126719.

[3] H. Taherdoost, "Cybersecurity vs. Information Security," in *Procedia Computer Science*, Elsevier B.V., 2022, pp. 483–487. doi: 10.1016/j.procs.2022.12.050.

[4] "Data protection - European Commission." Accessed: Mar. 09, 2024. [Online]. Available: https://commission.europa.eu/law/law-topic/data-protection_en

[5] "ISO 27001." Accessed: Mar. 09, 2024. [Online]. Available: https://www.iso.org/standard/27001

[6] M. Javaid, A. Haleem, S. Rab, R. Pratap Singh, and R. Suman, "Sensors for daily life: A review," *Sensors International*, vol. 2. KeAi Communications Co., Jan. 01, 2021. doi: 10.1016/j.sintl.2021.100121.

[7] J. Baranwal, B. Barse, G. Gatto, G. Broncova, and A. Kumar, "Electrochemical Sensors and Their Applications: A Review," *Chemosensors*, vol. 10, no. 9. MDPI, Sep. 01, 2022. doi: 10.3390/chemosensors10090363.

[8] "Sensor Characteristics and Physical Effects," in *Nanotechnology-Enabled Sensors*, Boston, MA: Springer US, 2008, pp. 13–62. doi: 10.1007/978-0-387-68023-1_2.

[9] R. M. Rangayyan, *Biomedical signal analysis : a case-study approach*, Wiley. 2001. doi: 10.1109/9780470544204.

[10] A. Jubran, "Pulse oximetry," *Crit Care*, vol. 19, no. 1, Jul. 2015, doi: 10.1186/s13054-015-0984-8.

[11] T. Leppänen *et al.*, "Pulse Oximetry: The Working Principle, Signal Formation, and Applications," in *Advances in the Diagnosis and Treatment of Sleep Apnea*, Springer, 2022, pp. 205–218. doi: 10.1007/978-3-031-06413-5_22.

[12] D. Fujita and A. Suzuki, "Evaluation of the Possible Use of PPG Waveform Features Measured at Low Sampling Rate," *IEEE Access*, vol. 7, pp. 58361–58367, 2019, doi: 10.1109/ACCESS.2019.2914498.

[13] M. Coutrot, E. Dudoignon, J. Joachim, E. Gayat, F. Vallée, and F. Dépret, "Perfusion index: Physical principles, physiological meanings and clinical implications in anaesthesia and critical care," *Anaesthesia Critical Care and Pain Medicine*, vol. 40, no. 6. Elsevier Masson s.r.l., Dec. 01, 2021. doi: 10.1016/j.accpm.2021.100964.

[14] D. Seok, S. Lee, M. Kim, J. Cho, and C. Kim, "Motion Artifact Removal Techniques for Wearable EEG and PPG Sensor Systems," *Frontiers in Electronics*, vol. 2, May 2021, doi: 10.3389/felec.2021.685513.

[15] G. A. Dildy, S. L. Clark, and C. A. Loucks, “Intrapartum fetal pulse oximetry: Past, present, and future,” 1996. doi: https://doi.org/10.1016/S0002-9378(96)70242-9.

[16] T. Tamura, Y. Maeda, M. Sekine, and M. Yoshida, “Wearable photoplethysmographic sensors—past and present,” *Electronics* , vol. 3, no. 2. MDPI AG, pp. 282–302, Apr. 23, 2014. doi: 10.3390/electronics3020282.

[17] A. Dupre, S. Vincent, and P. A. Iaizzo, “Basic ECG Theory, Recordings, and Interpretation,” in *Handbook of Cardiac Anatomy, Physiology, and Devices*, P. A. Iaizzo, Ed., Totowa, NJ: Humana Press, 2005, pp. 191–201. doi: 10.1007/978-1-59259-835-9_15.

[18] R. S. Khandpur, “Bioelectric Signals and Electrodes,” in *HANDBOOK OF BIOMEDICAL INSTRUMENTATION*, 3rd Edition., New York: McGraw-Hill Education, 2014.

[19] D. E. Becker, “Fundamentals of Electrocardiography Interpretation,” *Anesth Prog*, vol. 53, pp. 53–64, 2006, doi: 10.2344/0003-3006(2006)53[53:FOEI]2.0.CO;2.

[20] T. M. C. Pereira, R. C. Conceição, and R. Sebastião, “Initial Study Using Electrocardiogram for Authentication and Identification,” *Sensors*, vol. 22, no. 6, Mar. 2022, doi: 10.3390/s22062202.

[21] J. Romero *et al.*, “Anatomical considerations and clinical interpretation of the 12-lead ECG in the prone position: a prospective multicentre study,” *Europace*, vol. 25, no. 1, pp. 175–184, Jan. 2023, doi: 10.1093/europace/euac099.

[22] S. M. Lobodzinski, “ECG Instrumentation: Application and Design,” in *Comprehensive Electrocardiology*, P. W. Macfarlane, A. van Oosterom, O. Pahlm, P. Kligfield, M. Janse, and J. Camm, Eds., London: Springer, 2010, pp. 427–480.

[23] R. S. Khandpur, “Physiological Transducers,” in *Handbook of Biomedical Instrumentation*, 3rd edition., New York: McGraw Hill Education , 2014, pp. 66–110.

[24] R. J. Shephard, “The Objective Monitoring of Physical Activity,” *Progress in Preventive Medicine*, vol. 2, no. 4, Jul. 2017, doi: 10.1097/pp9.0000000000000007.

[25] R. Mc Ardle, S. Del Din, B. Galna, A. Thomas, and L. Rochester, “Differentiating dementia disease subtypes with gait analysis: feasibility of wearable sensors?,” *Gait Posture*, vol. 76, pp. 372–376, Feb. 2020, doi: 10.1016/j.gaitpost.2019.12.028.

[26] D. Pollreisz and N. TaheriNejad, “Detection and Removal of Motion Artifacts in PPG Signals,” *Mobile Networks and Applications*, vol. 27, no. 2, pp. 728–738, Apr. 2022, doi: 10.1007/s11036-019-01323-6.

[27] D. Grieshaber, R. MacKenzie, J. Vörös, and E. Reimhult, “Electrochemical Biosensors - Sensor Principles and Architectures,” *Sensors*, vol. 8, no. 3, pp. 1400–1458, 2008, doi: 10.3390/s80314000.

[28] U. Jain, N. Chauhan, and K. Saxena, “Fundamentals of sensors and biosensors: An overview,” in *Multifaceted Bio-sensing Technology*, Elsevier, 2023, pp. 31–44. doi: 10.1016/b978-0-323-90807-8.00005-1.

[29] J. P. Villagrasa, J. Colomer-Farrarons, and P. Ll. Miribel, “Bioelectronics for Amperometric Biosensors,” in *State of the Art in Biosensors*, T. Rinken, Ed., Rijeka: IntechOpen, 2013. doi: 10.5772/52248.

[30] J. Punter-Villagrasa, J. Colomer-Farrarons, F. J. del Campo, and P. Miribel-Català, “Introduction to Electronics. Study, Design and Validation Tests,” in *Amperometric and Impedance Monitoring Systems for Biomedical Applications*, Cham: Springer International Publishing, 2017, pp. 67–112. doi: 10.1007/978-3-319-64801-9_3.

[31] Y. Montes Cebrián, “Electrochemical Plug-and-Power e-readers for Point-of-Care Applications,” Universitat de Barcelona, Barcelona, 2020.

[32] M. M. Ahmadi and G. A. Jullien, “Circuits for Amperometric Electrochemical Sensors,” in *VLSI Circuits for Biomedical Applications*, K. Iniewski, Ed., Artech, 2008, pp. 265–283.

[33] J. Bobacka, “Electrochemical sensors for real-world applications,” *Journal of Solid State Electrochemistry*, vol. 24, pp. 2039–2040, Jun. 2020, doi: 10.1007/s10008-020-04700-4/Published.

[34] L. Wang, Y. Zhang, and P. G. Bruce, “Batteries for wearables,” *National Science Review*, vol. 10, no. 1. Oxford University Press, Jan. 01, 2023. doi: 10.1093/nsr/nwac062.

[35] Q. Yang, A. Chen, C. Li, G. Zou, H. Li, and C. Zhi, “Categorizing wearable batteries: Unidirectional and omnidirectional deformable batteries,” *Matter*, vol. 4, no. 10. Cell Press, pp. 3146–3160, Oct. 06, 2021. doi: 10.1016/j.matt.2021.07.016.

[36] L. Wang, Y. Zhang, and P. G. Bruce, “Batteries for wearables,” *National Science Review*, vol. 10, no. 1. Oxford University Press, Jan. 01, 2023. doi: 10.1093/nsr/nwac062.

[37] C. Dagdeviren, Z. Li, and Z. L. Wang, “Energy Harvesting from the Animal/Human Body for Self-Powered Electronics,” *Annu Rev Biomed Eng*, vol. 19, pp. 85–108, 2017, doi: 10.1146/annurev-bioeng-071516.

[38] M. Mansour *et al.*, “Internet of Things: A Comprehensive Overview on Protocols, Architectures, Technologies, Simulation Tools, and Future Directions,” *Energies*, vol. 16, no. 8. MDPI, Apr. 01, 2023. doi: 10.3390/en16083465.

[39] D. S. Bhatti *et al.*, “A Survey on Wireless Wearable Body Area Networks: A Perspective of Technology and Economy,” *Sensors*, vol. 22, no. 20. MDPI, Oct. 01, 2022. doi: 10.3390/s22207722.

[40] “ISO 14971.” Accessed: Mar. 19, 2024. [Online]. Available: https://www.une.org/encuentra-tu-norma/busca-tu-norma/norma?c=N0064637

3. Vital Signs Monitoring Device

The first chapter described every vital sign and highlighted the importance of measuring these parameters to assess the health status of a patient. Then, the second chapter presented the technologies involved to develop a wearable device capable of monitoring these biomarkers and the process that must be followed to design, implement, and validate a medical device. In the present section, a wearable device named ONAVITAL capable of measuring the vital signs of an individual is presented and characterized. This system is intended to be a medical device used by healthcare professionals as a tool to facilitate their job and enhance resource management, so this wearable device was meticulously developed to meet medical standards.

3.1. Architecture of the system

The ONAVITAL device (see Figure 3.1a) [1] is a wearable device that takes the form of a small bracelet. This bracelet is attached to the patient's wrist and measures the user's pulse rate (PR), peripheral oxygen saturation (SpO_2), arterial blood pressure (ABP), and skin temperature (STEMP). When the heart pumps blood, the ABP receives the name of systolic blood pressure (SABP), and when this muscle rests, ABP is named diastolic blood pressure (DABP).

This monitoring device is formed by a plastic case (see Figure 3.1b), an electronic board with a battery soldered to it (see Figure 3.1c), and a hypoallergenic strap (see Figure 3.1c). The device's design was kept as simple as possible to facilitate the system's adoption by the potential users. The target population is the geriatric population which normally has difficulties to use digitals systems, such as smartphones or smartwatches, so the system must be orientated to them [2]. Apart from helping the patient adherence, making the device simple reduces the manufacturing costs because the number of components is reduced.

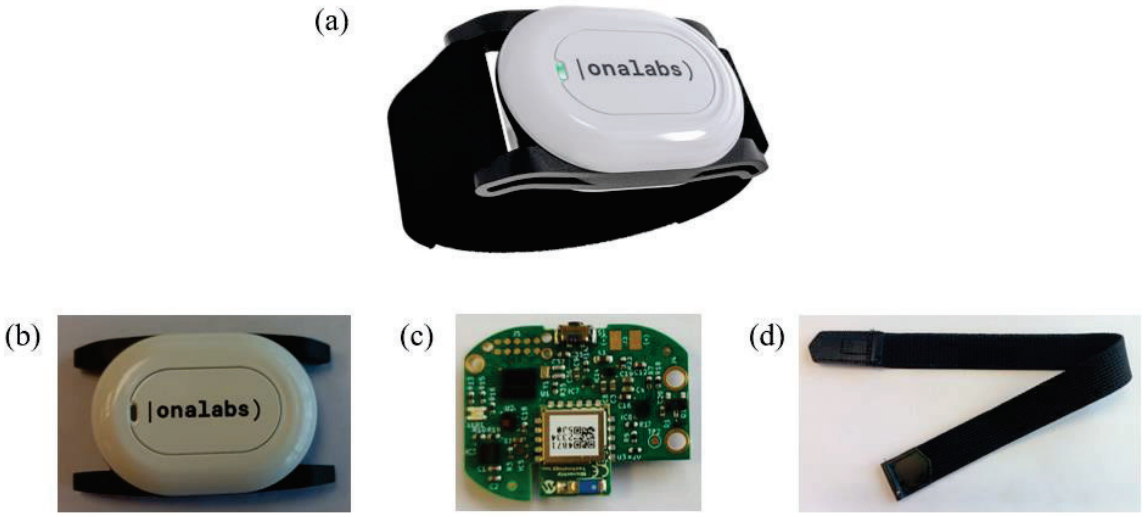

Figure 3.1. Structure of the ONAVITAL device. (a) Complete system, (b) plastic case, (c) electronics of the system, and (d) strap.

The wearable device case (see Figure 3.2) is made of biocompatible plastic, and it is the interphase between the system and the environment. It has several functions:

- **Interact with the user:** By means of a LED, the device indicates its state to the user. It also integrates a button which is utilized to reset the system.
- **Interphase between sensors and environment:** The case has a lens that transmit/receive the light produced by the pulse oximeters (PPGs) of the wearable device. It also has a metallic piece that conducts the heat from the patient's skin to the thermometer integrated onto the board.
- **Wear the device:** The plastic case holds the strap that allows to wear the product.
- **Charge the device:** This system can be charged using a custom cable that is attached to the case by means of a magnet.

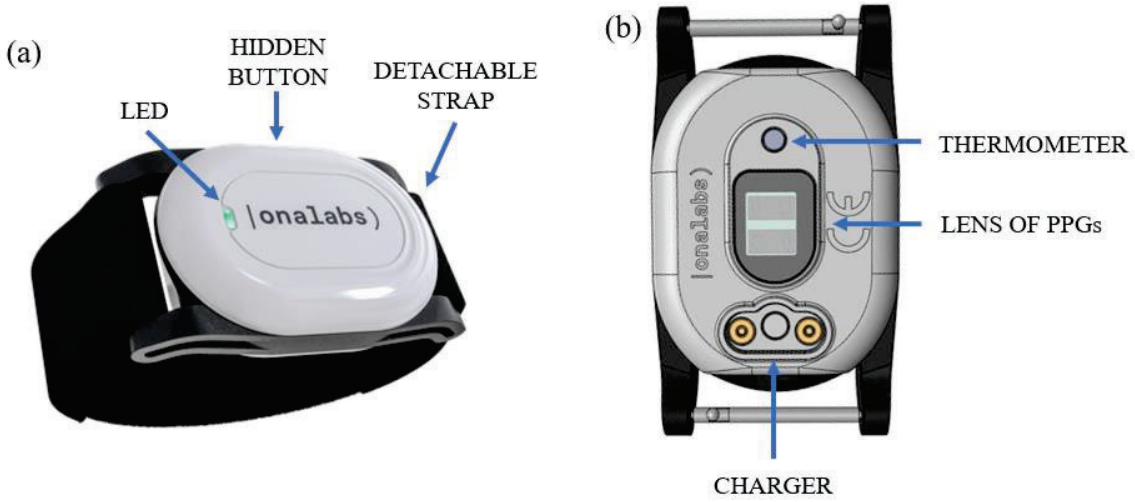

Figure 3.2. Parts of the ONAVITAL case. (a) Top and (b) bottom of the system.

To attach the wearable device to the patient, a cloth strap is utilized. The materials used to manufacture this strap are medical grade in order to ensure that the device is biocompatible and does not cause any harm to the user. Most of the potential users of this system are fragile patients that are susceptible to complications and infections, and their health can deteriorate rapidly if it is not properly cared [3]. The strap can be changed by another one by means of a detachable pin, so when a strap is damaged or must be washed, it can be rapidly replaced.

The ONAVITAL's electronics (see Figure 3.3) controls and performs every device's actions. These electronics capture the sensors' response, process the gathered data, and send the estimated health features to a gateway via Bluetooth Low Energy (BLE). BLE is a short-range wireless communication protocol that stands out by its low-power consumption and its versatility. Furthermore, it allows to exchange data with a multitude of systems because nowadays it is a standard of the electronics industry [4]. To power the device, a lithium polymer (LiPo) battery with a nominal voltage of 3.7 V and a rated capacity of 150 mAh is utilized. LiPo batteries possess a high energy density and are rechargeable, making it an ideal option to power a wearable device.

The electronics block represents almost 80 % of the device cost, so the economic scalability of the design has thoroughly been taken into account. All the electronics and sensors of the system are embedded in a single board to fulfill this goal.

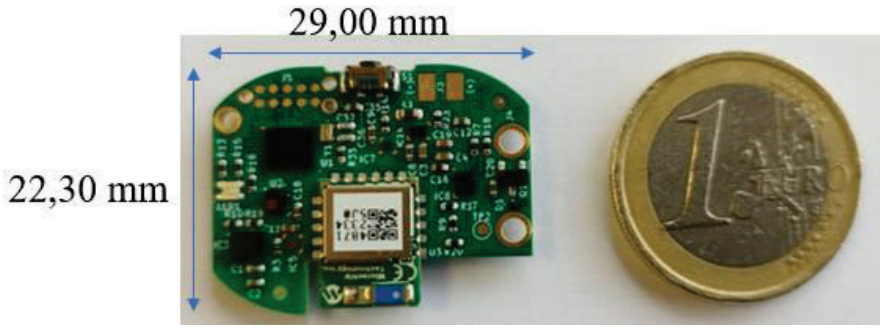

Figure 3.3. Photograph of the ONAVITAL electronics.

The data collected by the ONAVITAL device is sent to the cloud platform by means of a mobile phone application. Acting as a communication hub, the smartphone running this application not only facilitates the transmission but also provides a user-friendly interface for data visualization. To use this application, the patient must identify himself by means of both an email and a password. This authentication step is crucial, as each wearable device is linked to a unique patient profile. After the authentication phase is complete, the ONAVITAL device corresponding to the patient's profile establishes connection to the smartphone. Finally, the patient can visualize the last measurement taken by the system and perform new measurements by means of the ON-DEMAND button (see Figure 3.4).

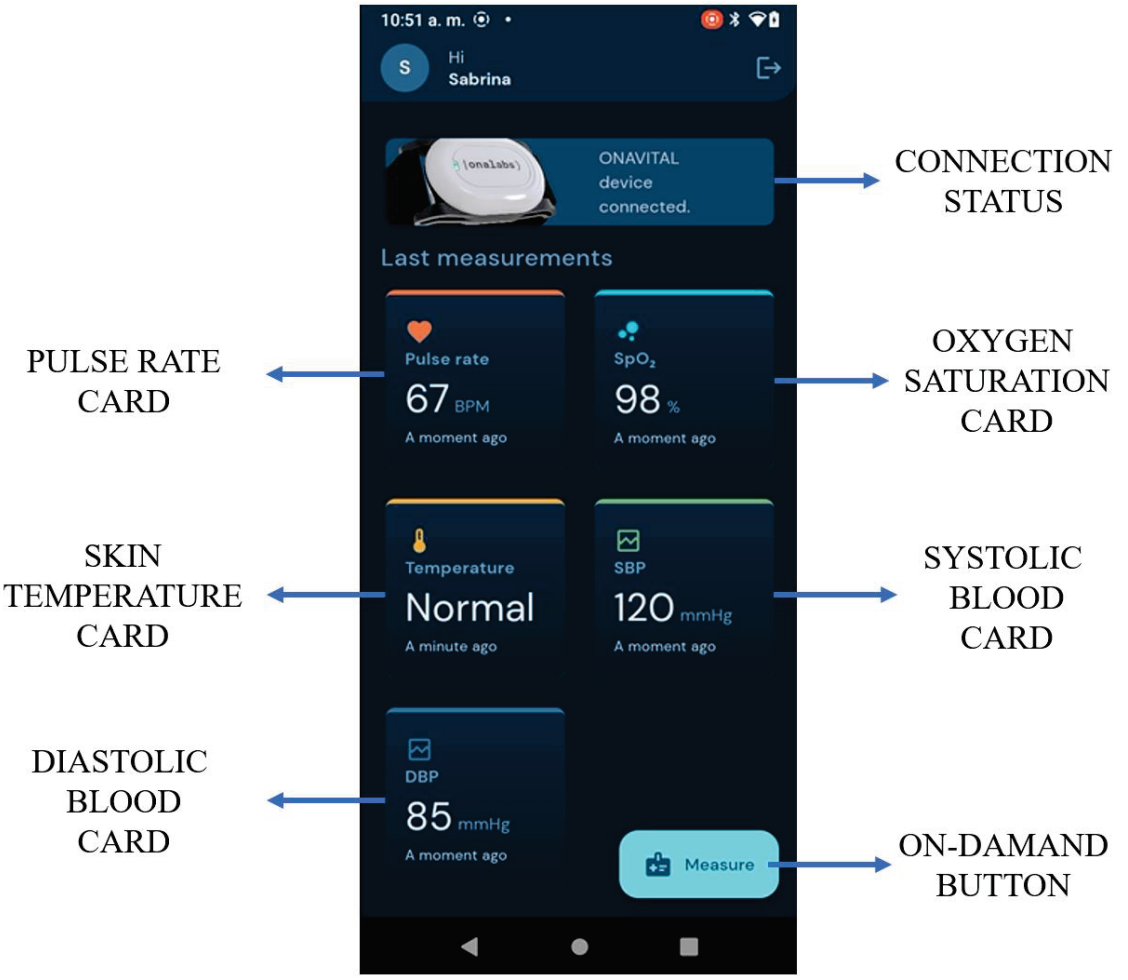

Figure 3.4. Mobile phone application of the ONAVITAL device.

The gathered data can be also sent to a specific hardware that acts as a gateway (see Figure 3.5). Most potential users of ONAVITAL device are elderly which are not accustomed to digital tools, such as mobile phone applications. Furthermore, smartphones are not always available, so an alternative gateway is very helpful in several settings. Utilizing a specific hardware address both issues at once. This hardware receives the information and sends the data to the cloud, acting only as a repeater. It consists of a board contained inside a plastic case and possesses every processing and communication capabilities of a smartphone. Authentication is not necessary when using this gateway, as each gateway is linked to one or more ONAVITALs.

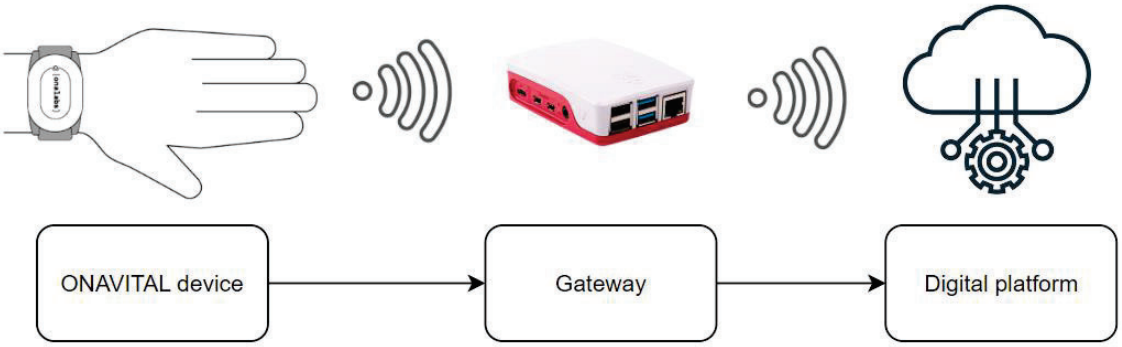

Figure 3.5. Gateway configuration.

The information collected by wearable devices is stored into a cloud-based platform. This platform is used to manage the registry of each bracelet, associate wearable devices with individuals, provide authentication to individuals accessing the ONAVITAL application or the gateway, and act as a data repository. The data gathered by the bracelets can be visualized through application programming interfaces (APIs) or a cloud-based dashboard.

3.2. Electronics of the system

The board architecture (see Figure 3.6) is the same as it is detailed in the previous chapter: control unit, power supply module, electronic instrumentation, wireless communication module, and external memory. Only one major difference is found which is both the instrumentation and sensors are included in the same module.

This wearable device has two operational modes: low-power and measurement states. Initially, the device remains in the low-power mode until it detects a patient. Then, the system switches to the second mode and starts to monitor the patient's vital signs. Measurements are taken every 15 minutes, but this frequency can be modified by means of the cloud-based platform. Multiple frequencies can be set and the selection of one or another depends on the criteria of the healthcare provider, but it must take into account that there is a tradeoff between the measurement frequency and battery life. The device consumption rises when the measurements are taken more often, and it falls when the period between measurements increases. A sampling frequency of 15 minutes is deemed sufficient to capture the evolution of every physiological parameter without an excessive power consumption. The ONAVITAL device monitors the vital signs until the user removes the bracelet. At this moment, the system returns to the first state.

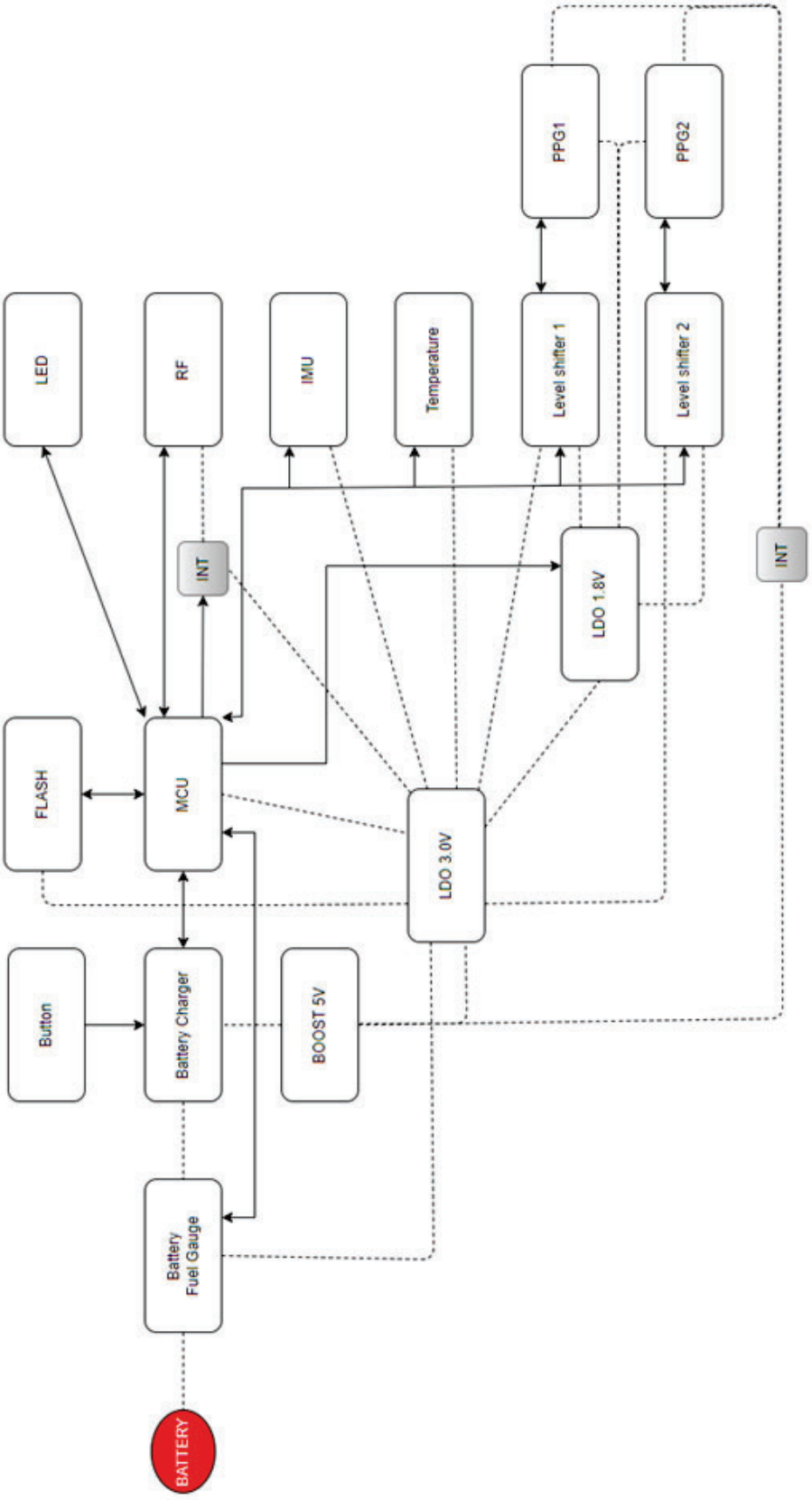

Figure 3.6. Architecture of the ONAVITAL electronic board.

To detect the presence of a patient, the ONAVITAL device uses an Inertial Measurement Unit (IMU) and a PPG. This IMU is continuously recording the acceleration and when it surpasses a fixed threshold, the system starts to look for the presence of an individual by means of the PPG, since considers that a patient wants to wear the device. The PPG emits infrared (IR) light and capture the environmental response. This response is analyzed, and the presence of an individual is determined when the signal is larger than a fixed threshold. Both fixed thresholds were established after analyzing the raw data of dozens of individuals.

The ONAVITAL board consumes 7.14 μA and 51 mA at low-power and measurement mode, respectively. This electronic board is capable of disabling and enabling different modules of the system to reduce power consumption. Furthermore, the processing of the sensors' raw data is carried out by the device itself instead of sending this information to the cloud for health features extraction. This latter approach consumes a lot of energy since many values must be sent rather than the estimated parameters. Given these characteristics, if the measurements of the ONAVITAL device are taken every 15 minutes, the expected battery life is five days.

3.2.1. Control unit

The control unit acts as the brain of the system. It manages all the actions performed by the wearable device and analyzes the sensors' response. These actions are controlled by the firmware embedded on the unit's microcontroller (MCU).

This module is composed by the MCU STM32L476JEY6TR (STMicroelectronics; Geneva, Switzerland) [5], its peripherals, and a RGB LED used to indicate different device states to the user, such as low charge of the battery. This component is an ultra-low-power MCU with a high-performance ARM Cortex-M4 32-bit RISC core. It includes in the same package several peripherals, such as analog to digital converters (ADCs) or digital to analog converters (DACs), and communication interfaces, like I2C or UART. These features allow to create electronic systems that perform complicated operations without consuming a lot of energy.

The power consumption of this unit depends on the system's operational mode. During the first state, the MCU is configured in a low-power mode resulting in an average consumption of 1.5 μA. When the system switches to the second mode, this component is activated and consumes an average current of 1 mA. It is important to reduce as much as possible the power consumption of this component since it is an element that usually consumes a lot of energy.

3.2.2. Power supply module

The energy used to supply the system is extracted from a battery. This electric energy is regulated by the power management module of this board. Furthermore, this module is utilized to recharge the battery and estimate its charge level.

A. Battery

To power this electronic board, a LiPo battery is utilized. These electrochemical cells are rechargeable batteries with high-energy density which means that they possess a lot of charge capacity in comparison to their weight. Besides, these batteries provide stable

current, but the voltage decays with the charge level [6]. Hence, the electrical potential must be regulated to power the circuit.

The LiPo battery used for the ONAVITAL device has a nominal voltage of 3.7 V, and a charge capacity of 150 mAh.

B. Regulation of the voltage

Most elements of the ONAVITAL device work at 3.0 V. Only the PPGs require different potentials to operate, which are 1.8 V and 5.0 V. Combining a BOOST converter and two low-dropout regulators (LDOs), these voltages are obtained. The first component elevates the voltage to 5.0 V and then it is regulated to 3.0 V by an LDO. Eventually, the other LDO is utilized to lower the potential from 3.0 V to 1.8 V (see Figure 3.7).

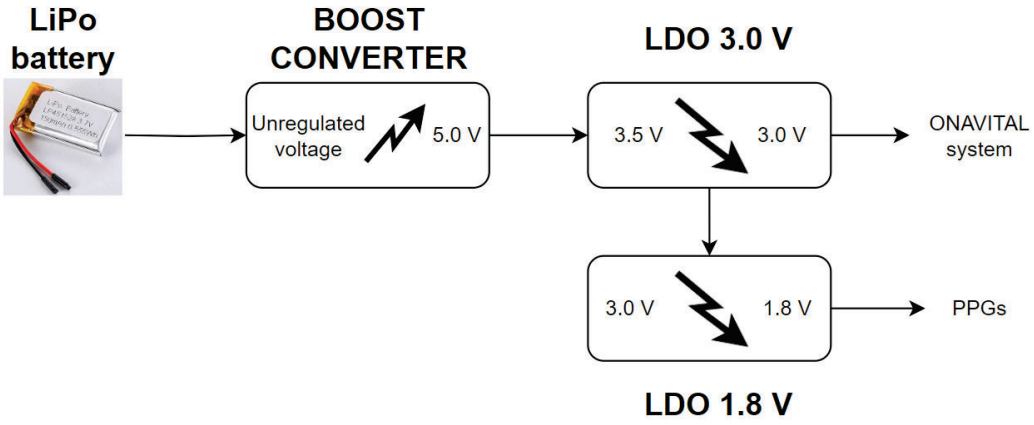

Figure 3.7. Schema of the ONAVITAL voltage regulation.

The boost converter and both LDOs are ultra-low-power integrated circuits (ICs) which only consumes 325 nA, enhancing the battery duration since these elements are always enabled. The 1.8 V LDO only consumes 25 nA and 3 nA when it is enabled and disabled, respectively. This LDO is controlled by the MCU to reduce the PPG consumption.

C. Charge of the battery

LiPo batteries are potentially dangerous because they can explode or burn when they are not handled properly. To manage this electrochemical cell, the battery charge management circuit BQ25150 (Texas Instruments; Dallas, TX, USA) [7] is used. The main function of this chip is to charge the battery in a controlled and secure way. It also monitors the state of the LiPo battery and disconnects this electrochemical cell from the system when a potential hazard is detected. This module communicates with the MCU by means of I2C and it consumes 18 µA when it is working.

D. Estimation of the battery level

The battery fuel gauge BQ27220 (Texas Instruments; Dallas, TX, USA) [8] is used to estimate the level of charge of the battery. This element determines the amount of charge remaining in the electrochemical cell and provides information about its state. The information recorded is sent to the MCU via I2C. This module consumes 600 nA and 50 µA when is disabled and enabled, respectively.

3.2.3. Sensors and instrumentation module

The ONAVITAL device integrates both the sensors and electronic instrumentation onto a single board. Different sensors are utilized depending on the physiological parameter being measured.

To monitor the PR, SpO_2, and ABP, two reflective PPGs MAX30101 (Analog Devices; Wilmington, MA, USA) [9] are utilized. This IC includes the LEDs and photodiodes required to carry out the pulse oximetry technique, along with the instrumentation necessary for their operation. The PPGs emit light at three wavelengths, which are 537nm (green), 660nm (red) and 880nm (IR). The response of the environment is captured by the system photodiodes and sent to the MCU via an I2C, which process the acquired signals to estimate the vital signs.

Temperature is measured using the digital thermometer TMP117 (Texas Instruments; Dallas, TX, USA) [10]. The heat is transferred from the skin to the thermometer using a metallic heat-conducting part built-in in the device case. The values extracted from the sensor are sent to the MCU via I2C.

Finally, to evaluate the patient's activity, the IMU ISM330DHCX (STMicroelectronics; Geneva, Switzerland) [11] is used. This IMU contains both an accelerometer and gyroscope, and it is used to detect when the patient takes the device to wear it. The data collected by this device is sent to MCU via I2C.

All these sensors consume 51 mA when they are measuring and 4.75 μA at low power. Since the measurement frequency is very low (15 minutes), there is no major concern with the battery life.

3.2.4. Wireless communication module

The gathered data by the wearable device is sent to a gateway. To perform this task, the certified BLE module RN4871 (Maxim Integrated; San Jose, CA, USA) [12] is used. This module sends/receives the information depending on the orders given by the MCU via UART.

BLE systems handle the transfer and storage of information through characteristics. A set of characteristics is known as a service. Several services and characteristics are defined to exchange information with the mobile phone application/gateway. For instance, there is a characteristic for the HR measurement and another one for the battery level.

To reduce the power consumption, an analog switch controlled by the MCU disables the power supply of this IC when it is not used. Despite BLE is a low-power communication protocol, it requires several mA (average of 5 mA) to send and receive information, so to enhance the battery life it is recommended to disable this system.

3.2.5. External memory

To ensure that any data is lost, a backup of the data collected is made after each measurement. This backup is stored in the external memory flash GD25Q128EWIGR (GigaDevice Semiconductor; Beijing, China) [13]. A flash memory is a non-volatile memory, which means that its content is not erased even when the power supply fails, i.e. the coin cell discharges. The storage capacity of the flash used is 16 Mbytes and can store

up to 20 years of measurements. Data is sent from the flash to the MCU via a Quad SPI interface.

This module consumes 12 mA and 100 nA when it is enabled and disabled, respectively. The elevated power consumption of the memory flash is associated with the process of saving/retrieving data. This process only longs 100 ms, so the impact on battery life is minimal.

3.3. Algorithms

The STEMP value is extracted from the device's thermometer. The other physiological parameters are estimated by processing the acquired PPG signals, so three custom algorithms were developed to obtain the PR, SpO_2, and ABP values. Given the limited resources of a MCU, algorithms cannot be very complex at computational level, because excessive resource usage drains a lot of energy reducing the device autonomy. Furthermore, the temperature of a MCU rises when many operations are carried out, which increases the board temperature, leading to erroneous STEMP recordings.

The first step of the three algorithms is acquiring the PPG signals. On one hand, the green light is used to estimate both the PR and ABP values. Green light is more energetic than other wavelengths of the visible spectra, so it penetrates deeply into the skin which improves the signal-to-noise ratio (SNR) [14]. A high SNR is crucial for PR and ABP algorithms to discern the details of the PPG signal corresponding to the cardiovascular system. On the other hand, red and IR light are utilized to calculate the SpO_2 value. As discussed in the previous chapter, the SpO_2 algorithm exploits the absorption difference between these two wavelengths to estimate the percentage of hemoglobin oxygenated and not (see Figure 3.8a).

PPG signals can be easily corrupted by movement, making it impossible to utilize these signals for estimating any physiological parameter. To reduce measurement error, an algorithm capable of distinguishing between high- and low-quality signals is employed before any estimation. This algorithm is referred as signal quality index (SQI) [15]. Acceptable or excellent quality signals are used to estimate both the PR and SpO_2 (see Figure 3.8b), or excellent in the case of ABP (see Figure 3.8c).

3.3.1. Signal quality index

Several physiological parameters can be estimated in a non-invasive way utilizing the pulse oximetry technique. Despite its versatility, there are different drawbacks that limit its use. On one hand, motion artifacts corrupt PPG signals by introducing random noise [16]. On the other hand, this technique presents reduced efficiency when it is applied to individuals with darker skins. This issue is caused by the elevated light absorption provoked by more prevalent melanin content of darker skins, leading to low SNR [17], [18].

There are several methods to reconstruct corrupted PPG signals, but these techniques require many computational resources [19], [20]. An alternative method to these techniques consists of a classifying algorithm that clusters the signals according to its quality and only the signals with acceptable or excellent quality are processed [21].

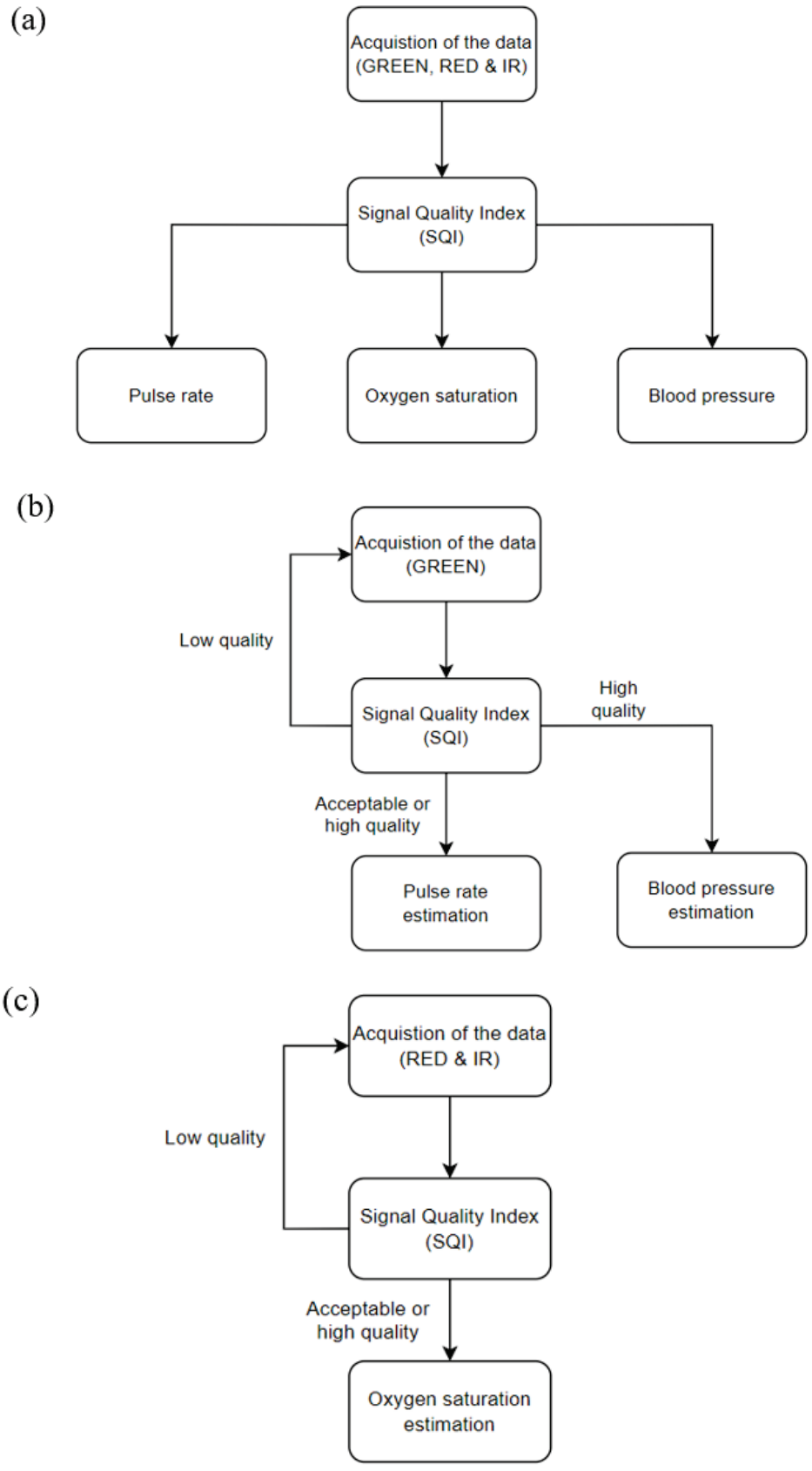

Figure 3.8. Signal processing decision tree. (a) General operation of the system, (b) SQI algorithm applied to PR and ABP estimation, and (c) SQI applied to SpO_2 calculation.

Most PPG manufacturers use the perfusion index as the gold standard for assessing signal quality [22]. Perfusion index is the ratio of pulsatile to the non-pulsatile blood in a patient's peripheral tissues. Despite this parameter is extensively used by transmissive PPG devices, which provide excellent quality signals by its own nature, this method is not effective for reflective systems because the recorded signals are normally noisier. Several alternative methods to the perfusion index assessing technique have been developed ranging from descriptive statistics to more complex approaches, such as deep learning [23]. These latter approaches are not feasible for wearable devices because their elevated computational complexity.

A SQI algorithm based on descriptive statistics is used by the ONAVITAL device. The statistics utilized are:

- **Mean value:** Arithmetic average of the signal (see Equation 3.1).

$$\bar{x} = \frac{\sum_{n=1}^{N} x_n}{N} \tag{3.1}$$

  where $\bar{x}$ is the mean value, x_n is each value of the signal, and N is the number of samples in the signal.

- **Standard deviation (STD):** Measurement of the signal dispersion (see Equation 3.2).

$$\sigma = \sqrt{\frac{\sum_{n=1}^{N}(x_n - \bar{x})}{N-1}} \tag{3.2}$$

  where σ is the STD, $\bar{x}$ is the mean value, x_n is each value of the signal, and N is the number of samples in the signal.

- **Kurtosis:** Measurement of symmetry of the data distribution (see Equation 3.3)

$$K = \frac{1}{N\sum_{n=1}^{N}[x_n - \frac{\bar{x}}{\sigma}]} \tag{3.3}$$

  where K is the kurtosis, x_n is each value of the signal, $\bar{x}$ is the mean value, σ is the STD, and N is the number of samples in the signal.

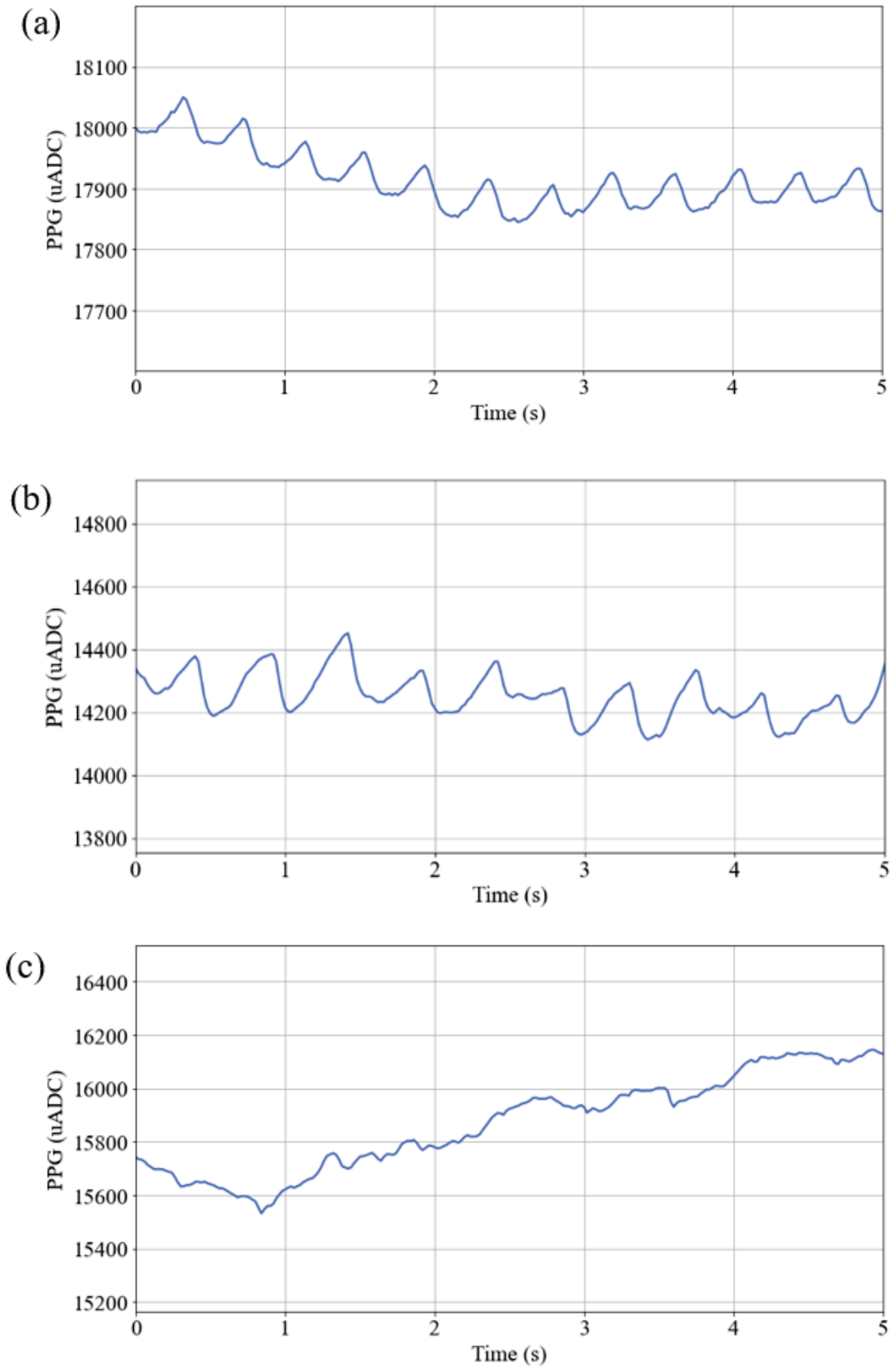

Figure 3.9. Signal classification. (a) Excellent, (b) acceptable, and (c) low quality PPG signals.

Two different thresholds are defined for each descriptive statistic. These thresholds were defined after a process of calibration with multiple volunteers. Using these thresholds, the signals are classified as low, acceptable, or excellent. Excellent quality signals (see Figure 3.9a) are those in which the systolic peaks can be clearly observed. These peaks can be also observed for acceptable PPG signals (see Figure 3.9b), but some noise is present on these signals. Finally, low quality signals (see Figure 3.9c) are those in which any peak is observed, or the noise corrupts entire sections of these signals.

3.3.2. Pulse rate

To estimate the PR, the green PPG signal is used. The PR algorithm is executed when the SQI algorithm classifies signals as acceptable or excellent. Each systolic peak within the acquired PPG signal is utilized to calculate the PR (see Figure 3.10a). These peaks correspond to the heartbeats, so the distance between peaks directly correlates with this vital sign.

The first step of the PR algorithm consists of reducing the noise from the PPG signal. To perform this task, a second order Butterworth band-pass filter with a pass band from 0.5 to 4 Hz is used. This band was selected to improve the detection of systolic peaks because PR typically ranges between these frequencies, which correspond to 30 to 220 bpm. Then, the autocorrelation of the filtered signal is calculated. The autocorrelation extracts the period of a signal by suppressing the aperiodic component which allows to extract the frequency of this signal. Finally, the autocorrelation peaks are detected, and the value of the PR is estimated using the following expression (see Equation 3.4):

$$PR = \frac{60 \cdot Sampling\ frequency}{Distance\ between\ peaks} \tag{3.4}$$

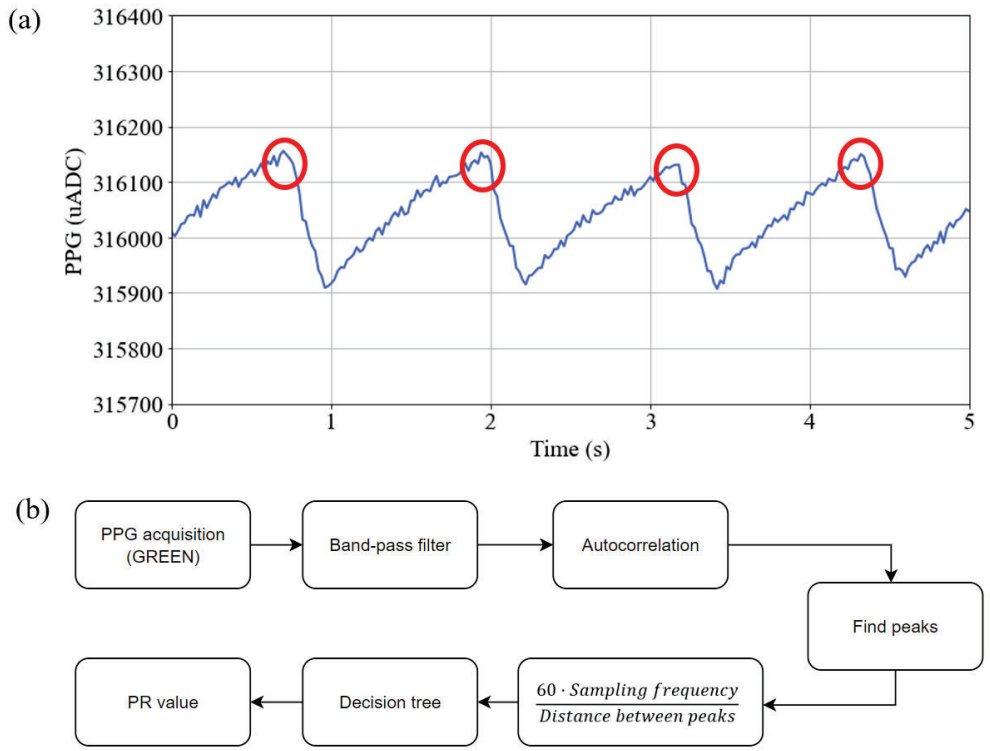

Figure 3.10. Pulse rate estimation. (a) Systolic peaks of the PPG signal, and (b) algorithm used to calculate this parameter.

The algorithm is applied to 10-second PPG signals. This window is split into several sliding windows of five seconds. The PR is calculated for each window and the results are stored in an array. An upper and lower limit are set using the mean and the STD of each element inside the array. Another limit is fixed using the maximum physiological PR value [24]. The values outside these limits are considered outliers and removed from the array. Eventually, the PR value is calculated by doing the mean of the values contained on this array (see Figure 3.10b).

3.3.3. Oxygen saturation

To estimate the patient SpO_2, the red and IR PPG signals are used. This operation is performed when the SQI algorithm classifies signals as excellent.

First, the direct component (DC) and the alternating component (AC) of each signal are estimated. The constant baseline and the pulsatile component are referred as DC and AC of the signal, respectively. On one hand, the root mean square (RMS) of the mean value of every signal is used to calculate the DC, and, on the other hand, the RMS (see Equation 3.5) of each signal without the DC component is utilized to estimate the AC.

$$RMS = \sqrt{\frac{1}{N}\sum_{n=1}^{N}|x_n|^2} \tag{3.5}$$

where N is the number of samples in the processed PPG signal and x_n is each value of this signal.

Then, both components of the red and the IR light are used to estimate the R value (see Equation 3.6):

$$R = \frac{AC_{RED}/DC_{RED}}{AC_{IR}/DC_{IR}} \tag{3.6}$$

where the AC_{RED} and AC_{IR} are the pulsatile component of the red and IR signal, and the DC_{RED} and DC_{IR} the baseline of both signals.

The R value is proportional to SpO_2, but it is not equivalent to this physiological parameter. To extract the oxygen saturation value the following equation is used (see Equation 3.7):

$$SpO_2 = a\,R^2 + b\,R + c \tag{3.7}$$

being SpO_2 the peripheral oxygen saturation, R the R value, and a, b, and c empiric coefficients. These coefficients depend on the device optical system and they are obtained after an initial calibration process (see Figure 3.11) [25].

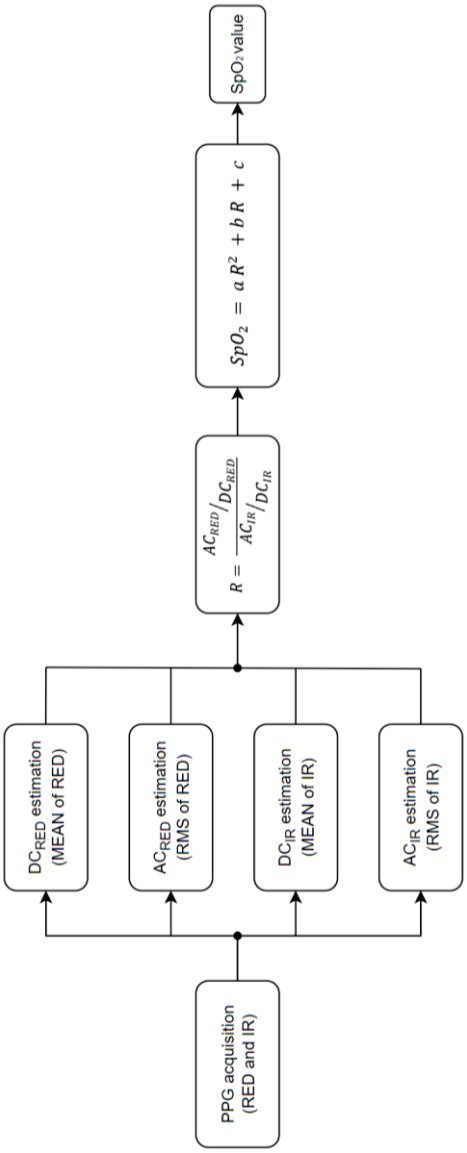

Figure 3.11. Algorithm used to calculate oxygen saturation.

3.3.4. Arterial blood pressure

The green PPG signal is utilized for estimating the ABP. This algorithm is executed when the SQI algorithm classifies PPG signals as excellent. PPG signals reflect the volume changes in blood vessels corresponding to the systolic and diastolic cycles of the heart. By analyzing the nature of these changes, the ABP can be estimated by calculating the area under the PPG signal (see Figure 3.12a).

First, the PPG signal is filtered separately by a third order Butterworth low-pass filter with a cut-off frequency of 15 Hz, a second order Bessel low-pass filter with a cut-off frequency of 2 Hz, and a DC filter. Then, the peaks and valleys corresponding to each filtered signal are detected and categorized as maximums and minimums, respectively. The area compressed between two valleys and one peak is considered as one complete cardiac cycle (systolic and diastolic). Following this categorization, the area under every triangle is calculated by integration. These values are intermediate results of both the SABP and DABP. Finally, a correction algorithm is applied to discard the unrealistic values and the final value of both SABP and DABP are estimated (see Figure 3.12b).

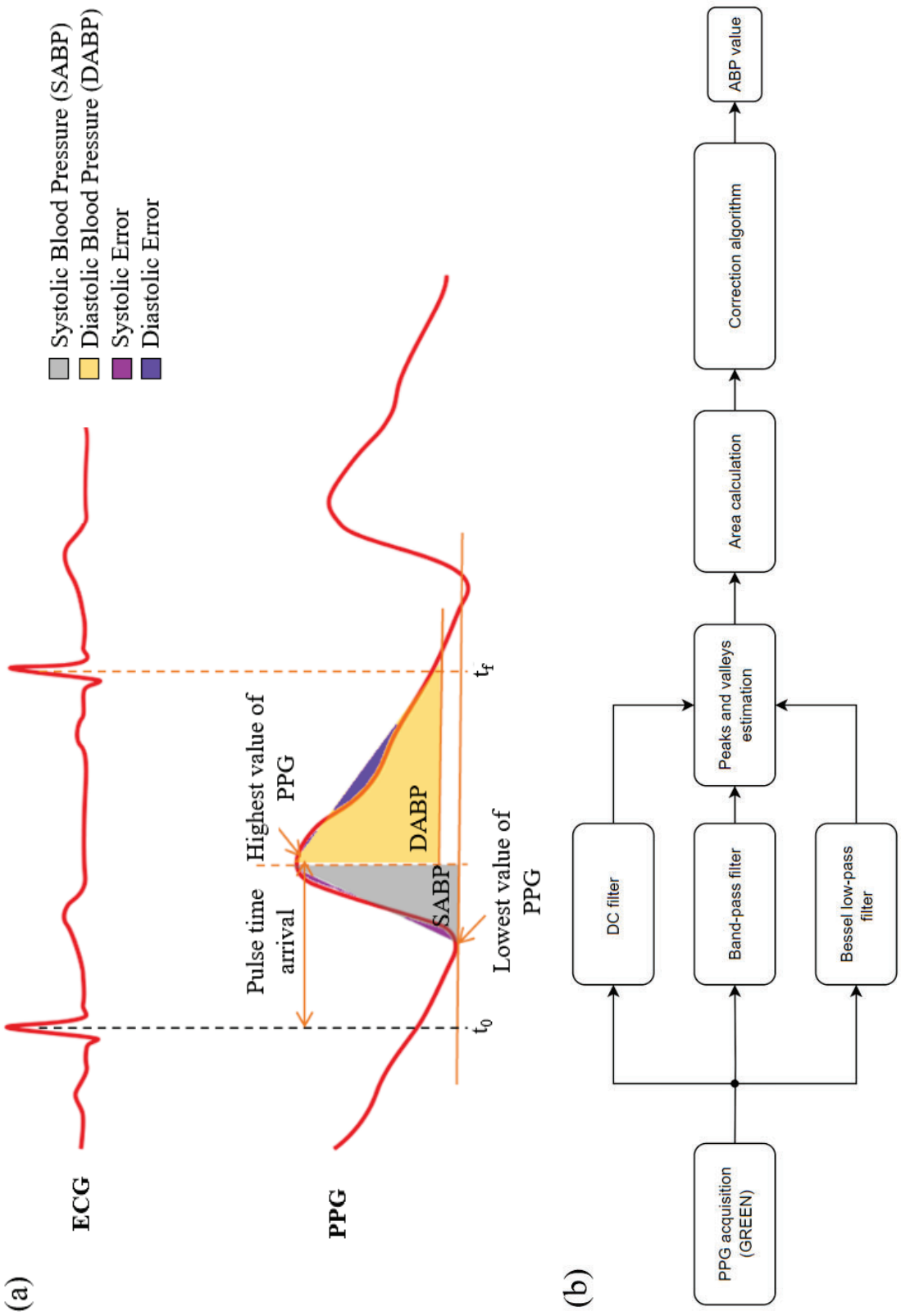

Figure 3.12. Blood pressure estimation technique. (a) Principle of the ABP estimation by means of a PPG signal, and (b) algorithm used to calculate this parameter.

3.4. Calibration process

Some of the algorithms used by the ONAVITAL device require a calibration process since these measurements depend on the system optics. These algorithms are the SQI, SpO_2, and ABP estimation methods. As humans were involved in this calibration process, the experiments were conducted in accordance with the international ethical declarations of Helsinki [26].

3.4.1. Signal quality index

The SQI algorithm must be calibrated because the characteristics of the PPG signals depend on the system optics. Variations in these characteristics are translated to the descriptive statistics used to cluster the signals as low, acceptable, or excellent quality.

To carry out this calibration process, multiple volunteers were recruited and gave their consent to treat their data (see appendix 2 – Data protection consent). Upon the consent was obtained, an ONAVITAL device was attached to the wrist of each volunteer and one minute of pulse oximetry (green, red, and IR wavelengths) was recorded using a sampling rate of 50 Hz. To reduce the number of motion artifacts on the recorded signals, the acquisition of the raw data was at rest while the partaker was sited. The recorded signals were labelled manually depending on their quality and stored in a custom database. This database comprises over 3000 PPG signals of multiple partakers.

Once the data collection was over, the generated database was split in two to calibrate the SQI algorithm: training and testing dataset. Using the training dataset, the thresholds corresponding to the descriptive statistics were defined. Then, the estimated thresholds were included on the algorithm and the performance of this system was assessed utilizing the training dataset. A confusion matrix [27] was utilized to evaluate if the SQI algorithm classifies the signals correctly depending on its quality. This matrix showed that almost every signal was classified properly, so this algorithm can be considered accurate (see Figure 3.13).

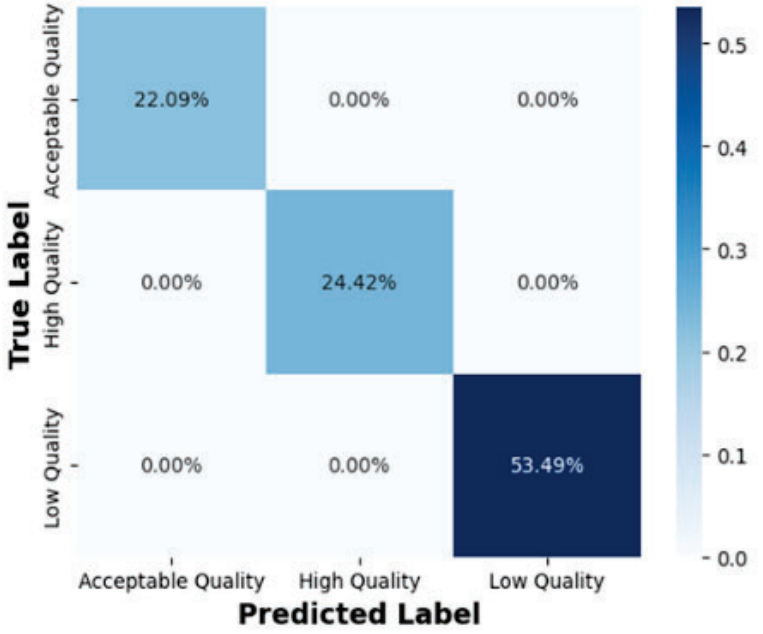

Figure 3.13. Accuracy of SQI algorithm represented by a confusion matrix.

3.4.2. Oxygen saturation

The DC and AC of both red and IR signals vary depending on the system optics, so the oxygen saturation measurement technique must be calibrated as well as the SQI algorithm. This calibration process provides the empiric coefficients of the equation that relates the R value and the SpO_2.

As it was discussed in the first chapter, the oxygen saturation barely changes and typically ranges between 95 and 100 %. This range is not enough to calibrate the system since critical values of this parameter are below 90 %. To calibrate this measurement, a set of partakers must be recruited, and their levels of oxygenation must be reduced artificially. This process is normally carried out using a mask which deprives the partaker oxygen intake and SpO_2 as low as 70 % can be obtained using this technique [28]. However, improper handling of this method can pose a danger to volunteers, so an alternative technique to calibrate this measurement is highly recommended.

Figure 3.14. Set-up used to calibrate the oxygen saturation measurement. (a) Hypobaric chamber from outside and (b) inside, and (c) a volunteer with the device ONAVITAL and the reference instrument.

A hypobaric chamber is a controlled environment used to simulate high altitude conditions and low atmospheric pressure. These chambers are used for training pilots, aerospace medicine, and mountain climbing research. The main purpose of a hypobaric chamber is to expose individuals to reduced atmospheric pressure, replicating the lower oxygen levels and reduced air density found at high altitudes [29]. High-altitude environments place considerable stress on the body causing variations on vital signs. For instance, when the SpO_2 is reduced by the low-pressure exposure, the HR increases to compensate lower oxygen levels in blood to deliver this molecule to every tissue [30]. Since the oxygen level is reduced along with the altitude, a hypobaric chamber can be utilized as an alternative method to calibrate the oxygen saturation measurement (see Figure 3.14). This calibration method was the method used to calibrate the oxygen saturation measurement of the ONAVITAL device.

To calibrate the SpO_2 measurement 21 males and 13 females with ages ranging from 18 to 34 (mean of 22.0 years and STD of 3.4 years) were recruited. They were informed about the trial and gave their consent (appendix 2 – Data protection consent) to use the gathered data during the experiments. Before each trial, the skin pigmentation of every partaker was recorded using the Fitzpatrick scale as reference system (mean of 1.9 and STD of 0.8). This scale is a numerical classification system utilized to categorize human skin types based on their response to ultraviolet light [31]. Several studies demonstrated a racial bias of pulse oximetry technology leading to undetected hypoxemias among individuals with darker skin tones, which poses a significant public health concern [32]. To address this issue, regulatory organizations, such as the federal agency of Food and Drug Administration (FDA) of the United States, demands to calibrate oxygen saturation measurement systems using volunteers representing diverse skin pigmentation.

Once consent was obtained, an ONAVITAL device was attached to the wrist of each volunteer and the partakers entered to the hypobaric chamber in groups of two. In this chamber, the calibration process was conducted as follows (see Figure 3.15):

- A simulated ascent in five minutes to 2000 meters. At this altitude, five minutes at rest and five minutes of gentle exercise using a stationary bicycle at a constant load.
- A simulated ascent in five minutes to 4000 meters. At this altitude, five minutes at rest and five minutes of gentle exercise using a stationary bicycle at a constant load.
- A simulated descent in five minutes to 2000m altitude. At this altitude, five minutes at rest and five minutes of gentle exercise using a stationary bicycle at a constant load.
- A simulated descent in five minutes to see level.

Every five minutes, 10 seconds of PPG signals (red and IR wavelengths) at a sampling rate 50 Hz were recorded by each ONAVITAL device. A reference measurement was also taken at the same time using the equipment Nonin Onyx Vantage 9590 (Nonin Medical; Plymouth, MA, USA) [33]. This instrument is a certified medical device regularly utilized in hospital Intensive Care Units (ICUs).

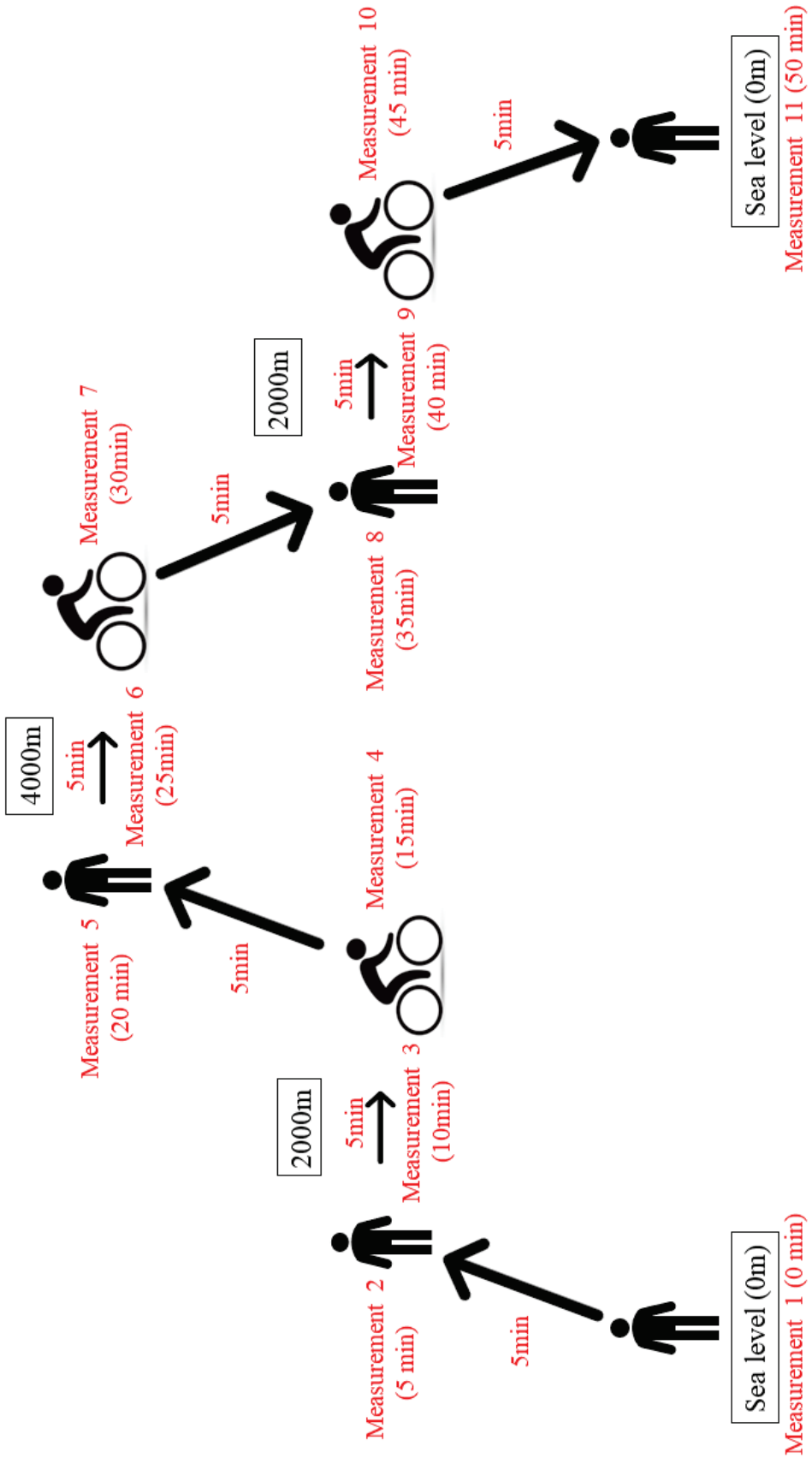

Figure 3.15. Protocol used to calibrate the oxygen saturation measurement.

A custom database was created using the gathered data and the R value was calculated for the signals classified as excellent by the SQI algorithm. Then, the results were plotted against the reference equipment using a linear regression [34]. A linear regression is a statistical method used to model the relationship between two different variables, typically to predict one variable based on the other. The regression was fine-tuned and each empiric coefficient that relates the R value and SpO_2 was extracted (see Figure 3.16).

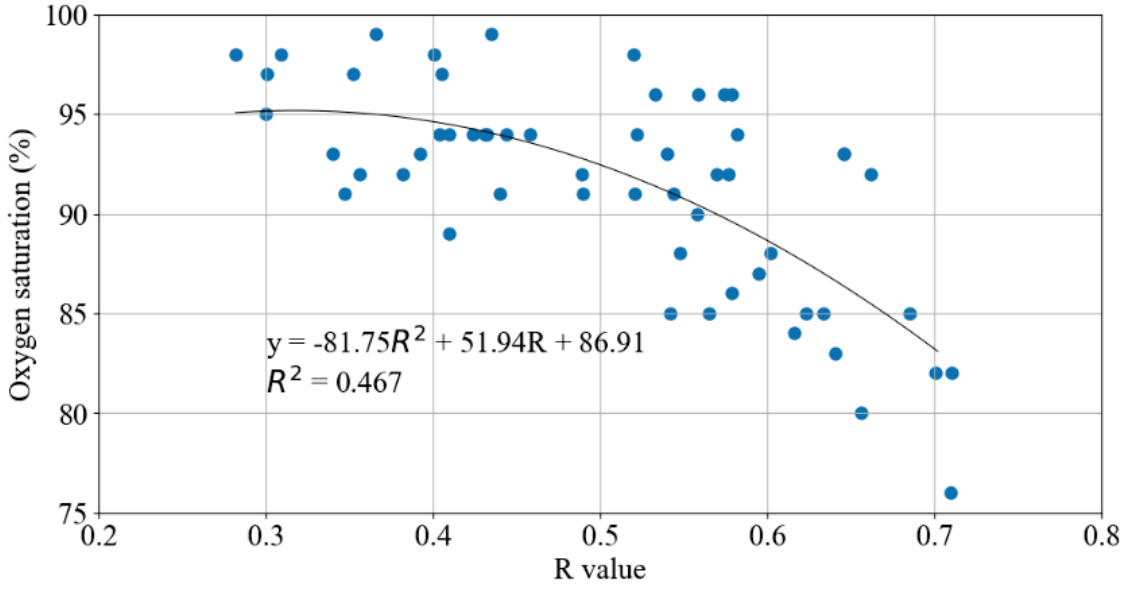

Figure 3.16. Oxygen saturation linear regression fit.

3.4.3. Blood pressure

The ABP algorithm must be calibrated because the PPG signals change in both shape and magnitude depending on the used optics. These variations affect the calculation of the area under the systolic peak, which is utilized to estimate this vital sign.

To calibrate the ABP measurement, 20 males and 12 females with ages ranging from 21 to 40 (mean of 27.8 years and STD of 8.5 years) were recruited. They were informed about the trial and gave their consent (appendix 2 – Data protection consent) to use the data gathered during the experiments. Upon the consent was obtained, an ONAVITAL device was attached to the volunteer wrist and three minutes of pulse oximetry (green light) were recorded using a sampling rate of 50 Hz. To reduce the number of motion artifacts and ensure the hemodynamics were always the same (forces and pressures involved in the circulation of blood within the cardiovascular system), the acquisition of the raw data was at rest while the partaker was sited. After acquiring the raw data from this wearable device, three consecutive reference measurements were taken using an X4 OMRON sphygmomanometer (Omron Corporation; Osaka, Japan) [35]. The arithmetic mean of the three measurements was utilized as the reference value.

Once the data collection was over, the SQI algorithm was used to classify the signals and those clustered as excellent were used to create a custom database. This database was split in two and utilized to adjust the ABP algorithm following the same methodology of the SQI calibration process.

3.5. Preliminary studies

After the calibration process, several studies were conducted to assess the accuracy of each measurement. These studies consisted of the direct comparison between the data provided by a reference equipment and an ONAVITAL device. As it was done with the calibration process, the international ethical declarations of Helsinki were followed.

3.5.1. Pulse rate

To assess the accuracy of the PR measurement, a custom database formed by PPG signals acquired from multiple ONAVITAL devices was used. This database was created by attaching a wearable device to the wrist of each volunteer, who was previously informed about the trial and gave consent to treat the gathered data (appendix 2 - Data protection consent). 10 seconds of pulse oximetry (green wavelength) were acquired using a sampling rate of 50 Hz. At the same moment of this recording, the PR registered by the reference equipment Onyx Vantage 9590 (Nonin Medical; Plymouth, MA, USA) was also taken.

The participants of this study were six males and three females with ages ranging from 21 to 61 (mean of 32.3 years and standard deviation of 11.5 years). Once the data was gathered, the SQI algorithm was used to classify the PPG signals and those clustered as acceptable or excellent were processed by the PR algorithm. A linear regression was used to compare the results of the ONAVITAL device in front of the reference equipment (see Figure 3.17). The determination coefficient of 0.933 shows a good fit between the values obtained and the reference data, so the system can be considered accurate.

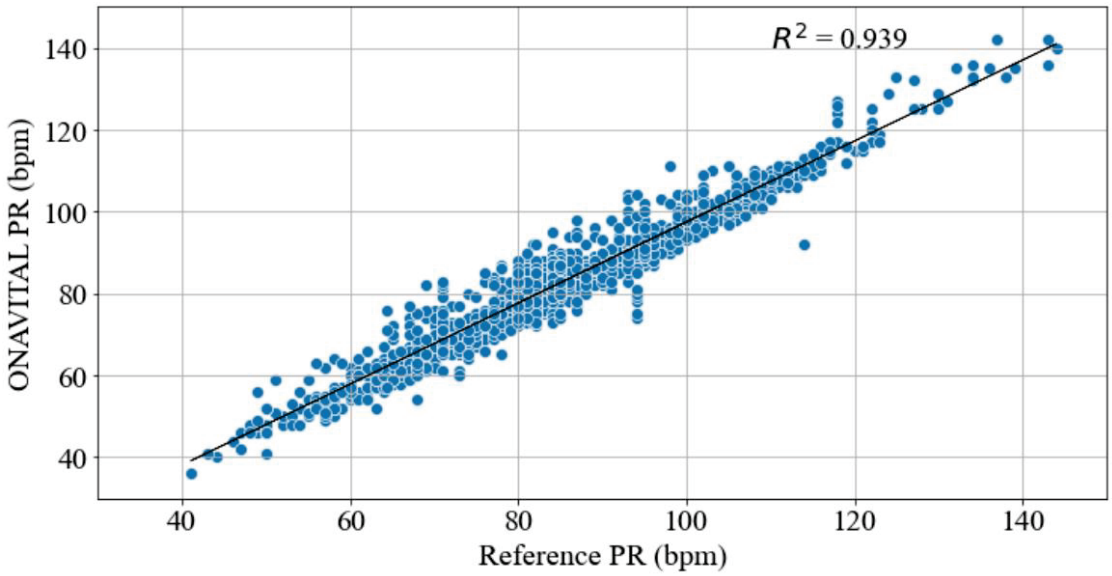

Figure 3.17. Comparison between the PR calculated by the wearable device and the reference equipment.

Moreover, a Bland-Altman plot [36] was employed to assess the agreement with the reference method (see Figure 3.18). This plot is a graphical method that allows to visually inspect the presence of any systematic bias or trends between the two measurement techniques, as well as to identify any potential outliers across the range of measurements. In this case, the Bland-Altman plot reveals few outliers within acceptable limits of agreement, underscoring the reliability of the PR algorithm.

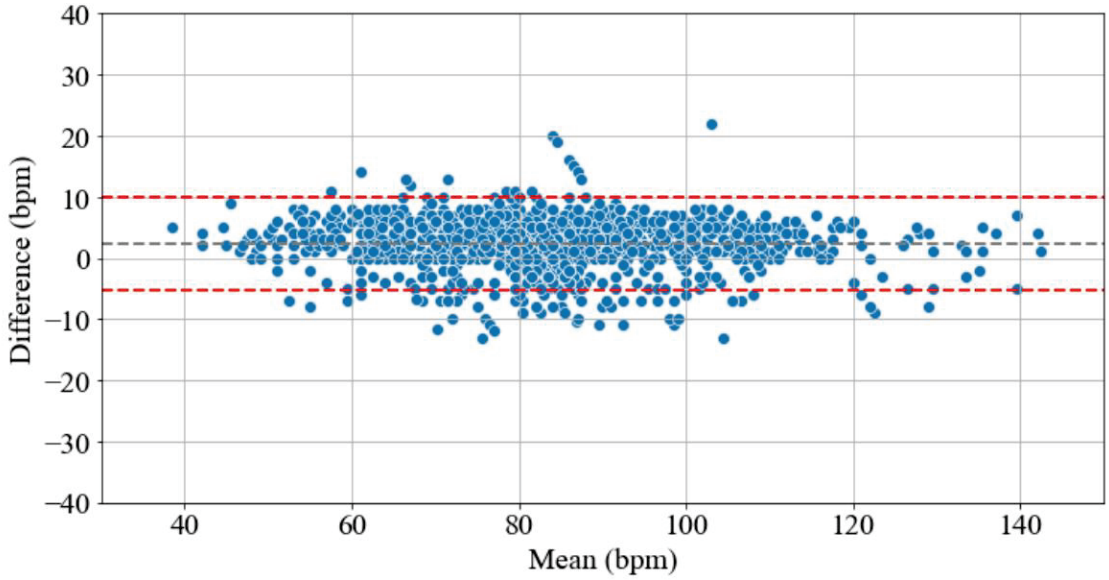

Figure 3.18. Bland-Altman of the PR values obtained.

In addition to these analytical methods, two metrics were calculated. These metrics were the mean absolute error (MAE), that expresses the agreement between the predicted and the reference value (see Equation 3.8), and the STD, which is used to assess the data dispersion.

$$MAE = \frac{1}{N}\sum_{n=1}^{N} x_n - \overline{x_n} \tag{3.8}$$

where x_n is the predicted value, $\bar{x}_n$ is the reference value, and N is the number of measurements for both metrics.

As the obtained MAE is below the limit of 3 bpm imposed by the international standard for pulse oximeters ISO 80601-2-61 [37], the system can be considered accurate for the PR measurement. Furthermore, the STD below 5 bpm indicates that this vital sign estimation is reliable and robust (see Table 3.1).

Metric	Value
MAE	2.99 bpm
STD	3.82 bpm

Table 3.1. PR metrics of the ONAVITAL device.

3.5.2. Oxygen saturation

To validate the oxygen saturation measurement, the same protocol as the calibration process was used. The main difference relied on the estimation of the SpO_2 value by the ONAVITAL device instead of recording raw data. The participants of this study were 18 males and 16 females with ages ranging from 19 to 29 (mean of 21.4 years and STD of 3.8 years). Each volunteer was informed before the trial and gave their consent to use the data extracted from the experiments (appendix 2 - Data protection consent).

Many of the recorded signals by the ONAVITAL device were classified as low-quality signals by the SQI algorithm due to motion artifacts. This issue gave as an outcome a

dataset with low data dispersion because the majority of the recorded values are comprised in the range from 90 to 100 %. Due to the low data dispersion, instead of a linear regression analysis, the root mean square error (RMSE), that expresses the agreement between the predicted and the reference value (see Equation 3.9), and the STD were calculated (see Table 3.2).

$$RMSE = \sqrt{\frac{1}{N}\sum_{n=1}^{N}|x_n - \overline{x_n}|^2} \tag{3.9}$$

where x_n is the predicted value, $\bar{x}_n$ is the reference value, and N is the number of measurements for both metrics.

Metric	Value
RMSE	3.35 %
STD	2.44 %

Table 3.2. SpO_2 metrics of the ONAVITAL device.

As the calculated RMSE is below the limit of 4 % marked by the norm for pulsi oximeters, the measurement can be considered accurate. Furthermore, the STD below 2 % indicates the low data dispersion.

3.5.3. Arterial blood pressure

To assess the accuracy of the ABP measurement, the same protocol of the calibration process was used but instead of recording the raw data, this vital sign was estimated. The volunteers of this preliminary study were 16 males and 18 females ranging from 19 to 50 (mean of 22.3 years and STD of 7.3 years). Every participant of this study was informed before the trial and gave the consent to treat the gathered data (appendix 2 - Data protection consent).

Two Bland-Altman plots were used to evaluate the agreement of the ONAVITAL device with the standard method (see Figure 3.19). The first plot was utilized to assess the performance of the SABP and the second to evaluate the DABP. Both plots show few outliers within reasonable limits of agreement, so the ABP algorithm can be considered accurate and reliable.

Furthermore, the MAE and the STD for both the SABP and DABP were calculated (see Table 3.3). The obtained MAE is below the maximum error of 5 mmHg accepted by the international norm for non-invasive sphygmomanometers ISO 81060-2 [38], so the system can be considered accurate for monitoring this vital sign. Besides, the STD lower than 8 mmHg shows acceptable data dispersion.

Metric	Value
MAE (SABP)	4.79 mmHg
STD (SABP)	6.24 mmHg
MAE (DABP)	4.55 mmHg
STD (DABP)	4.86 mmHg

Table 3.3. ABP metrics of the ONAVITAL device.

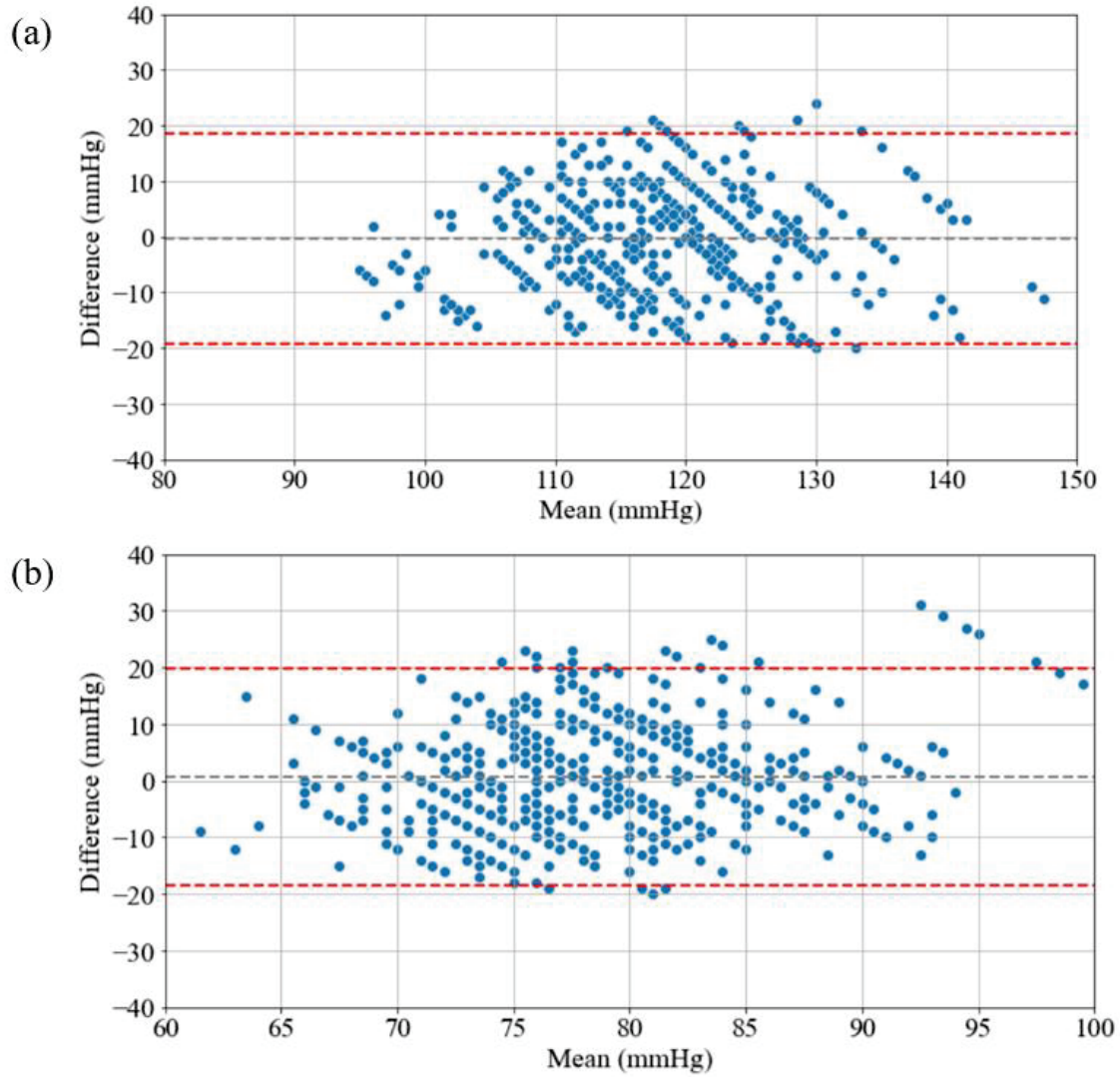

Figure 3.19. Bland-Altman of the ABP values obtained. (a) Systolic and (b) diastolic blood pressure.

3.5.4. Skin temperature

Eventually, to evaluate the accuracy of the STEMP measurement, the readings of an ONAVITAL device were compared to the measurements taken by a thermocouple. Both the wearable device and the reference equipment were placed on an IKA RCP B hot plate (IKA-Werke; Staufen im Breisgau, Germany) [39], which it controlled the environmental temperature. The temperature was incremented from 30 to 34 ºC at a rate of one degree per minute. A single measurement was recorded each minute, and the results were compared using a linear regression (see Figure 3.20). The results show a linear response and a determination coefficient of 0.921, so the STEMP measurement can be considered accurate.

Furthermore, the mean difference, which measures the mean difference between the actual values and the predicted values, was calculated (see Table 3.4). This metric below one degree demonstrates a good accuracy. There is no international standard for skin temperature measurement, so accuracy of this parameter is considered well-suited because the significant changes in STEMP typically span multiple degrees, as discussed in the first chapter.

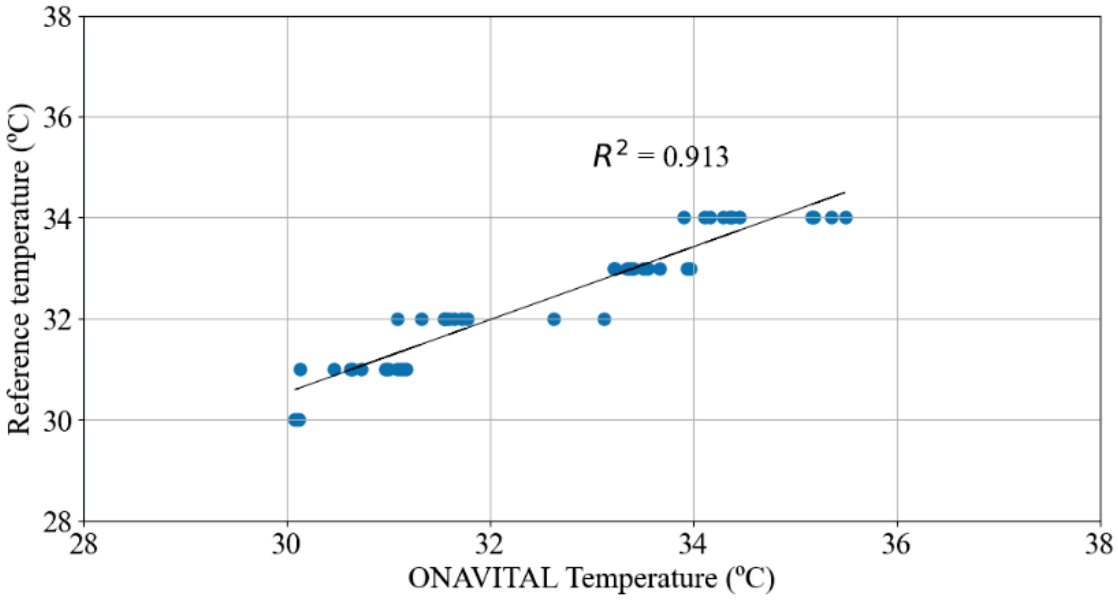

Figure 3.20. Comparison between the measurement taken by the temperature probe and the wearable device.

Metric	Value
Mean difference	0.18 ºC

Table 3.4. STEMP metrics of the ONAVITAL device.

3.6. Conclusions

In this section, a new wearable device for real-time tracking of vital signs is presented. This system is equipped with different sensors, enabling the collection, processing, and analysis of physiological data directly from the wearer's skin. The device conducts multiparametric measurements of multiple physiological parameters, allowing nurses and doctors to monitor the state of health of every patient remotely.

The ONAVITAL device takes the form of a bracelet that is attached on the patient's wrist. Its minimalistic design and conventional style make it easier for the users to adhere to the treatment and regularly wear this wearable device. The materials used to manufacture this device were selected carefully and all of them are biocompatible in order to not harm the user. Most of the potential users of the ONAVITAL device are fragile patients that are susceptible to complications, so special caution was taken when designing the device.

Every element of this wearable device has been described and characterized. The obtained results are satisfactory because the ONAVITAL system is capable of monitoring multiple physiological parameters accurately in a non-invasive and continuous way. Despite the good results, a clinical study is mandatory to assess the accuracy and robustness of this system.

The general characteristics of the developed wearable device are shown on the following table (see Table 3.5):

Form factor	Value	
Dimensions	46 x 26 x 14 mm	
Weight	15 grams	
Health features	**Range**	**Accuracy**
Pulse rate	40 to 180 bpm	± 3 bpm
Oxygen saturation	80 to 100 %	± 2 %
Arterial blood pressure	40 to 200 mmHg	± 5 mmHg
Skin temperature	30 to 34 ºC	± 1 ºC
Autonomy	**Value**	
Rated capacity of the battery	150 mAh	
Battery life	5 days (measurement frequency of 15 minutes)	
Connectivity	**Value**	
Range	Up to 10 meters	
Protocol	Bluetooth Low Energy	

Table 3.5. ONAVITAL device characteristics.

3.7. References

[1] "ONAVITAL device." Accessed: Mar. 09, 2024. [Online]. Available: https://onalabs.com/en/onavital/

[2] C. Chen, S. Ding, and J. Wang, "Digital health for aging populations," *Nat Med*, vol. 29, no. 7, pp. 1623–1630, Jul. 2023, doi: 10.1038/s41591-023-02391-8.

[3] T. Lu, S. Ji, W. Jin, Q. Yang, Q. Luo, and T. L. Ren, "Biocompatible and Long-Term Monitoring Strategies of Wearable, Ingestible and Implantable Biosensors: Reform the Next Generation Healthcare," *Sensors*, vol. 23, no. 6. MDPI, Mar. 01, 2023. doi: 10.3390/s23062991.

[4] C. Gomez, J. Oller, and J. Paradells, "Overview and evaluation of bluetooth low energy: An emerging low-power wireless technology," *Sensors (Switzerland)*, vol. 12, no. 9, pp. 11734–11753, Sep. 2012, doi: 10.3390/s120911734.

[5] "STM32L476JE." Accessed: Mar. 09, 2024. [Online]. Available: https://www.st.com/resource/en/datasheet/stm32l476je.pdf

[6] K. Hasan, N. Tom, and M. R. Yuce, "Navigating Battery Choices in IoT: An Extensive Survey of Technologies and Their Applications," *Batteries*, vol. 9, no. 12. Multidisciplinary Digital Publishing Institute (MDPI), Dec. 01, 2023. doi: 10.3390/batteries9120580.

[7] "BQ25150." Accessed: Apr. 03, 2024. [Online]. Available: https://www.ti.com/lit/ds/symlink/bq25150.pdf?ts=1712081856328&ref_url=https%253A%252F%252Fwww.ti.com%252Fproduct%252FBQ25150

[8] "BQ27220." Accessed: Mar. 09, 2024. [Online]. Available: https://www.ti.com/lit/ds/symlink/bq27220.pdf?ts=1712094478894&ref_url=https%253A%252F%252Fwww.google.com%252F

[9] “MAX30101.” Accessed: Mar. 09, 2024. [Online]. Available: https://www.analog.com/media/en/technical-documentation/data-sheets/MAX30101.pdf

[10] “TMP117.” Accessed: Mar. 09, 2024. [Online]. Available: https://www.ti.com/lit/ds/symlink/tmp117.pdf?ts=1712131034056&ref_url=https%253A%252F%252Fwww.ti.com%252Fproduct%252FTMP117%253FkeyMatch%253DTMP117

[11] “ISM330DHCX.” Accessed: Mar. 09, 2024. [Online]. Available: https://www.st.com/resource/en/datasheet/ism330dhcx.pdf

[12] “RN4871.” Accessed: Mar. 09, 2024. [Online]. Available: https://ww1.microchip.com/downloads/aemDocuments/documents/WSG/ProductDocuments/DataSheets/RN4870-71-Bluetooth-Low-Energy-Module-DS50002489.pdf

[13] “GD25Q128E.” Accessed: Mar. 09, 2024. [Online]. Available: https://www.gigadevice.com.cn/Public/Uploads/uploadfile/files/20220714/DS-00480-GD25Q128E-Rev1.2.pdf

[14] T. Tamura, “Current progress of photoplethysmography and SPO2 for health monitoring,” *Biomedical Engineering Letters*, vol. 9, no. 1. Springer Verlag, pp. 21–36, Feb. 08, 2019. doi: 10.1007/s13534-019-00097-w.

[15] M. Elgendi, “Optimal signal quality index for photoplethysmogram signals,” *Bioengineering*, vol. 3, no. 4, Dec. 2016, doi: 10.3390/bioengineering3040021.

[16] J. Lee, M. Kim, H. K. Park, and I. Y. Kim, “Motion artifact reduction in wearable photoplethysmography based on multi-channel sensors with multiple wavelengths,” *Sensors (Switzerland)*, vol. 20, no. 5, Mar. 2020, doi: 10.3390/s20051493.

[17] A. M. Cabanas, M. Fuentes-Guajardo, K. Latorre, D. León, and P. Martín-Escudero, “Skin Pigmentation Influence on Pulse Oximetry Accuracy: A Systematic Review and Bibliometric Analysis,” *Sensors*, vol. 22, no. 9. MDPI, May 01, 2022. doi: 10.3390/s22093402.

[18] B. Bent, B. A. Goldstein, W. A. Kibbe, and J. P. Dunn, “Investigating sources of inaccuracy in wearable optical heart rate sensors,” *NPJ Digit Med*, vol. 3, no. 1, Dec. 2020, doi: 10.1038/s41746-020-0226-6.

[19] N. M. H. Long and W. Y. Chung, “Reconstruction of Corrupted Photoplethysmography Signals Using Recursive Generative Adversarial Networks,” *IEEE Trans Instrum Meas*, vol. 73, pp. 1–15, 2024, doi: 10.1109/TIM.2023.3335524.

[20] S. M. A. Salehizadeh, D. Dao, J. Bolkhovsky, C. Cho, Y. Mendelson, and K. H. Chon, “A novel time-varying spectral filtering algorithm for reconstruction of motion artifact corrupted heart rate signals during intense physical activities using a wearable photoplethysmogram sensor,” *Sensors*, vol. 16, no. 1, Jan. 2016, doi: 10.3390/s16010010.

[21] C. Orphanidou, “Signal Quality Assessment in Physiological Monitoring: Requirements, Practices and Future Directions,” in *Signal Quality Assessment in Physiological Monitoring: State of the Art and Practical Considerations*, Springer, Cham, 2018, pp. 1–14. doi: 10.1007/978-3-319-68415-4.

[22] D. A. Colquhoun, K. T. Forkin, M. E. Durieux, and R. H. Thiele, “Ability of the Masimo pulse CO-Oximeter to detect changes in hemoglobin,” *J Clin Monit Comput*, vol. 26, no. 2, pp. 69–73, Apr. 2012, doi: 10.1007/s10877-012-9335-3.

[23] C. Orphanidou, T. Bonnici, P. Charlton, D. Clifton, D. Vallance, and L. Tarassenko, “Signal-quality indices for the electrocardiogram and photoplethysmogram: Derivation and applications to wireless monitoring,” *IEEE J Biomed Health Inform*, vol. 19, no. 3, pp. 832–838, May 2015, doi: 10.1109/JBHI.2014.2338351.

[24] N. Sydó, S. S. Abdelmoneim, S. L. Mulvagh, B. Merkely, M. Gulati, and T. G. Allison, “Relationship between exercise heart rate and age in men Vs women,” *Mayo Clin Proc*, vol. 89, no. 12, pp. 1664–1672, Dec. 2014, doi: 10.1016/j.mayocp.2014.08.018.

[25] J. Wan, Y. Zou, Y. Li, and J. Wang, “Reflective type blood oxygen saturation detection system based on MAX30100,” in *2017 International Conference on Security, Pattern Analysis, and Cybernetics (SPAC)*, 2017, pp. 615–619. doi: 10.1109/SPAC.2017.8304350.

[26] “World Medical Association declaration of Helsinki: Ethical principles for medical research involving human subjects,” *JAMA*, vol. 310, no. 20. American Medical Association, pp. 2191–2194, Nov. 27, 2013. doi: 10.1001/jama.2013.281053.

[27] C. Sammut and G. I. Webb, Eds., *Encyclopedia of Machine Learning*. New York: Springer , 2011. doi: https://doi.org/10.1007/978-0-387-30164-8.

[28] J. G. Webster, *Design of Pulse Oximeters*. IOP Publishing Ltd, 1997.

[29] T. Lorente-Aznar *et al.*, “Estimación de la saturación arterial de oxígeno en función de la altitud,” *Med Clin (Barc)*, vol. 147, no. 10, pp. 435–440, Nov. 2016, doi: 10.1016/j.medcli.2016.07.025.

[30] H. Casas, M. Casas, and G. Viscor, “Hypobaric Chamber: Use and applications,” 2003, pp. 243–246.

[31] Y. Mantri and J. V. Jokerst, “Impact of skin tone on photoacoustic oximetry and tools to minimize bias,” *Biomed Opt Express*, vol. 13, no. 2, p. 875, Feb. 2022, doi: 10.1364/boe.450224.

[32] M. W. Sjoding, R. P. Dickson, T. J. Iwashyna, S. E. Gay, and T. S. Valley, “Racial Bias in Pulse Oximetry Measurement,” *New England Journal of Medicine*, vol. 383, no. 25, pp. 2477–2478, Dec. 2020, doi: 10.1056/nejmc2029240.

[33] “Onyx Vantage 9590.” Accessed: Mar. 29, 2024. [Online]. Available: https://www.nonin.com/wp-content/uploads/2018/09/Instructions-for-Use-9590.pdf

[34] A. Schneider, G. Hommel, and M. Blettner, “Linear Regression Analysis,” *Dtsch Arztebl*, vol. 107, no. 44, pp. 776–782, Nov. 2010, doi: 10.3238/arztebl.2010.0776.

[35] “OMRON X4 Smart Blood Pressure Monitor.” Accessed: Mar. 29, 2024. [Online]. Available: https://www.omron-healthcare.com/storage/im-hem-7155t-esl-en-05-01-2022.pdf

[36] D. Giavarina, “Understanding Bland Altman analysis,” *Biochem Med (Zagreb)*, vol. 25, no. 2, pp. 141–151, 2015, doi: 10.11613/BM.2015.015.

[37] “ISO 80601-2-61.” Accessed: Mar. 30, 2024. [Online]. Available: https://www.une.org/encuentra-tu-norma/busca-tu-norma/norma?c=N0061425

[38] “ISO 81060-2.” Accessed: Mar. 30, 2024. [Online]. Available: https://www.une.org/encuentra-tu-norma/busca-tu-norma/norma?c=N0064845

[39] “IKA RCP B hot plate.” Accessed: Mar. 16, 2024. [Online]. Available: https://www.ika.com/en/Products-LabEq/Magnetic-Stirrers-pg188/RCT-basic-25005927/

4. Clinical evaluation

As stated in the first chapter, every device employed in a clinical setting must gain approval from the regulatory authorities of the country where it is distributed. This process is costly and time-consuming because each aspect of the device must undergo rigorous scrutiny. The accuracy and robustness of the physiological data provided are crucial functionalities of a monitoring medical device and must be validated in a clinical trial involving a healthcare institution. In this chapter, the clinical evaluation of the ONAVITAL device presented in the third section is described. This evaluation consisted of the direct comparison between the equipment used in the Intensive Care Units (ICUs) of a hospital and the wearable device under test.

4.1. Significance of a clinical study

The ONAVITAL device monitors the patient's vital signs providing valuable information to the medical personnel. To validate the accuracy and robustness of this wearable device, several clinical trials were performed in the hospital Germans Trias i Pujol (Badalona, Spain) [1]. This hospital provides care in the geographical area of *Barcelonès Nord* (*Badalona, Santa Coloma de Gramenet, and Sant Adrià del Besós*) and *Maresme Sud* (*El Masnou, Alella, Teià, Montgat, and Tiana*), which represents a population of 0.4 million inhabitants, more than 0.25 million assigned to this hospital as a basic referral. The hospital *Germans Trias i Pujol* promoted the creation of a Hospital at Home (HAH) unit at the beginning of 2000s to improve the attention provided to patients. Although this unit has a great number of advantages for patients and the organization, the physical separation from the hospital makes it difficult to monitor individuals during their stay at home, so a new tool is required to record the patient's status remotely.

To evaluate the accuracy of the data provided by the ONAVITAL device, three clinicals trials were carried out. Each study had different objectives:

- **Study 1:** This first trial involved assessing the accuracy of the data provided by this wearable device. The study was carried out with healthy volunteers. The main goal was to demonstrate that this system can be used in a clinical setting. Only the pulse rate (PR), oxygen saturation (SpO_2), and skin temperature (STEMP) were measured.
- **Study 2:** The following study consisted of monitoring patients with cardiovascular and/or respiratory diseases at ICUs. The primary objective was to validate the data accuracy when extreme values are involved. Only the PR, SpO_2, and STEMP were measured.
- **Study 3:** This final step consisted of repeating the first study to assess the accuracy of the arterial blood pressure (ABP) measurement.

Testing a new medical device in hospital facilities normally takes a lot of time, as an ethical protocol must be approved by a hospital committee to ensure patient safety and privacy. This period was longer than expected due to the COVID-19 pandemic, which collapsed the healthcare system from 2020 to 2022. For these reasons, different versions of the ONAVITAL device were utilized in the multiple stages of this clinical trial. During the first and second trials, a simpler version of the ONAVITAL was utilized (see Figure 4.1a), while the final system was used in the third test (see Figure 4.1b). This first version

included all the sensors of the definitive wearable device, but the Signal Quality Index (SQI) and the ABP algorithm were not developed yet.

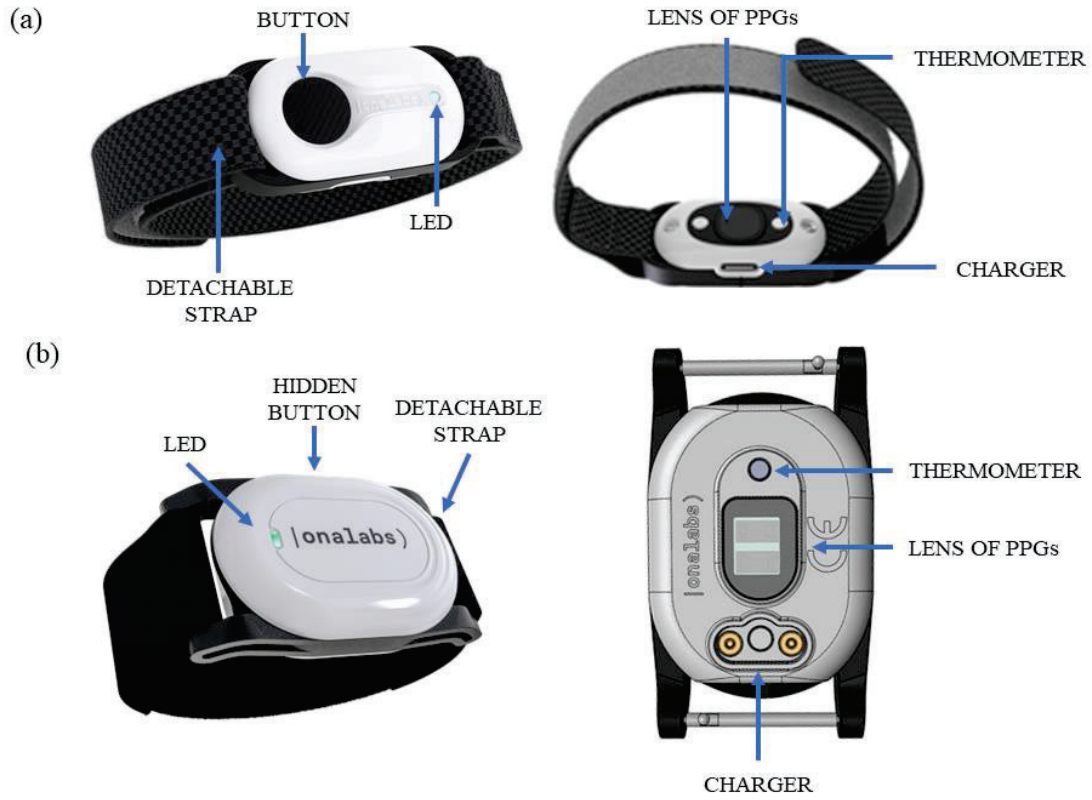

Figure 4.1. Versions of the ONAVITAL device. (a) Device used on the first and the second phase. Courtesy of Aguilar-Torán (2022) [2], used with permission. (b) Wearable device utilized in the third phase.

These studies were conducted in accordance with the international ethical declarations of Helsinki, the recommendations of the World Health Organization (WHO) [3], and the Biomedical Research Law of Spain [4]. Volunteers of each study were informed about the objectives, development, and scope of the study, and gave their consent to participate. The protocols were evaluated and approved by the Committee on Research Ethics (CEIM) of the hospital *Germans Trias i Pujol*.

4.2. Evaluation with healthy volunteers

The first trial was carried out at the Polyvalent Clinical Research Unit (UPIC) of the hospital *Germans Trias i Pujol*. This study had two main objectives:

- Validate the wearable device data by monitoring healthy volunteers.
- Assess the security of the ONAVITAL device in a clinical setting.

This phase consisted of the direct comparison between the data provided by the wearable device and the multiparametric monitors in the UPIC bedside area (see Table 4.1). These monitors are equipment regularly used in ICUs to measure the patient's vital signs.

Monitoring station	Parameters recorded
Philips SureSigns VS2	PR, SpO_2, and body temperature
Philips SureSigns VM4	Electrocardiogram (ECG) acquisition

Table 4.1. UPIC monitoring stations [5], [6].

A sample of volunteers were contacted to assess their willingness to participate in the study and to schedule a screening visit. At the visit, the UPIC's medical staff assessed the state of health of each partaker by a series of measurements. Partakers were included in the study if their vital signs were within the normal healthy range stated in the first chapter.

The participants were four males and two females with ages ranging from 23 to 26 years (mean of 23.7 years and standard deviation of 1.21 years). An ONAVITAL device was attached to the wrist of each volunteer. A single measurement of every parameter (PR, SpO_2, and STEMP) was recorded by this wearable device every five minutes. This measurement frequency was established in order to register as many points as possible without consuming the wearable device's battery. At the same time of each measurement, the monitoring station Philips SureSigns VS2 (Philips; Eindhoven, Netherlands) recorded the partaker's vital signs. This trial lasted five hours resulting in 60 data points per volunteer.

Volunteers alternated positions during the biometric recording. Measurements started at rest and alternated periods of gentle activity (walking inside the UPIC) lasting 30 minutes with periods of rest in decubitus position on the bed for another 30 minutes. These alternate positions allowed to assess the performance of this wearable device in different scenarios and evaluate if the movement affected measurements. Between these two scenarios, an ECG was recorded by the Philips SureSigns VM4 (Philips; Eindhoven, Netherlands) monitoring station.

4.2.1. Pulse rate

A linear regression was used to compare the PR measurement performance in front the reference system (see Figure 4.2a). There is a notable difference in the accuracy of the measurements when the volunteer was seated or standing. This is due to the technology itself, which is pulse oximetry. The pulse oximetry is sensitive to movement giving as a result corrupted pulse oximeter (PPG) signals and, consequently, erroneous estimations of the physiological parameters.

Apart from the linear regression, Bland-Altman plots were utilized to evaluate the agreement with the two methods. The first plot (see Figure 4.2b) shows the performance of the system when partakers were seated and the second plot (see Figure 4.2b) when they were standing. Few outliers were identified outside the confidence limits in the first scenario compared to the second one. As most of these outliers were related to the movement, the measurement can be considered accurate when no movement is present.

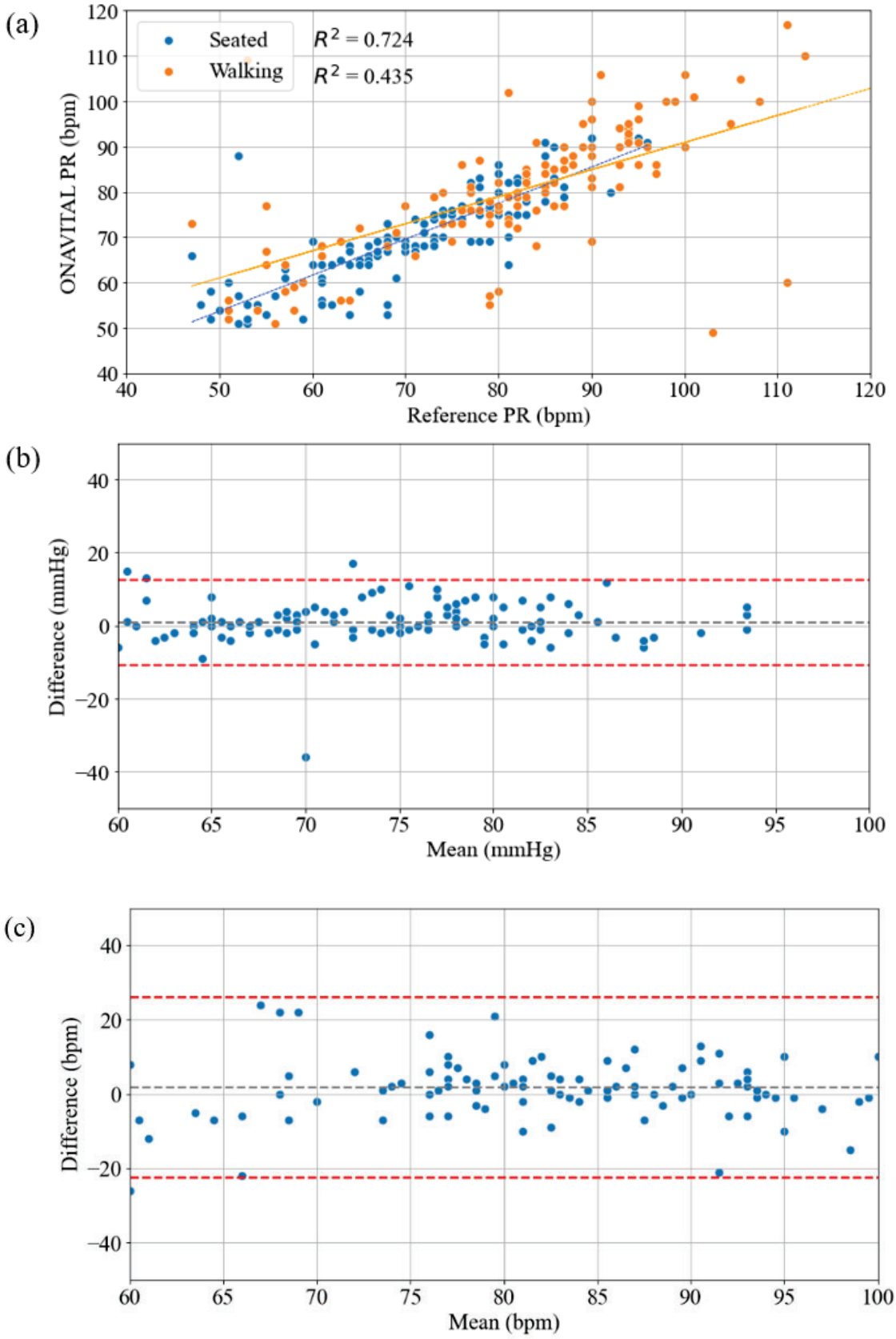

Figure 4.2. Pulse rate recorded by the ONAVITAL device and the monitoring station Philips SureSigns VS2. (a) Linear regression and Bland-Altman plot for (b) volunteers seated and (c) stand.

To test the motion artifact phenomena and conduct a reliability study, ECG heart rate (HR) measurements every 30 minutes were carried out during this study. The ECG HR is the gold standard for heart assessment, and this measurement is virtually unaffected by movement. Another linear regression and a Bland-Altman plot were employed to analyze the obtained results (see Figure 4.3). The results show a good fit between both systems, so the measurement errors observed above can be mostly associated with the measurement technology and not relevant to the purpose of the device's operation.

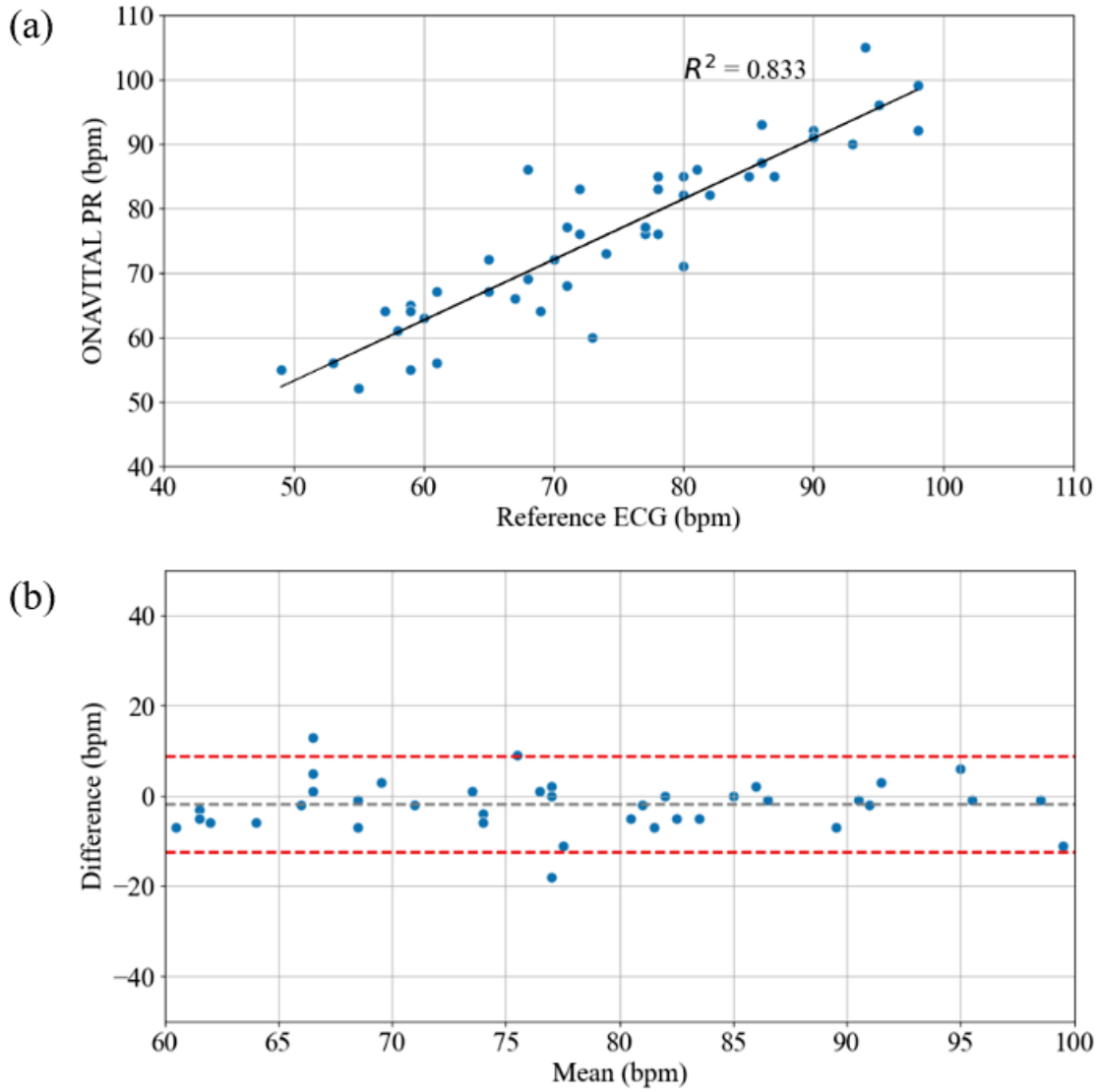

Figure 4.3. Pulse rate recorded by the ONAVITAL device and the monitoring station Philips SureSigns VM4. (a) Linear regression and (b) Bland-Altman plot.

Furthermore, two different metrics were calculated to assess the performance of this system when the volunteer is not moving. These metrics were the mean absolute error (MAE), which expresses the mean error between the predicted and the reference value, and the standard deviation (STD), which quantifies the data dispersion (see Table 4.2).

Metric	Value
MAE	2.66 bpm
STD	3.32 bpm

Table 4.2. Metrics of pulse rate comparison corresponding to the first study.

As the obtained MAE is below the limit of 3 bpm imposed by the international standard ISO 80601-2-61 for pulse oximeters, the system can be considered accurate for the PR measurement. Besides, the STD below 5 bpm indicates that this vital sign estimation is reliable and robust.

4.2.2. Oxygen saturation

Oxygen saturation for healthy individuals normally varies between 95 to 100 %. The values recorded by this wearable device during the trial consistently ranged from 97 to 100 %, aligning with the expected values. Due to the low dispersion of the gathered data, instead of a linear regression analysis, the root mean square error (RMSE) and the STD were calculated (see Table 4.3).

Metric	Value
RMSE	1.96 %
STD	1.26 %

Table 4.3. Metrics of the oxygen saturation comparison corresponding to the first study.

As the calculated RMSE is below the limit of 4 % marked by the norm ISO 80601-2-61 for pulse oximeters, the system can be considered accurate for the SpO_2 measurement. Furthermore, the STD below 2 % indicates the low dispersion of this vital sign estimation.

4.2.3. Skin temperature

The core body temperature typically varies between 36.5 and 37.5 ºC in healthy individuals. When measuring the STEMP of the upper body extremities, temperatures ranging from 30°C to 34°C are expected. During tests, temperatures similar to those expected were obtained (see Figure 4.4). Variations of up to 4ºC were observed depending on whether the patient was seated or standing. This fluctuation can be attributed to the cooling effect caused by air movement and sweat generated by body activity.

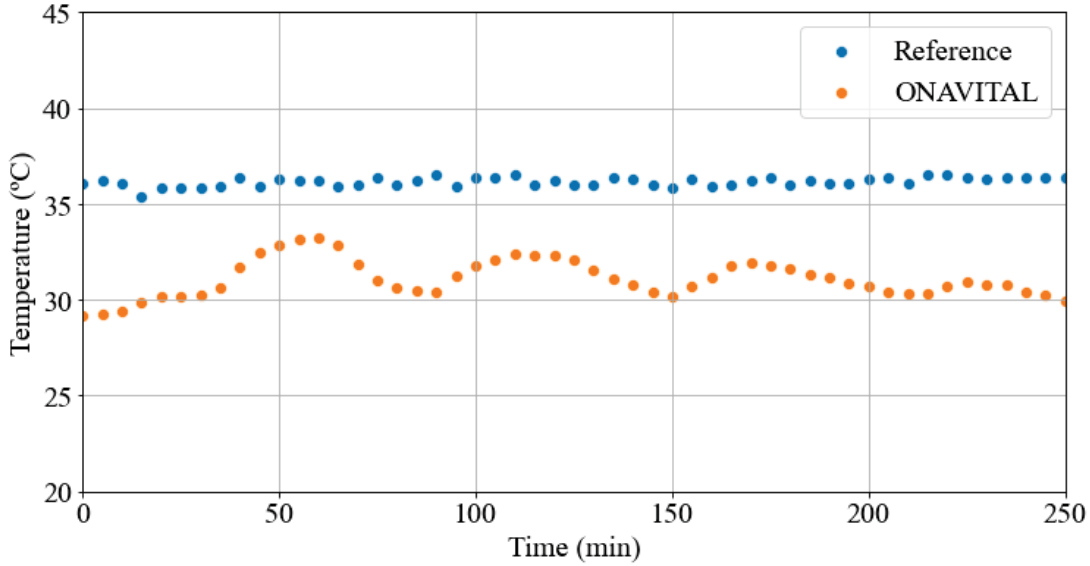

Figure 4.4. Temperature recorded by the ONAVITAL device and the monitoring station Philips SureSigns VS2 for a single individual.

4.2.4. Discussion about healthy volunteers' evaluation phase

In terms of PR, the results obtained during the trial can be considered satisfactory due to the linearity of the data and the low STD. The main issue of the system are the motion artifacts, which hamper the PR measurement. This issue can be solved by means of the SQI algorithm presented in the previous chapter.

The SpO_2 recorded at the clinical trial is the expected for healthy individuals. Despite these favorable results, more variability is required to evaluate how the system estimates oxygen saturation. To verify the wearable device measurement, the second trial with respiratory patients was carried out.

Eventually, the STEMP recorded is not the same as the core body temperature. This was expected and another approach is applied on the following trials to evaluate this measurement.

4.3. Evaluation with semi-critical patients

The second study was performed at the Intermittent Respiratory Care Unit (UCRI) and the Coronary Care Unit (UCO) of the hospital *Germans Trias i Pujol*. The main goal of this study was to validate the ONAVITAL device for remotely, continuously, and real-time collection of biometric data across various groups of individuals:

- Patients with cardiac and/or respiratory pathologies.
- Those in severe clinical decompensation.
- Individuals admitted to the semi-critical care units.

This phase also consisted of the direct comparison between the data provided by the wearable device and the multiparametric monitors of both units (see Table 4.4). The monitoring stations recorded the patient's PR, SpO2, and STEMP.

Monitoring station	Unit
Philips Intellivue MX550	UCO
Mindray ePM15	UCRI

Table 4.4. UCO and UCRI monitoring stations [7], [8].

The selection criteria (inclusion and exclusion) of patients were as follows:

Inclusion criteria:

- Patients both sexes ≥ 18 years.

Exclusion criteria:

- Patients with pathologies that interfere with an adequate assessment (i.e. terminal illness or serious psychiatric illness).
- Patient in palliative care or with limited life expectancy.
- Patients with a cognitive impairment that prevents them from understanding or completing the informed consent form.
- Patients who have participated in an interventional clinical trial during the previous three months.

The recruited participants were seven males and three females with ages ranging from 41 to 88 years (mean of 64.8 years and STD of 11.9 years). After recruiting the patients, an ONAVITAL device was attached to the wrist of each volunteer. A single measurement of each parameter (PR, SpO_2, and STEMP) was recorded with a frequency of 15 minutes. A sampling period of 15 minutes is considered enough to capture the evolution of every physiological parameter without an excessive power consumption. At the same time of the wearable device measurement, the monitoring station recorded the vital signs of each partaker. The trial lasted 24 hours resulting in 96 data points taken per volunteer.

4.3.1. Pulse rate

The dataset obtained from the trials was divided into two based on the unit where the trials were conducted (UCRI or UCO).

On one hand, a linear regression (see Figure 4.5a) was used to compare the PR results of the ONAVITAL device versus the UCRI monitoring station Philips Intellivue MX550 (Philips; Eindhoven, Netherlands). There was a good fit between the data provided by both systems since the coefficient of determination is close to one. On the other hand, a Bland-Altman plot was utilized to evaluate the agreement between the two monitoring methods (see Figure 4.5b). A few outliers were detected outside the confidence limits of the plot, so the dispersion was very low.

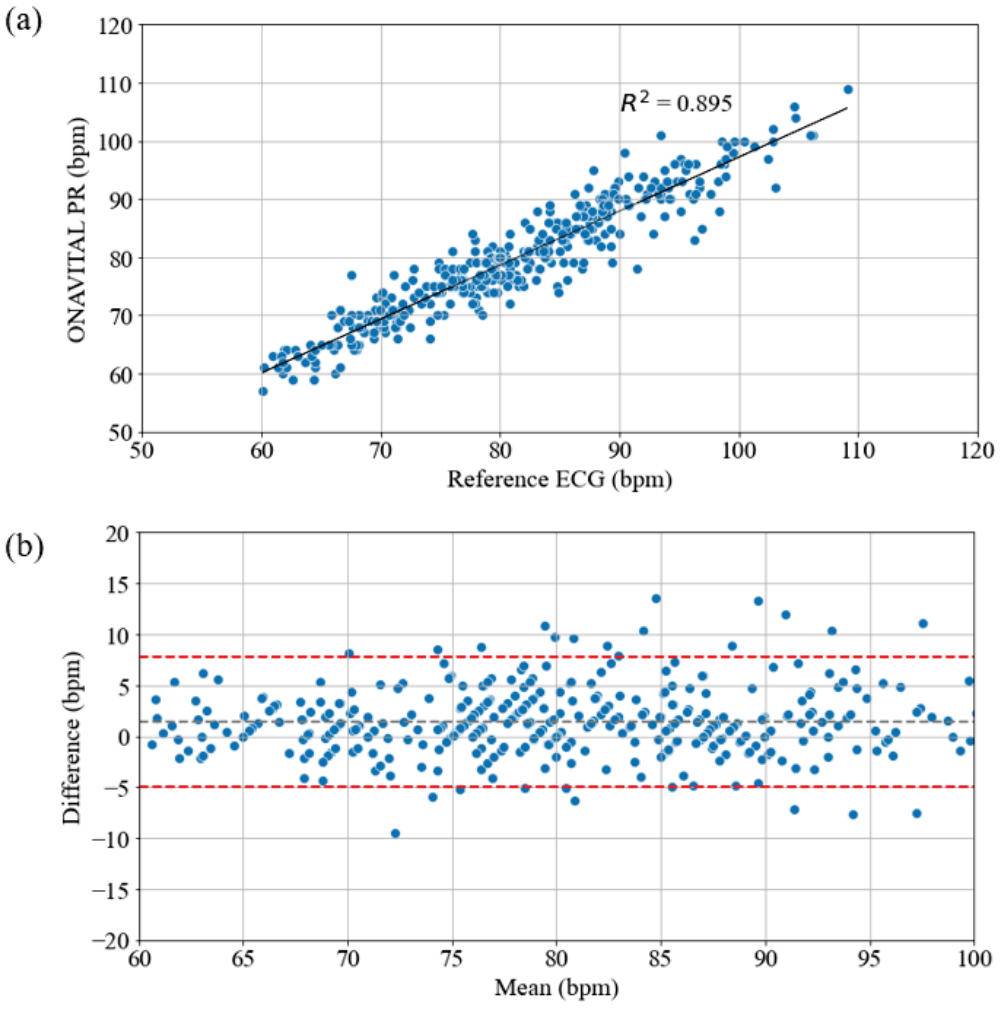

Figure 4.5. Pulse rate recorded by the ONAVITAL device and the monitoring station Mindray ePM15 from the UCRI. (a) Linear regression and (b) Bland-Altman plot.

The same methodology was used to analyze the results obtained in the UCO by the monitoring station Mindray ePM15 (Mindray Medical International Limited; Shenzhen, China). On one hand, the coefficient of determination (see Figure 4.6a) is worse than the previous analysis. On the other hand, the value of the Bland-Altman plot confidence limits is higher than expected (see Figure 4.6b), which means a large dispersion between measurements.

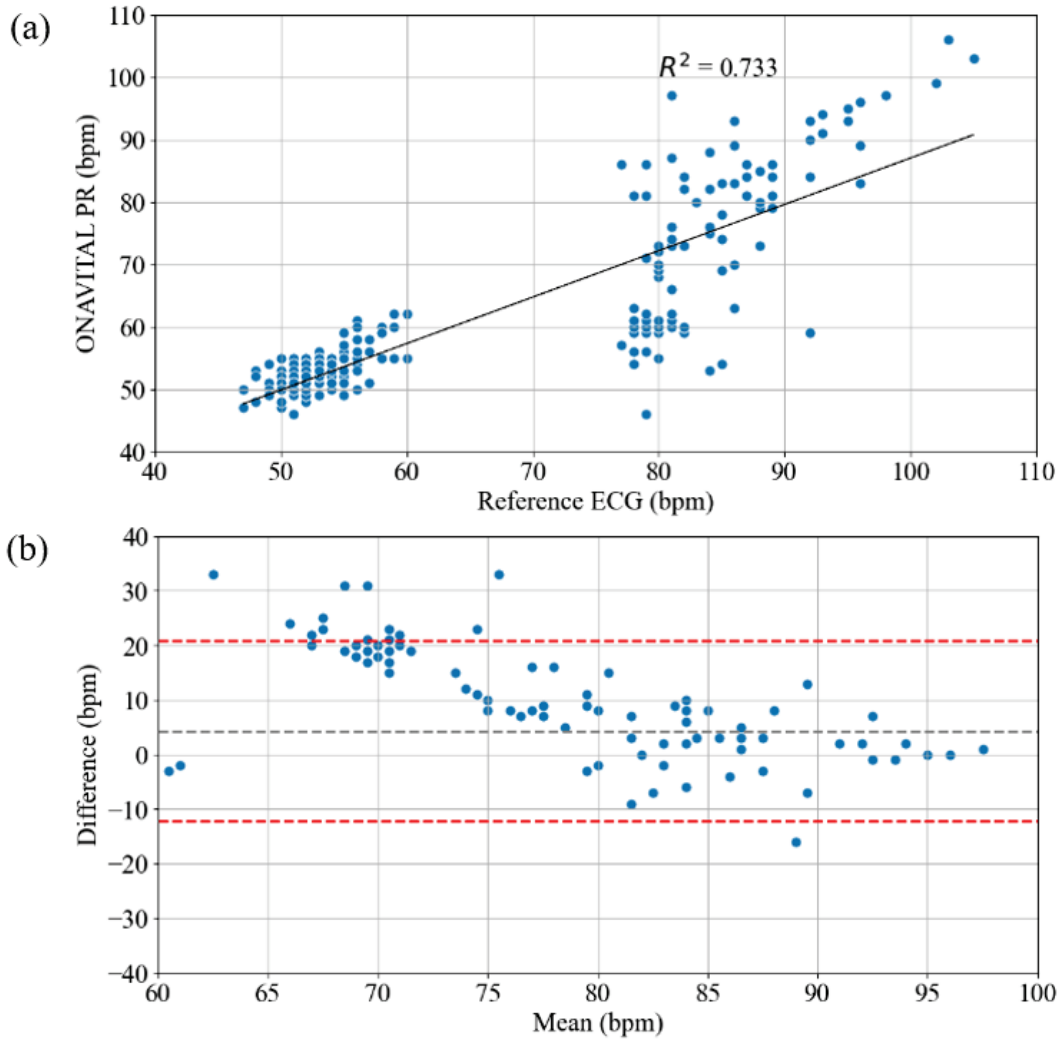

Figure 4.6. Comparison between the pulse rate recorded by the ONAVITAL device and the monitoring station Philips Intellivue MX550 from the UCO. (a) Linear regression and (b) Bland-Altman plot.

The larger error on the UCO dataset comes from a single patient (see Figure 4.7a). During the night, the PR recorded by the wearable device was lesser than the reference equipment which monitors the HR using an ECG. This issue can be attributed to the technology itself, since the PR recorded by the bedside monitor presented the same tendency as the ONAVITAL device (see Figure 4.7b). For individuals who have certain heart conditions, the heart may not efficiently push blood through the body with each contraction resulting in a PR lower than HR. Discarding the data collected from this patient, the coefficient of determination of the linear regression increases to 0.973 (see Figure 4.7c).

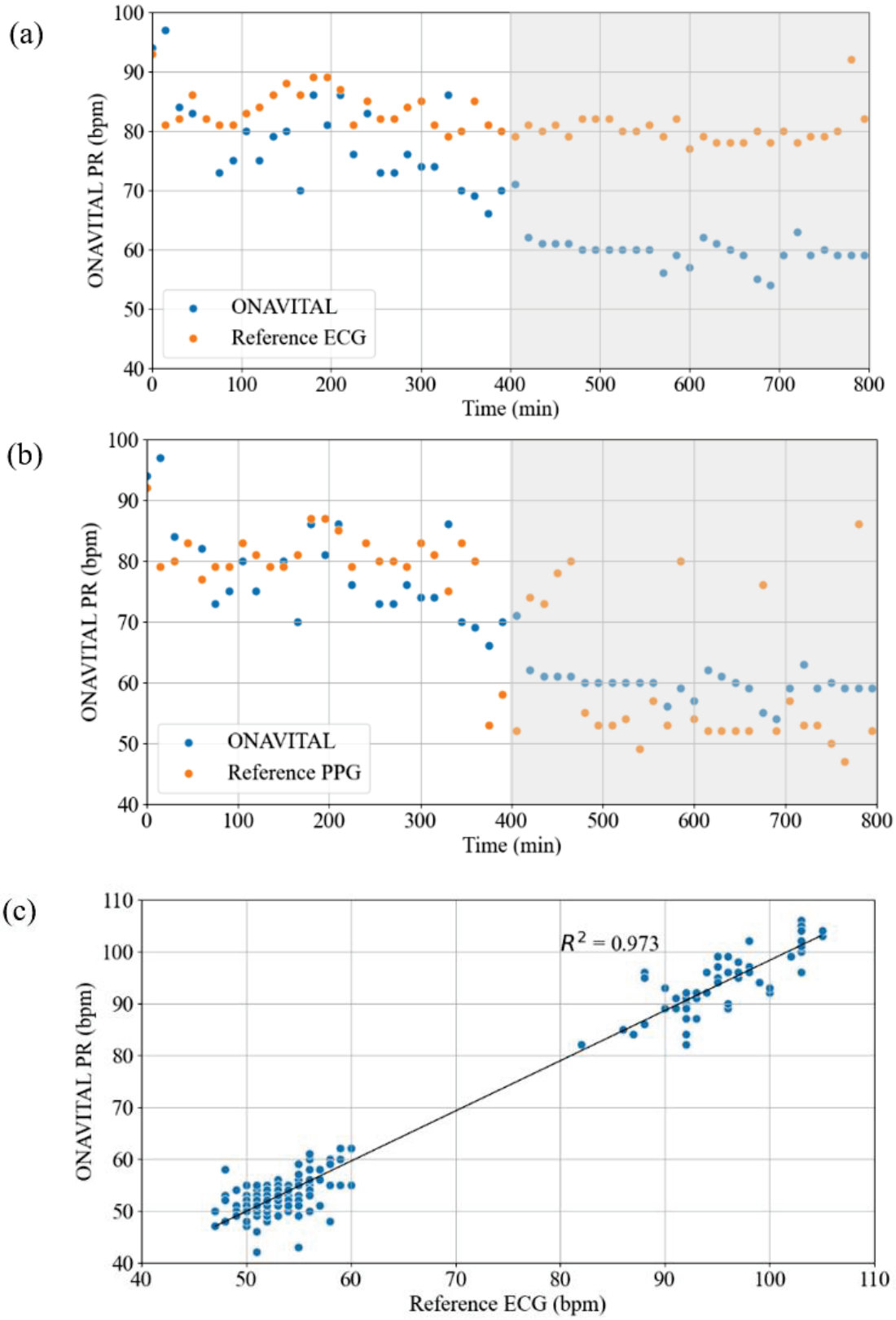

Figure 4.7. Analysis of the PR when the outlier patient is discarded. (a) Comparison between the PR measured by the ONAVITAL device, and the HR recorded by the bedside monitor from the UCO (in gray is highlighted the night). (b) Comparison between the PR measured by the wearable device and the reference equipment (in gray is highlighted the night). (c) Linear regression after discarding the outliers' values.

Furthermore, both the MAE and STD for both units were calculated after discarding the aforementioned outlier values (see Table 4.5). The obtained MAE is practically equal to the limit of 3 bpm imposed by the international standard ISO 80601-2-61 for pulse oximeters, so the system measures PR with acceptable accuracy. Besides, the STD below 5 bpm indicates that this vital sign estimation is reliable.

Metric	Value
MAE	3.15 bpm
STD	3.75 bpm

Table 4.5. Metrics of the UCO and UCRI pulse rate comparison.

4.3.2. Oxygen saturation

Lower values of SpO_2 were recorded at both units compared to the previous study. Despite lower saturations were obtained, many volunteers were administered with artificial oxygen, which maintains the SpO_2 levels stable and within the healthy range. This situation gives as an outcome a low data dispersion. Due to this fact, instead of a linear regression analysis, the RMSE and the STD were estimated for both units (see Table 4.6).

Metric	Value
RMSE	1.75 %
STD	1.01 %

Table 4.6. Metrics of the UCO and UCRI oxygen saturation comparison.

The obtained results are positive since the RMSE was below the limit imposed by the international norm for pulse oximeters and the STD is less than 2 %.

4.3.3. Skin temperature

During this clinical trial, the reference STEMP was also measured using a temperature probe attached to the patient's arm (see Figure 4.8). The adherence of this probe was not very reliable, so during some phases of this test the temperature acquired by the bedside monitor was the environment temperature.

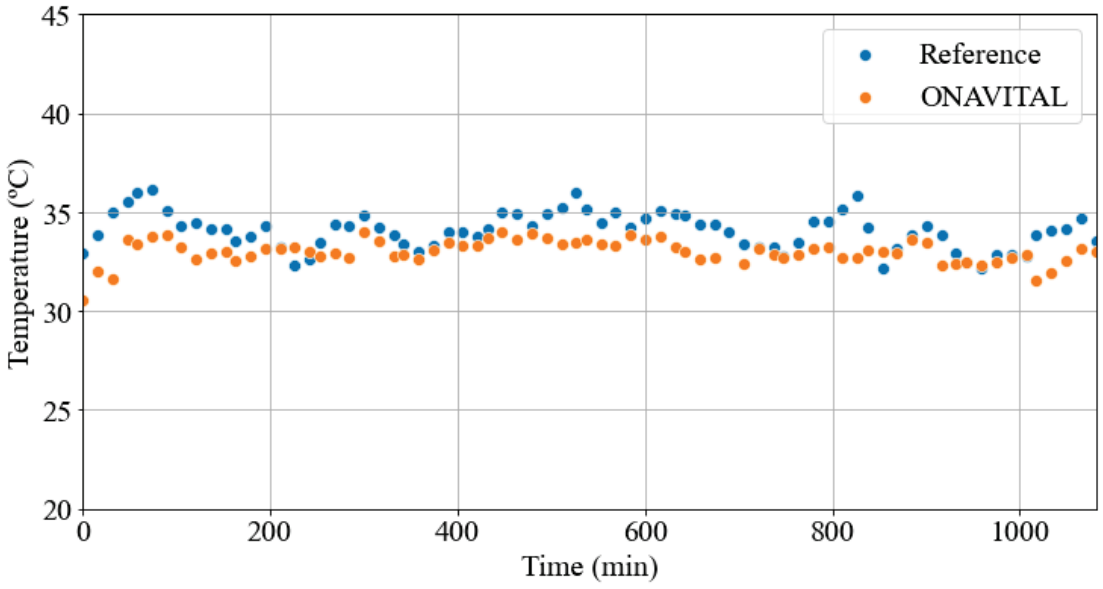

Figure 4.8. STEMP evolution of a single patient.

Due to the low dispersion of the recorded data, both the mean difference and STD were estimated and used to analyze the system performance (see Table 4.7).

Metric	Value
Mean difference	1.49 ºC
STD	1.10 ºC

Table 4.7. Metrics of the UCO and UCRI skin temperature comparison.

The mean difference and the STD calculated were greater than expected and can be attributed to the bad adherence of the temperature probe. Despite this fact, the results can be considered acceptable due to the low dispersion of the gathered data.

4.3.4. Discussion about semi-critical patients' evaluation phase

The obtained PR results can be considered satisfactory for both the UCRI and UCO trials due to the data linearity and the high correlation coefficients. The main issue was found in the OCU dataset, since the PR of one patient was different to the recorded HR. This is a limitation of the PPG technology since individuals who have certain cardiac conditions can present lower PR than HR. The same trend of PR was followed by the reference equipment and the wearable device, so the ONAVITAL PR measurement can be considered accurate.

Graphs related to SpO_2 and STEMP are not presented due to the low dispersion of the recorded data. Instead, RMSE and STD were the metrics used to analyze the obtained results. These results can be considered satisfactory for both measurements due to the low value of the metrics calculated.

4.4. Arterial blood pressure validation

Eventually, the first trial was carried out again using the final version of the ONAVITAL device. The main goal of this trial was to assess the accuracy of the ABP measurement. The same procedure of the first study was followed except for the position of the body, which was always seated to minimize motion artifacts.

Once the volunteers were recruited and included in the study, an ONAVITAL device was attached to the wrist of each volunteer. The participants consisted of four males and four females with ages ranging from 20 to 25 years (mean of 22.6 years and STD of 1.3 years). A single measurement of every parameter (PR, SpO_2, ABP, and STEMP) was recorded by this wearable device every 20 minutes. At the same time, the monitoring station Philips SureSigns VS2 (Philips; Eindhoven, Netherlands) recorded the partaker's vital signs.

The 20-minute recording frequency was set to reduce the inconvenience caused by constant measurement of the ABP by the reference equipment. This measurement was made using a sphygmomanometer, which blocks the flow of blood to carry out this estimation leading to major discomfort. Given this measurement period, 18 data points per volunteer were recorded as the trial lasted 6 hours.

Despite measuring every parameter, only the PR and ABP were analyzed. The other parameters did not vary enough, and the same results as those obtained in the first clinical trial were expected.

4.4.1. Pulse rate

As was done previously, a linear regression (see Figure 4.9a) and a Bland-Altman plot (see Figure 4.9b) were used to analyze the obtained results. There is a good fit between the data recorded and the reference equipment as the coefficient of determination is close to one. Besides, the plot shows scarce outliers outside reasonable limits of confidence, so the measurement is reliable.

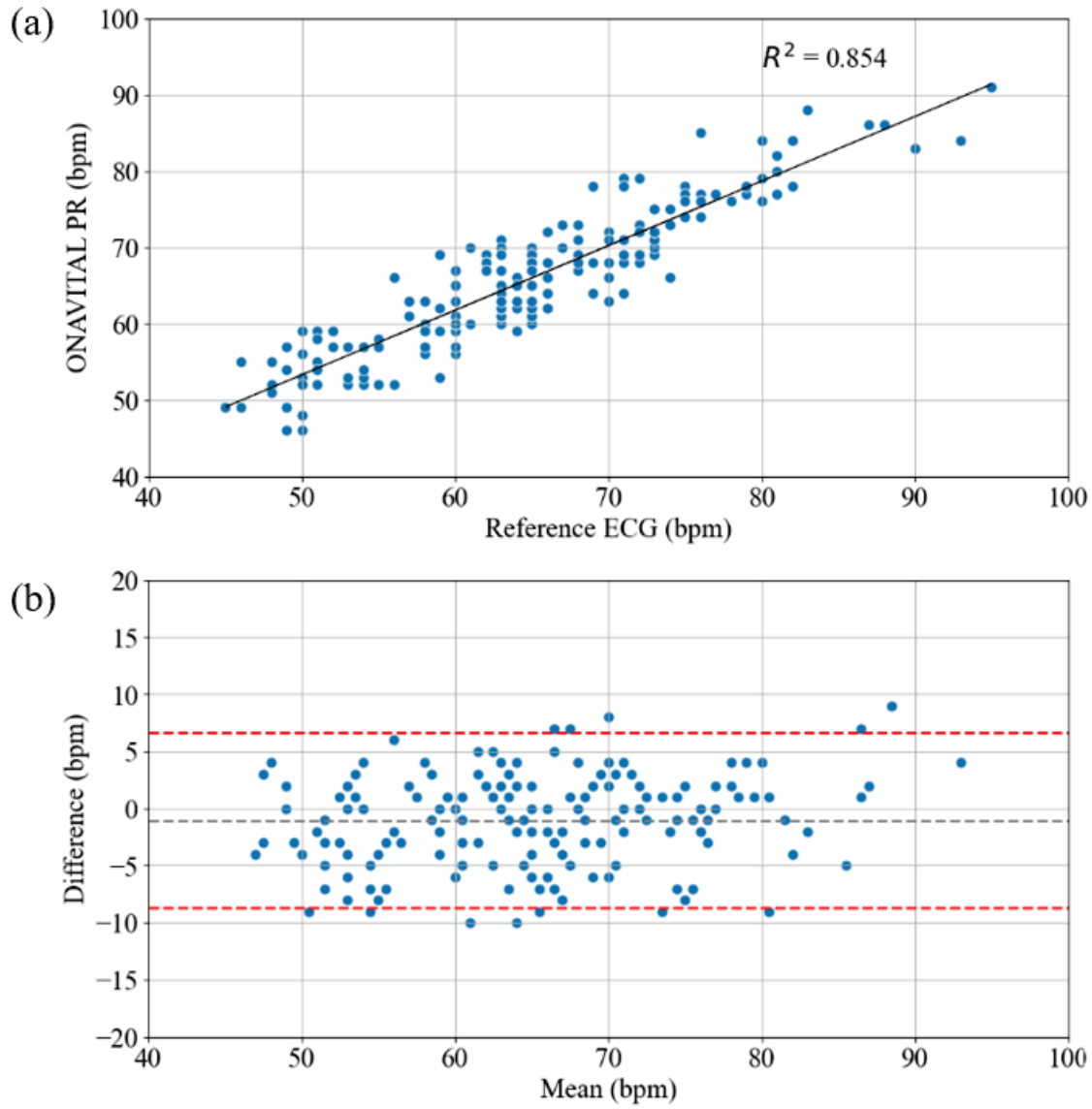

Figure 4.9. Pulse rate recorded by the final version of the ONAVITAL device and the UPIC's monitoring station. (a) Linear regression and (b) Bland-Altman plot.

Furthermore, the metrics were calculated again (see Table 4.8). This final system complies with the norm ISO 80601-2-61 as the MAE is lower than 3 bpm and STD is below 5 bpm.

Metric	Value
MAE	2.01 bpm
STD	3.91 bpm

Table 4.8. Metrics of the final version of the ONAVITAL pulse rate measurement.

4.4.2. Arterial blood pressure

The ABP pressure for healthy individuals normally oscillates within a well-defined range. Due to the nature of this vital sign, the dispersion of the data is not enough to use a linear regression and other statistical methods must be used. Two different Bland-Altman plots were used to assess the robustness of this measurement technique for both the systolic blood pressure (SABP) and diastolic blood pressure (DABP).

More outliers were identified for the SABP (see Figure 4.10a) than the DABP (see Figure 4.10b). Despite this fact the number of these points is residual, which means that both measurements are reliable.

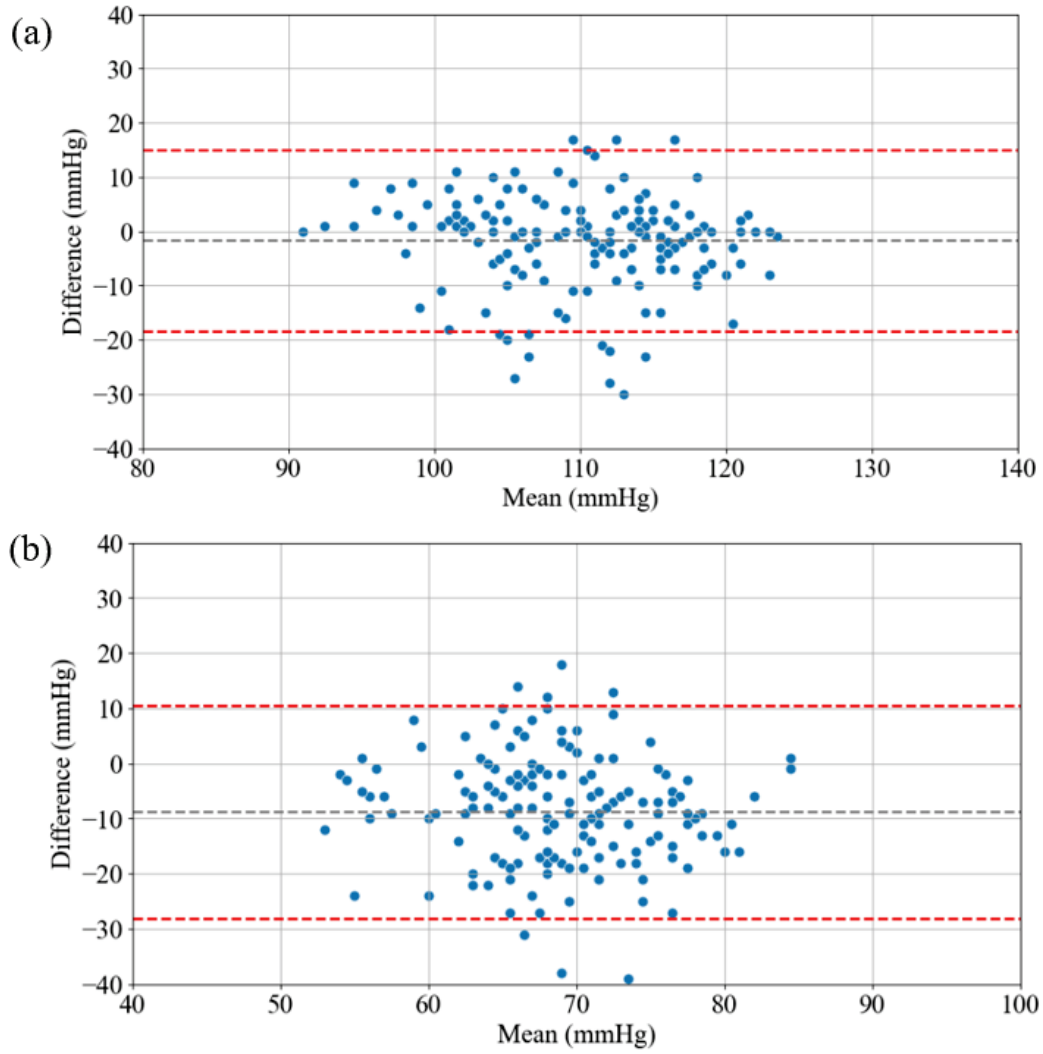

Figure 4.10. Bland-Altman plot of the (a) SABP and (b) DABP values recorded by the ONAVITAL and the reference device.

Apart from the Bland-Altman plot analysis, the MAE and the STD for both measurements were calculated (see Table 4.9).

Metric	Value
MAE (SABP)	4.50 mmHg
STD (SABP)	6.12 mmHg
MAE (DABP)	10.34 mmHg
STD (DABP)	8.08 mmHg

Table 4.9. Metrics of the ONAVITAL arterial blood pressure measurement.

On one hand, the MAE of the SABP measurement is below the 5 mmHg imposed by the international norm for non-invasive sphygmomanometers ISO 81060-2, so it can be considered accurate. Furthermore, the STD indicates an acceptable data dispersion because it is inferior to the 8 mmHg marked by this standard.

On the other hand, the MAE of the DABP measurement is higher than the expected, but the STD is close to the limit marked by the norm. This discrepancy can be associated with the simultaneous measurement of the ABP using the sphygmomanometer and the ONAVITAL device since the cuff changes the body's hemodynamics. The variation of hemodynamics leads to a negative constant bias as it is observed in the Bland-Altman plot.

To evaluate and confirm that the DABP calculation is affected by the simultaneous measurement of a sphygmomanometer, another study was carried out. This study consisted of measuring the ABP three consecutive times using the ONAVITAL device prior, during, and after the recording of the reference equipment X4 OMRON (Omron Corporation; Osaka, Japan).

The participants of this study were six males and four females ranging from 62 to 22 (mean of 33.4 years and STD of 12.9 years). Once each measurement was carried out, both the MAE and STD for the DABP were calculated for every scenario (see Table 4.10).

Scenario	MAE	STD
Before sphygmomanometer measurement	3.96 mmHg	4.87 mmHg
Simultaneous measurement	13.48 mmHg	14.61 mmHg
After sphygmomanometer measurement	7.66 mmHg	14.13 mmHg

Table 4.10. DABP metric calculated for every measurement scenario.

An increase of the error is observed in the calculated metrics. This error can be attributed to the occlusion caused by the sphygmomanometer, so the results can be considered acceptable given this harsh scenario.

4.4.3. Discussion about the arterial blood pressure evaluation

The obtained results for the PR are satisfactory since this measurement complies with the standard for pulse oximeters. Besides, an improvement compared to the first version of the device is observed. This enhancement can be associated with the SQI algorithm incorporated on the last version of the system.

On the other side, the ABP results can be considered acceptable for both the SABP and DABP. On one hand, the metrics of the SABP are below the limit imposed by the international norm for non-invasive sphygmomanometers. On the other hand, the DABP metrics are worse than expected, but these results are caused by the reference equipment. This data discrepancy does not hamper to use the ONAVITAL device to measure this parameter because the study carried out to assess this issue reveals an increase of the error of this measurement. If the sphygmomanometer is not used at the same time, an error inferior to the limit imposed by the norm is expected.

4.5. Conclusions

In this chapter, the clinical evaluation of the ONAVITAL device is presented and described. This process is an essential step for every system intended to be used in a clinical setting, such as a hospital. The clinical evaluation assesses the system accuracy and security of the device under study. Furthermore, it is crucial to demonstrate in front of the notified bodies that the system can be certified as a medical device.

Every measurement of the ONAVITAL device was compared to the results obtained by multiparametric monitors regularly used in ICUs (see Table 4.11). The outcomes of these trials reveal a close correlation between the values recorded by this wearable device and the reference equipment. This alignment demonstrates the accuracy of this system and makes the ONAVITAL device feasible to be used in a clinical setting to monitor the health state of patients with multiple pathologies.

Health features	Metric	Value	Acceptance criteria	Norm
Pulse rate	MAE	2.01 bpm	≤ 3 bpm	ISO 80601-2-61
	STD	3.91 bpm	≤ 5 bpm	ISO 80601-2-61
Oxygen saturation	RMSE	1.75 %	≤ 4 %	ISO 80601-2-61
	STD	1.01 %	≤ 2 %	
Systolic blood pressure	MAE	4.50 mmHg	≤ 5 mmHg	ISO 81060-2
	STD	6.12 mmHg	≤ 8 mmHg	
Diastolic blood pressure	MAE	10.34 mmHg (*)	≤ 5 mmHg	ISO 81060-2
	STD	8.08 mmHg (*)	≤ 8 mmHg	
Skin temperature	Mean difference	1.49 ºC (*)	≤ 1 ºC	N/A
	STD	1.10 ºC (*)	≤ 1ºC	

Table 4.11. ONAVITAL measurements performance. The (*) indicates the discrepancies observed and discussed previously.

4.6. References

[1] "Hospital Germans Trias i Pujol." Accessed: Mar. 09, 2024. [Online]. Available: https://www.hospitalgermanstrias.cat/web/guest

[2] J. Aguilar-Torán, J. Punter-Villagrasa, X. Muñoz, and P. Miribel-Catala, "Home hospitalization system for the remotely and continuous monitoring of chronic patients," in *IECON 2022 – 48th Annual Conference of the IEEE Industrial Electronics Society*, 2022, pp. 1–6. doi: 10.1109/IECON49645.2022.9968342.

[3] "Health Ethics & Governance." Accessed: Mar. 20, 2024. [Online]. Available: https://www.who.int/teams/health-ethics-governance/governance/research

[4] "Biomedical Research Law of Spain." Accessed: Mar. 31, 2024. [Online]. Available: https://www.boe.es/boe/dias/2007/07/04/pdfs/A28826-28848.pdf

[5] "SureSigns VS2+." Accessed: Mar. 31, 2024. [Online]. Available: https://www.usa.philips.com/healthcare/product/HC863278/suresigns-vs2-vital-signs-monitor

[6] “SureSigns VM4.” Accessed: Mar. 31, 2024. [Online]. Available: https://www.philips.ie/healthcare/product/HC863063/suresigns-vm4-bedside-monitor

[7] “ePM Series.” Accessed: Mar. 31, 2024. [Online]. Available: https://www.mindray.com/en/products/patient-monitoring/continuous-patient-monitoring/epm-series

[8] “Philips Intellivue MX550.” Accessed: Mar. 31, 2024. [Online]. Available: https://www.usa.philips.com/healthcare/product/HC866066/intellivue-mx550-patient-monitor

5. Certification and industrialization

The clinical evaluation presented in the previous chapter is an essential part of the medical certification process, but other steps are also involved. On one hand, the safety of the system must be tested and evaluated by regulatory authorities. On the other hand, the manufacturing process must be handled properly to ensure that every fabricated device has the same characteristics. In this section, both certification and industrialization process of the ONAVITAL device are described.

5.1. ONAVITAL certification process

As it is explained in the first chapter, any device utilized in a clinical setting must be approved by the regulatory authorities of the country where it is distributed. Medical devices in the European Union (EU) are regulated by the Medical Device Regulation (MDR), which is a set of norms that every system must comply with to receive the CE mark. Notified bodies are the organizations responsible for evaluating medical devices.

The medical certification process is divided in the following steps:

- **Intended use definition:** The intended use refers to the purpose for which a device is designed and produced. Every medical device must define its intended use to classify the equipment in one of the four MDR categories.
- **Classifying the medical device:** There are four categories in the MDR regulation that classify devices depending on its inherent risk. Depending on the category, different requirements must be fulfilled.
- **Obtain evidence:** The device must be safe and performs as is intended. Evidence verifying compliance with the MDR category requirements must be gathered.
- **Evaluation by a notified body:** Once the information is collected, the evidence is presented to the notified body. If the presented information demonstrates that the device is accurate and safe, the notified body grants CE mark to the system.

The above steps were followed to certify the ONAVITAL wearable device as a medical device.

5.1.1. Product classification

The first step of the medical certification process is classifying the device in one of the four MDR categories. To do that, its characteristics, functionalities, and intended use must be considered.

The ONAVITAL device has the following characteristics:

- Standalone, so it is not used in conjunction with another medical device or accessory.
- Non-invasive and does not come into contact with injured skin.
- Intended to monitor vital physiological parameters.
- Intended to be used directly for the medical benefit of individual patients.

According to the nature of this wrist band and its purpose, the ONAVITAL device can be classified as an IIa or IIb medical device. The difference between the two classes is a thin line that depends mainly on the intended use:

- **Class IIa:** “Active devices intended for diagnosis or monitoring of vital physiological processes”.
- **Class IIb:** “Active devices monitoring of vital physiological parameters and the nature of variations of those parameters is such that it could result in immediate danger to the patient”.

As the variations of the recorded parameters can result in immediate danger for the patient, the ONAVITAL device is classified as a IIb medical device.

In addition, considering the device intended use and classification of this system, and according to what it is stipulated on the ISO 60601-1-11 [1] entitled "Medical electrical equipment - Part 1-11: General requirements for basic safety and essential performance”, the device it is additionally classified as Transit-Operable and Portable, which defines the safety validations that must be carried out.

5.1.2. Safety assessment

Once the device is classified in one of the four categories, evidence about its safety must be collected. The clinical evaluation presented in the previous section demonstrates its accuracy, but other tests must be carried out to verify its safety: biocompatibility, electrical safety, electromagnetic compatibility, ingress protection, and shocks, vibrations, and free falls tests. These tests were performed by certified regulatory agencies.

A. Biocompatibility

Biocompatibility refers to the ability of a material to perform the function for which it has been designed without producing any harm to the user [2]. Every medical device must be biocompatible to not cause any undesirable effect on the patient. The most restrictive biocompatibility requirements are found on the class III, since many of these systems are invasive devices, such as pacemakers or prosthetics.

The ONAVITAL device is a non-invasive system that is in direct contact with the skin’s patient. Due to its non-invasive nature just one major risk must be considered which is skin irritation. To avoid this unwanted situation, the elements in contact with the patient must be biocompatible. These elements are both the cloth strap and plastic case.

The norm ISO 10993-10 [3] was utilized to evaluate if the device can cause skin irritation to the user. A dilution of 100 ml using 20 grams of the elements in-contact with the skin was prepared. Different doses of this dilution were applied on the skin of 10 guinea pigs, as these animals exhibit similar immune responses to humans. As no response was observed on the guinea pigs in comparison to the control group formed by six other guinea pigs, the ONAVITAL devices passed this test successfully.

B. Electrical and electromagnetic safety

Electronic devices of any kind must undergo thorough testing and certification before its commercialization. The main goal of this testing process is assessing the electrical security of the system and ensuring that the device does not cause interferences with other electronic equipment. To do that, electrical and electromagnetic trials are carried out. These tests characterize the device electromagnetic compatibility (EMC), which is the

ability of an electronic equipment to function satisfactorily in its electromagnetic environment without introducing intolerable electromagnetic disturbance to anything in that environment [4].

The electrical and electromagnetic trials depend on the medical device classification, its characteristics, and its intended use. In the case of the ONAVITAL device, these tests were the following ones:

- **Emission test:** Emission test measures the amount of energy emitted by an electronic system. Devices that emit large quantities of energy can interfere with other systems and represent a harm to the patient's health. To pass this test, the emission level registered during the trial must be below a certain threshold.
- **Immunity test:** It characterizes the ability of an electronic device to operate in presence of an electromagnetic disturbance. To pass this test, the device must remain unaffected by any disturbance throughout the trial.
- **Electrostatic discharge (ESD) test:** ESD is a sudden and momentary flow of electric current between two electrically charged objects. An ESD provokes multiple types of failure, such as burn or metallization defects, that may cause the device to behave abnormally or to stop operating [5], [6]. To pass the ESD test, the device must remain unaffected by a discharge applied directly on the system and operate without any interruption.

The emission and immunity trials were carried out in an anechoic chamber (see Figure 5.1). An anechoic chamber is a room designed to minimize reflections of electromagnetic waves. This room also isolates from electromagnetic energy entering from their surroundings being a perfect scenario to characterize the device EMC [7].

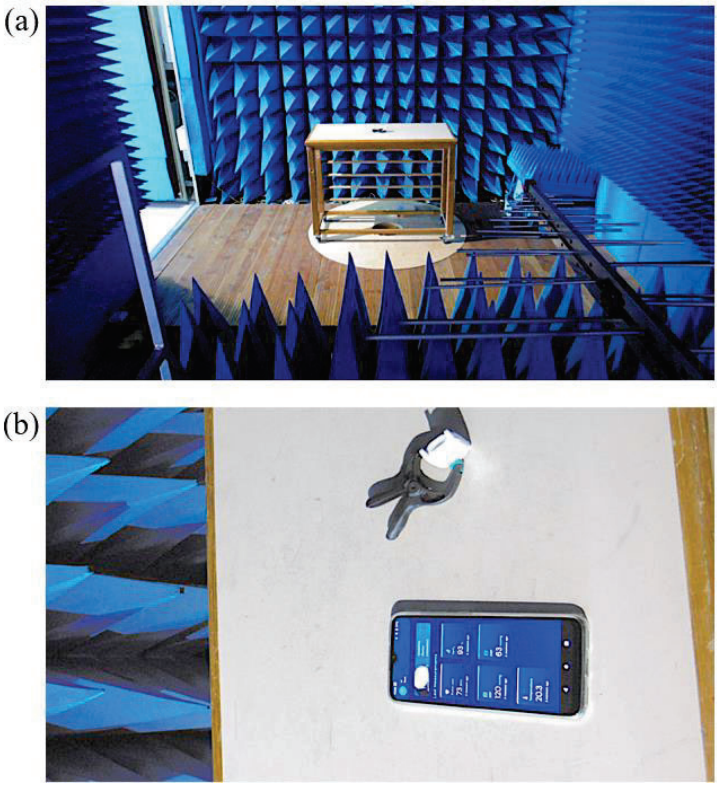

Figure 5.1. Set-up of emission and immunity trials. (a) Anechoic chamber and (b) the device under test.

For the emission testing the norms ETSI EN 303 446-1 [8], ETSI EN 301 489-1/-3 /-17 [9], and UNE-EN 60601-1-2 [10] were used. An operating ONAVITAL device was placed inside an anechoic chamber and measurements of its emissions were recorded. The frequencies measured during this trial ranged from 30 MHz to 6 GHz (see Figure 5.2). Recordings were taken using a receiver antenna in both horizontal and vertical polarization. Levels of radiation recorded were below the limit imposed by the norm except for the Bluetooth's exclusion band. Peaks between 2.40 and 2.48 GHz are allowed by the norms in order to the communication system to establish connection and exchange data. Therefore, the device passed the emission testing successfully.

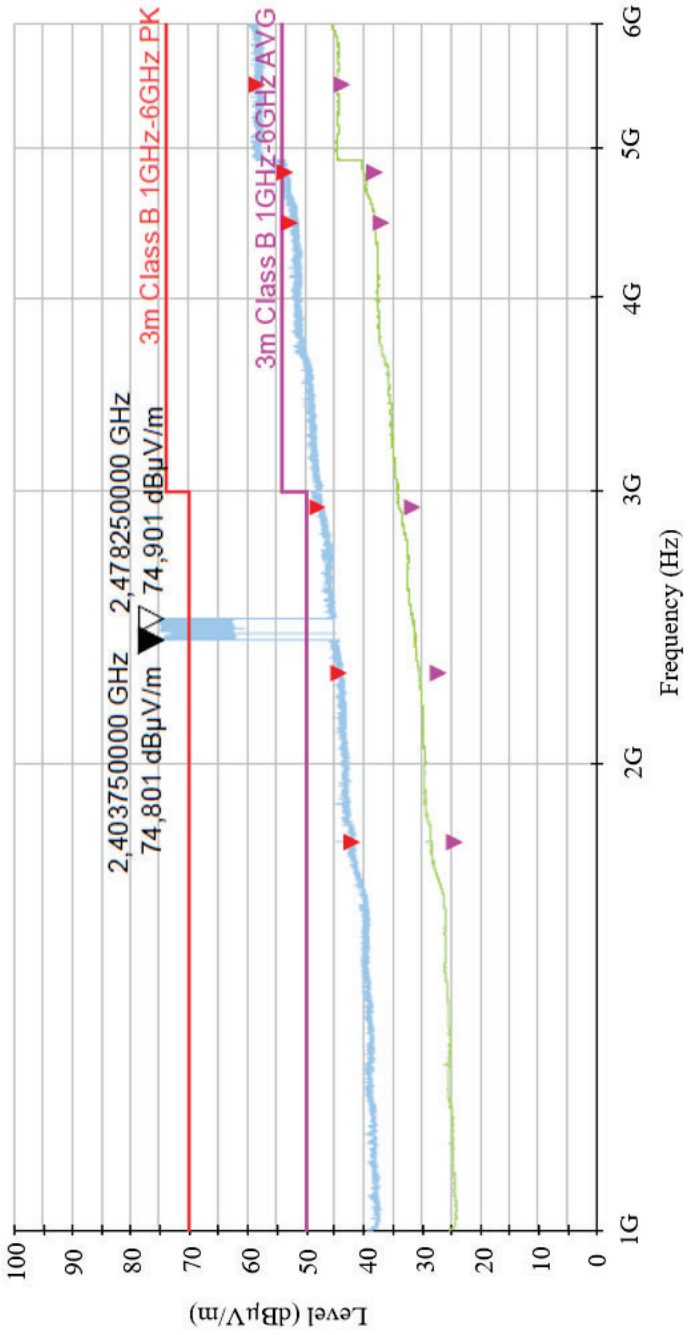

Figure 5.2. Emission spectra of the ONAVITAL device from 1 to 6 GHz. The green line corresponds to the average radiation emitted by the device, the blue line corresponds to the maximum peaks emitted by the wearable, the purple line corresponds to the average emission limit allowed by the norm, and the red line correspond to the peak emitted limit allowed by the norm. Triangles mark the peaks detected by the analysis software.

The aforementioned norms were also utilized for immunity testing. An ONAVITAL device that sends data continuously to a mobile phone was used and placed inside an anechoic chamber. A disturbance electromagnetic field that varies from 0.15 to 100 GHz was generated inside this room. During this trial, the wearable device did not interrupt the communication with the mobile phone except for the 2.4 GHz band. This band is the BLE carrier frequency, and it is an exception to the norm, so the device passed the test successfully.

Eventually, the same norms were used to evaluate immunity to ESD. An operating ONAVITAL device that exchange information continuously with a mobile phone was utilized. Discharges of ±8 kV at a frequency of 1 Hz were applied to the charge connections and the thermometer a total of 10 times. The same procedure was applied to the plastic case, but this time a voltage of ±15 kV was used. Discharges did not affect the functionality of the wearable device, so the test passed successfully (see Figure 5.3).

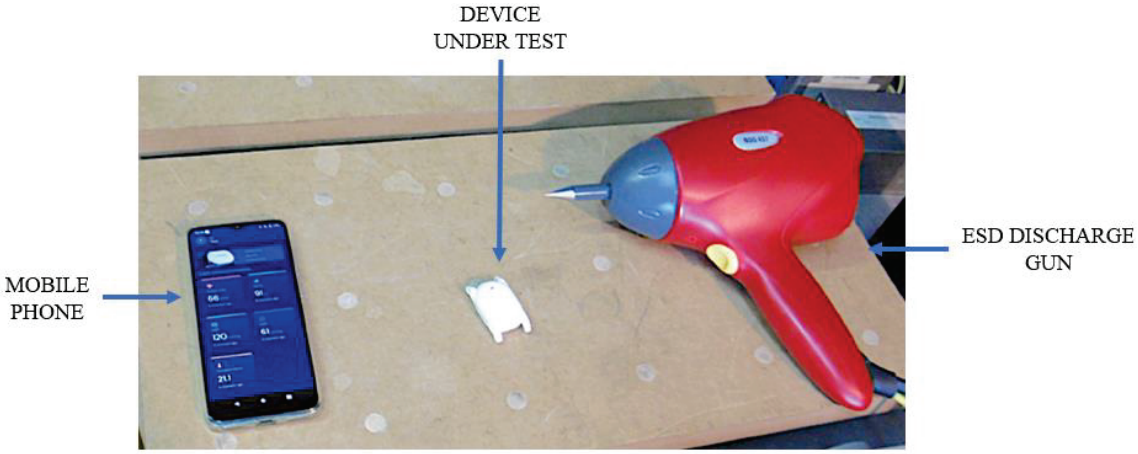

Figure 5.3. ESD testing set-up.

C. Ingress protection

Electronic equipment deteriorates or malfunction when water or dust enters inside the device. The ingress protection (IP) rating is an international standard that grades the resistance of an enclosure against the intrusion of solid particles (i.e. dust and dirt) or liquids. The IP code is composed of two digits: the first one indicates the protection against solid objects, and it is rated on a scale from 0 (no protection) to 6 (no ingress of dust), and the second one rates the enclosure's protection against liquids and uses a scale from 0 (no protection) to 9 (high-pressure hot water from different angles) [11].

The minimum IP for a medical device is IP22, which means that it is protected against objects greater than 12.5mm diameter and it is protected against drops of water. To allow patients to perform their daily routine, the ONAVITAL plastic case was designed as a grade IP65. An IP65 case does not permit ingress of dust and it is protected against powerful water jets. These characteristics allow to use the device even when the patient is taking a shower.

To ensure that the ONAVITAL device is a grade IP65, the case design was carried out with this feature in mind. All the components comprising the case must be sealed to prevent liquid entering inside the device. To do that, some elements of the plastic case are glued together, and others are joined by a sonotrode. A sonotrode is a tool utilized in

ultrasonic welding, which it is a technique that uses high-frequency ultrasonic vibrations to join materials together (see Figure 5.4) [12].

The norm UNE-EN 60529 [13] was used to evaluate the ingress protection level of the ONAVITAL device. On one hand, to evaluate the solid particle protection, a functional device was placed inside a chamber where fine particles are suspended in the air. After the exposure, the ONAVITAL device was still working, thus achieving a rating of level six for protection against solid objects. On the other hand, to evaluate the liquid protection, the same device was placed inside a chamber and subjected to powerful water jets. Since the ONAVITAL device operated correctly after the test, the level five against liquids was granted to the system.

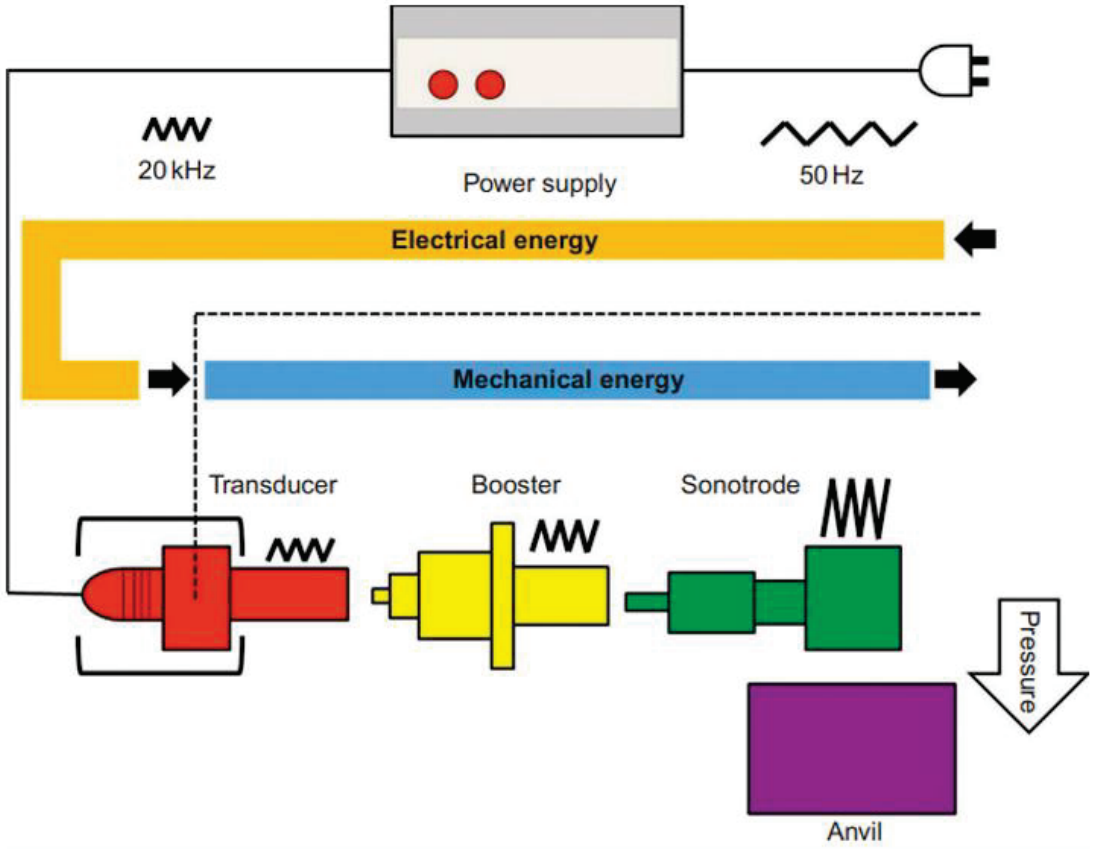

Figure 5.4. Ultrasound welding schema. Courtesy of Friel (2015) [14], used with permission.

D. Shocks, vibrations, and free falls

Mechanical stress can damage an electronic device and lead to malfunctions. Medical devices must be resistant to shocks, vibrations, and accidental falls to avoid unwanted and unexpected situations. Portable medical devices, like the ONAVITAL device, operate in harsh conditions because they are utilized in uncontrolled environments, so these systems must be resistant to mechanical stress. To evaluate this characteristic, shocks, vibration, and free falls tests were carried out. The shock test is regulated by the norm UNE-EN 60068-2-64 [15], the vibration test by the norm UNE-EN 60068-2-27 [16], and the free falls test by the norm ISO 60601-1-11.

The shock test consisted of fixing an ONAVITAL device onto a platform and applying a series of shocks to it with predefined magnitudes, durations, and directions. This wearable device was tested in every axis during 6 milliseconds using an acceleration of 300 m/s^2. The wearable device remained fully functional despite the shocks, thus passing the test successfully.

To evaluate its resistance to vibrations, a functional device was fixed on a vibration test platform. This platform generates random vibrations across a range of frequencies and amplitudes. The frequency range used was between 10 and 2000 Hz and each axis of the device was tested for 30 minutes. After the exposure, the wearable device was still working, thus the test passed successfully.

Eventually, the free fall test consisted of suspending an ONAVITAL device in the air at a height of 0.25 meters and dropping it from this altitude. The drop was conducted for each axis of this wearable device. Falls did not affect the functionality of the wearable device, so the test passed successfully.

E. Summary

Each test to evaluate the ONAVITAL device safety was conducted, and the outcomes of these trials were successful (see Table 5.1). Thus, this wearable device can be considered safe for users because it complies with the corresponding safety norms.

Test	Description	Norm
Biocompatibility	Assessment of skin irritation produced by the components in contact with the human body.	ISO 10993-10
Emission	Evaluation of the amount of energy emitted by the wearable device.	ETSI EN 303 446-1
		ETSI EN 301 489-1/-3/-17
		UNE-EN 60601-1-2
Immunity	Evaluation of the ability to operate in presence of electromagnetic disturbances.	ETSI EN 303 446-1
		ETSI EN 301 489-1/-3/-17
		UNE-EN 60601-1-2
ESD	Assessment of the device resistance against ESD discharges.	ETSI EN 303 446-1
		ETSI EN 301 489-1/-3/-17
		UNE-EN 60601-1-2
Ingress protection	Rating of the device protection against solid objects and liquids.	UNE-EN 60529
Shocks	Assessment of resistance against shocks.	EN 60068-2-64
Vibrations	Assessment of resistance against vibrations.	EN 60068-2-27
Falls	Evaluation of resistance against shocks.	IEC 60601-1-11

Table 5.1. Safety assessment summary.

5.2. ONAVITAL industrialization process

An underestimated step of the medical device development is the industrialization process. Industrialization is the process of transitioning a product from its initial design and development phase to mass production on an industrial scale. This involves setting-up the manufacturing processes, systems, and infrastructure to produce the device efficiently, cost-effectively, and in large quantities [17]. A medical device must be industrialized in a proper way since the quality of the system depends on this process and the outcomes of a medical device must be excellent regardless of the system used.

The industrialization process involves several steps which are the following ones:

- **Concept and design:** In this phase, the initial concept of the system is carried out and the detailed design specifications are created.
- **Prototyping:** It consists of assembling prototypes for testing and validation.
- **Design for manufacturing:** In this step, the product's design is optimized for efficient and cost-effective manufacturing.
- **Process planning:** This process consists of developing a detailed plan for the manufacturing process, including workflow and quality control points.
- **Quality control systems:** Quality control consists of implementing quality control measures, including testing protocols and inspection processes.
- **Production trials runs:** During this phase small-scale production runs are carried out to identify and address any issues that may arise during the manufacturing process.
- **Scaling production:** In this last phase, the production volumes gradually increase while maintaining quality and efficiency.

The mentioned steps were followed to industrialize the ONAVITAL device. Once this process is completed, large amounts of this system can be manufactured in a cost-efficient and effective manner. The process to produce this wearable encompasses the next phases:

- **Manufacturing process:** Every element that forms an ONAVITAL device is manufactured or purchased. These components must meet the quality standards of a medical device, so this step is crucial for the well-function of this system.
- **Assembly process:** To create an ONAVITAL device, these components must be assembled. This phase must be properly handled to ensure that any part of the system is damaged.
- **Quality control:** Quality control guarantees the performance and reliability of every manufactured device. Each wearable device undergoes to a rigorous scrutiny to check if every system operates as it is intended.

5.2.1. Manufacturing process

The ONAVITAL device is composed of various elements, not all of which are custom-made, some are commercial components. The off-the-shelf components are:

- Lithium polymer (LiPo) battery
- Charging cable
- Cloth strap
- Metallic piece for the thermometer

The remaining components must be manufactured since they are unique for this system:

- Electronic board
- Plastic case

A. Electronic board

First, the printed circuit board (PCB) of the ONAVITAL device is fabricated. This PCB contains each electronic component and sensor in a small area (29.0 x 22.3 mm) due to the device's reduced dimensions. The result of this area limitation is a high-density interconnected (HDI) PCB composed of multiple layers. A multilayer board is well-suited for small devices because it provides more routing space (electrical connections between components) by means of its internal layers, improving the signal integrity, and reducing the electromagnetic compatibility (EMC).

This board was designed as a 4-layer PCB. It counts with a stack-up (arrangement layers that make up a PCB) composed by power and ground planes at the external and inner layers, respectively. FR4 is the core material of this PCB, which is standard material in the electronics industry. This choice of characteristics (stack-up and core material) was made to reduce the manufacturing costs while retaining excellent specifications.

Once the PCB is manufactured, the electronic components and sensors are soldered onto this board. This is done using a surface-mount technology (SMT) assembly line (see Figure 5.5a). A SMT line is utilized because every component is a surface-mount device (SMD), which they are more integrated compared to traditional through-hole technology (THT) components. Using only SMD components not only reduces costs but also simplifies the assembly process, as a consistent technology is employed throughout the soldering process.

The first step of the soldering process is placing the solder paste on the board's exposed pads using an automated screen-printing system. Then, a pick and place machine places every component in its well-defined position. Eventually, an oven is used to solder each element to the PCB (see Figure 5.5b).

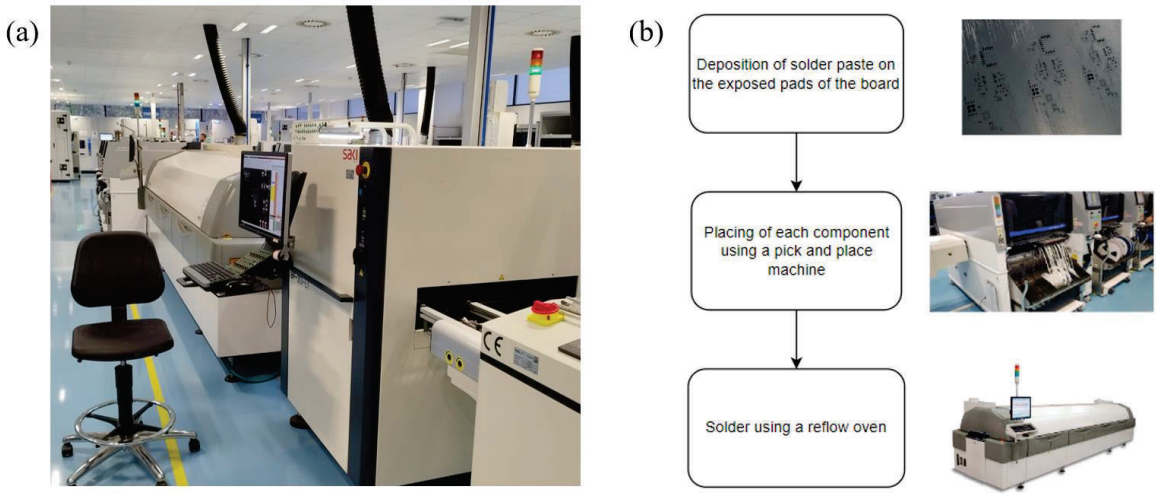

Figure 5.5. Assembly of the ONAVITAL PCB. (a) Image of the SMT line and (b) schema of the soldering process.

After soldering every component, a test for assessing the assembly process must be carried out. There are several testing methods and the use one or another depends on the board characteristics and the production rate (see Table 5.2).

Test	Description	Advantages	Drawbacks
Bed-of-nails/In-Circuit Test (ICT)	Involves a fixture with a bed of spring-loaded probes (nails) that make contact with specific test points on the PCB	Checks for shots, opens, resistance, and capacitance to show whether the assembly was correctly fabricated	Space on PCB for test points
			High fixture costs (only available for large productions)
Flying Probe (FPT)	Uses a set of movable probes controlled by a computer that move around the board to make contact with test points	Checks for shots, opens, resistance, and capacitance to show whether the assembly was correctly fabricated	Space on PCB for test points
			Long test times
Automated Optical Inspection (AOI)	AOI uses cameras and image recognition software to inspect PCBs for defects	Non-contact test	Speed and access limited
			No functional testing
		Can observe solder quality or component skew problems	No programming
			Ambiguous results

Table 5.2. Board testing methods [18], [19], [20].

An alternative to the traditional board testing techniques, such as the bed-of-nails/in-circuit test or flying probe, is the JTAG testing methodology. JTAG is a testing technology that is widely used in the electronics industry for testing and programming circuits. This system can be used to test almost every element of an electronic board without requiring physical access to the circuit. It also allows to program the circuit after a successful test.

The JTAG core is the boundary scan architecture. Each integrated circuit (IC) designed with JTAG capabilities includes a set of registers called boundary scan registers. These registers are at the boundary of the chip, between its functional core and its connection pins/balls to the rest of the system. When a JTAG test is carried out, the functional core of the integrated circuit (IC) is disconnected, and the pins are controlled by the boundary scan registers. Thus, values can be driven onto every net and the response can be monitored, which allows to detect electrical faults, such as short-circuits. JTAG testing can be also utilized to verify the board logic functionality by using the JTAG enabled devices on a board to communicate with non-JTAG peripheral devices, like DDR RAM and flash [21].

To test the ONAVITAL board, the JTAG testing technology is used. The JTAG provides excellent test coverage for this board, as most of the chips establish communication with the microcontroller (MCU) using a digital interface. This fact allows to perform a functional testing of almost every element of the manufactured board (see Figure 5.6).

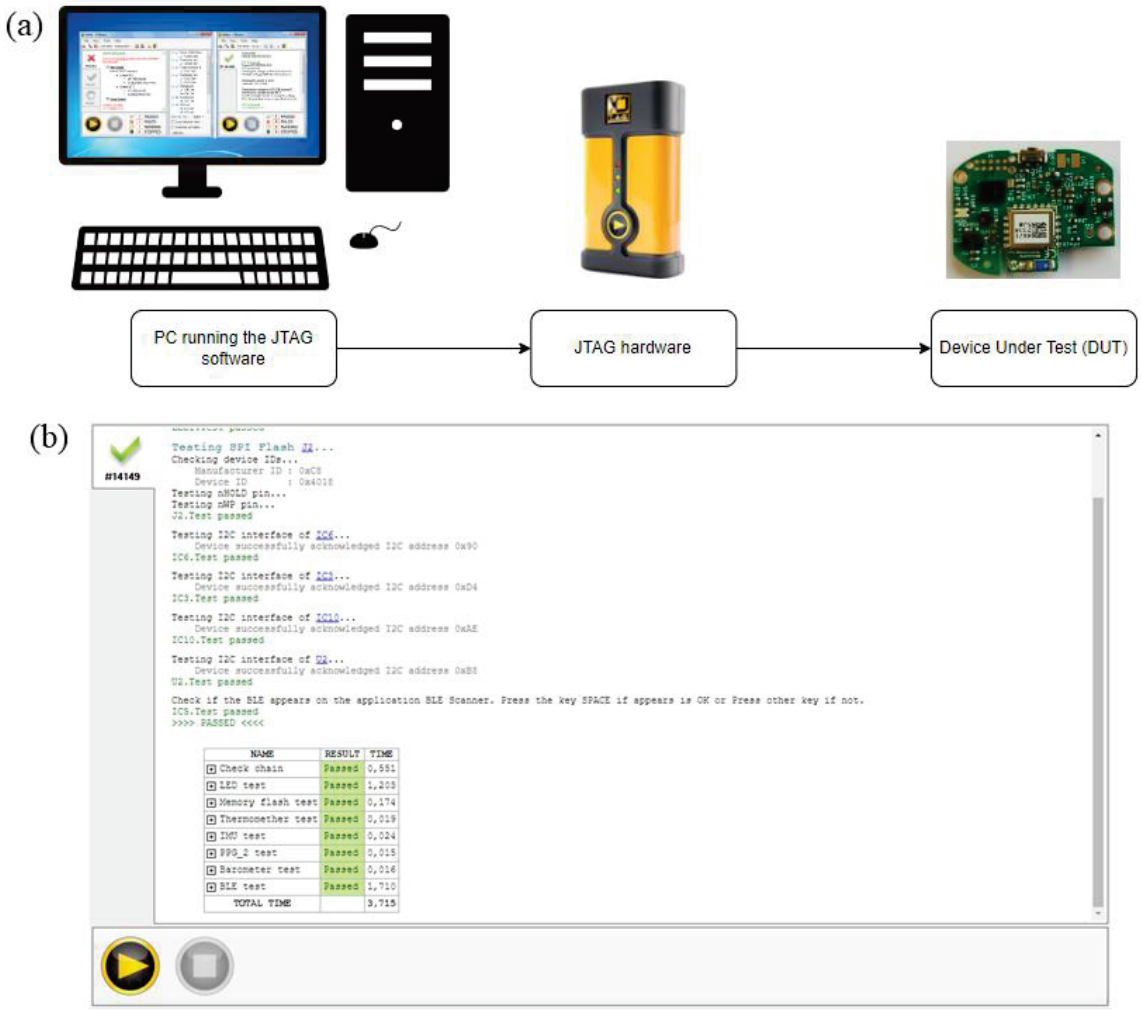

Figure 5.6. JTAG testing technique. (a) Set-up and (b) program used to test the ONAVITAL board.

B. Plastic case

There are multiple methods to manufacture a plastic case (see Table 5.3) and the choice of the technique depends on factors such as the production volume, part complexity, material properties, and cost considerations.

Technique	Description	Advantages	Drawbacks
3D printing	Layer-by-layer additive manufacturing technique where a digital model is created layer by layer using plastics	No tooling required	Limited material options
		Rapid prototyping capabilities	Slow production speed
		Minimal material waste	Surface finish requires post-processing
CNC machining	Computer Numerical Control (CNC) machines remove material from a solid block of plastic to create a desired shape	High precision and tight tolerances	High material wastage
		Wide range of materials	Long lead times
		Suitable for both prototyping and production runs	High tooling costs

Thermoforming	Plastic sheet is heated until pliable and then stretched over a mold using vacuum, pressure, or both	Cost-effective for low to medium production volumes	Limited to simple shapes
		Low tooling costs	Limited precision
		Fast manufacturing process	Not be suitable for parts with intricate details or complex geometries

Table 5.3. Plastic case manufacturing techniques [22], [23], [24].

When the production volume is large, the cost of each plastic case must be as low as possible to maintain competitive prices. Injection molding is a manufacturing technique that consists of injecting molten material into a mold cavity, where it solidifies and takes the shape of the mold (see Figure 5.7) [25], [26], [27]. This technique has several advantages:

- Injection molding allows high production rates with minimal material waste.
- This technique produces parts highly detailed with tight tolerances.
- The injection molding process provides repeatable results.
- The cost per unit decreases as production volume increases.

Despite these advantages, it also has different drawbacks. The most significant limitations are the high cost of the initial tooling cost and the long lead times for tooling. However, this method is widely used in the industry to manufacture plastic pieces.

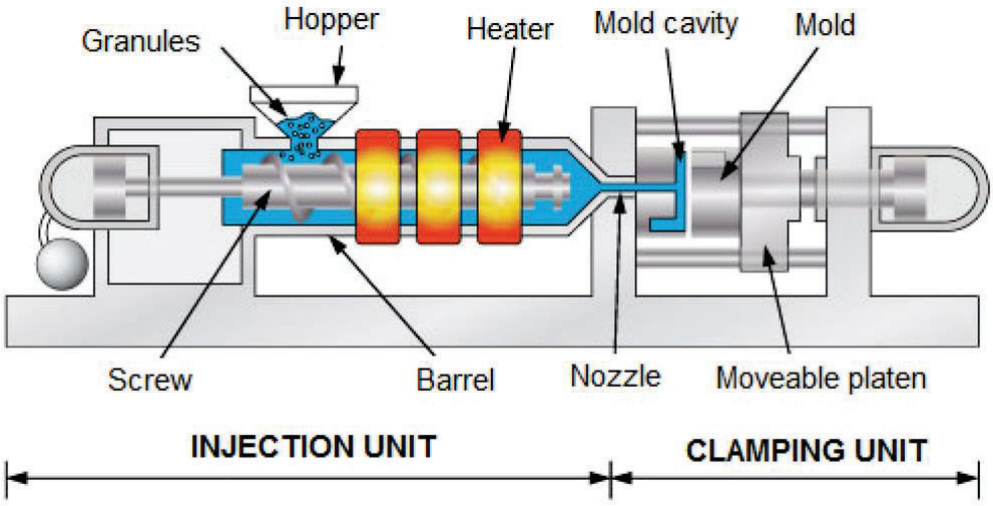

Figure 5.7. Injection molding technique. Courtesy of Svečko (2013) [28], used with permission.

The ONAVITAL case is manufactured using this technique. Two different molds are utilized to fabricate the different parts of the case. These parts are the following ones:

- Bottom case
- Upper case
- PPG lens
- Light guide of the RGB LED

5.2.2. Assembly of the device

After manufacturing every device part and acquiring the off-the-shelf components, the assembly of this wearable is carried out. The first step is screwing the board to the bottom plastic case. Then, the serial number of the device is engraved along with the required symbols (CE Mark, IP grade, etc.). Next, the pulse oximeter (PPG) lens and the metallic piece that transmits the skin temperature to the thermometer are glued to the bottom case and the RGB LED's light guide to the upper case. Following this step, the upper case is welded to the bottom case by means of a sonotrode. Eventually, the cloth straps are attached to the plastic case (see Figure 5.8).

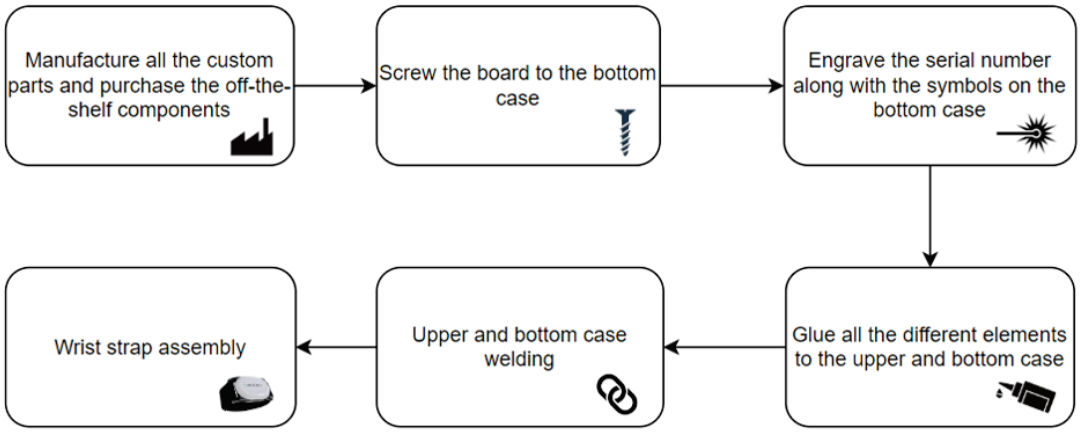

Figure 5.8. Flow diagram of the product assembly.

5.2.3. Quality control

The last step of the production process is testing every assembled device. This operation ensures that each manufactured wearable device operates as intended. The next steps are followed during this process:

- First, the tester (person who performs the product testing) initiates the testing program.
- Subsequently, the tester logs into the testing software using both a username and password.
- Then, a series of questions are asked by the software to the tester. These questions are related to the visual inspection of each device and must be answered with YES or NO. If every answer is YES, the next steps of the process are followed. Otherwise, the device is disposed, revised, and repaired if it is possible.
- Next, the device is activated by connecting the charge cable. Once the LED starts to shine, the charging cable is disconnected.
- Following the activation of the wearable device, the tester reads the data matrix engraved on the bottom of this wearable using a scanning tool.
- Then, the tester uses the testing program to establish a connection between the device and the computer.
- Next, the testing software reads the serial number of the ONAVITAL device under test and the identifier (ID) of each sensor. This information is sent to the computer and the program provides a PASS / NOT PASS outcome. If the test result is PASS, the product is ready for packaging. Otherwise, the product is disposed, revised, and repaired if it is possible.

- A report is automatically generated and stored on the computer.
- The reports are collected using a USB storage device and uploaded to a database that stores the information of every manufactured device.
- Eventually, a reset pin is used to shut down the device.

5.3. Traceability

Traceability refers to the ability to trace a product through every stage of production, processing, and distribution. Medical devices must be traceable and easily identifiable by both the end-user and the manufacturer. In the case of any event, such as a malfunction caused by a manufacturing issue, the equipment must be identified and retired or replaced as quickly as possible.

The Unique Device Identifier (UDI) [29] is a unique alphanumeric code related to a medical device. This code allows clear and unambiguous identification of specific devices on the market and facilitates their traceability. Each UDI consists of two parts: the device identifier, which identifies the version or model of the system, and the production identifier, that includes information such as the device batch number, serial number, and manufacturing date.

The ONAVITAL device is traceable at every step of its life cycle. Before the fabrication of this wearable, a manufacturing batch is generated. This code identifies each manufactured element, such as the electronics or the plastic case, that is part of the end-product. The manufactured code is 1YYMMDDX, where 1 is the internal product code, YY are the last two digits of the year, MM the month and DD the day of the manufacturing order, and the X is the hexadecimal number of the batch in ascending order (0 to F) for each manufactured batch in the same day. This only applies to the electronic circuits, as 1000 units batch were defined, for the rest of the components the X is 0, as the whole order is considered a batch.

Then, a serial number that identifies every produced unit is generated and associated with each manufactured board by attaching a sticker to it. This sticker contains the serial number encoded inside a data matrix. After attaching the data matrix to the board, the serial number is read using a barcode scanner and it is stored in the device internal memory. The ONAVITAL serial number is ManBatchIDAAA, where ManBatch is the manufactured code and AAA is each single device of the batch (0 to 999).

Eventually, when the electronic board is screwed to the case, the sticker is read again, and the UDI of the device is generated. This UDI contains the device identifier, the manufactured code, and the serial number. Eventually, the UDI is laser engraved on the bottom plastic case (see Figure 5.9).

The UDI is sent to an online database during the final product testing. In this database, not only the UDI is stored, but the testing results and the information related to the product are saved.

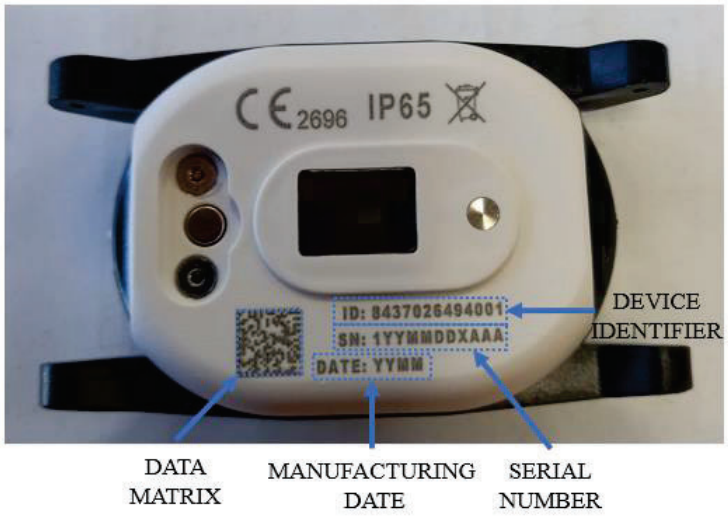

Figure 5.9. Traceability symbols engraved on the ONAVITAL case.

5.4. Conclusions

In this chapter, the medical certification process of the ONAVITAL device has been presented and described. This process is costly and time-consuming, so a lot of manufacturers avoid it. However, the only way to use a device in a clinical setting and impact the patients' lives is obtaining the medical CE mark. This process has several steps that include defining the intended use of the system, classifying the device in one of the four MDR categories, obtaining evidence about the performance and safety of the system, and presenting this data to a notified body. Only the CE mark is granted if each phase is completed successfully.

Apart from the certification process, the industrialization of this wearable device has been described in this section. Industrialization is the process of transitioning a product from its initial design and development phase to mass production. Every medical device must successfully complete this process to ensure that each distributed system has the same characteristics. This process encompasses from manufacturing to product testing, so it is a complex task that must be carried out meticulously.

Both the certification and industrialization processes are essential for the deployment of a medical device. Any device must obtain the medical CE mark to be used in ambulatories and hospitals, but if the industrialization is not handled correctly, the devices distributed do not perform this function as it is intended. Therefore, both processes are complementary and must be carried out successfully.

5.5. References

[1] "UNE-EN 60601-1-11." Accessed: Mar. 09, 2024. [Online]. Available: https://www.une.org/encuentra-tu-norma/busca-tu-norma/norma?c=N0054998

[2] D. F. Williams, "On the mechanisms of biocompatibility," *Biomaterials*, vol. 29, no. 20, pp. 2941–2953, Jul. 2008, doi: 10.1016/j.biomaterials.2008.04.023.

[3] "ISO 10993-10." Accessed: Mar. 09, 2024. [Online]. Available: https://www.une.org/encuentra-tu-norma/busca-tu-norma/norma?c=N0071963

[4] R. Keller, “Introduction,” in *Design for Electromagnetic Compatibility–In a Nutshell, Theory and Practice*, Springer, Cham, 2022, pp. 1–8. doi: 10.1007/978-3-031-14186-7.

[5] D. C. Smith, “Techniques for Investigating the Effects of ESD on Electronic Equipment,” in *Journal of Physics: Conference Series*, Institute of Physics Publishing, Oct. 2015. doi: 10.1088/1742-6596/646/1/012036.

[6] J. E. Vinson and J. J. Liou, “Electrostatic discharge in semiconductor devices: an overview,” *Proceedings of the IEEE*, vol. 86, no. 2, pp. 399–420, 1998, doi: 10.1109/5.659493.

[7] S. Guo, D. Guo, Q. Zhang, and N. Wu, “Research on design of electromagnetic compatibility shielded anechoic chamber,” in *IOP Conference Series: Earth and Environmental Science*, Institute of Physics Publishing, May 2020. doi: 10.1088/1755-1315/474/7/072062.

[8] “EN 303 446-1.” Accessed: Mar. 10, 2024. [Online]. Available: https://www.etsi.org/deliver/etsi_en/303400_303499/30344601/01.02.00_20/en_30344601v010200a.pdf

[9] “EN 301 489-1.” Accessed: Mar. 10, 2024. [Online]. Available: https://www.etsi.org/deliver/etsi_en/301400_301499/30148901/02.02.03_60/en_30148901v020203p.pdf

[10] “UNE-EN 60601-1-2.” Accessed: Mar. 09, 2024. [Online]. Available: https://www.en.une.org/encuentra-tu-norma/busca-tu-norma/norma?c=N0065565

[11] H. P. Bloch, “Ingress Protection code explained,” *World Pumps*, vol. 2009, no. 11, p. 26, Nov. 2009, doi: 10.1016/S0262-1762(09)70418-3.

[12] S. K. Bhudolia, G. Gohel, K. F. Leong, and A. Islam, “Advances in ultrasonic welding of thermoplastic composites: A review,” *Materials*, vol. 13, no. 6, Mar. 2020, doi: 10.3390/ma13061284.

[13] “UNE-EN 60529.” Accessed: Mar. 09, 2024. [Online]. Available: https://www.une.org/encuentra-tu-norma/busca-tu-norma/norma?c=N0060015

[14] R. J. Friel, “Power ultrasonics for additive manufacturing and consolidating of materials,” in *Power Ultrasonics: Applications of High-Intensity Ultrasound*, Elsevier Inc., 2015, pp. 313–335. doi: 10.1016/B978-1-78242-028-6.00013-2.

[15] “UNE-EN 60068-2-64.” Accessed: Mar. 10, 2024. [Online]. Available: https://www.une.org/encuentra-tu-norma/busca-tu-norma/norma?c=N0044016

[16] “UNE-EN 60068-2-27.” Accessed: Mar. 10, 2024. [Online]. Available: https://www.une.org/encuentra-tu-norma/busca-tu-norma/norma?c=N0046798

[17] J.-P. Dal Pont, “Industrialization: From Research to Final Product,” in *Process Industries 2: Digitalization, a New Key Driver for Industrial Management*, J.-P. Dal Pont and M. Debacq, Eds., Wiley, 2020, pp. 79–108.

[18] A. A. R. M. A. Ebayyeh and A. Mousavi, “A Review and Analysis of Automatic Optical Inspection and Quality Monitoring Methods in Electronics Industry,” *IEEE Access*, vol. 8, pp. 183192–183271, 2020, doi: 10.1109/ACCESS.2020.3029127.

[19] P. Radev and M. Shirvaikar, “Enhancement of Flying Probe Tester Systems with Automated Optical Inspection,” in *Southeastern Symposium on System Theory*, Cookeville, TN, USA: IEEE, Apr. 2006.

[20] R. Oliveira *et al.*, “A Systematic Analysis of Printed Circuit Boards Bending during In-Circuit Tests,” *Machines*, vol. 10, no. 2, Feb. 2022, doi: 10.3390/machines10020135.

[21] “IEEE Standard for Test Access Port and Boundary-Scan Architecture,” *IEEE Std 1149.1-2013 (Revision of IEEE Std 1149.1-2001)*, p. 200, 2013, doi: 10.1109/IEEESTD.2013.6515989.

[22] A. Jandyal, I. Chaturvedi, I. Wazir, A. Raina, and M. I. Ul Haq, “3D printing – A review of processes, materials and applications in industry 4.0,” *Sustainable Operations and Computers*, vol. 3, pp. 33–42, Jan. 2022, doi: 10.1016/j.susoc.2021.09.004.

[23] P. J. Martin, “Thermoforming of polymers,” in *Advances in Polymer Processing: From Macro- To Nano- Scales*, Elsevier, 2009, pp. 352–383. doi: 10.1533/9781845696429.3.352.

[24] I. P. Okokpujie, C. A. Bolu, O. S. Ohunakin, E. T. Akinlabi, and D. S. Adelekan, “A review of recent application of machining techniques, based on the phenomena of CNC machining operations,” in *Procedia Manufacturing*, Elsevier B.V., 2019, pp. 1054–1060. doi: 10.1016/j.promfg.2019.06.056.

[25] M. Czepiel, M. Bańkosz, and A. Sobczak-Kupiec, “Advanced Injection Molding Methods: Review,” *Materials*, vol. 16, no. 17. Multidisciplinary Digital Publishing Institute (MDPI), Sep. 01, 2023. doi: 10.3390/ma16175802.

[26] C. Fernandes, A. J. Pontes, J. C. Viana, and A. Gaspar-Cunha, “Modeling and Optimization of the Injection-Molding Process: A Review,” *Advances in Polymer Technology*, vol. 37, no. 2. John Wiley and Sons Inc., pp. 429–449, Mar. 01, 2018. doi: 10.1002/adv.21683.

[27] P. D. Kale, P. D. Darade, and A. R. Sahu, “A literature review on injection moulding process based on runner system and process variables,” in *IOP Conference Series: Materials Science and Engineering*, IOP Publishing Ltd, Jan. 2021. doi: 10.1088/1757-899X/1017/1/012031.

[28] R. Svečko, D. Kusić, T. Kek, A. Sarjaš, A. Hančič, and J. Grum, “Acoustic emission detection of macro-cracks on engraving tool steel inserts during the injection molding cycle using PZT sensors,” *Sensors (Switzerland)*, vol. 13, no. 5, pp. 6365–6379, May 2013, doi: 10.3390/s130506365.

[29] “Unique Device Identifier (UDI).” Accessed: Mar. 09, 2024. [Online]. Available: https://health.ec.europa.eu/medical-devices-topics-interest/unique-device-identifier-udi_en

6. Sweat Monitoring Device

The first chapter presented the sweat analysis as an alternative to the traditional blood testing. Then, the second section described the technologies involved to develop a wearable device capable of performing this analysis. In this chapter, a novel wearable device named ONASPORT, able to capture sweat from the user's skin and quantify its content during a physical activity, is presented and characterized. When an exercise is performed, large amounts of sweat are generated to cool down the internal temperature of the body. The analysis of this biofluid during a physical activity allows sport medicine doctors to assess the performance and health state of an athlete. This information can be used to plan trainings and recovery plans in an efficient way.

The ONASPORT device is not intended to be a medical device unlike the other wearable presented in this thesis. The sensing technology behind the sweat measurement carried out by this wearable device is a starting point for translating this monitoring system into the healthcare field. Despite not being a medical device, the medical development procedure presented in the second chapter was followed to design, implement, and validate this system.

6.1. System architecture

The ONASPORT device [1] is conceived as a band that it is placed on the athlete's chest. This band was modified to integrate a microfluidic system, an array of sensors, and device's electronics. The system is intended for estimating the user's heart rate (HR), dehydration, and blood lactate levels during physical activity. Despite this device measures all these parameters, the methods for the obtention of blood lactate levels and dehydration state from the gathered data are not developed here because this thesis focuses on the wearable device's development.

Monitoring physiological parameters using wearable devices during a physical activity helps to prevent injuries and enhance the performance of athletes [2]. However, mainly the HR is used by sport professionals to determine the athlete's state during the exercise [3]. Other parameters are rarely measured, and when they are monitored, a special test must be carried out.

This system (see Figure 6.1a) is formed by three different elements:

- Central module (see Figure 6.1b)
- Cartridge (see Figure 6.1c)
- Chest strap (see Figure 6.1d)

The central module contains the system electronics (see Figure 6.2). These electronics capture the response of the device's sensors by means of a custom analog front-end, process the raw data obtained from the sensors, and send the results to a mobile phone application via Bluetooth Low Energy (BLE). BLE is a low-power communication system that can be used to establish communication to a multitude of devices, such as smartphones, fitness trackers, and smartwatches. Nowadays, the interconnectivity between devices is more demanded by users, so be able to connect with different technological garments to display the acquired data is very useful to ease the adoption of this system.

Figure 6.1.Structure of the ONASPORT device. (a) Complete system, (b) central module (electronics of the system), (c) cartridge and (d) chest strap. Courtesy of Aguilar-Torán (2023) [4], used with permission.

To power the whole system, a lithium coin cell battery is utilized. Coin cell batteries are a popular power source solution for wearable devices because they are commonly available in any store, their compact size, and their long shelf life.

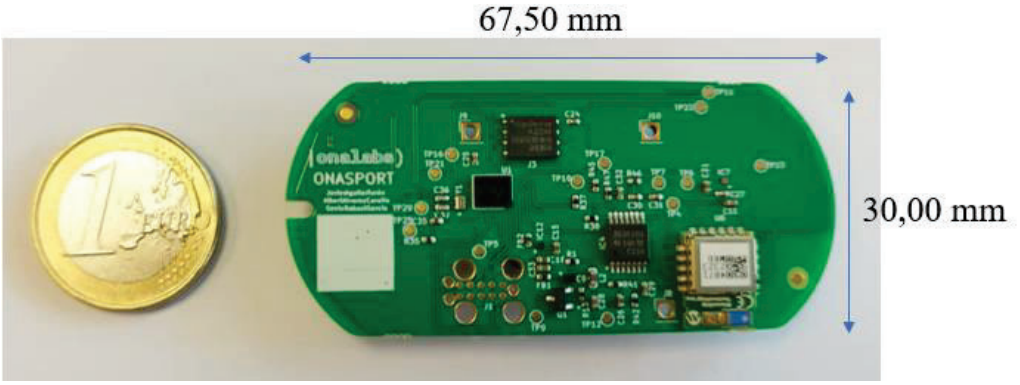

Figure 6.2. Photograph of the ONASPORT electronics.

The cartridge (see Figure 6.3) is the element that collects sweat from the skin and canalizes it into a microfluidic channel. Inside this channel there are several sensors which analyze the content of this biofluid. This cartridge is a single-use component (disposable) that must be changed after each test. However, continuous measurements can be carried out for a given test, obtaining the evolution profile of every parameter during the exercise.

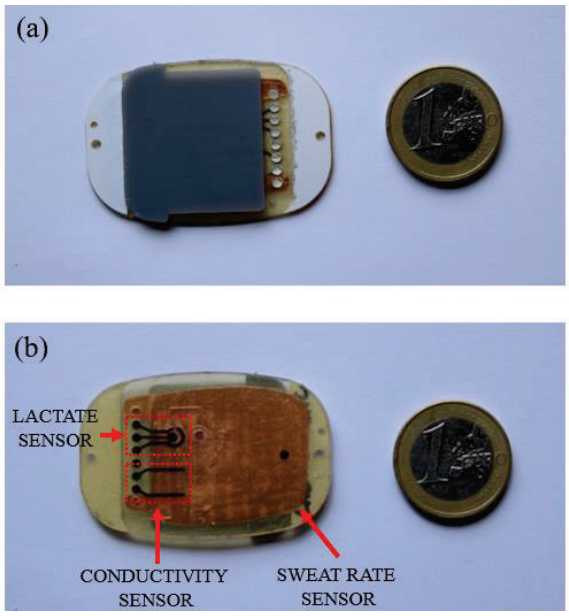

Figure 6.3. Photograph of the cartridge. (a) Front and (b) back of the disposable. At the back of the cartridge is highlighted each sensor (lactate, conductivity, and sweat rate sensors). Adapted with permission from Aguilar-Torán (2023) [4].

The chest strap provides a comfortable and robust attachment to the body, and it is utilized to carry out HR measurements. This measurement is possible thanks to two rubber electrodes integrated inside the band.

Every mentioned element must be connected together in order to take measurements. The chest strap and the cartridge are attached to the central module (see Figure 6.4).

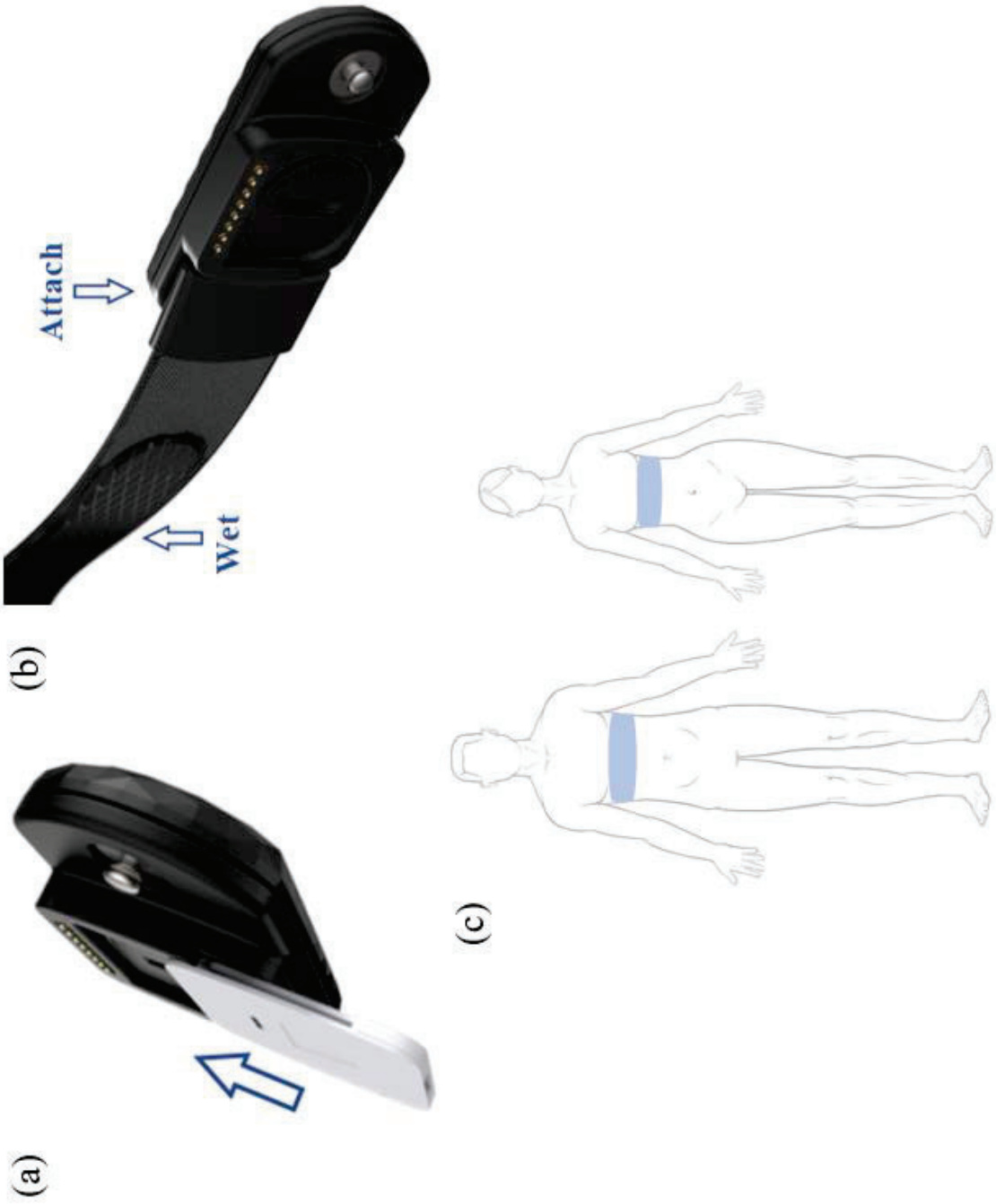

Figure 6.4. How to connect the different elements of the system. (a) First, slide the cartridge into the central module, (b) then, attach the strap to the electronics, and (c) finally, place the band around the chest. Courtesy of Aguilar-Torán (2023) [4], used with permission.

The information gathered by the ONASPORT device is sent to a smartphone. This smartphone runs an application, which enables data visualization during the physical activity (see Figure 6.5). After finishing each training session, the data collected is sent to the cloud platform. The platform stores the information and allows to the user see the evolution of every physiological parameter by means of a web dashboard.

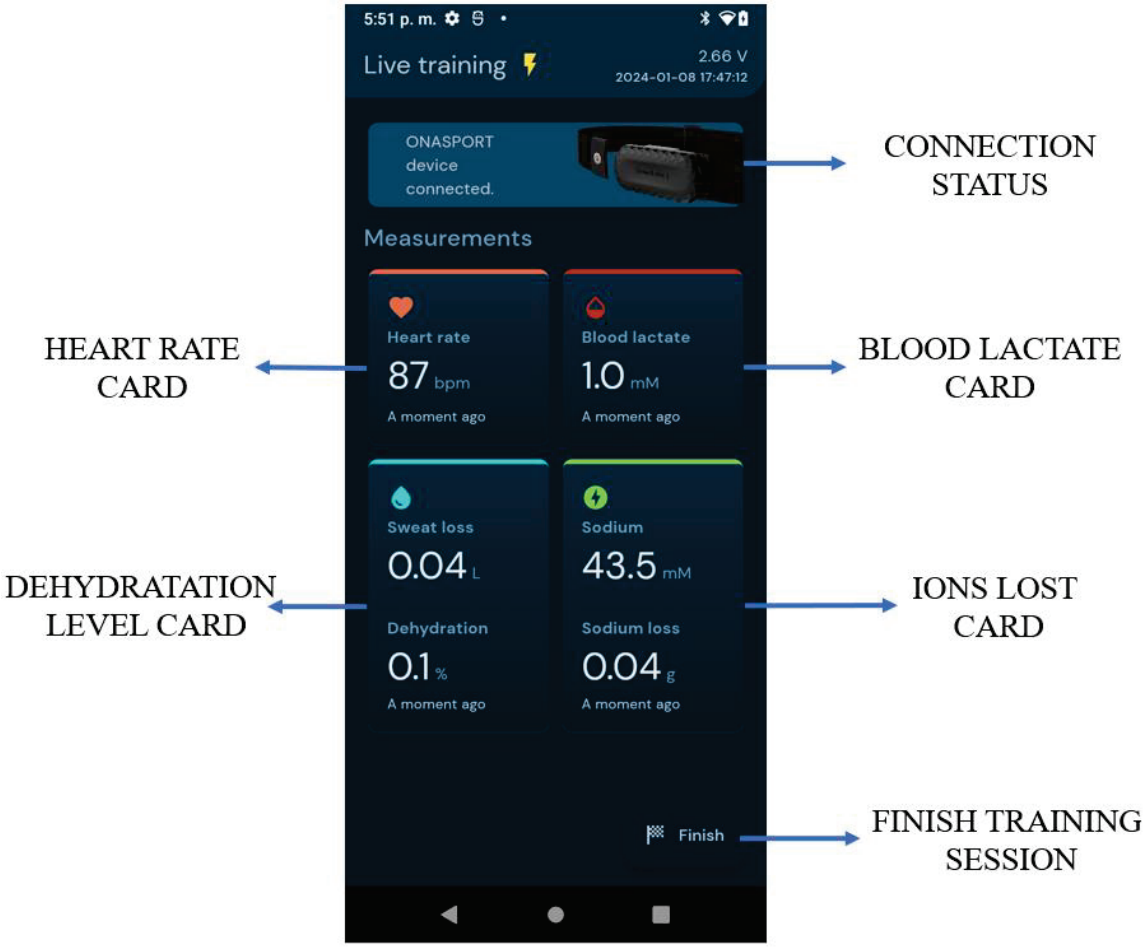

Figure 6.5. Mobile phone application of the ONASPORT device.

6.2. Sensing elements

The sensing elements of this wearable device are the chest strap and the sensors integrated inside the cartridge. The chest strap is employed for HR measurement, while the sensors within the disposable are utilized to estimate the sweat content.

6.2.1. Chest strap

The chest strap has two rubber electrodes that are in contact with the athlete's skin. These electrodes are used to record an electrocardiogram (ECG). Rubber electrodes are typically utilized in sport bands because they are reusable and washable. A single-lead ECG is recorded using this configuration of electrodes, which lacks the necessary quality to be used in clinical settings, but the QRS complex can be identified easily in the obtained signals (see Figure 6.6). This complex indicates that one beat has taken place, so it can be used to estimate the HR value.

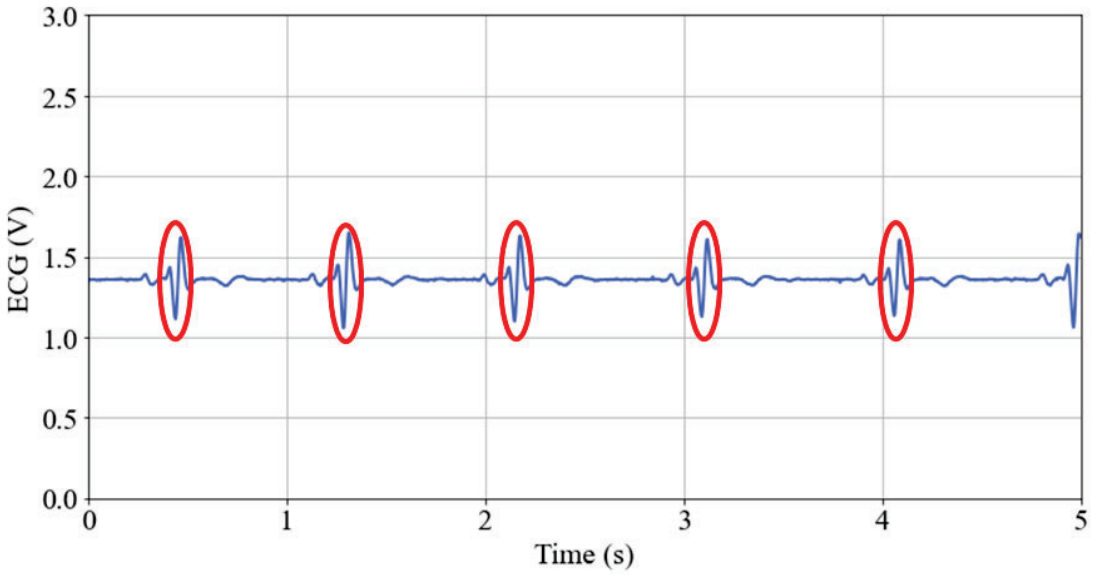

Figure 6.6. Example of the ECG recorded using the ONASPORT electrodes. Each QRS complex in this signal is highlighted.

The system uses the chest strap from the heart rate monitor TICKR product (Wahoo Fitness; Atlanta, GA, USA) [5].

6.2.2. Cartridge

The cartridge is an adhesive patch attached directly to the athlete's skin as well to the central module of the device. This patch collects sweat from the skin and canalizes it inside a microfluidic channel. There are different sensors in this channel that are used to estimate both the dehydration and lactate levels of the athlete (see Figure 6.7).

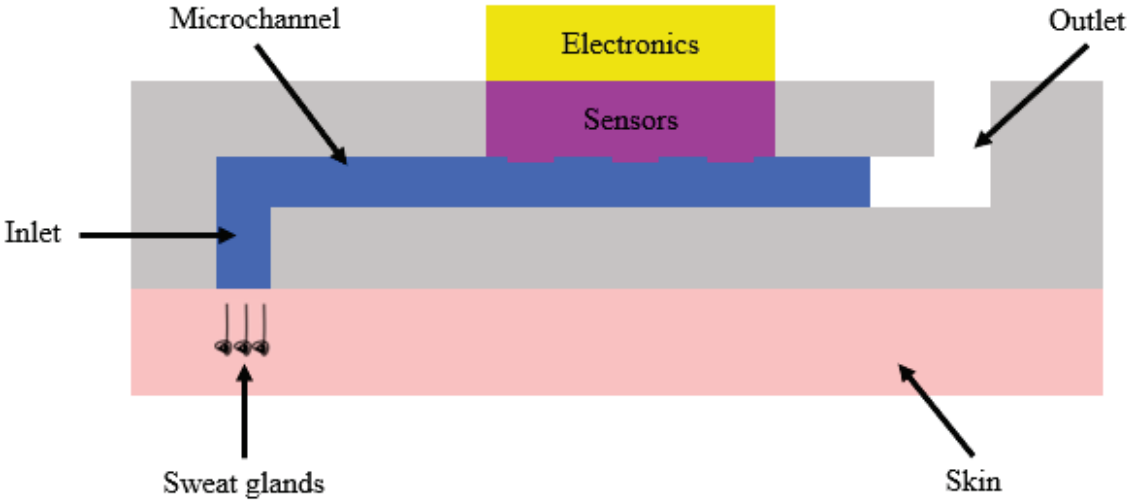

Figure 6.7. Schema of the microfluidic system.

A detailed description of the sensors and the microfluidics is not given here, since it is out of the scope of this thesis.

A. Dehydration sensors

Dehydration is the condition that occurs when the body loses too much water. It can be caused by several reasons, such as sweating too much or not drinking enough water. If left untreated, this condition can lead to poor body function and, in extreme cases, death [6], [7], [8].

During a physical activity, water is lost due to thermoregulatory sweating. The sweat glands of the body collectively secrete between 0.8 and 1.5 L of water in the course of a moderate-intensity workout [9], [10]. This fluid loss can lead to the athlete dehydration, and it also produces imbalance of the salts, since a lot of ions are lost through sweat [11].

Two different sensors are used to estimate the athlete's dehydration. These sensors are a capacitive sensor [12], [13] utilized to know the perspiration rate of the athlete, and a conductometric sensor used to estimate the sweat ionic strength.

The capacitive sensor (see Figure 6.8a) is formed by two layers of copper and a microfluidic channel that is placed in the middle of two metal sheets. All these elements are laminated forming the sensing system. This sensor can be modeled as a parallel plate capacitor which capacitance varies as follows (see Equation 3.1):

$$C = \varepsilon_o \varepsilon_d \frac{A}{d} \tag{3.1}$$

where ε_o is the permittivity of space, ε_d is the relative permittivity of dielectric material between the metal layers, d is the separation between these sheets, and A is the area of the sheets.

At the beginning of each trial, the chamber is full of air, and once the test initiates, the channel starts to be filled with sweat. When the content inside the chamber changes, the dielectric constant of the sensor varies as well. This variation is translated to a modification of the system capacitance, so the volume changes within the channel can be detected by measuring this parameter. The volume measured during a certain period of time can be related to the total volume of fluid lost by the user and thus the dehydration level can be estimated.

The ionic strength sensor (see Figure 6.8b) is formed by two screen-printed electrodes that are integrated inside the microfluidic channel. Screen-printing is a technique that deposits ink onto a substrate, such as fabric, plastic, or metal, using a mesh screen with a defined pattern. This printing technique is extensively utilized in the industry to miniaturize sensors at low cost [14]. The electrodes of the ionic strength sensor are in direct contact with the sweat that flows in the channel, and they are used to measure the impedance of this fluid. The main contribution of the sweat impedance is the resistance of this biofluid, which directly depends on the number of ions present in the medium. Therefore, the concentration of ions can be estimated by measuring the conductivity of this biofluid. Specifically, the sodium concentration can be easily calculated, as it is the most abundant ion in sweat and dominates the conductivity response [15].

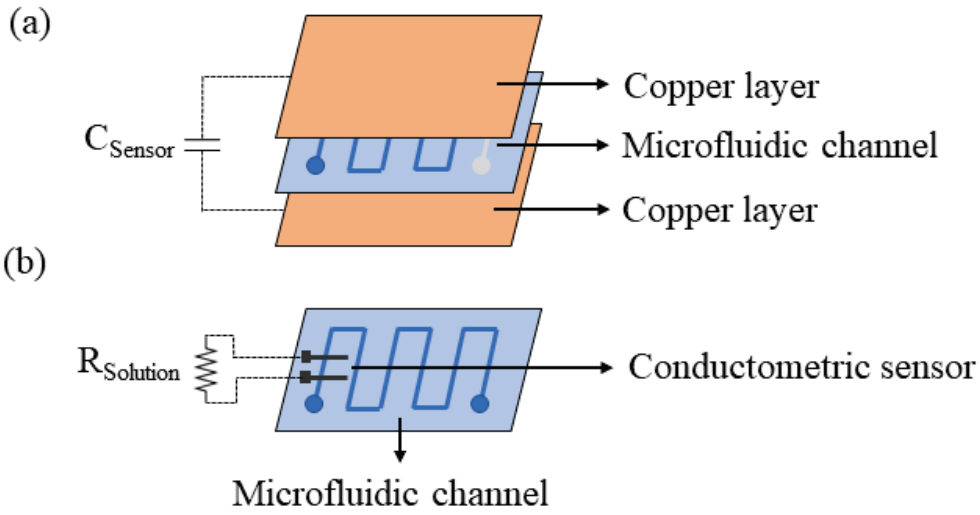

Figure 6.8. Dehydration sensors. (a) Scheme of the capacitive and (b) the conductometric sensors, respectively. Courtesy of Aguilar-Torán (2023) [4], used with permission.

B. Lactate sensor

Lactate is a molecule produced through the breakdown of glucose under anaerobic conditions. Elevated blood lactate levels indicate an oxygen deficiency in some tissues of the body. During exercise, lactate is generated because there is insufficient oxygen reaching the muscles. The increase in lactate implies a higher concentration of protons within the cells, so if the lactate production rate is high, it may exceed the buffering capacity of protons and cause a decrease in pH, generating lactic acid that affects the performance of muscles [16], [17].

The blood lactate concentration varies from 0.6 to 2.0 mM, but it can increase up to 10 mM during intense physical effort [18]. Many factors affect sweat lactate concentration, but it is estimated that it varies between 1 mM and 100 mM during physical activity [19]. Currently, lactate tests need a blood sample, generally taken from the earlobe through a needle, that causes great disadvantage in real-time monitoring. Using this method can be difficult for taking a series of measurements during training and therefore obtaining follow-up results [20].

The lactate sensor used in this wearable device is an enzyme-based amperometric sensor. This sensor consists of a working electrode (WE) made of a mixture of carbon and Prussian blue mediator, a silver reference electrode (RE), and a carbon counter electrode (CE). These electrodes are screen-printed on the surface of a polyethylene terephthalate (PET) foil. The WE is functionalized with lactate oxidase, which it is immobilized in a biopolymeric membrane whose function is to retain the enzyme on the electrode's surface.

To know the relationship between the lactate levels in blood and sweat, a bioequivalence study was carried out. In this study, physiological data from more than 30 volunteers was collected and analyzed. The study concludes that does not exist a direct equivalence between the lactate level at blood and sweat without considering other parameters. To estimate the equivalence, a custom algorithm that takes HR, perspiration level, and sweat lactate concentration as inputs is required (see Figure 6.9) [21].

6.3. Electronics of the system

The system electronics are embedded in a single board. The board architecture (see Figure 6.9) follows the schema described in the second chapter: control unit, power supply module, electronic instrumentation, wireless communication module, and external memory.

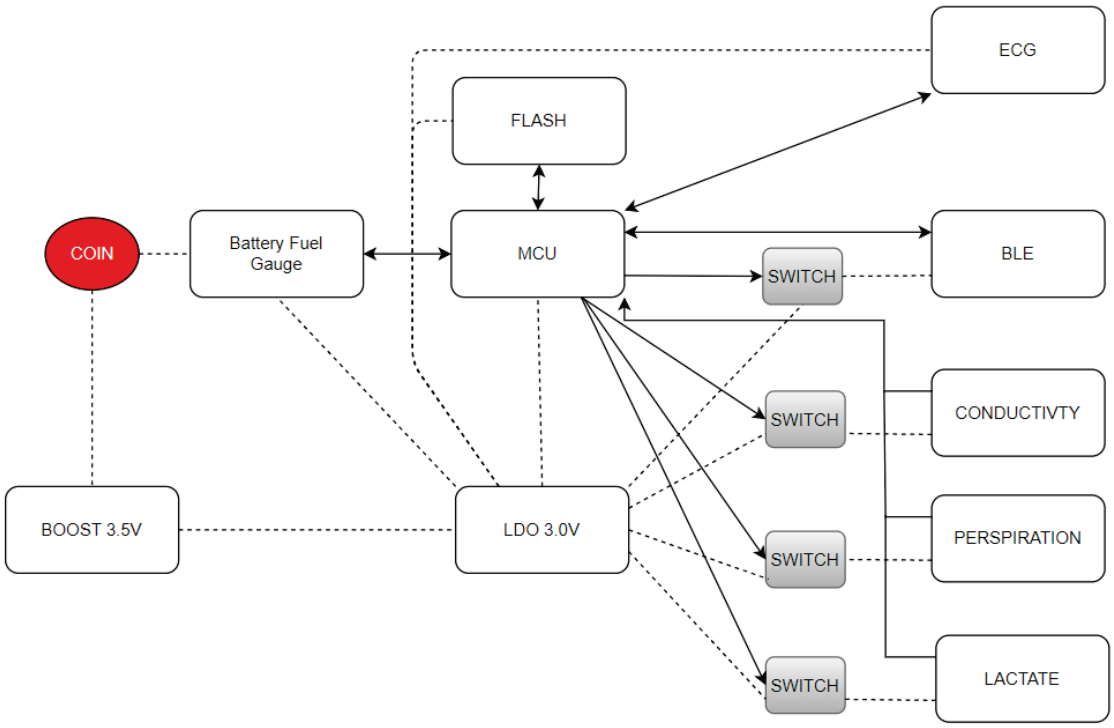

Figure 6.9. Architecture of the ONASPORT board.

This wearable device has the same operational modes as the ONAVITAL system: low-power and measurement states. Initially, the system remains in the low-power mode until the athlete wears the device. Upon detection by a skin detector system, the device switches to measurement mode. In this state, the wearable device records the HR dynamics and analyzes the sweat content. The measurement frequency is not the same for every parameter since the dynamics of each biomarker are different and depend on the nature of the physiological process behind it. On one hand, HR is measured every five seconds, and, on the other hand, the other parameters are estimated every two minutes. Once the activity is completed, it returns to the low-power state.

The ONASPORT board consumes 27 µA and 1.77 mA at low-power and measurement mode, respectively. This device is capable of disabling and enabling different modules of the system in order to reduce power consumption. Furthermore, as the ONAVITAL device, the processing of the sensors' raw data is carried out by the device itself to enhance the battery autonomy. Given these characteristics, if the user uses the device one hour per day (training average time) with a coin cell with a capacity of 235 mAh, the expected battery life is 100 days.

Whenever possible, the same electronic components are used for the ONASPORT and ONAVITAL board. This approach cuts the manufacturing costs because the price of each element is greatly reduced when large amounts of the same components are purchased.

Furthermore, using the same elements simplifies their maintenance and reduces the inherent risks.

6.3.1. Control unit

The control unit is based on the same microcontroller (MCU) of the ONAVITAL device but does not include a RGB LED for indicating device states. The MCU runs the firmware that manages all the actions performed by the system and analyzes the sensors' response. The current consumption of this module depends on the operational mode of the system. During the first mode the MCU only consumes 1.5 µA and in the second mode 1 mA.

6.3.2. Power supply and power management module

The energy used to supply the system is extracted from a coin cell battery. This electric energy is regulated by the power management module of the ONASPORT board. Apart from performing this task, this module is also used to estimate the charge level of the battery.

A. Coin cell

To power the board, a CR2032 battery is utilized. This electrochemical cell is a non-rechargeable battery of lithium-manganese dioxide (Li-MnO_2). The specifications of this battery vary depending on the manufacturer, although some characteristics, such as dimension (20 mm of diameter and 3.2 mm of thickness) and nominal voltage (3.0 V) are always the same. CR2032 coin cells provide a stable current, but the voltage decays with the level of charge as lithium polymer batteries. Hence, the potential must be regulated to power the circuit.

ONASPORT device can use any CR2032 coin cell available on the market, but it is recommended to power the system utilizing a coin cell with a rated capacity of 235 mAh [22].

B. Voltage regulation

Every ONASPORT's components work at 3.0 V. To obtain this voltage, the potential provided by the coin cell is elevated to 3.5 V by boost converter and then it is regulated to 3.0 V by a low-dropout regulator (LDO) (see Figure 6.10). The boost converter cannot be used to power the system directly since a ripple appears on the component's output. This ripple can cause malfunctions on the system, particularly in the analog instrumentation. The LDO removes the noise from this signal and provides a stable power source. Using this configuration, coin cells that are nearly dead can be used due to battery tensions as low as 1.25 V can be elevated.

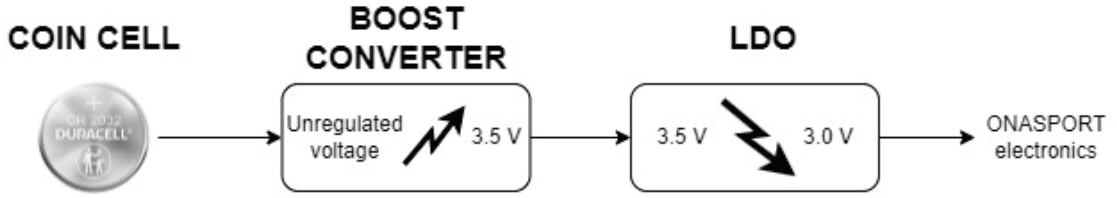

Figure 6.10. Schema of the ONASPORT regulation voltage.

Both the boost converter and 3.0 V LDO are the same as the ONASPORT device and only consumes 325 nA combined. This current consumption is very low, which it is crucial since the power supply module is always enabled.

C. Estimation of the battery level

To estimate the battery charge level, the battery fuel gauge BQ35100 (Texas Instruments; Dallas, TX, USA) [23] is used. This component determines the amount of charge remaining in an electrochemical cell by means of a coulomb meter and provides information about its state of health using custom algorithms. The data recorded by this IC is sent to the MCU via I2C. This module consumes 50 nA and 40 µA when is disabled and enabled, respectively.

6.3.3. Instrumentation

The ONASPORT system has several instrumentations that capture the sensors' response. This front-end adapts their output signals to the levels of the MCU's ADC, which acquires its response.

A. ECG recording and heart rate estimation

To record the athlete's ECG, the commercial IC AD8233 (Analog Devices; Wilmington, MA, USA) [24] is used. This chip is an analog front-end for the signal conditioning of cardiac biopotentials. It is composed of an instrumentation amplifier, an operational amplifier, and a right leg drive amplifier.

Two different filters are implemented to eliminate the noise present on the ECG signal. The first filter is a first-order high-pass filter with a cutoff frequency of 7 Hz, and it is used to delete motion artifacts and the electrode half-cell potential. The second filter is a second-order low-pass filter with a cutoff frequency of 25 Hz, and it is utilized to remove other interference signals.

Apart from the signal conditioning circuitry, this IC contains a skin detector system. This system monitors the impedance between the two rubber electrodes. To do that, it injects an AC current of 100 kHz to one of these electrodes and measures the potential at the other one. If the tension measured surpasses a certain level, it is considered that a user wears the chest strap.

The Pan-Tompkins algorithm is used to calculate the HR from the ECG recorded by the analog front-end [25]. To estimate the HR, windows of five seconds of the ECG recording are utilized. The sampling rate of this recording is 50 Hz. The current consumption of this module is 150 µA and 500 µA when it is activated and deactivated, respectively.

B. Sweat rate and conductivity instrumentations

On one hand, a modified Schmitt Trigger oscillator is utilized to measure the capacitive sensor response (see Figure 6.11a). This circuit is based on the OPAMP OPA348AQDBVRQ1 (Texas Instruments; Dallas, TX, USA) [26]. The oscillator generates a square signal whose frequency depends on the capacitance of the system (see Figure 6.11b). The capacitance is the sensor itself, so the changes in the period of the signal are directly related to the variation in the sensor impedance. As was mentioned

before, the perspiration sensor modifies its capacitance as sweat enters inside the microfluidic channel, so the changes in volume inside this channel can be easily detected.

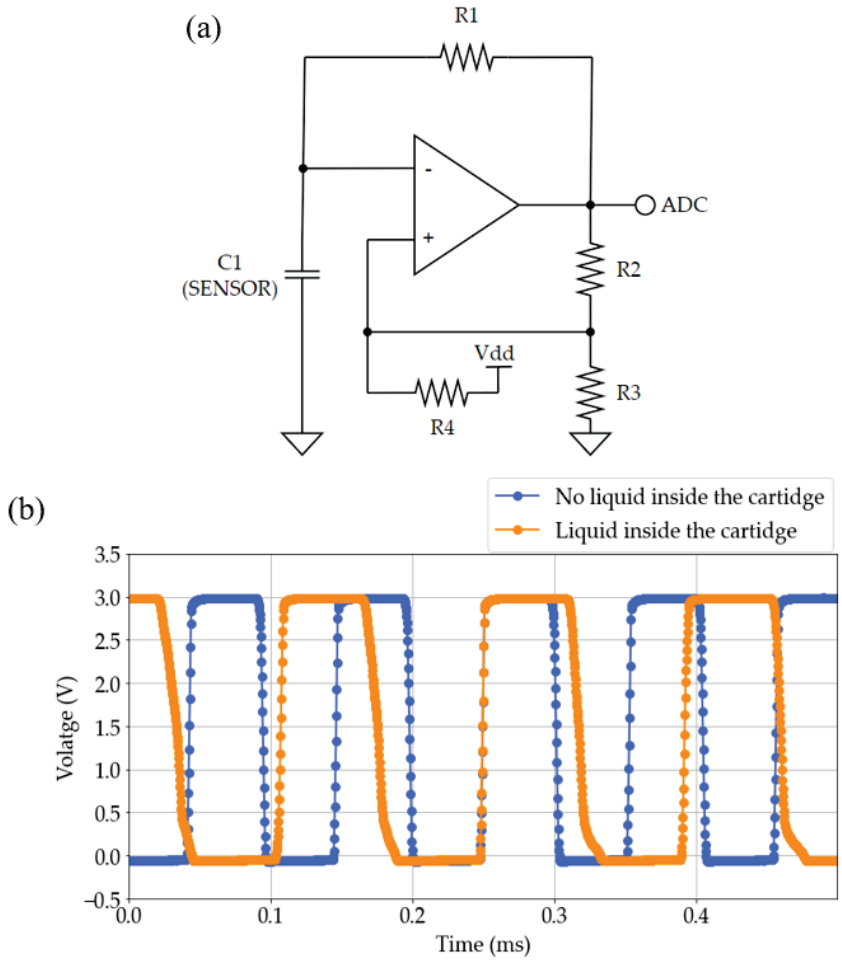

Figure 6.11. Modified Schmitt Trigger Oscillator. (a) Schematic of the circuit and (b) response of this instrumentation. In blue is highlighted the output signal when the disposable is empty and in orange is the response of the instrumentation when the cartridge is full of fluid. Courtesy of Aguilar-Torán (2023) [4], used with permission.

On the other hand, a circuit that combines an amplification stage and a transimpedance amplifier are used to quantify the sweat ionic strength (see Figure 6.12a). This circuit uses the operational amplifier (OPAMP) OPA4348AQPWRQ1 (Texas Instruments; Dallas, TX, USA) [27]. The control unit MCU generates a square signal of 8 kHz using a digital to analog converter (DAC) and injects this signal into the circuit (see Figure 6.12b). Then, the signal amplitude is reduced by the amplification stage in order to not saturate the conductivity sensor. Finally, this signal is applied to the sensor, and the response is captured by a transimpedance amplifier. The bandgap reference REF35102QDBVR (Texas Instruments; Dallas, TX, USA) [28] is used to provide a bias to adjust the signal to the ADC levels of the MCU. From the amplitude of the acquired signal, the conductivity of the biofluid is estimated. To obtain this value, the cell constant of this sensor is utilized. This constant depends on the geometry of the sensor, and it defines the resolution of this measurement [29]. Once the conductivity is calculated, the number of ions present in this biofluid can be estimated.

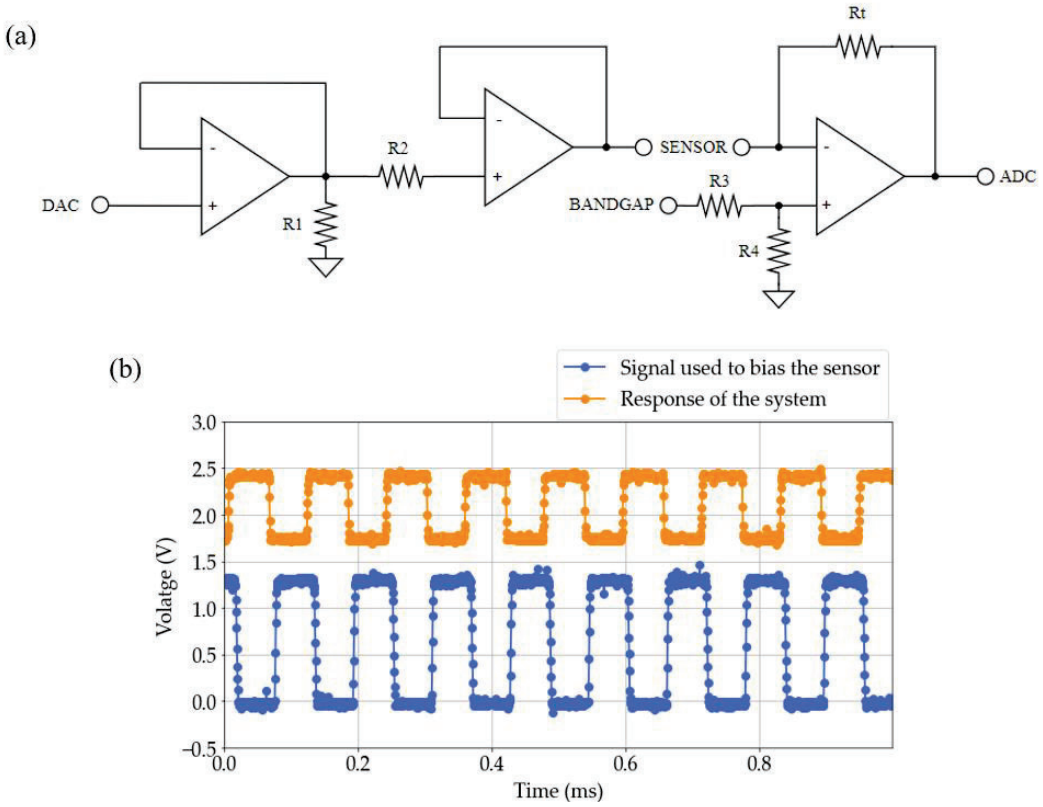

Figure 6.12. Conductivity instrumentation. (a) Schematic of the instrumentation and (b) response of this circuit. In blue is the signal used to bias the sensor and in orange is the response of the system to a conductive fluid inside the disposable. The amplitude of the signal provided by the instrumentation changes depending on conductivity of the medium. Adapted with permission from Aguilar-Torán (2023) [4].

The current consumption of the first module is 250 µA and the second one is 800 µA when they are activated. These two modules are enabled or disabled by two different analog switches that are placed in the middle of the power supply of these circuits.

C. Potentiostat

A custom potentiostat based on the OPAMP ADA4505-4 (Analog Devices; Wilmington, MA, USA) [30] is used to estimate the lactate concentration (see Figure 6.13a). This potentiostat is designed to work along two or three electrodes amperometric sensors. Three electrode configuration is normally used due to the extra electrode helps to stabilize the potential on the electrochemical cell. Its architecture is based on a transimpedance amplifier with a direct voltage bias application and a final non-inverting amplifier, as low current levels are expected from the lactate sensor. Moreover, a capacitor is introduced as a first-order low-band-pass filter. This potentiostat can provide a whole voltage supply compliance voltage as well as read both oxidation (negative current) and reduction currents (positive current) from the amperometric sensor. It is complemented by the same bandgap used for the conductometric instrumentation and the MCU DAC, which provides the necessary voltage bias to the sensor [31].

This circuit is capable of carrying out both cyclic voltammetries (CV) and chronoamperometries (CA), depending on the DAC's configuration. On one hand, a CV is performed when the DAC potential varies until it reaches an established potential value, then it changes direction (triangular waveform). On the other hand, a CA is carried out

when the generated voltage is fixed. To quantify the sweat lactate concentration, CA is performed (see Figure 6.13b), since this technique is faster than CV.

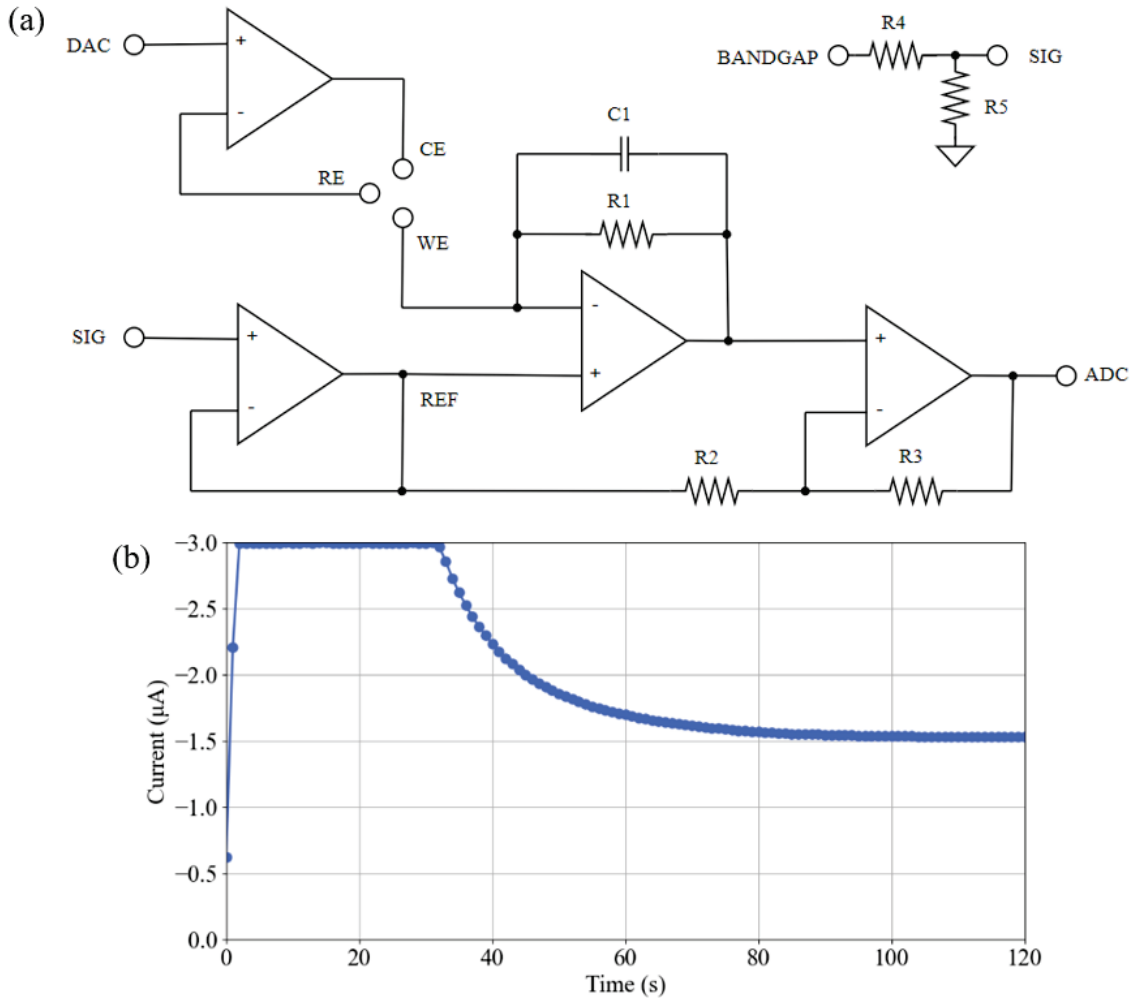

Figure 6.13. Potentiostat. (a) Schematic of the instrumentation and (b) response of this circuit when a CA is carried out. Adapted with permission from Aguilar (2020) [31].

This module consumes 150 µA when it is enabled. The potentiostat is enabled or disabled by means of an analog switch placed in the middle of the power supply.

6.3.4. Communication system

The data gathered by the ONASPORT device is sent to a mobile phone that acts as a gateway. To carry out this task, the same communication module as the ONAVITAL device is used. The main difference between both systems lies in the BLE services and characteristics implemented, since the information sent to the gateway is completely different.

6.3.5. External memory

To ensure that no information is lost, a backup of the collected data is constantly made during each training session. This backup is stored in the same external memory as the ONAVITAL device. After finishing each training session, the data stored in the memory flash is sent to the mobile phone via BLE (if the connection is established) and this memory is erased. The flash memory used can store up to 1000 hours of training.

6.4. Preliminary studies

The system was validated by means of several in vitro and in vivo tests. In vitro trials ensured good functioning of each measurement and in vivo tests demonstrated their functionality in a real environment.

6.4.1. In-vitro tests

Each sensor and instrumentation were tested individually and validated by comparing the data obtained using the gold standard method of every type of measurement. Unlike the ONAVITAL device presented in the third chapter, the performance of each system was not valued utilizing international standards because no norms exist due to the novelty of sweat measurement technology.

A. Heart rate

To characterize the HR parameter, a specific protocol was created. This protocol consisted of an equivalence study between the wearable device and the sports band Suunto Smart HR Belt (Suunto; Vantaa, Finland) [32]. It has been demonstrated that this kind of band has an accuracy similar to an ECG Holter monitor [33]. The protocol of this study is as follows:

- Moisten the rubber electrodes of the wearable device and the reference band, before placing them on the chest of a volunteer.
- Collect the data from each device using a mobile phone application, while the volunteer is sitting, for five minutes.
- Collect the data from each device using a mobile phone application, while the volunteer is pedaling on a stationary bicycle at a constant load, for five minutes.
- Collect the data from each device using a mobile phone application, while the volunteer is sitting, again, for five minutes.

Using this protocol, nine tests were performed, and the results of these trials were analyzed. The volunteers of this study included six males and three females with ages ranging from 21 to 61 (mean of 32.3 years and standard deviation of 11.5 years). These volunteers were informed about the trial and gave their consent to treat their data (see appendix 2 – Data protection consent). Besides, this study was conducted according to the international ethical declarations of Helsinki.

A linear regression was used to compare the performance of the ONASPORT device with the reference band (see Figure 6.14). The coefficient of determination of 0.884 is close to one, so the HR obtained by the wearable device shows no significant difference when is compared with the data provided by the Suunto Smart HR Belt.

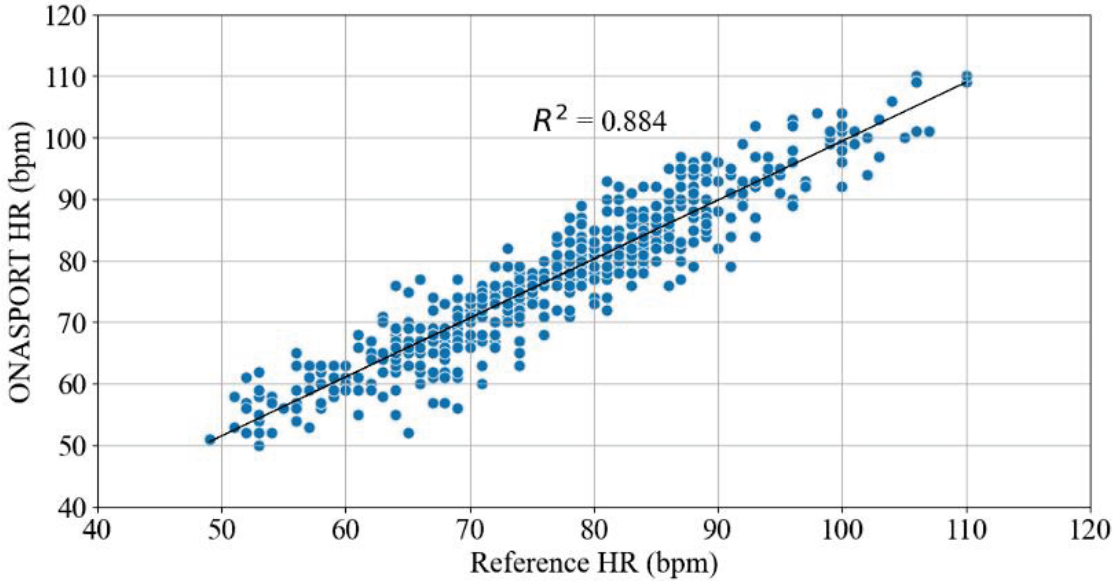

Figure 6.14. Fit between the HR calculated by the ONASPORT device and the Suunto Smart HR Belt.

B. Ionic strength

To validate the ionic strength measurement, a direct comparison was carried out between the wearable device and the reference equipment LAQUAtwin EC-11 (Horiba; Kioto, Japan) [34]. The analyte utilized to perform this analysis was artificial sweat. This artificial sweat was prepared using deionized water with 0.5 % sodium chloride, 0.1 % potassium chloride, 0.1 % lactic acid, and 0.1 % urea. From this solution, ionic strength dilutions of 10, 30, 50, 70, 100, and 130 mM were made.

Multiple measurements were taken using three different conductometric sensors. A linear regression was employed to compare the device performance with the reference equipment (see Figure 6.15). The coefficient of determination of 0.995 shows a good fit between the data, so the system can be considered accurate.

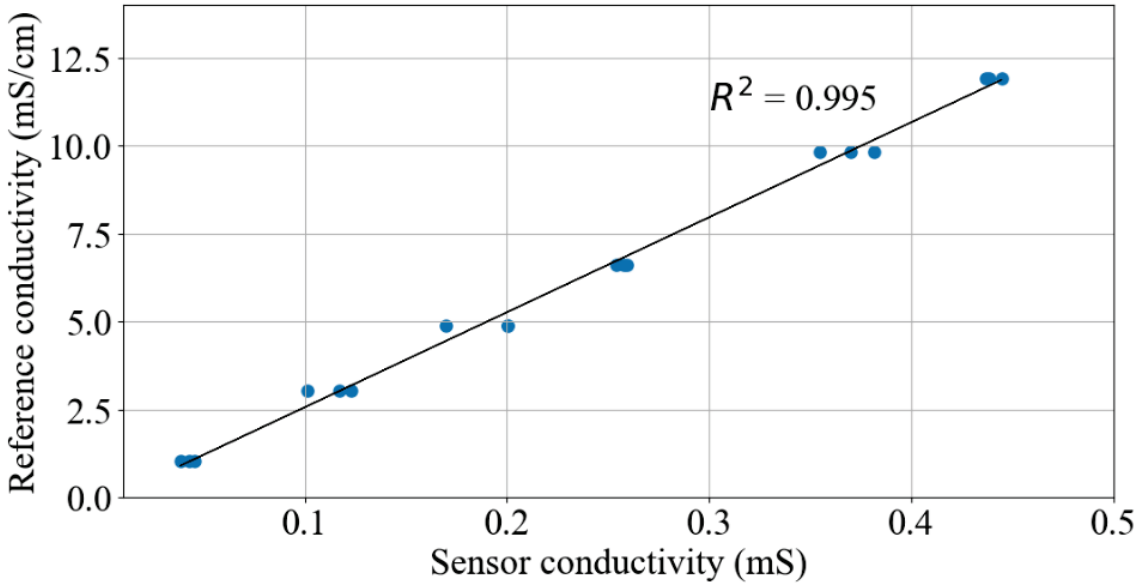

Figure 6.15. Fit between the conductivity calculated by the wearable device and the reference equipment. Courtesy of Aguilar-Torán (2023) [4], used with permission.

C. *Sweat rate*

To validate the perspiration level measurement, no reference equipment was used because there does not exist standard instrumentation to estimate the sweat rate. Instead, a KDS Legato 101 syringe pump (KD Scientific; Holliston, MA, USA) [35] was utilized to simulate the perspiration of the user. This element continuously pumped artificial sweat inside the disposable at a fixed rate of 2 µL/min, which it is an expected perspiration rate for an individual exercising [36].

A trial of 30 min was performed using this syringe pump and a cartridge. During this test, both sweat rate value and conductivity were recorded (see Figure 6.16). The response of the capacitive and the conductometric sensors remained constant at the beginning of the test since the fluid had not yet entered inside the microfluidic channel. When the liquid entered the chamber, the conductometric sensor gave an unstable output that was stabilized at a fixed value after two minutes. The sweat rate sensor was activated immediately, and it gave a response that is linearly time dependent. Finally, when the microfluidic channel was full of liquid, the sensor response stayed constant because the system capacitance could no longer change.

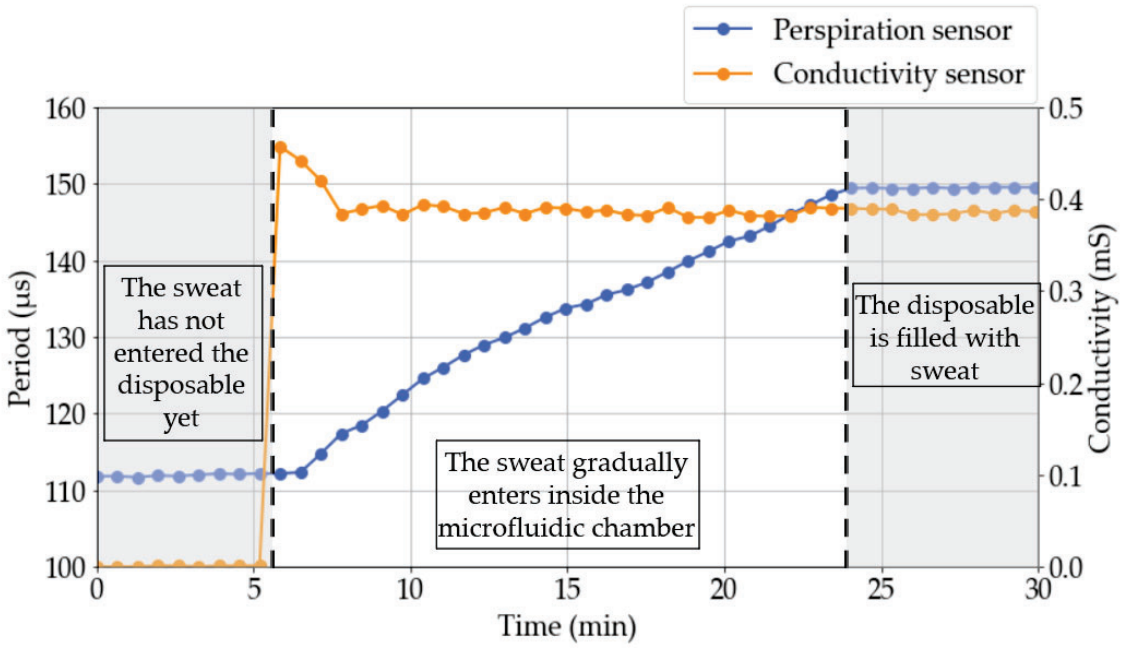

Figure 6.16. Conductivity and sweat rate obtained during an in-vitro test. Courtesy of Aguilar-Torán (2023) [4], used with permission.

D. *Lactate*

Eventually, the lactate measurement was characterized using artificial sweat. This solution was modified to obtain 0, 10, 30, 50, 70, and 100 mM lactate concentrations. Multiple measurements with six different lactate sensors were made using the custom potentiostat and the reference equipment PalmSens4 (Palmsens BV; Houten, Netherlands) [37]. Chronoamperometries using a working potential of −0.3 V during 60 seconds were carried out. Only the last value was taken because it is the moment when the sensor stabilizes its response.

To evaluate the performance of this system, two different metrics were calculated. These metrics were the mean difference, which measures the difference between the actual values and the predicted values, and the standard deviation, which assesses the dispersion of a dataset (see Table 6.1).

Metric	Value
Mean difference	-0.043 µA
Standard deviation	0.064 µA

Table 6.1. Performance of the ONASPORT potentiostat.

The level of current (when its response is stable) varies from -0.2 to -1.5 µA for concentrations of 10 to 100 mM. Since both calculated metrics are lower than the minimum value of current recorded, this measurement can be considered accurate.

6.4.2. In-vivo tests

Once both the sensors and the electronics were validated in vitro, the system was ready to be tested in vivo. This test consisted of the utilization of this wearable system to analyze the sweat content of volunteers during a physical activity.

All the participants of the study were informed and gave their consent to use the data extracted from the experiments (appendix 2 - Data protection consent). This study was conducted in accordance with the international ethical declarations of Helsinki. The volunteers included two males and one female. Before starting the test, the participants were asked to provide the researchers with a series of personal data (see Table 6.2).

Parameters	Volunteer 1	Volunteer 2	Volunteer 3
Sex	Male	Female	Male
Age (years)	30	21	39
Height (cm)	175	164	176
Weight (kg)	80.4	52.0	75.0
BMI (kg/m^3)	26.3	19.3	24.2

Table 6.2. Characteristics of the volunteers of the in-vivo tests.

The protocol of the in-vivo tests was as follows:

- Clean with water the skin area where the disposable is placed, and then, dry the area to ensure that the disposable's adherence to the skin is good.
- Attach the heart rate monitor strap to the central module and wet both rubber electrodes.
- Remove the adhesive liner of the disposable and adhere the central module carrying the cartridge to the skin.
- Collect the data from the wearable device while the volunteer is pedaling on a stationary bicycle at a constant load (see Figure 6.17a). The data is gathered using the ONASPORT mobile application, and this information is downloaded as a CSV file.

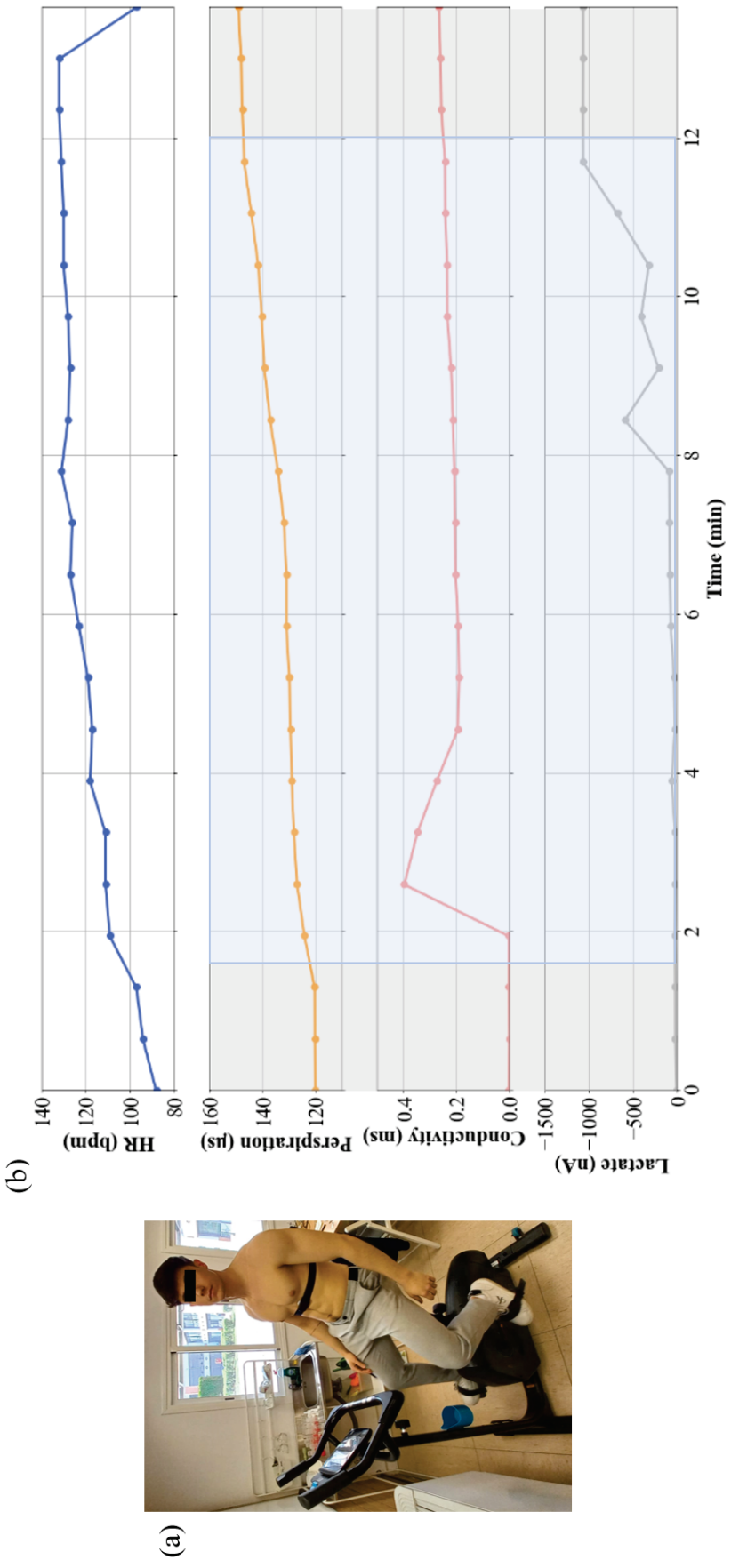

Figure 6.17. Real-time perspiration analysis during stationary cycling. (a) Photograph of the experimental set-up. (b) Results obtained by one in-vivo trial. In gray are highlighted the moments when the cartridge is empty and full. The time in which the cartridge is filled is marked in blue. Adapted with permission from Aguilar-Torán (2023) [4].

The in-vivo results were the expected ones for every partaker (see Figure 6.17b). At the beginning of the test, the HR increased until it reached its maximum value and remained stable. When the HR value increased, the perspiration of the athlete began. A few minutes passed until the cartridge started to collect sweat from the skin, as is observed in the response of the conductometric sensor. This sensor gave an initial peak that can be associated with the trapped minerals (iron, zinc, magnesium, etc.) in the sweat duct [10]. The progressive increase when the activity continued could be explained by the dependence on sweat rate (reabsorption channels in the sweat duct) [38]. More importantly, these results mean that the microfluidic system associated with the sensor was making the sweat continuously circulate and was able to determine the chronological evolution of the different biomarkers. Meanwhile, the capacitive sensor gave an increasing response over time until the microfluidic channel was full of liquid. Eventually, the lactate sensor started its measurement by giving an increasing output until it stabilized its response at a fixed value after a few minutes elapsed.

The behavior of every sensor was almost the same as in the in-vitro trials. Only small changes were observed in the response time and the absolute value of the sensors. The first difference was expected since the perspiration rate of the in vivo test was not constant over time and every volunteer had different perspiration profiles. On the other hand, the second difference can be associated with the sweat composition. Artificial and real sweat are not the same, so different responses were expected. Sweat contains a large quantity of ions that modify the properties of the medium. Enzymatic electrochemical sensors are affected a lot by environmental conditions. In this case, the saltiness of the medium interacted with the activity of the lactate sensor enzyme, producing higher current levels than initially expected.

6.5. Conclusions

In this chapter, a wearable device designed for continuous athlete monitoring in real-time through sweat analysis is presented. This innovative and patented system (appendix 2 – Patent 1) utilizes a conventional sports band that incorporates a single-use cartridge capable of collecting, processing, and analyzing sweat from the user's skin, all thanks to an array of sensors integrated in this disposable.

Two aspects of the device make this approach exceptional. On one hand, the ONASPORT device provides instant assessment of the athlete's health without disruptions to their routine. This device is not only non-invasive, but is seamlessly integrated into the user's daily life, making adoption effortless. On the other hand, this device performs multiparametric measurements of sweat which allows to analyze its content with precision. Sweat is a complex fluid that contains a lot of components that interact with each other, so a multiparametric analysis must be performed to carry out a good assessment.

Apart from enhancing the daily life of athletes, this technology has the potential to play a crucial role in the medical field. The non-invasive and continuous measurement of the composition of sweat could provide to doctors' information about biochemical parameters, such as the glucose level, that allows them to improve the attention given to the patients and improve their treatments. To translate this device from the sports to medical field, a lot of work is required in the field of sensing and microfluidics in order

to be capable of processing low volumes of sweat. These modifications also imply to adjust the electronic instrumentation of this device to meet with the specifications of the new measurement methods.

Apart from modifying this system, it is imperative to conduct a clinical trial to assess the accuracy of the performed measurements. Furthermore, the safety of this wearable device must be demonstrated by means of several trials. Eventually, the accumulated evidence needs to be presented to a notified body for the certification of this system as a medical device.

The general characteristics of this wearable device are shown on the following table (see Table 6.3):

Form factor	**Value**	
Central module dimensions	75 x 35 x 16 mm	
Disposable dimensions	34 x 33 x 3 mm	
Central module weight	26 grams	
Disposable weight	4 grams	
Health features	**Range**	**Accuracy**
Heart rate	40 to 220 bpm	± 1 bpm
Perspiration rate	0 to 2 µL/min	± 0.1 µL/min
Conductivity	0 to 12 mS/cm	± 0.1 mS/cm
Lactate Level	0 to 100 mM	± 1 mM
Autonomy	**Value**	
Recommended coin cell capacity	235 mAh	
Battery life using the recommended battery	100 hours of training	
Connectivity	**Value**	
Range	Up to 10 meters	
Protocol	Bluetooth Low Energy	

Table 6.3. ONASPORT device characteristics.

6.6. References

[1] "ONASPORT device." Accessed: Mar. 09, 2024. [Online]. Available: https://onalabs.com/en/onasport/

[2] A. Ç. Seçkin, B. Ateş, and M. Seçkin, "Review on Wearable Technology in Sports: Concepts, Challenges and Opportunities," *Applied Sciences (Switzerland)*, vol. 13, no. 18, Sep. 2023, doi: 10.3390/app131810399.

[3] C. Schneider *et al.*, "Heart rate monitoring in team sports—A conceptual framework for contextualizing heart rate measures for training and recovery prescription," *Front Physiol*, vol. 9, May 2018, doi: 10.3389/fphys.2018.00639.

[4] J. Aguilar-Torán *et al.*, "Novel Sweat-Based Wearable Device for Advanced Monitoring of Athletic Physiological Biometrics," *Sensors*, vol. 23, no. 23, Dec. 2023, doi: 10.3390/s23239473.

[5] "TICKR Replacement Heart Rate Strap." Accessed: Mar. 09, 2024. [Online]. Available: https://eu.wahoofitness.com/devices/heart-rate-monitors/tickr-replacement-heart-rate-strap

[6] B. M. Popkin, K. E. D'Anci, and I. H. Rosenberg, "Water, hydration, and health," *Nutr Rev*, vol. 68, no. 8, pp. 439–458, 2010, doi: 10.1111/j.1753-4887.2010.00304.x.

[7] J. Lacey *et al.*, "A multidisciplinary consensus on dehydration: definitions, diagnostic methods and clinical implications," *Ann Med*, vol. 51, no. 3–4, pp. 232–251, May 2019, doi: 10.1080/07853890.2019.1628352.

[8] N. A. Shaheen, A. A. Alqahtani, H. Assiri, R. Alkhodair, and M. A. Hussein, "Public knowledge of dehydration and fluid intake practices: Variation by participants' characteristics," *BMC Public Health*, vol. 18, no. 1, Dec. 2018, doi: 10.1186/s12889-018-6252-5.

[9] L. E. Armstrong and D. J. Casa, "Methods to Evaluate Electrolyte and Water Turnover of Athletes," *Athl Train Sports Health Care*, vol. 1, no. 4, pp. 169–179, Jul. 2009, doi: 10.3928/19425864-20090625-06.

[10] L. B. Baker, "Sweating Rate and Sweat Sodium Concentration in Athletes: A Review of Methodology and Intra/Interindividual Variability," *Sports Medicine*, vol. 47, pp. 111–128, Mar. 2017, doi: 10.1007/s40279-017-0691-5.

[11] K. A. Barnes *et al.*, "Normative data for sweating rate, sweat sodium concentration, and sweat sodium loss in athletes: An update and analysis by sport," *J Sports Sci*, vol. 37, no. 20, pp. 2356–2366, 2019, doi: 10.1080/02640414.2019.1633159.

[12] A. Hourlier-Fargette *et al.*, "Skin-interfaced soft microfluidic systems with modular and reusable electronics for: In situ capacitive sensing of sweat loss, rate and conductivity," *Lab Chip*, vol. 20, no. 23, pp. 4391–4403, Dec. 2020, doi: 10.1039/d0lc00705f.

[13] D. H. Choi, M. Gonzales, G. B. Kitchen, D. T. Phan, and P. C. Searson, "A Capacitive Sweat Rate Sensor for Continuous and Real-Time Monitoring of Sweat Loss," *ACS Sens*, vol. 5, no. 12, pp. 3821–3826, Dec. 2020, doi: 10.1021/acssensors.0c01219.

[14] C. Foster, R. Kadara, and C. Banks, "Fundamentals of Screen-Printing Electrochemical Architectures," in *SpringerBriefs in Applied Sciences and Technology*, 2016, pp. 13–23. doi: 10.1007/978-3-319-25193-6_2.

[15] C. A. Riedi, A. F. Zavadniak, D. C. Silva, A. Franco, and N. A. R. Filho, "Comparison of conductivity with sodium determination in the same sweat sample," *J Pediatr (Rio J)*, vol. 76, no. 6, pp. 443–6, Nov. 2000, doi: 10.2223/jped.91.

[16] H. Cunha-Silva and M. J. Arcos-Martinez, "Dual range lactate oxidase-based screen printed amperometric biosensor for analysis of lactate in diversified samples," *Talanta*, vol. 188, pp. 779–787, Oct. 2018, doi: 10.1016/j.talanta.2018.06.054.

[17] S. E. Allen and J. L. Holm, "Lactate: Physiology and clinical utility," *Journal of Veterinary Emergency and Critical Care*, vol. 18, no. 2, pp. 123–132, Apr. 2008, doi: 10.1111/j.1476-4431.2008.00286.x.

[18] M. L. Goodwin, J. E. Harris, A. Hernández, and L. B. Gladden, “Blood Lactate Measurements and Analysis during Exercise: A Guide for Clinicians,” *J Diabetes Sci Technol*, vol. 1, no. 4, pp. 558–569, 2007, doi: 10.1177/193229680700100414.

[19] P. J. Derbyshire, H. Barr, F. Davis, and S. P. J. Higson, “Lactate in human sweat: A critical review of research to the present day,” *Journal of Physiological Sciences*, vol. 62, no. 6. pp. 429–440, Nov. 2012. doi: 10.1007/s12576-012-0213-z.

[20] Takashi Yamagata, Daisuke Kume, Toshihiro Wakimoto, and Noriki Nagao, “The Influence of Sampling Site on Blood Lactate Response to Steady State Exercise,” *Journal of Sports Science*, vol. 6, no. 5, Oct. 2018, doi: 10.17265/2332-7839/2018.05.003.

[21] G. Rabost-Garcia *et al.*, “Non-Invasive Multiparametric Approach To Determine Sweat-Blood Lactate Bioequivalence,” *ACS Sens*, vol. 8, no. 4, pp. 1536–1541, Apr. 2023, doi: 10.1021/acssensors.2c02614.

[22] “Energizer CR2032.” Accessed: Mar. 17, 2024. [Online]. Available: https://data.energizer.com/pdfs/cr2032.pdf

[23] “BQ35100.” Accessed: Mar. 23, 2024. [Online]. Available: https://www.ti.com/lit/ds/symlink/bq35100.pdf?ts=1712046910813&ref_url=https%253A%252F%252Fnl.mouser.com%252F

[24] “AD8233.” Accessed: Mar. 09, 2024. [Online]. Available: https://www.analog.com/media/en/technical-documentation/data-sheets/ad8233.pdf

[25] J. Pan and W. J. Tompkins, “A Real-Time QRS Detection Algorithm,” *IEEE Trans Biomed Eng*, vol. BME-32, no. 3, pp. 230–236, 1985, doi: 10.1109/TBME.1985.325532.

[26] “OPA348-Q1.” Accessed: Mar. 09, 2024. [Online]. Available: https://www.ti.com/lit/ds/symlink/opa2348-q1.pdf?ts=1712060277642

[27] “OPA4348.” Accessed: Mar. 09, 2024. [Online]. Available: https://www.ti.com/lit/ds/symlink/opa4348.pdf?ts=1712132398097&ref_url=https%253A%252F%252Fwww.ti.com%252Fproduct%252Fes-mx%252FOPA4348

[28] “REF35.” Accessed: Mar. 09, 2024. [Online]. Available: https://www.ti.com/lit/ds/symlink/ref35.pdf?ts=1712066203799&ref_url=https%253A%252F%252Fwww.ti.com%252Fproduct%252FREF35%252Fpart-details%252FREF35102QDBVR

[29] W. Olthuis, W. Streekstra, and P. Bergveld, “Theoretical and experimental determination of cell constants of planar-interdigitated electrolyte conductivity sensors,” *Sens Actuators B Chem*, vol. 24, no. 1, pp. 252–256, 1995, doi: https://doi.org/10.1016/0925-4005(95)85053-8.

[30] “ADA4505-4.” Accessed: Mar. 09, 2024. [Online]. Available: https://www.analog.com/media/en/technical-documentation/data-sheets/ada4505-1_4505-2_4505-4.pdf

[31] J. Aguilar *et al.*, “Autonomous self-powered potentiostat architecture for biomedical wearable applications,” in *2020 XXXV Conference on Design of Circuits and Integrated Systems (DCIS)*, 2020, pp. 1–6. doi: 10.1109/DCIS51330.2020.9268667.

[32] “Suunto Smart Heart Rate Belt.” Accessed: Mar. 09, 2024. [Online]. Available: https://www.suunto.com/Products/Heart-Rate-Belts/suunto-smart-heart-rate-belt/

[33] R. Gilgen-Ammann, T. Schweizer, and T. Wyss, “RR interval signal quality of a heart rate monitor and an ECG Holter at rest and during exercise,” *Eur J Appl Physiol*, vol. 119, no. 7, pp. 1525–1532, Jul. 2019, doi: 10.1007/s00421-019-04142-5.

[34] “LAQUAtwin EC-11.” Accessed: Mar. 09, 2024. [Online]. Available: https://www.horiba.com/esp/water-quality/productos/detail/action/show/Product/laquatwin-ec-11-872/

[35] “Legato 101.” Accessed: Mar. 09, 2024. [Online]. Available: https://www.kdscientific.com/legato-101-syringe-pump.html?___SID=U

[36] S. J. Montain, S. N. Cheuvront, and M. N. Sawka, “Exercise associated hyponatraemia: Quantitative analysis to understand the aetiology,” *Br J Sports Med*, vol. 40, no. 2, pp. 98–105, Feb. 2006, doi: 10.1136/bjsm.2005.018481.

[37] “PalmSens4.” Accessed: Mar. 19, 2024. [Online]. Available: https://www.palmsens.com/product/palmsens4/

[38] Z. Sonner *et al.*, “The microfluidics of the eccrine sweat gland, including biomarker partitioning, transport, and biosensing implications,” *Biomicrofluidics*, vol. 9, no. 3, May 2015, doi: 10.1063/1.4921039.

7. Conclusions and future work

This final chapter summarized the monitoring system presented in this thesis along with its main elements. The characteristics of every element are presented focusing on the wearable devices designed, implemented, and validated. Eventually, the future lines of work derived from this research are presented.

7.1. Conclusions

The process of developing a medical wearable device for remote physiological data collection is presented in this thesis. This process encompasses the system design to the medical certification and even the industrialization. Devices implemented using this well-defined methodology are robust products ready to be used in clinical settings, such as hospitals or ambulatories.

Two different wearable devices were designed, implemented, and validated following the abovementioned procedure. Both devices are intended for remote, continuous, and non-invasive assessment of the individuals' health status. These monitoring tools address several issues related to the aging population due to the rise of longevity.

As it is discussed in the first chapter, increased life expectancy makes diseases associated with age more prevalent causing a huge raise in health expenditure. In addition, seasonal infections, such as the flu, or pandemics, like the recent COVID-19 crisis, can collapse the healthcare system and drastically reduce its efficiency. To mitigate these problems, Hospital at Home (HAH) units were created. These units have demonstrated to be a well-rounded solution, but most of the visits are focused on the acquisition of biometric data related to patient physiological status. To improve the efficiency of HAH units, novel tools capable of monitoring the patients' health state continuously and remotely are required. The company Onalabs developed a monitoring medical system for HAH units based on the two wearable devices presented in this thesis.

In the second chapter, the functional characteristics of the aforementioned monitoring system are presented and described. This system uses wearable devices to collect physiological information from patients and send the gathered data to a digital platform by means of a gateway. Apart from presenting the functionalities, the technologies involved in the operation of this system are presented too. Every element is described, focusing on the sensing technologies of the implemented wearable devices. Finally, the development procedure followed during the design, implementation, and validation of a medical device is presented.

The third chapter presents and characterizes a new medical wearable device named ONAVITAL which it is capable of monitoring the vital signs of a patient continuously, remotely, and in a non-invasive way. Vital sign monitoring allows medical personnel to determine the individual's health status and evaluate the efficiency of treatments. This wearable device is a bracelet that is worn on the user's wrist and contains multiple sensors, enabling the collection, processing, and analysis of physiological data directly from the wearer's skin. It measures the pulse rate, oxygen saturation, arterial blood pressure, and skin temperature providing valuable information to assess the patient status.

In the fourth chapter, the clinical evaluation of the ONAVITAL device is presented. The clinical evaluation assesses the accuracy of the developed system and evaluates the viability to use this wearable device in a clinical setting. Both the clinical evaluation with healthy volunteers and critical patients are described. This clinical trial consisted of the direct comparison between the data provided by the ONAVITAL device and the equipment regularly used to monitor patients at the hospital facilities.

The fifth chapter presents the ONAVITAL medical certification process. To use a device in a clinical setting, it must be approved by the regulatory authorities of the country where it is distributed. Certifying a equipment as a medical device verifies both the accuracy and safety of this system. Apart from the certification process, the industrialization of this wearable device is described in this section. This process allows to produce a large number of devices with the same characteristics and functionalities at a reduced cost. The industrialization phase is normally overshadowed during the technological development but it is critical since the well-function of the final devices depends on this process.

Eventually, the sixth chapter presents and describes a novel wearable device capable of collecting and analyzing the sweat content of an individual. Sweat is a biofluid that contains many biomarkers, which can be used to determine the patient's health status, but it is barely utilized in clinical settings because it is difficult to process it. To overcome this issue, a microfluidic system able to analyze this biofluid was created. This microfluidic system is inside a single-use cartridge which collects sweat from the skin and canalizes it into a microfluidic channel. Inside this channel there are several sensors that analyze the content of this biofluid. The cartridge is connected to the wearable device named ONASPORT, and it is used to monitor the state of an athlete during a physical activity. This patented device estimates the user's heart rate alongside the dehydration level and blood lactate levels in real-time. Monitoring all these parameters during a trial gives a lot of information to sport medicine doctors and allows for efficient training and recovery.

7.2. Future work and perspectives

The monitoring system described in this thesis can be used in countless scenarios, but there are two main applications for the developed technology. On one hand, this system can be utilized to improve the efficiency of HAH units. The ONAVITAL device measures the vital signs of individuals, allowing for continuous and non-invasive assessment of the patient's health status remotely. These characteristics enable more effective resource allocation, thereby improving the attention provided by nurses and doctors. On the other hand, this monitoring system can be also used to monitor the athletes' status during a physical activity and improve their training methodology. The ONASPORT device measures continuously the content of sweat giving insights about the user performance.

Apart from the mentioned applications mentioned, the work developed in this thesis open a wide range of opportunities and research lines:

- Personalized care can be provided to every patient monitored by an ONAVITAL device. Unique patterns can be identified through the study of the physiological parameters recorded by this wearable device. Identifying these patterns allows healthcare professionals to treat conditions even before symptoms appear. To

perform this task, artificial intelligence (AI) algorithms must be developed using as dataset the huge amount generated by this device during extensive periods of time [1], [2], [3]. AI applied to the healthcare field can revolutionize the diagnosis and treatment, improving the attention provided while reducing costs.

- From the signals recorded by the ONAVITAL sensors, more physiological parameters can be estimated. The patient's respiratory rate can be measured by processing the recorded pulse oximetry (PPG) signals [4], [5]. Monitoring this parameter would allow a complete assessment of an individual health status because every vital sign would be measured.

- Not only the vital signs can be monitored using the PPG sensors. Heart rate variability can be also measured this system. Heart rate variability is the variance in time between heart beats and it is typically used to determine the emotional state of an individual [6], [7], so the ONAVITAL device can be a tool for assessing the patient' psychological status.

- Another sensor of the ONAVITAL device is an inertial measurement unit (IMU) formed by an accelerometer and a gyroscope. This sensor monitors the user's movement and relevant information can be extracted analyzing this data. For instance, the gait evolution can be analyzed which is an indicator of mortality [8], [9].

- The ONASPORT device is capable of providing information about the athlete's status during a physical activity but does not give advises and recommendations. To exploit this novel technology, a huge dataset must be created and analyzed. Through AI algorithms more useful information can be provided to sport medicine doctors and athletes.

- Heart rate variability is regularly used in the athletic world to identify periods of optimal training and to monitor recovery status and any potential overtraining [10]. The ONASPORT device can measure this physiological parameter by processing the electrocardiogram (ECG) used to estimate the user's heart rate.

- Apart from enhancing the daily lives of athletes, the sweat monitoring technology has the potential to play a crucial role in the medical field. Non-invasive and continuous measurements of sweat can provide healthcare providers with information about patient's biochemical parameters, improving the attention to patients and their treatment. To translate this system to the healthcare field, the sensors and microfluidics must be modified to process low volumes of sweat (range of nanoliters).

- Other biomarkers can be estimated from sweat analysis. For instance, several studies demonstrated that exists a strong correlation between blood and sweat glucose concentration [11], [12]. A sweat based wearable device capable of

monitoring glucose has the potential to improve the lives of millions of diabetic patients since every glucose monitoring device available on the market is invasive.

- Despite the two wearable devices presented in this thesis were designed for different applications, they can be used together. These systems used in conjunction allow a complete monitoring of an individual because both the vital signs and chemical analysis are performed at the same time. Furthermore, the study of the physiological parameters monitored can generate new health features that complement the current ones.

- Both systems use batteries as power sources. Batteries have a limited lifespan which produce a hiatus in the measurements when they discharge. Energy harvesting represents the energy derived from the ambient sources that is extracted and directly converted into electrical energy [13]. The power source of the wearable devices could be substituted by an energy harvesting system that supplies the system electronics and sensors.

7.3. References

[1] S. A. Alowais *et al.*, "Revolutionizing healthcare: the role of artificial intelligence in clinical practice," *BMC Medical Education*, vol. 23, no. 1. BioMed Central Ltd, Dec. 01, 2023. doi: 10.1186/s12909-023-04698-z.

[2] F. Kitsios, M. Kamariotou, A. I. Syngelakis, and M. A. Talias, "Recent Advances of Artificial Intelligence in Healthcare: A Systematic Literature Review," *Applied Sciences (Switzerland)*, vol. 13, no. 13, Jul. 2023, doi: 10.3390/app13137479.

[3] T. Davenport and R. Kalakota, "The potential for artificial intelligence in healthcare," *Future Healthc J*, vol. 6, no. 2, pp. 94–98, 2019, doi: 10.7861/futurehosp.6-2-94.

[4] C. Massaroni, A. Nicolò, D. Lo Presti, M. Sacchetti, S. Silvestri, and E. Schena, "Contact-based methods for measuring respiratory rate," *Sensors (Switzerland)*, vol. 19, no. 4. MDPI AG, Feb. 02, 2019. doi: 10.3390/s19040908.

[5] H. Liu, J. Allen, D. Zheng, and F. Chen, "Recent development of respiratory rate measurement technologies," *Physiological Measurement*, vol. 40, no. 7. IOP Publishing Ltd, Aug. 02, 2019. doi: 10.1088/1361-6579/ab299e.

[6] H. G. Kim, E. J. Cheon, D. S. Bai, Y. H. Lee, and B. H. Koo, "Stress and heart rate variability: A meta-analysis and review of the literature," *Psychiatry Investigation*, vol. 15, no. 3. Korean Neuropsychiatric Association, pp. 235–245, Mar. 01, 2018. doi: 10.30773/pi.2017.08.17.

[7] K. Georgiou, A. V. Larentzakis, N. N. Khamis, G. I. Alsuhaibani, Y. A. Alaska, and E. J. Giallafos, "Can Wearable Devices Accurately Measure Heart Rate Variability? A Systematic Review," *Folia Med (Plovdiv)*, vol. 60, no. 1, pp. 7–20, Mar. 2018, doi: 10.2478/folmed-2018-0012.

[8] D. K. White *et al.*, "Trajectories of gait speed predict mortality in well-functioning older adults: The health, aging and body composition study," *Journals of Gerontology - Series*

A Biological Sciences and Medical Sciences, vol. 68, no. 4, pp. 456–464, Apr. 2013, doi: 10.1093/gerona/gls197.

[9] L. J. Dommershuijsen, B. M. Isik, S. K. L. Darweesh, J. N. van der Geest, M. Kamran Ikram, and M. Arfan Ikram, "Unraveling the association between gait and mortality-one step at a time," *Journals of Gerontology - Series A Biological Sciences and Medical Sciences*, vol. 75, no. 6, pp. 1184–1190, 2021, doi: 10.1093/GERONA/GLZ282.

[10] A. E. Aubert, B. Seps, and F. Beckers, "Heart Rate Variability in Athletes," *Sports Medicine*, vol. 33, no. 12, pp. 889–919, 2003, doi: 10.2165/00007256-200333120-00003.

[11] E. V. Karpova, E. V. Shcherbacheva, A. A. Galushin, D. V. Vokhmyanina, E. E. Karyakina, and A. A. Karyakin, "Noninvasive diabetes monitoring through continuous analysis of sweat using flow-through glucose biosensor," *Anal Chem*, vol. 91, no. 6, pp. 3778–3783, Mar. 2019, doi: 10.1021/acs.analchem.8b05928.

[12] J. Moyer, D. Wilson, I. Finkelshtein, B. Wong, and R. Potts, "Correlation between sweat glucose and blood glucose in subjects with diabetes," *Diabetes Technol Ther*, vol. 14, no. 5, pp. 398–402, May 2012, doi: 10.1089/dia.2011.0262.

[13] A. Ali, H. Shaukat, S. Bibi, W. A. Altabey, M. Noori, and S. A. Kouritem, "Recent progress in energy harvesting systems for wearable technology," *Energy Strategy Reviews*, vol. 49, p. 101124, 2023, doi: https://doi.org/10.1016/j.esr.2023.101124.

Appendix 1

Resumen

La esperanza de vida no ha dejado de crecer durante las últimas décadas. Esta situación sin precedentes es debida a los avances técnicos producidos tanto en el campo de la medicina como el de los cuidados. El aumento de la longevidad provoca que el conjunto de la población envejezca de forma dramática haciendo que el porcentaje de personas de la tercera edad no pare de crecer. Esta situación trae consigo multitud de problemáticas que las sociedades modernas deben abordar.

La población mayor de 65 años es propensa a presentar enfermedades crónicas como la osteoporosis, la diabetes, o las enfermedades cardiovasculares. Estas afecciones requieren de atención constante por parte del personal médico, ya que los pacientes deben ser monitorizados continuamente y tienen que recibir tratamiento específico para paliar los efectos de sus enfermedades. Para poder atender a una población envejecida, se necesitan nuevos métodos y herramientas que ayuden al personal sanitario a llevar a cabo su labor. Si no se aborda esta situación se corre el riesgo que muchas personas queden desatendidas e incluso que el sistema sanitario colapse si hay un aumento inusual de pacientes, como ya sucedió en la reciente pandemia de COVID-19.

Los dispositivos *wearable*, como las pulseras inteligentes, han demostrado ser una herramienta muy útil para el personal médico, ya que permiten monitorizar de forma continua y remota a los pacientes. De esta forma, se elimina la necesidad de que médicos y enfermeros realicen las tareas de seguimiento. Al reducir la carga de trabajo, los recursos se pueden usar de forma más eficiente haciendo que el sistema sanitario sea más sostenible.

Aunque estos dispositivos son de gran utilidad, la mayoría de los *wearables* actuales no son fiables. Esto es debido a que son dispositivos de electrónica de consumo, los cuales no están certificados como equipo médico. La certificación médica es indispensable para que un sistema sea utilizado en un entorno clínico, como un ambulatorio o un hospital, y asegura que el equipo tiene un estándar de calidad alto además de que es seguro tanto para el paciente como para el personal sanitario.

Para saber el estado de salud de una persona se pueden medir multitud de parámetros, aunque la monitorización de los signos vitales suele ser el método más extendido. Las constantes vitales son un conjunto de parámetros fisiológicos que reflejan las funciones esenciales del organismo. Estos parámetros tienden a mantenerse dentro de un rango bien definido, y cualquier desviación de estos puede indicar la presencia de una enfermedad o condición médica.

Aunque la monitorización de los signos vitales es muy útil, no da una visión completa del estado de salud de una persona. Para complementar la información proporcionada por estos parámetros, es necesario recoger y analizar datos bioquímicos, como por ejemplo el nivel de glucosa en sangre. El análisis de sangre es el método de referencia para el análisis bioquímico, pero presenta varios inconvenientes que limitan su uso: son invasivos, requieren personal cualificado y sólo permite conocer el estado del paciente en el

momento de la extracción. Un método alternativo consiste en el análisis del sudor de los pacientes.

El sudor es un biofluido compuesto mayoritariamente por agua, pero contiene multitud de electrolitos, iones, aminoácidos, proteínas y otras moléculas pequeñas. Debido a su rico contenido, este fluido se ha convertido en un gran candidato para ser analizado. El análisis del sudor no es invasivo, no requiere que un profesional recoja la muestra y puede realizarse de forma continua, ya que este fluido está siempre presente en la piel debido a la termorregulación del organismo.

El objetivo de esta tesis es desarrollar dispositivos *wearable* para un sistema de monitorización integral de salud. Estos dispositivos son capaces de medir las constantes vitales de un paciente y analizar el contenido de su sudor. La monitorización de tanto los signos vitales como de los biomarcadores de este biofluido permite una evaluación precisa y completa del estado de salud de un individuo.

Por un lado, se presenta el desarrollo de un dispositivo *wearable* de grado médico capaz de monitorizar las constantes vitales de los pacientes. No sólo se ha desarrollado el dispositivo, sino que se ha llevado a cabo la certificación e industrialización de este sistema dando como resultado un producto robusto listo para ser utilizado en entornos clínicos.

Por otro lado, junto a este dispositivo médico, se desarrolla un novedoso sistema capaz de capturar y analizar el contenido del sudor de una persona de forma no invasiva y continua. Este dispositivo puede ser una herramienta inestimable para el personal médico, ya que puede proporcionar información sólo disponible mediante análisis invasivos como lo es el análisis de sangre.

Estos dos dispositivos wearables están conectados a la misma plataforma, por lo que los datos recogidos de ambos sistemas pueden utilizarse para evaluar el estado de los individuos. El sistema de monitorización desarrollado tiene el potencial de revolucionar el campo de la asistencia sanitaria ya que puede llevar a cabo una monitorización remota, no invasiva y continua del paciente.

List of publications

JOURNALS

Authors: Genis Rabost-Garcia, Valeria Colmena, Javier Aguilar-Torán, Joan Vieyra Galí, Jaime Punter-Villagrasa, Jasmina Casals-Terré, Pere Miribel-Catala, Xavier Muñoz, Joan Cadefau, Josep Padullés and Daniel Brotons Cuixart

Title: Non-Invasive Multiparametric Approach To Determine Sweat–Blood Lactate Bioequivalence

Journal: ACS Sensors

DOI: https://doi.org/10.1021/acssensors.2c02614

Authors: Javier Aguilar-Torán, Genis Rabost-Garcia, Samantha Toinga-Villafuerte, Albert Álvarez-Carulla, Valeria Colmena-Rubil, Andrea Fajardo-Garcia, Andrea Cardona-Bonet, Jasmina Casals-Terré, Xavier Muñoz-Pascual, Pere Miribel-Català and Jaime Punter-Villagrasa

Title: Novel Sweat-Based Wearable Device for Advanced Monitoring of Athletic Physiological Biometrics

Journal: MDPI Sensors

DOI: https://doi.org/10.3390/s23239473

CONFERENCES

Authors: Javier Aguilar-Torán, Alvert Alvarez-Carulla, Valeria Colmena-Rubil, Oscar Carreras, Genis Rabost, Manel Puig-Vidal, Jordi Colomer-Farrorons, Xavier Muñoz, Pere Miribel-Catala and Jaime Punter-Villagrasa

Title: Autonomous self-powered potentiostat architecture for biomedical wearable applications

Conference: 2020 XXXV Conference on Design of Circuits and Integrated Systems (DCIS)

Place: Segovia, Spain

Date: 18-20 November 2020

Authors: Javier Aguilar-Torán, Jaime Punter-Villagrasa, Xavier Muñoz, and Pere Miribel-Catala

Title: Home hospitalization system for the remotely and continuous monitoring of chronic patients

Conference: IECON 2022 – 48th Annual Conference of the IEEE Industrial Electronics Society

Place: Brussels, Belgium

Date: 17-20 October 2022

Authors: Javier Aguilar-Torán, Albert Castellano-Tallón, Jordi Colomer-Farrarons, Albert Alvarez-Carulla, Samantha Toinga-Villafuerte, Xavier Muñoz, Jaime Punter-Villagrasa, and Pere Miribel-Catala

Title: Towards a self-powered cardiac monitoring device

Conference: XXXVII Conference on Design of Circuits and Integrated Systems - DCIS 2022

Place: Pamplona, Spain

Date: 16-18 November 2022

List of patents

Authors: Genis Rabost-Garcia, Xavier Muñoz-Pascual, Javier Aguilar-Torán, Jaime Punter-Villagrasa and Valeria Colmena-Rubil

Title: A Wearable Device for Continuous Monitoring of Health Parameters

Patent country: European Patent Office

Patent number: EP4205644A1

Publication: 07/05/2023

State: Patent Requested

Appendix 2

Data protection consent

Document used to obtain the consent of each volunteer that participated in the multiple experiments performed.

CONSENTIMIENTO PROTECCION DE DATOS

Nombre completo:
Documento de identidad:
Email:

ONALABS INNO-HUB SL con NIF/CIF B66905936, y domicilio social en 08290 – Cerdanyola del Vallès, Avinguda Parc Tecnològic, 3, se compromete a tratar de forma absolutamente confidencial todos sus datos de carácter personal, según lo establecido en el Reglamento General de Datos UE 2016/679 (RGPD) y Ley Orgánica 3/2018, de 5 de diciembre, de Protección de datos personales y Garantía de los Derechos Digitales (LOPDGDD).

El titular de este consentimiento autoriza a ONALABS INNO-HUB SL a tratar sus datos personales y otorga esta autorización de manera expresa, precisa, inequívoca e informada. En cumplimiento de lo dispuesto en los artículos 13 y 14 del RGPD y en el artículo 11 de la LOPDGDD se informa de los siguientes datos:

Responsable del tratamiento de sus datos personales: ONALABS INNO-HUB SL con NIF/CIF B66905936, y domicilio social en 08290 – Cerdanyola del Vallès, Avinguda Parc Tecnològic, 3 – Email: legal@onalabs.com.

Finalidad del trato de sus datos: ONALABS INNO-HUB SL tratará toda la información que nos facilita para el testeo y el desarrollo de sistemas de monitorización sanitarios no invasivos.

Conservación: Los datos personales proporcionados se conservarán mientras no se solicite la supresión por parte del interesado o durante el tiempo necesario para cumplir con las obligaciones legales.

Destinatarios: Sus datos serán tratados por ONALABS INNOHUB, S.L. y prestadores de servicio o colaboradores.

Derechos: Puede ejercer sus derechos de acceso, rectificación, supresión, portabilidad de sus datos y a la limitación u oposición de su tratamiento, así como no ser objeto de decisiones individuales automatizadas, dirigiéndose a nuestro domicilio social o a través del correo electrónico, debiéndose identificar debidamente y solicitar claramente el derecho a ejercer.

☐ Consiento expresamente en el tratamiento de mis datos. Firma:

En....., a..... de..... de .....

Publication 1

Novel Sweat-Based Wearable Device for Advanced Monitoring of Athletic Physiological Biometrics

Javier Aguilar-Torán, Genis Rabost-Garcia, Samantha Toinga-Villafuerte, Albert Álvarez-Carulla, Valeria Colmena-Rubil, Andrea Fajardo-Garcia, Andrea Cardona-Bonet, Jasmina Casals-Terré, Xavier Muñoz-Pascual, Pere Miribel-Català and Jaime Punter-Villagrasa

Sensors 2023, Volume 23, Issue 23, 9473

sensors

MDPI

Article

Novel Sweat-Based Wearable Device for Advanced Monitoring of Athletic Physiological Biometrics

Javier Aguilar-Torán [1,2,*], Genis Rabost-Garcia [1,3], Samantha Toinga-Villafuerte [1], Albert Álvarez-Carulla [1], Valeria Colmena-Rubil [1,4], Andrea Fajardo-Garcia [1], Andrea Cardona-Bonet [1], Jasmina Casals-Terré [3], Xavier Muñoz-Pascual [1], Pere Miribel-Català [2] and Jaime Punter-Villagrasa [1]

[1] Onalabs Inno-Hub SL, 08290 Cerdanyola del Vallès, Spain
[2] Department of Electronics and Biomedical Engineering, Barcelona University, 08028 Barcelona, Spain
[3] Department of Mechanical Engineering, Polytechnic University of Catalonia, 08222 Terrassa, Spain
[4] Department of Chemistry, Autonomous University of Barcelona, 08193 Cerdanyola del Vallès, Spain
* Correspondence: j.aguilar@onalabs.com

Abstract: Blood testing has traditionally been the gold standard for the physiological analysis and monitoring of professional athletes. In recent years, blood testing has moved out of the laboratory thanks to portable handheld devices, such as lactate meters. However, despite its usefulness and widespread use, blood testing has several drawbacks and limitations, such as the need for the athlete to stop exercising for blood extraction and the inability to have data continuously collected. In this scenario, sweat has become an alternative to blood testing because of its rich content of electrolytes and metabolites, as well as small quantities of sugars, proteins, and ions. Nevertheless, there are few devices capable of analyzing this biofluid and providing useful information to users. In this paper, an electronic system designed for the autonomous analysis of sweat electrolytes and metabolites along with heart rate dynamics is presented. This system is part of a novel wearable device tailored for athletes that offers to the user a real-time assessment of their physiological status and performance.

Keywords: sweat monitoring; perspiration level; dehydration; lactate; heart rate; wearable device; sports medicine

Citation: Aguilar-Torán, J.; Rabost-Garcia, G.; Toinga-Villafuerte, S.; Álvarez-Carulla, A.; Colmena-Rubil, V.; Fajardo-Garcia, A.; Cardona-Bonet, A.; Casals-Terré, J.; Muñoz-Pascual, X.; Miribel-Català, P.; et al. Novel Sweat-Based Wearable Device for Advanced Monitoring of Athletic Physiological Biometrics. *Sensors* **2023**, *23*, 9473. https://doi.org/10.3390/s23239473

Academic Editors: Giovanni Saggio and Ki H. Chon

Received: 12 October 2023
Revised: 13 November 2023
Accepted: 17 November 2023
Published: 28 November 2023

1. Introduction

Blood tests are regularly used by clinicians to assess the state of health of patients. This trial is the gold standard for biochemical analyses, but it has several drawbacks that limit its use. Blood tests are invasive, require trained personnel, and only provide the state of the patient at the moment of the extraction. An alternative analysis that has gained a lot of interest during the past few years is based on the use of sweat as the sample to be analyzed [1,2].

Sweat is a biofluid composed mainly of water, but it contains various electrolytes, ions, amino acids, proteins, and other small molecules. Due to its rich content, this fluid has become a great candidate for analysis. Sweat analysis is non-invasive, does not require a professional to collect the sample, and can be carried out continuously, since this biofluid is always present on the skin due to the body's thermoregulation [3].

Despite these advantages, nowadays, sweat is barely used, and only some trials, such as the cystic fibrosis test, utilize this biofluid [4]. The lack of tests that use sweat as a sample is because a standardized method to extract sweat from skin does not exist. This fact, along with the low volume of the sample available (range of nanoliters) and liquid evaporation, makes sweat a biofluid that is difficult to measure. These issues are solved by attaching sensors to the skin, but this methodology produces a major issue: contamination of the sample due to the accumulation of sweat on the sensor. To avoid this unwanted situation, a microfluidic system can be used to renew the sample and expel the generated waste [5].

Several research groups have developed systems capable of collecting sweat from the skin, processing it, and analyzing its content using different sensors. Liang et al. developed a paper-based microfluidic device for the real-time monitoring of sweat potassium [6]. Martín et al. presented a microfluidic detection platform for the monitoring of glucose and lactate levels [7]. Kim et al. developed a microfluidic patch that allowed for rapid colorimetric assessments of the concentrations of multiple essential nutrients in sweat [8]. Noura et al. presented a paper-based microfluidic electrochemical integrated device for measuring the glucose concentration in sweat in real time [9].

Most of the systems intended to analyze the content of sweat were tested while performing a physical activity, such as cycling. This method was used to validate the developed systems because it is an easy way to obtain significant volumes of this biofluid passively. During physical activity, sweat is generated to regulate the body's internal temperature. The analysis of sweat at the time of an activity allows sports medicine doctors to assess an athlete's performance and state of health.

It has been demonstrated that the monitoring of physiological parameters using wearable devices during a physical activity helps to prevent injuries and enhance the performance of athletes [10]. However, mainly the heart rate (HR) is used by sport professionals to determine the state of the athlete during the exercise [11]. Other parameters that give a lot of information, such as the blood lactate level and user's dehydration , are rarely measured, and when they are monitored, a special test must be carried out.

In this paper, we present a novel wearable device capable of collecting sweat from the skin, canalizing it inside a microfluidic chamber, and analyzing its content using an array of sensors. The device was based on a sport chest strap that was modified to integrate the microfluidic system, the sensors, and the device's electronics. This system is intended for estimating the user's heart rate, dehydration, and blood lactate levels during physical activity. This paper focuses on the development of the system, sensors, and involved electronics and the initial results. Materials and methods for the obtention of blood lactate levels and dehydration state from the data collected are not developed here.

2. Materials and Methods

2.1. System Architecture

The wearable device (Figure 1a) was conceived as a band that can be placed on the athlete's chest. This system is formed by three different elements: a central module (Figure 1b), a cartridge (Figure 1c), and a chest strap (Figure 1d).

Figure 1. Structure of the wearable device. (**a**) Complete system, (**b**) central module (electronics of the system), (**c**) cartridge, and (**d**) chest strap.

The central module contains the electronics of the system (Figure 2). These electronics capture the response of the device's sensors by means of a custom analog front-end, process the raw data obtained from the sensors, and send the results to a mobile phone application via Bluetooth Low Energy (BLE). The entire system is controlled by a STM32L476JEY6TR microcontroller (STMicroelectronics; Geneva, Switzerland).

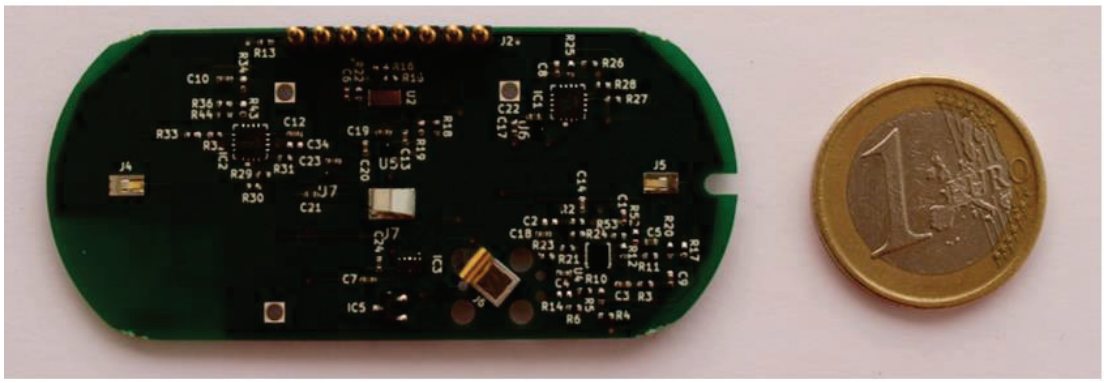

Figure 2. Photograph of the electronics of the device.

To power the system, a lithium coin cell battery with a nominal voltage of 3.0 V and a rated capacity of 210 mAh is used [12]. The voltage is regulated to 3.0 V, and this is the operational voltage of the system.

The cartridge (Figure 3) is the element that collects sweat from the skin and canalizes it into a microfluidic channel. There are several sensors inside this channel that analyze the content of this biofluid. This cartridge is a single-use component (disposable) that must be changed after each test. However, continuous measurements can be carried out for a given test, obtaining the evolution profile of every parameter during the exercise.

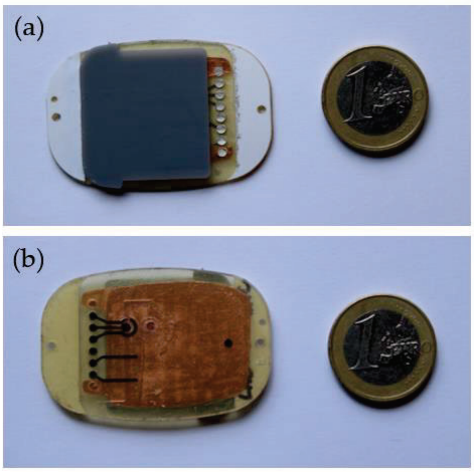

Figure 3. Image of the cartridge. (**a**) Front and (**b**) back of the disposable.

The chest strap provides a comfortable and robust attachment to the body and is utilized to perform HR measurements. This measurement is possible thanks to two rubber electrodes integrated inside the band.

All the mentioned elements of the wearable device must be connected together in order to take measurements. The chest strap and the cartridge are attached to the central module (Figure 4).

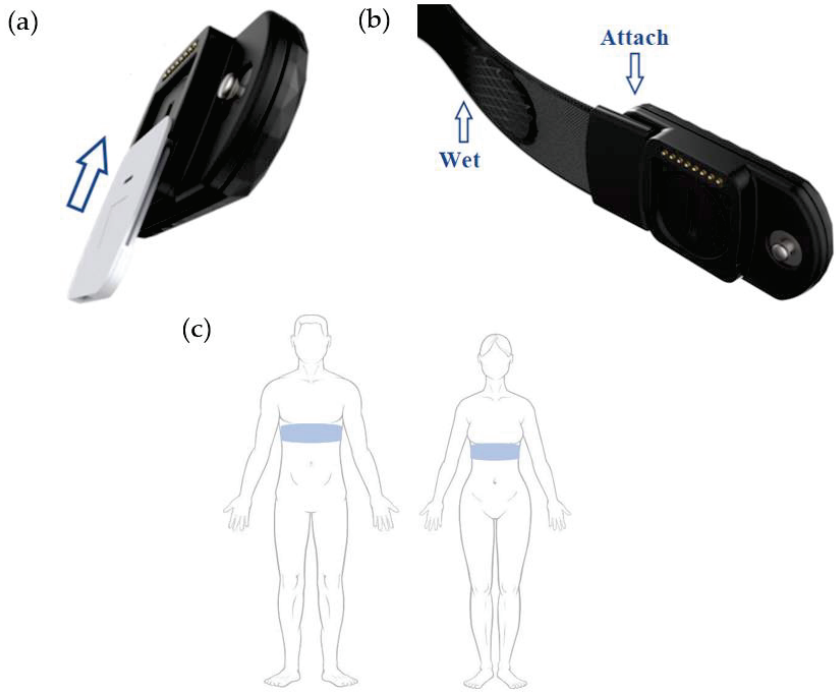

Figure 4. How to connect the different elements of the wearable device. (**a**) First, peel the protective layer and slide the cartridge into the central module (as is indicated by the arrow). This procedure ensures that the connections are isolated from the environment and the cartridge is robustly attached during the exercise. (**b**) Then, clip the strap to the central module and (**c**) put it on the chest. At the end, attach the cartridge to the skin. To remove the disposable, detach the adhesive from the skin and slide down the cartridge.

The system has two operational modes: low-power and measurement states. Initially, the system remains in the low-power mode until the athlete wears the device. Upon detection by a skin detector system, the device switches to measurement mode. In this state, the wearable device records the heart rate dynamics and analyzes the sweat content. Once the activity is completed, it returns to the low-power state.

The device consumes 85 μA and 5 mA in low-power and measurement modes, respectively. This device is capable of disabling and enabling different modules of the system in order to reduce consumption. If the user uses the device for one hour per day, the expected battery life is 30 days.

2.2. Chest Strap and Cartridge

The sensing elements of the wearable device are the chest strap and the sensors integrated inside the cartridge. The chest strap is employed for HR measurement, while the sensors within the disposable are utilized to estimate the sweat content.

2.2.1. Chest Strap

The chest strap has two rubber electrodes that are in contact with the athlete's skin. These electrodes are used to record the athlete's cardiac electrical activity by measuring the difference in potential between the electrodes. An electrocardiogram (ECG) is a plot of the electric activity recorded during this process. The signals of an ECG have multiple waves that reflect the heart state. The P wave represents the depolarization of the atria, the QRS complex represents the depolarization of the ventricles, and the T wave represents the repolarization of the ventricles [13,14].

Rubber electrodes are typically utilized in sports bands because they are reusable and washable. The ECG recorded using these electrodes lacks the necessary quality to be used in clinical settings, but the QRS complex can be identified easily in the signals obtained.

This complex indicates that one beat has taken place, so it can be used to estimate HR. HR is the number of heartbeats per unit of time, usually per minute.

The system presented in this paper utilized the chest strap from the heart rate monitor TICKR product (Wahoo Fitness; Atlanta, GA, USA) [15].

2.2.2. Cartridge

The cartridge is an adhesive patch attached directly to the user's skin as well as to the central module of the device. This patch collects sweat from the skin and canalizes it inside a microfluidic channel. There are different sensors in this channel that are used to estimate the dehydration and the lactate levels of the athlete. The disposable design is not described here because it is outside the scope of this paper, and only the sensors are presented.

Dehydration is the condition that occurs when the body loses too much water. It can be caused by several reasons, such as sweating too much or not drinking enough water. If left untreated, this condition can lead to poor body function and, in extreme cases, death [16–18].

During physical activity, water is lost due to thermoregulatory sweating. The sweat glands of the body collectively secrete between 0.8 and 1.5 L of water in the course of a moderate-intensity workout [19,20]. This loss of fluids can lead to dehydration in the athlete, and it also produces an imbalance of body salts, since a lot of ions are lost through sweat [21].

Two different sensors are used to estimate the athlete's dehydration. These sensors are a capacitive sensor [22,23] utilized to know the perspiration rate of the athlete, and a conductometric sensor used to estimate the sweat ionic strength.

The capacitive sensor (Figure 5a) is formed of two layers of copper and a microfluidic channel that it is placed in the middle of the two metal sheets. At the beginning of each trial, the chamber is full of air, and once the test initiates, the channel starts to be filled with sweat. When the content inside the chamber changes, the dielectric constant of the sensor varies as well. This variation is translated to a modification of the system capacitance, so the volume changes within the channel can be detected by measuring this parameter. The volume monitored during a certain period of time can be related to the total volume of fluid lost by the athlete, and thus, the dehydration level can be estimated.

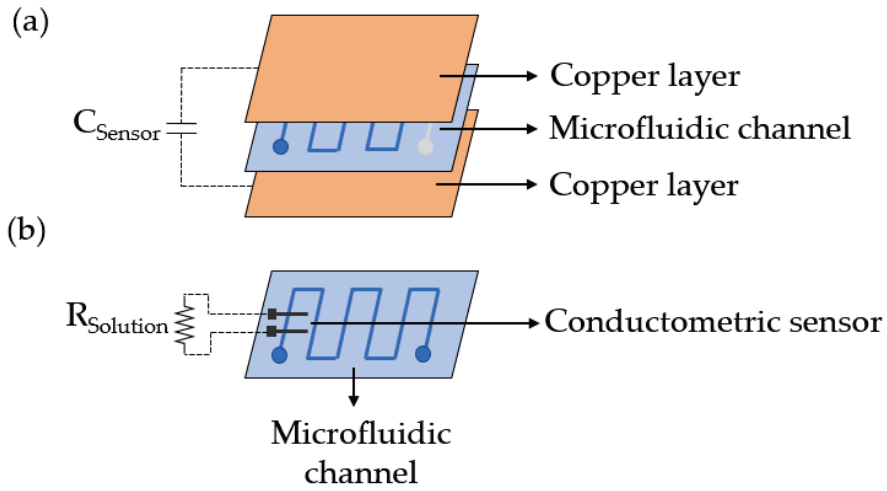

Figure 5. Dehydration sensors. (**a**) Scheme of the capacitive and (**b**) the conductometric sensors, respectively.

The ionic strength sensor (Figure 5b) is formed of two screen-printed electrodes integrated inside the microfluidic channel. These electrodes are in direct contact with the sweat that flows in the channel, and they are used to measure the impedance of this fluid. The main contribution of sweat impedance is the resistance of this biofluid, which depends on the number of ions present in the medium. Therefore, the concentration of ions

can be estimated by measuring the conductivity of this biofluid. Specifically, the sodium concentration can be easily estimated, as it is the most abundant ion in sweat and dominates the conductivity response [24].

Lactate is a molecule produced through the breakdown of glucose under anaerobic conditions. Elevated blood lactate levels indicate an oxygen deficiency in some tissues of the body. During exercise, lactate is generated because there is insufficient oxygen reaching the muscles. The increase in lactate implies a higher concentration of protons within the cells, so if the lactate production rate is high, it may exceed the buffering capacity of protons and cause a decrease in pH, generating lactic acid that affects the performance of muscles [25–27].

The blood lactate concentration varies from 0.6 to 2.0 mM, but it can increase up to 10 mM during intense physical effort [28]. Many factors affect sweat lactate concentration, but it is estimated that it varies between 1 mM and 100 mM during physical activity [29,30]. Currently, lactate tests need a blood sample, generally taken from the earlobe through a needle, that causes a great disadvantage in real-time monitoring. Using this method can be difficult for taking a series of measurements during training and therefore obtaining follow-up results [31].

To know the relationship between the lactate levels in blood and sweat, a bioequivalence study was carried out by the authors of this work. The study is described in [32], which concludes that there is no direct equivalence between blood lactate and sweat lactate without considering other parameters. To estimate the equivalence, a custom algorithm that takes HR, perspiration level, and sweat lactate concentration as inputs is required.

There are different methods to estimate the concentration of a molecule, such as ultraviolet spectrophotometry or refractive index detection. However, these tests are time-consuming and very complex. Electrochemical biosensors have several advantages over traditional methods, like speed, high specificity, low cost, and possible miniaturization/integration into circuits to perform the measurement [33].

The lactate sensor used in this device is an enzyme-based amperometric sensor that combines the specificity and selectivity of enzymes with the high sensitivity of electrochemical sensing. This sensor consists of a working electrode made of a mixture of carbon and Prussian blue mediator, a silver reference electrode, and a carbon counter-electrode. These electrodes are screen-printed on the surface of a PET foil. The working electrode is functionalized with lactate oxidase, which is immobilized in a biopolymeric membrane whose function is to retain the enzyme on the electrode's surface.

2.3. Electronics of the System

The disposable and the chest strap are attached to the central module of the device which contains the system electronics. The electronics capture the response of every sensor using custom analog instrumentations and the ADCs of the microcontroller.

2.3.1. ECG Recording and Heart Rate Estimation

To record the user's ECG, a commercial integrated AD8233 circuit (Analog Devices; Wilmington, MA, USA) is utilized. This chip is an analog front-end for the signal conditioning of cardiac biopotentials. It is composed of an instrumentation amplifier, an operational amplifier, and a right leg drive amplifier. The component also incorporates leads-on or -off detection circuitry.

Two different filters are implemented to eliminate the noise present on the ECG signal. The first filter is a first-order high-pass filter with a cutoff frequency of 7 Hz, and it is used to delete motion artifacts and the electrode half-cell potential. The second filter is a second-order low-pass filter with a cutoff frequency of 25 Hz, and it is utilized to remove other interference signals.

The Pan–Tompkins algorithm is used to calculate the HR from the ECG recorded by the analog front-end [34]. To estimate the HR, windows of 5 s of the ECG recording are utilized. The current consumption of this module is 150 μA at 3.0 V, when it is activated.

2.3.2. Sweat Rate and Conductivity Instrumentations

As mentioned before, a capacitive sensor is used to estimate the user's perspiration level, and a conductivity sensor is used to know the ionic strength of the sweat.

On one hand, a modified Schmitt Trigger oscillator is utilized to measure the response of the capacitive sensor (Figure 6a). This circuit is based on the operational amplifier TSX564IQ4T (STMicroelectronics; Geneva, Switzerland). The oscillator generates a square signal whose frequency depends on the capacitance of the system (Figure 6b). This capacitance is the sensor, so the changes in the period of the signal are directly related to the variation in the sensor impedance. As was mentioned before, the perspiration sensor modifies its capacitance as sweat enters inside the microfluidic channel, so the changes in volume inside this channel can be easily detected.

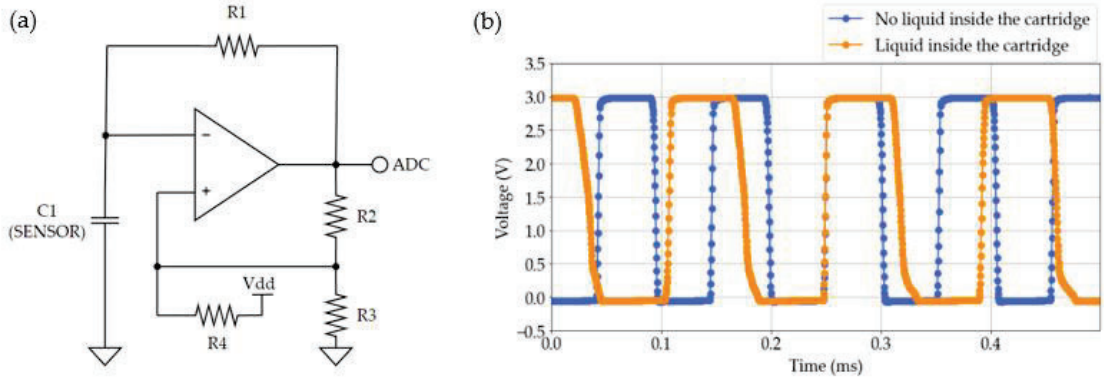

Figure 6. Modified Schmitt Trigger Oscillator. (**a**) Schematic of the circuit and (**b**) response of this instrumentation. The output signal is highlighted in blue when the disposable is empty, and in orange is the response of the instrumentation when the cartridge is full of fluid. The first signal has a period of 103 µs and the second one of 141 µs.

On the other hand, a circuit that combines the modified Schmitt Trigger oscillator, an amplification stage, and a transimpedance amplifier is used to quantify the sweat ionic strength (Figure 7a). This circuit uses the same operational amplifier as in the previous case. It generates a square signal of 8 kHz using the mentioned oscillator. Then, the amplitude of this signal is reduced by the amplification stage in order to not saturate the conductivity sensor. Finally, this signal is applied to the sensor, and the response is captured by a transimpedance amplifier (Figure 7b). The bandgap reference REF2920AIDBZR (Texas Instruments; Dallas, TX, USA) is used to provide a bias in order to adjust the signal to the ADC levels of the microcontroller. From the amplitude of the signal acquired, the conductivity of the biofluid is estimated. To obtain this value, the cell constant of this sensor is utilized. This constant depends on the geometry of the sensor, and it defines the resolution of the measurement [35]. Once the conductivity is calculated, the number of ions present in this biofluid can be estimated.

The current consumption of the first module is 650 µA at 3.0 V and the second one is 800 µA at the same operating voltage when they are activated.

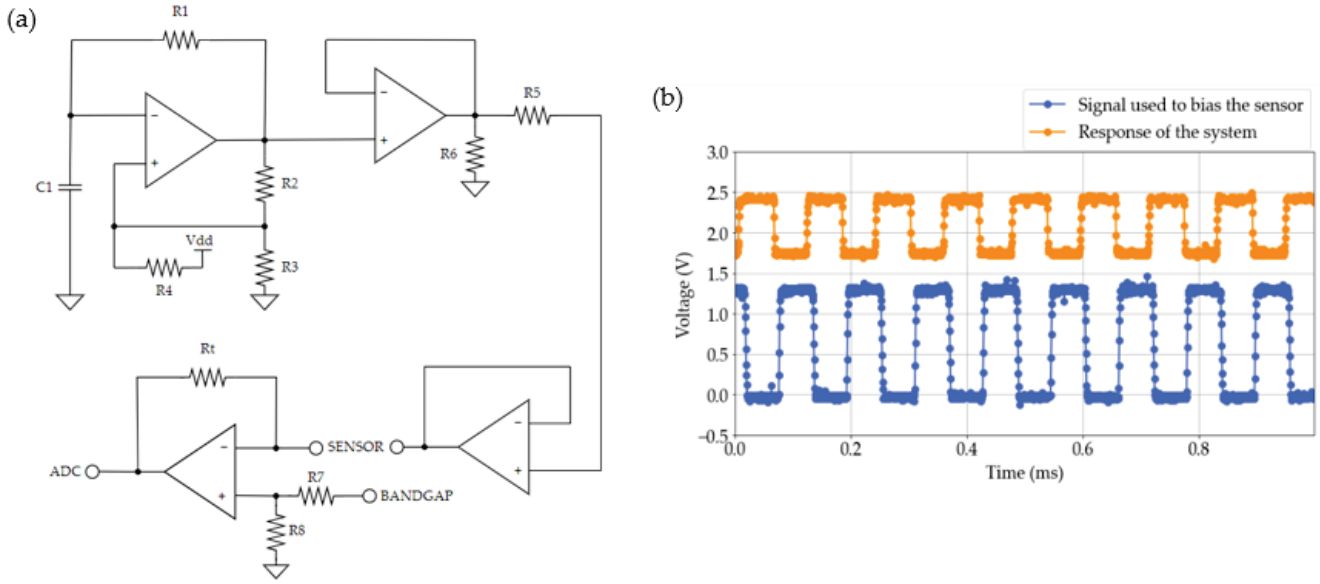

Figure 7. Conductivity instrumentation. (**a**) Schematic of the instrumentation and (**b**) response of this circuit. The signal used to bias the sensor is shown in blue, while the system's response to a conductive fluid inside the disposable is indicated in orange. The amplitude of the signal provided by the instrumentation changes depending on the medium conductivity.

2.3.3. Potentiostat

A potentiostat is an electronic instrument used to carry out several electrochemical techniques, such as chronoamperometry and cyclic voltammetry. It is a circuit that biases the electrochemical cell under study and captures its response [36].

A custom potentiostat based on the operational amplifier ADA4505-4 (Analog Devices; Wilmington, MA, USA) is utilized (Figure 8). This potentiostat is designed to work along three electrode amperometric sensors. Its architecture is based on a transimpedance amplifier with a direct voltage bias application and a final non-inverting amplifier, as low current levels are expected from the lactate sensor. Moreover, a capacitor is introduced as a first-order low-band-pass filter. This potentiostat can provide a whole voltage supply compliance voltage as well as read both oxidation (negative current) and reduction currents (positive current) from the amperometric sensor. It is complemented by the same bandgap used for the conductometric instrumentation and the microcontroller's DAC, which provides the necessary voltage bias to the sensor. The complete characterization of this potentiostat can be found in article [37].

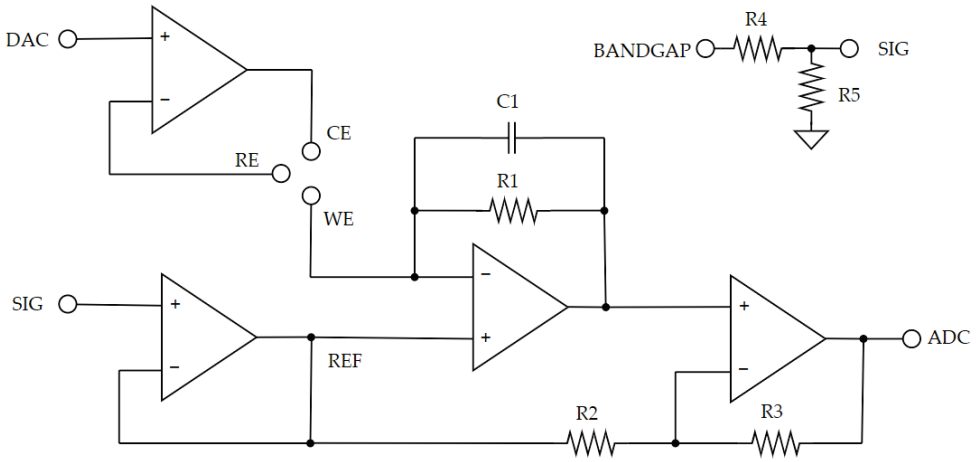

Figure 8. Potentiostat used to bias the lactate sensor and capture its response.

3. Results and Discussion

The system was validated by means of several in vitro and in vivo tests. In vitro trials ensured good functioning of each measurement and in vivo test demonstrated their functionality in a real environment.

3.1. In Vitro Tests

Each sensor and instrumentation was tested individually and validated by comparing the data obtained using the gold-standard method of each type of measurement.

To characterize the HR parameter, a specific protocol was created. This protocol consisted of an equivalence study between the wearable device and the sports band Suunto Smart HR Belt (Suunto; Vantaa, Finland) [38]. It has been demonstrated that this kind of band has an accuracy similar to an ECG Holter monitor [39]. The protocol of this study is as follows:

- Moisten the rubber electrodes of the wearable device and the reference band, before placing them on the chest of a volunteer.
- Collect the data from each device using a mobile phone application, while the volunteer is sitting, for five minutes.
- Collect the data from each device using a mobile phone application, while the volunteer is pedaling on a stationary bicycle at a constant load, for five minutes.
- Collect the data from each device using a mobile phone application, while the volunteer is sitting, again, for five minutes.

Using this protocol, eight tests were performed, and the results of these trials were analyzed. The volunteers of this study included five males and three females with ages ranging from 21 to 39 (mean of 28.6 years and standard deviation of 5.9 years). Both the correlation coefficient and the mean standard deviation were utilized to determine the accuracy of this measurement (Table 1). The correlation coefficient is close to one, so the HR obtained by the wearable device shows no significant difference when compared with the data provided by the Suunto Smart HR Belt. Additionally, the mean standard deviation is less than three beats per minute (bpm), indicating low measurement dispersion.

Table 1. Statistical analysis of the comparison between the HR calculated by the wearable device and the reference instrument.

Participants	Correlation Coefficient	Mean Standard Deviation
Males	0.81	2.9 bpm
Females	0.83	2.8 bpm

To validate the ionic strength measurement, a direct comparison was carried out between the wearable device and the reference equipment, LAQUAtwin EC-11 (Horiba; Kioto, Japan) [40]. The analyte utilized to perform this analysis was artificial sweat. This artificial sweat was prepared using deionized water with 0.5% sodium chloride, 0.1% potassium chloride, 0.1% lactic acid, and 0.1% urea. From this solution, ionic strength dilutions of 10, 30, 50, 70, 100, and 130 mM were made.

Multiple measurements were taken using three different conductometric sensors. A linear regression was employed to compare the performance of the device with the reference equipment (Figure 9). The coefficient of determination of 0.995 shows a good fit between the data, so the system can be considered accurate.

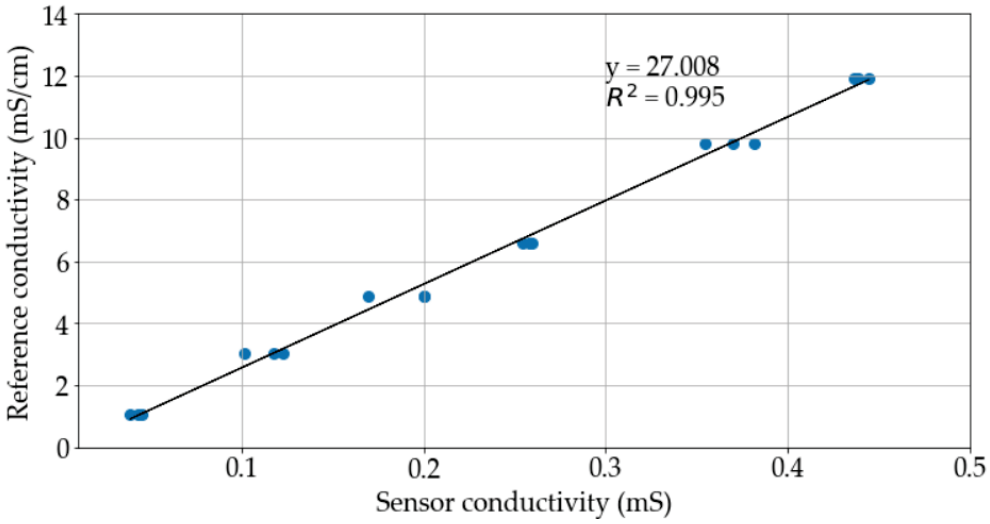

Figure 9. Fit between the conductivity calculated by the wearable device and the reference equipment. The dots correspond to each measurement carried out by the wearable device.

To validate the perspiration level measurement, no reference equipment was used because there does not exist standard instrumentation to estimate the sweat rate. Instead, a KDS Legato 101 syringe pump (KD Scientific; Holliston, MA, USA) was utilized [41] to simulate the perspiration of the user. This element continuously pumped artificial sweat inside the disposable at a fixed rate of 2 µL/min.

A trial of 30 min was performed using this syringe pump and a cartridge. During this test, both sweat rate value and conductivity were recorded (Figure 10). The response of the capacitive and the conductometric sensors remained constant at the beginning of the test since the fluid had not yet entered inside the microfluidic channel. When the liquid entered the chamber, the conductometric sensor gave an unstable output that was stabilized at a fixed value after 2 min. The sweat rate sensor was activated immediately, and it gave a response that is linearly time dependent. Finally, when the microfluidic channel was full of liquid, the sensor response stayed constant because the system capacitance could no longer change.

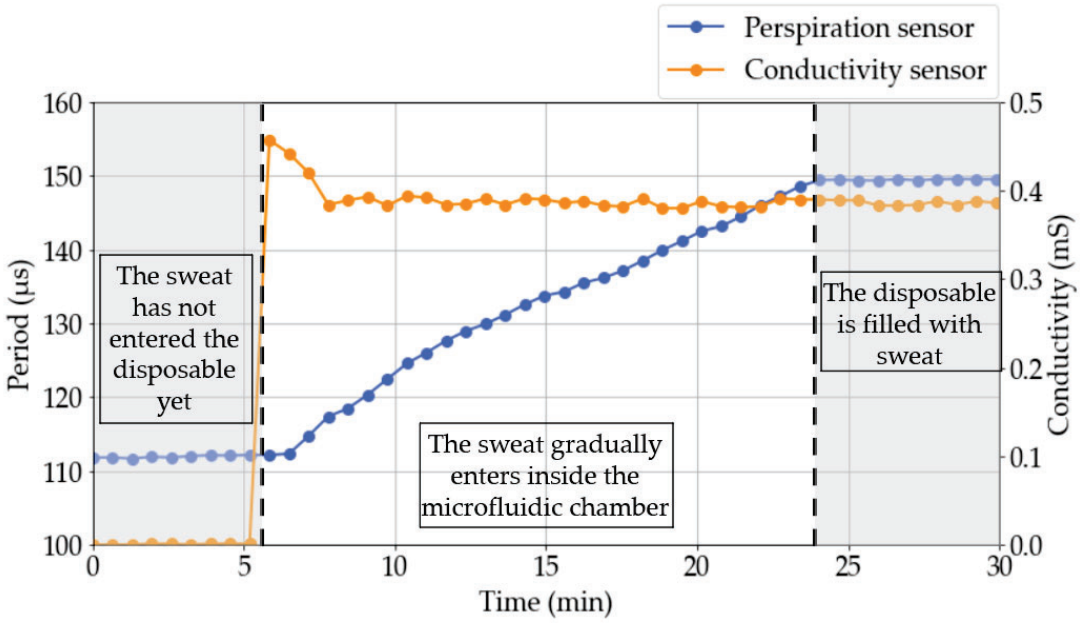

Figure 10. Conductivity and sweat rate obtained during an in vitro test.

Eventually, the lactate measurement was characterized using artificial sweat. This solution was modified to obtain 0, 10, 30, 50, 70, and 100 mM lactate concentrations. Different measurements with three different lactate sensors were made using the custom potentiostat. Chronoamperometries of 60 s using a working potential of −0.3 V were performed. Only the last value was taken because it is the moment when the sensor stabilizes its response (Figure 11). No comparison with reference instrumentation was carried out since the characterization of this potentiostat can be found in [37].

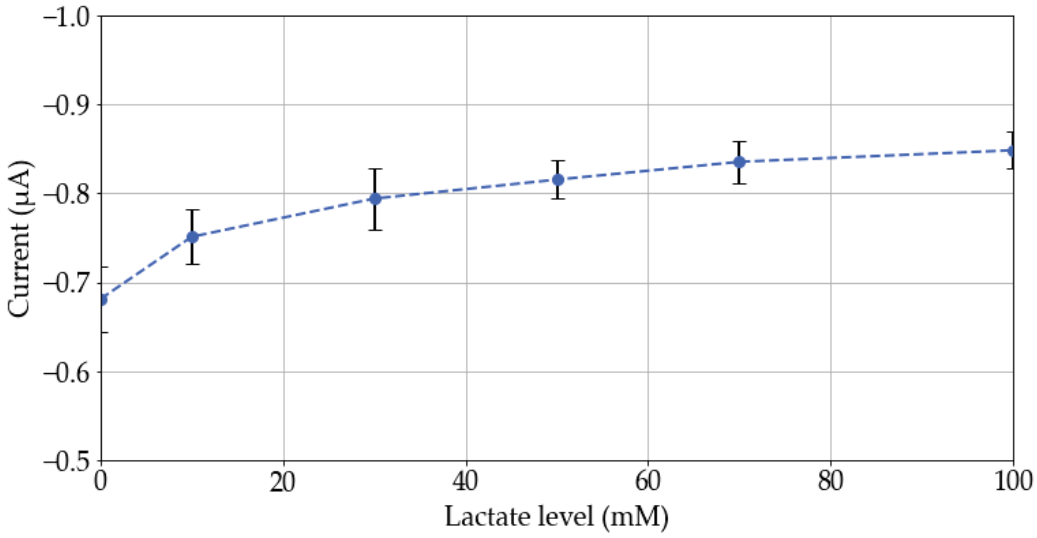

Figure 11. Response of each sensor and potentiostat to different concentrations of lactate. The error bars correspond to the standard deviation between measurements of multiple sensors.

A trend in the system's response is observed: the current produced by the sensor increases as the lactate concentration rises. This response allows to monitor the level of this molecule and predict the sweat lactate concentration.

3.2. In Vivo Tests

Once both the sensors and the electronics were validated in vitro, the system was ready to be tested in vivo. This test consisted of the utilization of the wearable system to analyze the sweat content of volunteers during physical activity.

All the participants of the study were informed and gave their consent to use the data extracted from the experiments. The volunteers included two males and one female. Before starting the test, the participants were asked to provide the researchers with a series of personal data (Table 2).

Table 2. Characteristics of the volunteers of the in vivo tests.

Parameters	Volunteer 1	Volunteer 2	Volunteer 3
Sex	Male	Female	Male
Age (years)	30	21	39
Height (cm)	175	164	176
Weight (kg)	80.4	52.0	75.0
BMI (kg/m^3)	26.3	19.3	24.2

The in vivo testing protocol is as follows:

Clean with water the skin area where the disposable is placed, and then, dry the area to ensure that the disposable's adherence to the skin is good.

- Attach the heart rate monitor strap to the central module and wet both rubber electrodes.

- Remove the adhesive liner of the disposable and adhere the central module carrying the cartridge to the skin.
- Collect the data from the wearable device while the volunteer is pedaling on a stationary bicycle at a constant load (Figure 12a). All the data are gathered using a mobile application, and these data are downloaded as a CSV file (Figure 12b).

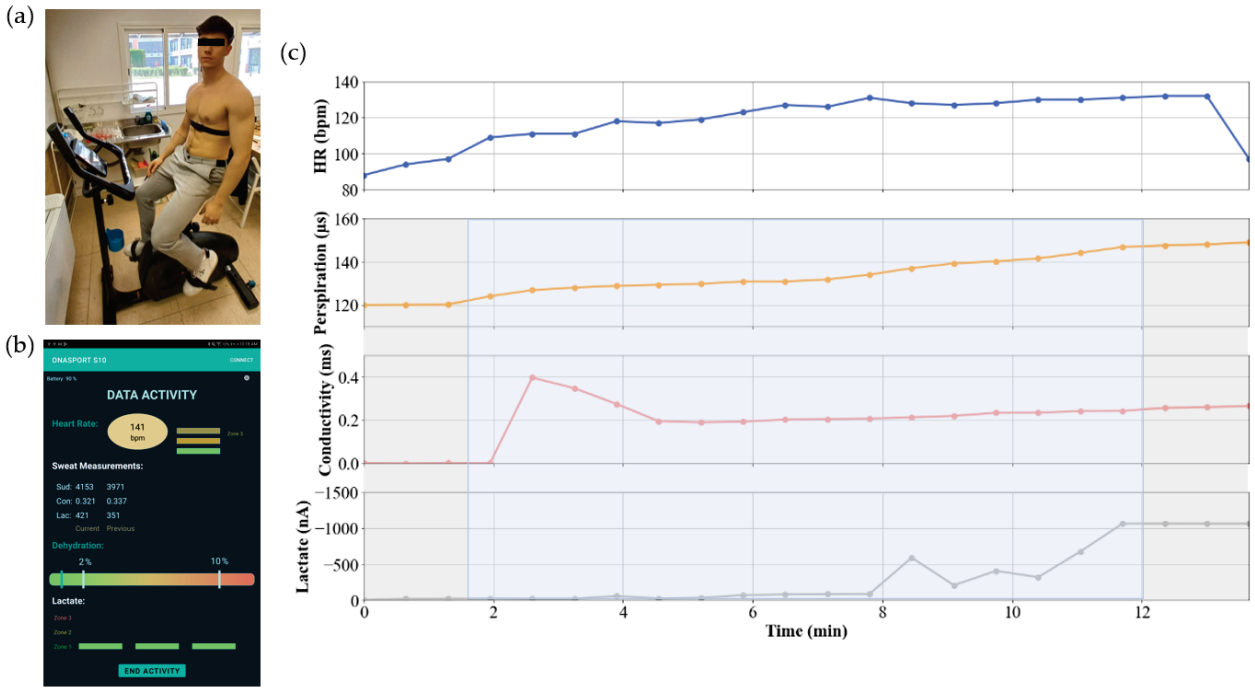

Figure 12. Real-time perspiration analysis during stationary cycling. (**a**) Photograph of the experimental set-up and (**b**) the application used to capture the data produced by the wearable device. (**c**) Results obtained via one in vivo trial. In gray are highlighted the moments when the cartridge is empty and full. The time in which the cartridge is filled is marked in blue.

The results of the in vivo trials were the expected ones for every partaker (Figure 12c). At the beginning of the test, the HR increased until it reached its maximum value and remained stable. When the HR value increased, the perspiration of the athlete began. A few minutes passed until the cartridge started to collect sweat from the skin, as is observed in the response of the conductometric sensor. This sensor gave an initial peak that can be associated with the trapped minerals (iron, zinc, magnesium, etc.) in the sweat duct [20]. The progressive increase when the activity continued could be explained by the dependence on sweat rate (reabsorption channels in the sweat duct) [5]. More importantly, these results mean that the microfluidic system associated with the sensor was making the sweat continuously circulate, and was able to determine the chronological evolution of the different biomarkers. Meanwhile, the capacitive sensor gave an increasing response over time until the microfluidic channel was full of liquid. Eventually, the lactate sensor started its measurement by giving an increasing output until it stabilized its response at a fixed value after a few minutes elapsed.

The behavior of all these sensors was almost the same as in the in vitro trials. Only small changes were observed in the response time and the absolute value of the sensors. The first difference was expected since the perspiration rate of the in vivo test was not constant over time and every volunteer had different perspiration profiles. On the other hand, the second difference can be associated with the sweat composition. Artificial and real sweat are not the same, so different responses were expected. Sweat contains a large quantity of ions that modify the properties of the medium. Enzymatic electrochemical sensors are affected a lot by environmental conditions. In this case, the saltiness of the

medium interacted with the activity of the lactate sensor enzyme, producing higher current levels than expected.

The outcomes of these trials can be considered a great success since real-time sweat analysis was performed. Despite this fact, more work needs to be carried out in order to fully understand the obtained results. To achieve this, more in vivo tests must be performed and the physiology of perspiration must be studied.

The microfluidic system defines the capabilities of the cartridge in terms of sensor response time and durability. This could be adapted by modifying the collection area, which determines the total fluid volume, and the configuration of the microfluidic channels to maximize volume capability.

Eventually, improvements in the consumption of the system can be made, and additional measures such as heart rate variability (HRV) can be added. HRV is the variance in time between heart beats and it is regularly used in the athletic world to identify periods of optimal training and to monitor recovery status and any potential overtraining [42].

4. Conclusions

In this paper, we present a groundbreaking advancement in the field of sports monitoring: a wearable device designed for continuous athlete monitoring in real time through sweat analysis. This innovative system utilizes a conventional sports band that incorporates a single-use cartridge capable of collecting, processing, and analyzing sweat from the user's skin, all thanks to an array of sensors integrated into this disposable. What makes our approach exceptional is its ability to provide an instant assessment of the athlete's health without disrupting their routine. This device is not only non-intrusive, but is seamlessly integrated into the user's daily life, making adoption effortless.

Every component of the device has undergone rigorous testing, both in vitro and in vivo. Promising results that open the door to an exciting future for health monitoring in sports have been achieved. However, the true potential of this system lies in its ability to translate the collected data into valuable insights for athletes. This means that there is still much to be done in order to interpret these data and provide athletes with a deep understanding of their performance and health. To interpret these data, dozens of trials with multiple athletes must be performed to create a large database and analyze all the collected data.

Apart from enhancing the daily lives of athletes, this technology has the potential to play a crucial role in the medical field. Non-invasive and continuous measurements of sweat composition can provide healthcare providers with information about biochemical parameters, such as glucose level, that could allow them to improve the attention given to patients and their treatment. A direct application of this system is the assessment of cystic fibrosis since the conductivity of sweat rises a lot when a user has this disease. Despite this fact, to translate this device from the sports to the medical field, a lot of work is required in the field of sensing and microfluidics in order to enable it to process low volumes of sweat.

Author Contributions: Conceptualization, J.A.-T. and G.R.-G.; methodology, J.A.-T. and G.R.-G.; software, J.A.-T., S.T.-V., A.Á.-C. and A.C.-B.; validation, G.R.-G., V.C.-R., S.T.-V. and A.F.-G.; formal analysis, G.R.-G., V.C.-R. and S.T.-V.; investigation, J.A.-T. and G.R.-G.; resources, X.M.-P.; data curation, A.C.-B.; writing—original draft preparation, J.A.-T.; writing—review and editing, J.A.-T. and G.R.-G.; visualization, J.A.-T., G.R.-G. and J.P.-V.; supervision, P.M.-C., J.C.-T. and J.P.-V.; project administration, J.P.-V.; funding acquisition, X.M.-P. All authors have read and agreed to the published version of the manuscript.

Funding: This work was supported by the Spanish Ministerio de Indústria, Energía y Turismo, grant numbers AEI-010500-2020-198 and AEI-010500-2022b-111, and AGAUR, grant numbers 2019 DI 18 and 2019 DI 29.

Institutional Review Board Statement: All subjects gave their informed consent for inclusion before they participated in this study. The study was conducted in accordance with the Declaration of Helsinki, and the protocol was approved by the ethics committee of INEFC (National Institute of

Physical Education of Catalonia) regulating the projects AEI-010500-2020-198 and AEI-010500-2022b-111 of the Spanish Ministerio de Indústria, Energía y Turismo.

Informed Consent Statement: Informed consent was obtained from all subjects involved in this study.

Data Availability Statement: Data is contained within the article.

Conflicts of Interest: J.A.-T., G.R.-G., S.T.-V., A.Á.-C., V.C.-R., A.F.-G., A.C.-B., X.M.-P. and J.P.-V. were employed by the company Onalabs Inno-Hub SL. The remaining authors declare that the research was conducted in the absence of any commercial or financial relationships that could be construed as a potential conflict of interest.

References

1. Yang, D.S.; Ghaffari, R.; Rogers, J.A. Sweat as a Diagnostic Biofluid. *Science* **2023**, *379*, 760–761. [CrossRef] [PubMed]
2. Yang, P.; Wei, G.; Liu, A.; Huo, F.; Zhang, Z. A Review of Sampling, Energy Supply and Intelligent Monitoring for Long-Term Sweat Sensors. *NPJ Flex. Electron.* **2022**, *6*, 33. [CrossRef]
3. Hussain, J.N.; Mantri, N.; Cohen, M.M.; Hussain, J. Working Up a Good Sweat-The Challenges of Standardising Sweat Collection for Metabolomics Analysis. *Clin. Biochem. Rev.* **2017**, *38*, 13.
4. Gokdemir, Y.; Karadag, B.T. Sweat Testing and Recent Advances. *Front. Pediatr.* **2021**, *9*, 649904. [CrossRef]
5. Sonner, Z.; Wilder, E.; Heikenfeld, J.; Kasting, G.; Beyette, F.; Swaile, D.; Sherman, F.; Joyce, J.; Hagen, J.; Kelley-Loughnane, N.; et al. The Microfluidics of the Eccrine Sweat Gland, Including Biomarker Partitioning, Transport, and Biosensing Implications. *Biomicrofluidics* **2015**, *9*, 031301. [CrossRef] [PubMed]
6. Liang, B.; Cao, Q.; Mao, X.; Pan, W.; Tu, T.; Fang, L.; Ye, X. An Integrated Paper-Based Microfluidic Device for Real-Time Sweat Potassium Monitoring. *IEEE Sens. J.* **2021**, *21*, 9642–9648. [CrossRef]
7. Martín, A.; Kim, J.; Kurniawan, J.F.; Sempionatto, J.R.; Moreto, J.R.; Tang, G.; Campbell, A.S.; Shin, A.; Lee, M.Y.; Liu, X.; et al. Epidermal Microfluidic Electrochemical Detection System: Enhanced Sweat Sampling and Metabolite Detection. *ACS Sens.* **2017**, *2*, 1860–1868. [CrossRef]
8. Kim, J.; Wu, Y.; Luan, H.; Yang, D.S.; Cho, D.; Kwak, S.S.; Liu, S.; Ryu, H.; Ghaffari, R.; Rogers, J.A. A Skin-Interfaced, Miniaturized Microfluidic Analysis and Delivery System for Colorimetric Measurements of Nutrients in Sweat and Supply of Vitamins Through the Skin. *Adv. Sci.* **2021**, *9*, 2103331. [CrossRef]
9. Noura, Z.; Shah, I.; Aziz, S.; Ahmed, A.; Jung, D.W.; Brahim, L.; ElMostafa, R. Wearable Healthcare Monitoring Based on a Microfluidic Electrochemical Integrated Device for Sensing Glucose in Natural Sweat. *Sensors* **2022**, *22*, 8971. [CrossRef]
10. Seçkin, A.Ç.; Ateş, B.; Seçkin, M. Review on Wearable Technology in Sports: Concepts, Challenges and Opportunities. *Appl. Sci.* **2023**, *13*, 10399. [CrossRef]
11. Schneider, C.; Hanakam, F.; Wiewelhove, T.; Döweling, A.; Kellmann, M.; Meyer, T.; Pfeiffer, M.; Ferrauti, A. Heart Rate Monitoring in Team Sports-A Conceptual Framework for Contextualizing Heart Rate Measures for Training and Recovery Prescription. *Front. Physiol.* **2018**, *9*, 639. [CrossRef] [PubMed]
12. CR2032 Multicomp, Battery, Coin Cell, 3 V | Farnell Spain. Available online: https://es.farnell.com/en-ES/multicomp/cr2032/cell-lithium-cr2032-210mah-3v/dp/2065171 (accessed on 16 April 2023).
13. Zhang, Y.; Wang, Z. Research on Intelligent Algorithm for Detecting ECG R Waves. In Proceedings of the ICEIEC 2015—Proceedings of 2015 IEEE 5th International Conference on Electronics Information and Emergency Communication, Beijing, China, 14–16 May 2015; Institute of Electrical and Electronics Engineers Inc.: New York, NY, USA, 2015; pp. 47–50.
14. Pereira, T.M.C.; Conceição, R.C.; Sencadas, V.; Sebastião, R. Biometric Recognition: A Systematic Review on Electrocardiogram Data Acquisition Methods. *Sensors* **2023**, *23*, 1507. [CrossRef] [PubMed]
15. TICKR Replacement Heart Rate Strap | Wahoo Fitness, EU. Available online: https://eu.wahoofitness.com/devices/heart-rate-monitors/tickr-replacement-heart-rate-strap (accessed on 16 April 2023).
16. Popkin, B.M.; D'Anci, K.E.; Rosenberg, I.H. Water, Hydration, and Health. *Nutr. Rev.* **2010**, *68*, 439–458. [CrossRef] [PubMed]
17. Lacey, J.; Corbett, J.; Forni, L.; Hooper, L.; Hughes, F.; Minto, G.; Moss, C.; Price, S.; Whyte, G.; Woodcock, T.; et al. A Multidisciplinary Consensus on Dehydration: Definitions, Diagnostic Methods and Clinical Implications. *Ann. Med.* **2019**, *51*, 232–251. [CrossRef] [PubMed]
18. Shaheen, N.A.; Alqahtani, A.A.; Assiri, H.; Alkhodair, R.; Hussein, M.A. Public Knowledge of Dehydration and Fluid Intake Practices: Variation by Participants' Characteristics. *BMC Public Health* **2018**, *18*, 1346. [CrossRef] [PubMed]
19. Armstrong, L.E.; Casa, D.J. Methods to Evaluate Electrolyte and Water Turnover of Athletes. *Athl. Train. Sports Health Care* **2009**, *1*, 169–179. [CrossRef]
20. Baker, L.B. Sweating Rate and Sweat Sodium Concentration in Athletes: A Review of Methodology and Intra/Interindividual Variability. *Sports Med.* **2017**, *47*, 111–128. [CrossRef]
21. Barnes, K.A.; Anderson, M.L.; Stofan, J.R.; Dalrymple, K.J.; Reimel, A.J.; Roberts, T.J.; Randell, R.K.; Ungaro, C.T.; Baker, L.B. Normative Data for Sweating Rate, Sweat Sodium Concentration, and Sweat Sodium Loss in Athletes: An Update and Analysis by Sport. *J. Sports Sci.* **2019**, *37*, 2356–2366. [CrossRef]

22. Choi, D.H.; Gonzales, M.; Kitchen, G.B.; Phan, D.T.; Searson, P.C. A Capacitive Sweat Rate Sensor for Continuous and Real-Time Monitoring of Sweat Loss. *ACS Sens.* **2020**, *5*, 3821–3826. [CrossRef]
23. Hourlier-Fargette, A.; Schon, S.; Xue, Y.; Avila, R.; Li, W.; Gao, Y.; Liu, C.; Kim, S.B.; Raj, M.S.; Fields, K.B.; et al. Skin-Interfaced Soft Microfluidic Systems with Modular and Reusable Electronics for: In Situ Capacitive Sensing of Sweat Loss, Rate and Conductivity. *Lab Chip* **2020**, *20*, 4391–4403. [CrossRef]
24. Riedi, C.A.; Zavadniak, A.F.; Silva, D.C.; Franco, A.; Filho, N.A.R. Comparison of Conductivity with Sodium Determination in the Same Sweat Sample. *J. Pediatr.* **2000**, *76*, 443–446. [CrossRef]
25. Cunha-Silva, H.; Arcos-Martinez, M.J. Dual Range Lactate Oxidase-Based Screen Printed Amperometric Biosensor for Analysis of Lactate in Diversified Samples. *Talanta* **2018**, *188*, 779–787. [CrossRef] [PubMed]
26. Allen, S.E.; Holm, J.L. Lactate: Physiology and Clinical Utility. *J. Vet. Emerg. Crit. Care* **2008**, *18*, 123–132. [CrossRef]
27. Robergs, R.A.; Ghiasvand, F.; Parker, D. Lactate Accumulation, Proton Buffering, and PH Change in Ischemically Exercising Muscle. *Am. J. Physiol. Regul. Integr. Comp. Physiol.* **2004**, *287*, 502–516. [CrossRef] [PubMed]
28. Goodwin, M.L.; Harris, J.E.; Hernández, A.; Bruce Gladden, L. Blood Lactate Measurements and Analysis during Exercise: A Guide for Clinicians. *J. Diabetes Sci. Technol.* **2007**, *1*, 558–569. [CrossRef] [PubMed]
29. Van Hoovels, K.; Xuan, X.; Cuartero, M.; Gijssel, M.; Swarén, M.; Crespo, G.A. Can Wearable Sweat Lactate Sensors Contribute to Sports Physiology? *ACS Sens.* **2021**, *6*, 3496–3508. [CrossRef]
30. Derbyshire, P.J.; Barr, H.; Davis, F.; Higson, S.P.J. Lactate in Human Sweat: A Critical Review of Research to the Present Day. *J. Physiol. Sci.* **2012**, *62*, 429–440. [CrossRef]
31. Yamagata, T.; Kume, D.; Wakimoto, T.; Nagao, N. The Influence of Sampling Site on Blood Lactate Response to Steady State Exercise. *J. Sports Sci.* **2018**, *6*, 276–284. [CrossRef]
32. Rabost-Garcia, G.; Colmena, V.; Aguilar-Torán, J.; Vieyra Galí, J.; Punter-Villagrasa, J.; Casals-Terré, J.; Miribel-Catala, P.; Muñoz, X.; Cadefau, J.; Padullés, J.; et al. Non-Invasive Multiparametric Approach To Determine Sweat–Blood Lactate Bioequivalence. *ACS Sens.* **2023**, *8*, 1536–1541. [CrossRef]
33. Grieshaber, D.; Mackenzie, R.; Vörös, J.; Reimhult, E. Electrochemical Biosensors-Sensor Principles and Architectures. *Sensors* **2008**, *8*, 1400–1458. [CrossRef]
34. Pan, J.; Tompkins, W.J. A Real-Time QRS Detection Algorithm. *IEEE Trans. Biomed. Eng.* **1985**, *BME-32*, 230–236. [CrossRef] [PubMed]
35. Olthuis, W.; Streekstra, W.; Bergveld, P. Theoretical and Experimental Determination of Cell Constants of Planar-Interdigitated Electrolyte Conductivity Sensors. *Sens. Actuators B Chem.* **1995**, *24*, 252–256. [CrossRef]
36. Punter-Villagrasa, J.; Colomer-Farrarons, J.; del Campo, F.J.; Miribel, P. *Amperometric and Impedance Monitoring Systems for Biomedical Applications*; Springer: Cham, Switzerland, 2017.
37. Aguilar, J.; Alvarez-Carulla, A.; Colmena, V.; Carreras, O.; Rabost, G.; Puig-Vidal, M.; Colomer-Farrarons, J.; Munoz, X.; Miribel-Catala, P.; Punter-Villagrasa, J. Autonomous Self-Powered Potentiostat Architecture for Biomedical Wearable Applications. In Proceedings of the 2020 35th Conference on Design of Circuits and Integrated Systems, DCIS 2020, Segovia, Spain, 18–20 November 2020; Institute of Electrical and Electronics Engineers Inc.: New York, NY, USA, 2020.
38. Suunto Smart Heart Rate Belt—Accurate and Comfortable Multisport HR Belt. Available online: https://www.suunto.com/Products/Heart-Rate-Belts/suunto-smart-heart-rate-belt/ (accessed on 16 April 2023).
39. Gilgen-Ammann, R.; Schweizer, T.; Wyss, T. RR Interval Signal Quality of a Heart Rate Monitor and an ECG Holter at Rest and during Exercise. *Eur. J. Appl. Physiol.* **2019**, *119*, 1525–1532. [CrossRef] [PubMed]
40. LAQUAtwin EC-11 Pocket Water Quality Meters—HORIBA. Available online: https://www.horiba.com/esp/water-quality/productos/detail/action/show/Product/laquatwin-ec-11-872/ (accessed on 16 April 2023).
41. Infuse Only Dual Syringe Pump—Legato 101. Available online: https://www.kdscientific.com/legato-101-syringe-pump.html?___SID=U (accessed on 16 April 2023).
42. Aubert, A.E.; Seps, B.; Beckers, F. Heart Rate Variability in Athletes. *Sports Med.* **2003**, *33*, 889–919. [CrossRef] [PubMed]

Patent 1

A Wearable Device for Continuous Monitoring of Health Parameters.

Genis Rabost-Garcia, Xavier Muñoz-Pascual, Javier Aguilar-Torán, Jaime Punter-Villagrasa and Valeria Colmena-Rubil

EP4205644A1

(19) Europäisches Patentamt
European Patent Office
Office européen des brevets

(11) EP 4 205 644 A1

(12) EUROPEAN PATENT APPLICATION

(43) Date of publication:
05.07.2023 Bulletin 2023/27

(21) Application number: **21383240.5**

(22) Date of filing: **30.12.2021**

(51) International Patent Classification (IPC):
A61B 5/024 *(2006.01)* ***A61B 5/145*** *(2006.01)*
A61B 5/00 *(2006.01)*

(52) Cooperative Patent Classification (CPC):
A61B 5/4266; A61B 5/024; A61B 5/14517; A61B 5/6831

(84) Designated Contracting States:
AL AT BE BG CH CY CZ DE DK EE ES FI FR GB GR HR HU IE IS IT LI LT LU LV MC MK MT NL NO PL PT RO RS SE SI SK SM TR
Designated Extension States:
BA ME
Designated Validation States:
KH MA MD TN

(71) Applicant: **Onalabs Inno-Hub**
08012 Barcelona (ES)

(72) Inventors:
- **RABOST GARCIA, Genís**
08012 Barcelona (ES)
- **MUÑOZ PASCUAL, Francesc Xavier**
08012 Barcelona (ES)
- **AGUILAR TORÁN, Javier**
08012 Barcelona (ES)
- **PUNTER VILLAGRASA, Jaime**
08012 Barcelona (ES)
- **COLMENA RUBIAL, Valeria**
08012 Barcelona (ES)

(74) Representative: **Hoffmann Eitle**
Hoffmann Eitle S.L.U.
Paseo de la Castellana 140, 3a planta
Edificio LIMA
28046 Madrid (ES)

(54) A WEARABLE DEVICE FOR CONTINUOUS MONITORING OF HEALTH PARAMETERS

(57) The present invention refers to a device for the continuous monitoring of health condition of patients or sport persons without the need of blood extraction. In particular the invention refers to a wearable device that comprises: at least one sweat sensor for measuring a sweat biomarker, a sweat collection inlet arranged in the device for collecting sweat when the device is worn by a user, a microfluidic channel for conveying collected sweat from the inlet to the sweat sensor, at least one vital-sign sensor arranged in the device for measuring a vital-sign or physiological sign of the user, a sweat volume sensor for measuring volume of the collected sweat, and a processing unit adapted for receiving and processing data provided by the sweat sensor, the vital-sign biosensor and the sweat volume measuring device. The invention can advantageously be used in sports medicine and/or sports health sectors for remote effort and/or fatigue assessment.

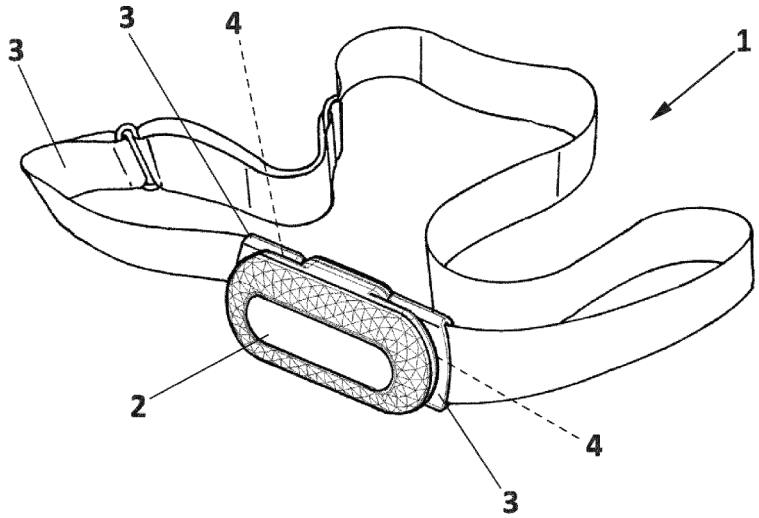

FIG. 1

EP 4 205 644 A1

Description

Field and object of the invention

[0001] The present invention belongs to the technical filed of medical devices, in particular to the area of wearable medical devices both for clinical and sport applications.

[0002] An object of the invention, is the provision of a multi-sensor device for the continuous remote, and real-time monitoring of health condition of patients or sport persons, without blood extraction.

[0003] The invention can advantageously be used in sports medicine and/or sports health sectors for remote effort and/or fatigue assessment.

Background of the invention

[0004] Blood tests are the reference clinical methods that show the most important physiological parameters that allow an accurate diagnosis of a patient's condition. In the health sector, the analysis of most of the metabolites of interest (various amino acids, sugars, carboxylic acids and fatty acids, ...) requires blood collection, creating an obstacle for their use in real-time monitoring in both clinical health and sports medicine.

[0005] Therefore, there is a need in the medical personnel in charge of clinical protocols as well as in the training and recovery of the athletes, for devices capable of monitoring biomarkers in a non-invasive, continuous and remote way by means of sweat. In this regard, although the use of blood is the reference, analyzing sweat has been a challenge to obtain bioequivalence between both measurement formats.

[0006] The current clinical trend is to be less invasive contemplates the tendency to combine both non-invasive measurement techniques: on skin and on biofluid (urine, saliva, sweat, etc.).

[0007] To measure sweating volume and rate, there are different strategies like: using humidity sensors, calorimetric measurements or volumetric determination. Using humidity sensors or calorimetric sensors are highly sensitive, but require a high level of complexity that limits their integration into portable devices. In contrast, volumetric measurements, determining the volume collected in a controlled period of time, allows simple and direct monitoring. There are visual monitoring options that are simple for the research setting as they require little instrumentation. However, for continuous monitoring applications it is better to use impedimetric detection (electrical resistance is reduced proportionally to the sample volume) which allows autonomous and real-time measurement.

Summary of the invention

[0008] The present invention is defined in the attached independent claim, and satisfactorily solves the drawbacks of the prior art, by providing a wearable device that integrates different sensors to obtain simultaneous measurements of biomarkers in sweat (metabolites, ions or amino acids, etc.), and vital physiological parameters (heart and respiratory rate, blood pressure, etc.), for the determination of lactate concentration in blood, in a non-invasive, continuous, real-time and remote manner.

[0009] More specifically, an aspect of the invention refers to a wearable device for continuous monitoring of health parameters of a user, wherein the device comprises: at least one sweat sensor for measuring a sweat biomarker, a sweat collection inlet arranged in the device for collecting sweat when the device is worn by a user, and a microfluidic channel for conveying collected sweat from the inlet to the sweat sensor.

[0010] Additionally, the device comprises: at least one vital-sign sensor arranged in the device for measuring a vital-sign or physiological sign of the user, a sweat volume sensor for measuring volume of the collected sweat, and a processing unit adapted for receiving and processing data provided by the sweat sensor, the vital-sign biosensor and the sweat volume measuring device.

[0011] Preferably, the vital-signs or signs sensors is one or more of the following sensors: a heart rate sensor, a respiratory rate sensor, a blood pressure sensor, a body temperature sensor, and an oxygen saturation sensor.

[0012] The processing unit is further adapted to calculate or predict a blood lactate concentration based on data provided by the sweat sensor, the sweat volume sensor, and a vital sign-sensor. Preferably, the data is the form of electric signals that can be processed by the processing unit to perform calculations based on that data.

[0013] In a preferred embodiment, the sweat sensor is a sweat lactate sensor and the vital-sign sensor is a heart rate sensor, and the processing unit is further adapted to calculate, preferably by means of machine learning algorithms in a known manner for a skilled person in the art, predictive values of lactate concentration in blood, based on data in the form of electric signals, provided by: the sweat lactate sensor, the sweat volume sensor and heart rate sensor.

[0014] Therefore, the wearable device of the invention is a smart wearable device for lactate monitoring, that integrates a microfluidic system that ensures efficient sweat capture and continuous circulation of a fresh sweat sample. The invention is capable of providing real time health status of athletes and report when an athlete enters the anaerobic phase, thus, creating a new paradigm in sports training planning, as well as the health status of the athlete.

[0015] A direct and proportional relationship between lactate measurement (key biomarker in the monitoring of intensive physical exertion or fatigue) in blood and sweat is unknown, thus, in the present invention it has been found that taking into account additional parameters to sweat lactate, would establish a more accurate bioequivalence with blood lactate.

[0016] In particular, the invention involves the processing of the following additional parameters to sweat lactate for the blood lactate estimation: sweat rate, sweat volume excreted by the subject, and heart rate. In the invention, the sweating rate is also taken into account as a factor of dilution of lactate and the other analytes present in sweat.

[0017] The sweating rate gives an indication of the decrease in sweat lactate concentration in the tests and the variation observed with the blood lactate trend. Moreover, the heart rate provides a good estimation of the intensity of the physical activity performed by a user, and it is a common parameter in the monitoring of the athlete's condition and fatigue.

[0018] The wearable device of the invention integrates a microfluidic system for collecting sweat, that in contrast to prior art devices that are only capable of providing time isolated sweat measurements of no practical use, includes a sweat sample renewal system, such that fresh sweat measurement is always performed, which provide a faithful indication of the physical effort made at that time by a user.

[0019] Furthermore, the device incorporates a communication module adapted for the wireless transmission of data processed by the processing unit, preferably for transmitting the estimated or calculated blood lactate concentration.

[0020] The device is provided with a sensing chamber and at least one of the following sensors placed in the sensing chamber: a sweat lactate sensor, a sweat conductivity sensor, metabolites sensor, ions sensors, amino acids sensor. The microfluidic channel communicates the sweat inlet with the sensing chamber.

[0021] The sweat volume sensor comprises a microfluidic circuit or a microfluidic reservoir, fluidly communicated with the sensing chamber and arranged downstream the sensing chamber, and a pair of electrodes such that the microfluidic reservoir is arranged in between the two electrodes, in a way that a capacitance value between the two electrodes is variable depending on the amount of sweat in the reservoir. The two electrodes are a pair of strips opposite each other, and more preferably the electrodes are embodied as conductive flexible strips.

[0022] The microfluidic reservoir can have any form, for example the microfluidic reservoir can be a straight or curved conduit, or it can be formed as a conduit having a meander configuration.

[0023] Preferably, the wearable device comprises three main parts, namely: a main housing, means for attaching the main housing to a part of the user's body, and a fungible or consumable part disposable after use, which is configured to be manually attachable and detachable from the main housing.

[0024] The means for attaching the main housing to a part of the user's body, preferably consist of a flexible band having two ends respectively couplable with the main housing.

[0025] In a preferred embodiment, the processing unit is integrally contained in the main housing, but in other preferred embodiments of the invention, the processing unit or part of it, is external to the device, for example, it is implemented in a smart phone, a smart watch, a tablet or similar devices. The main housing additionally includes a power source like a battery, for supplying power to the electronics implementing the processing unit, and electric connectors for the communication with the consumable part.

[0026] The flexible band is fitted with at least one biosensor for measuring a vital-sign or physiological sign of the user, such as a heart rate sensor, thus, in addition to the sweat measurements, heart rate measurements are also taken in direct contact with the skin, with the same de device, and simultaneously as the sweat parameters are measured.

[0027] The flexible band is implemented as an elastic textile tape that would have a good hold on the body and would contain a pair of electrodes to measure the heart rate. The electrodes are made of bioelectric silicone to capture the electrocardiogram signal and extract the heart rate. They have sufficient conductivity to obtain a quality heart rate signal and are resistant to continuous use and washing.

[0028] The flexible band can be provided with other sensors, like a respiratory rate sensor to obtain additional parameters.

[0029] The consumable component has a contact surface provided to be in contact with the user's skin when the main housing is attached to a user's body part, and the consumable component is coupled with the main body.

[0030] Alternatively, the means for attaching the main housing to a part of a user's body, comprises an adhesive material for example an adhesive surface suitable to be adhered on a user's skin. For example, this adhesive surface is provided on a surface of the consumable component meant to be in contact with the user's skin.

[0031] The consumable component incorporates: the sweat collection inlet formed in the consumable component's contact surface at least one sweat sensor, the sweat rate measuring device, and the microfluidic channel, and electric connection means for electrically connecting the consumable component with the processing unit when the consumable component is coupled with the main housing.

[0032] Preferably, the consumable component is a generally flat body embodied as a card-like component.

[0033] In a preferred implementation of the wearable device, the main housing has a front surface and a back surface provided with a pair of guides opposite each other, and the consumable component has a pair of sides wings, such that the consumable component is couplable with the main housing by inserting its side wings respectively in the guides and by moving the consumable component on the back surface of the main housing.

[0034] A part of the back surface of the main housing

is generally flat, and the consumable component is couplable with the main housing by moving the consumable component on a plane parallel to said generally flat part of the back surface.

[0035] The main body is provided by a pair of electric connectors and each end of the flexible band is fitted with metallic connectors for mechanically and electrically connecting the flexible band and the biosensor with the main body.

[0036] The main body includes a battery for supplying power to the processing unit, and the main body has a lid at its back surface for providing access to the battery. The consumable component is overlapped with the lid, when the consumable component is operatively coupled with the main housing.

[0037] The wearable device of the invention, provides an advanced and integral personalized health management capability, through the combined analysis of key metabolic and physiological health indicators, like blood glucose measurement data, in addition to heart rate, oxygen saturation and temperature measurements, to achieve accurate equivalence with blood glucose measurements.

[0038] In summary, some of the main advantages of the invention are the followings:

- the diagnostic capacity of a biofluid like sweat is increased; much more patient data is generated by monitoring in a non-invasive, continuous and remote way;
- the format of the wearable device, is already used by athletes (heart rate monitor) to which they are accustomed in their regular training;
- the permanent part of the device (main housing) can be used by itself, in case the chemical measurement with the fungible or consumable part is not necessary (already known training routine, etc...);
- the permanent part (main housing) is compatible with different consumable part depending on the parameters to be measured. Useful tool not only for the end user but also for the clinic/sports physician who can adapt the device to the requirements of the patient/study;
- simple to use by insertion of the consumable and placement of the heart rate monitor. Guarantees placement in the same place every time, limiting the variability that the user's own operation may entail;
- it allows to have more advanced electronics with advanced functionalities compared to patch wearables such as battery management, data processing, flash memory in case there is no possibility of communicating the data;
- the consumable part might have an adhesive surface to enhance its fastening with the permanent part.

[0039] The main application of the invention is focused on sports medicine or sports health sector, for example for monitoring dehydration monitoring in athletes, but depending on the combination of sensors used, the device can be adapted to different applications as explained below.

[0040] Therefore, in a preferred embodiment, the wearable device is adapted to operate as a device for dehydration monitoring in athletes. A combination of sensors for measuring sweating, conductivity and some salt such as sodium can give real-time information on the state of dehydration of an athlete during physical exertion. Important to improve the control of dehydration in tests, and to be able to be treated in time (as an alarm system for the user) and with measurable variables in order to create an objective scale.

[0041] In another preferred embodiment, the wearable device comprises a heart rate and sweat rate measurement sensors, and the device is adapted to operate as a device for monitoring user fatigue.

[0042] In another preferred embodiment, the wearable device is adapted to operate as a device for nocturnal hypoglycaemia monitoring. In this embodiment, the device is a non-invasive device provided with sensors for measuring: heart rate, sweating, conductivity and a glucose sensor adapted to low ranges. The user would put the device on during the night, and the device can generate alarms when an episode of this type is detected. With the addition of predictive models, the onset of an episode could be predicted in advance to prevent and limit its consequences.

[0043] In another preferred embodiment, the wearable device is adapted to operate as a device for peritoneal dialysis remote monitoring. In this embodiment, the device comprises a heart rate sensor, an accelerometer, a sweat rate sensor, and sensors for measuring: conductivity, ions such as sodium, and lactate.

Brief description of the drawings

[0044] Preferred embodiments of the invention are henceforth described with reference to the accompanying drawings, wherein:

Figure 1.- shows a perspective view of a preferred embodiment of the invention including an attachment band or strap.

Figure 2.- shows a perspective view of the main housing and the consumable part partially coupled together.

Figure 3.- shows another perspective view of the main housing from above, and part of the band ends.

Figure 4.- shows a front elevational view of the main housing.

Figure 5.- shows a perspective view of the main housing from below.

Figure 6.- shows an exploded view of the main housing components.

Figure 7.- shows in Figure A a perspective view of the main housing from below. In Figure B with the consumable part partially coupled, and in Figure C with the consumable part fully coupled.

Figure 8.- shows an schematic representation of the sweat volume sensor. The figure represents four stages (A - B) of filling of the microfluidic channel.

Figure 9.- shows a perspective view of the consumable device from the face opposite the surface meant to be in contact with the skin.

Figure 10.- shows a schematic representation in plan view of the consumable device.

Figure 11.- shows a cross-sectional view of the consumable device, taken at cutting plane A-A in figure 10.

Figure 12.- shows another cross-sectional view of the consumable device, taken at cutting plane B-B in figure 10.

Figure 13.- shows a graph illustrating the characterization of the sweat volume sensor.

Figure 14.- shows a graph illustrating the effects of sweat conductivity on measured capacitance of the sweat volume sensor.

Preferred embodiment of the invention

[0045] Figure 1 shows an exemplary embodiment of a wearable device (1) according to the invention comprising a main housing (2) and a flexible band or strap (3) for attaching the main housing to a part of a user's body, and a pair of electric and mechanic connectors or snap buttons (4) provided in the main housing (2) for mechanically and electrically connecting the flexible band ends with the main housing (2).

[0046] The flexible band (3) is fitted conventionally with at least one biosensor for measuring a vital-sign or physiological sign of the user, in a known manner. The vital-signs or signs sensors are at least one of the following: a heart rate sensor, a respiratory rate sensor, blood pressure sensor, body temperature sensor, and oxygen saturation sensor.

[0047] As shown more clearly in **Figure 2,** the device (1) includes a consumable component (5) configured to be manually coupled and uncoupled with the main housing (2), and having a contact surface (6) provided to be in contact with the user's skin when the consumable component (5) is coupled with the main housing (2), and the main housing (2) is attached to a user's body.

[0048] As shown in **Figure 6,** the main housing (2) is formed by two couplable parts, a base (2a) and a lid or cover (2b) that configure a space within which an electronic circuit (7) is enclosed. This electronic circuit (7) implements the processing unit, sensors instrumentation, battery management, data processing and communication module for the wireless transmission of data processed by the processing unit.

[0049] The main housing (2) in particular the base (2a) has a receptacle (8) for receiving a battery (9) for supplying power to the electronic circuit (7), and a lid (10) for closing and opening the receptable (8).

[0050] The consumable component (5) is generally a flat body, and the main housing (2) and the consumable component (5) are configured, such that the consumable component (5) is couplable with the main housing (2) by moving the consumable component (5) on the same lane as the generally flat back surface (19) of the main housing (2) or a plane parallel to it, as illustrated in **Figures 2, 7B** and **7C,** such that the lid (10) can only be accessed when the consumable component (5) has been taken off from the main housing (2).

[0051] In particular, the consumable component (5) is overlapped with the lid (10) when the consumable component (5) is operatively coupled with the main housing (2), as it can be observed in **Figures 7A - 7C.**

[0052] The consumable component (5) incorporates: a sweat collection inlet (11) formed in the consumable component's contact surface (6) for collecting sweat when the device is worn by a user, at least one sweat sensor, a sweat volume measuring device, and a microfluidic channel for conveying collected sweat from the inlet (11) to the sweat sensor.

[0053] In particular, consumable component (5) has a sensing chamber and at least one of the following sensors: a sweat lactate sensor, a sweat conductivity sensor, metabolites sensor, ions sensors, amino acids sensor, and, placed in the sensing chamber. The microfluidic channel communicates the sweat inlet (11) with the sensing chamber.

[0054] The consumable component (5) is manufactured as a stack of layers of plastic materials where the microfluidic channels are formed by laser cutting or die cutting. The integrated sensors are electrochemical in nature and therefore require electrodes that are fabricated by screen printing.

[0055] A set of electric connectors (12) are provided at the back surface (13) of the base (2a) of the main housing (2), in order to realise electric communication between the sensors located in the consumable component (5) and the processing unit (7). These connectors (12) are known spring-biased connectors, that stablish

electric contact with corresponding electric pads (17) (provided in the consumable component (5), in a known manner when this is coupled with the main housing (2).

[0056] The consumable component (5) can be mechanically coupled and uncoupled from the main housing (2), in a quick and intuitive manner for a user, while ensuring functionality and good electrical connection with the main housing.

[0057] The main housing (2) has a back surface (13) provided with a pair of guides (15) opposite each other, and the consumable component (5) has a pair of sides wings (16), such that the consumable component (5) is couplable with the main housing (2) by inserting its side wings (16) respectively in the guides (15), and by moving the consumable component on the back surface (13) of the main housing (2).

[0058] The sweat volume sensor (18) is represented schematically in **Figure 8,** and comprises a microfluidic circuit or a microfluidic reservoir (19), fluidly communicated with the sensing chamber and arranged downstream the sensing chamber. In addition, the sweat volume sensor (18) comprises a pair of electrodes (20,20') and the microfluidic reservoir (19) arranged in between the two electrodes, such that a capacitance value between the two electrodes is variable depending on the amount of sweat in the reservoir.

[0059] The entry of sweat into the microfluidic reservoir (19) results in a change in capacitance between the two electrodes (dielectric constant difference between air and water which is the main component of sweat). This approach, apart from giving a very robust response with the added volume, has integration advantages, as it is only necessary to add two layers of copper tape in the lamination of the device, which is a cheap and easily available material. In addition, it does not require the fabrication of electrodes inside the channel and has sensitivity over the entire measurement area of the copper layers.

[0060] The electrodes (20,20') allow determination of the flow of sweat as it advances filling the reservoir (19) with limited influence of the ionic strength of the sweat sample.. The local sweat flow for each measurement interval can be estimated (we know the time and volume of sweat advancement) and thus be able to correct the sweat lactate measurement as a dilution factor.

[0061] The experimental validation of this novel sweat volume sensor has been carried out by injecting a controlled volume with a syringe pump into the microfluidic reservoir while monitoring the capacitance between the two electrodes. The microfluidic reservoir consisted in a long serpentine microfluidic channel, fabricated using adhesive materials and laser cutting, entrapped between the electrodes made of copper conductive tape. A 100 mM NaCl solution, which replicates the typical ionic strength of sweat, was injected at a constant flow rate of 5 μL/min. In **Figure 13,** it can be seen that, as the injection starts, the capacitance starts increasing linearly until the solution reaches the end of the sensing region. Then, the capacitance will remain stable although we keep injecting fluid because the sensing region is already completely filled. Converting time to volume injected, the calibration curve between capacitance and volume for the sweat volume sensor can be build.

[0062] Most impedimetric sweat volume or rate sensors have a response which depends significantly on the conductivity or ionic strength of the sweat sample. This is because they have a resistive nature, where free ions present in sweat have a greater effect than in capacitive measurements, as the sensor proposed here. This can be observed in **Figure 14** where the increment in capacitance (between an empty and filled sweat volume sensor) is measured for different solutions of increasing ionic strength (NaCl solutions ranging from 0 to 100 mM). There is a slight increase in the increment of capacitance when the solution contains a higher concentration of ions, but for the range of interest (low, 30 mM, to high, 100 mM, concentrations) the change produced by the conductivity of the sample is found between the margins of the variability of the sensor.

[0063] Preferably, the two electrodes are a pair of conductive flexible strips opposite each other.

[0064] As shown in **Figures 11** and **12,** in this particular embodiment, the sweat inlet (11), the microfluidic channel (22) and the sensing chamber (21), are placed above the microfluidic reservoir (19).

Claims

1. A wearable device for continuous monitoring of health parameters of a user,
   the device comprising:

   at least one sweat sensor for measuring a sweat biomarker,
   a sweat collection inlet arranged in the device for collecting sweat when the device is worn by a user,
   a microfluidic channel for conveying collected sweat from the inlet to the sweat sensor,
   at least one vital-sign sensor arranged in the device for measuring a vital-sign or physiological sign of the user,
   a sweat volume sensor for measuring volume of the collected sweat, and
   a processing unit adapted for receiving and processing data provided by the sweat sensor, the vital-sign biosensor and the sweat volume measuring device.

2. A wearable device according to claim 1, wherein the sweat sensor is a sweat lactate sensor, and the vital-sign sensor is a heart rate sensor, and wherein the processing unit is further adapted to calculate, preferably by means of machine learning algorithms, a blood lactate concentration based on data provided

by: the sweat lactate sensor, the sweat volume sensor and heart rate sensor.

3. A wearable device according to claim 1 or 2, further comprising a communication module adapted for the wireless transmission of data processed by the processing unit.

4. A wearable device according to any of the preceding claims further comprising sensing chamber and at least one of the following sensors: a sweat lactate sensor, a sweat conductivity sensor, metabolites sensor, ions sensors, amino acids sensor, and, placed in the sensing chamber, and wherein the microfluidic channel communicates the sweat inlet with the sensing chamber.

5. A wearable device according to any of the preceding claims, comprising at least one of the following vital-signs or signs sensors: a heart rate sensor, a respiratory rate sensor, blood pressure sensor, body temperature sensor, and oxygen saturation sensor.

6. A wearable device according to any of the preceding claims, wherein the sweat volume sensor comprises a microfluidic circuit or a microfluidic reservoir, fluidly communicated with the sensing chamber and arranged downstream the sensing chamber.

7. A wearable device according to claim 6, wherein the sweat volume sensor comprises a pair of electrodes and a microfluidic reservoir fluidly communicated with the sensing chamber and arranged relative to each other, such that a capacitance value between the two electrodes is variable depending on the amount of sweat in the reservoir.

8. A wearable device according to claim 7, wherein the two electrodes are a pair of strips opposite each other, and the microfluidic reservoir is arranged in between the two electrodes, wherein preferably the electrodes are embodied as conductive strips, and more preferably the electrodes are embodied as conductive flexible strips.

9. A wearable device according to any of the preceding claims, further comprising:

a main housing having at least part of the processing unit enclosed therein,
means for attaching the main housing to a part of the user's body,
a consumable component configured to be manually attachable and detachable from the main housing, and having a contact surface provided to be in contact with the user's skin when the main housing is attached to a user's body part, and the consumable component is coupled with the main housing,
wherein the consumable component incorporates: the sweat collection inlet formed in the consumable component's contact surface at least one sweat sensor, the sweat rate measuring device, and the microfluidic channel, and
electric connection means for electrically connecting the consumable component with the processing unit when the consumable component is coupled with the main housing.

10. A wearable device according to claim 9, wherein the means for attaching the main housing to a part of a user's body, comprises a flexible band having two ends respectively couplable with the main housing, and wherein the flexible band is fitted with at least one biosensor for measuring a vital-sign or physiological sign of the user.

11. A wearable device according to claim 9, wherein the means for attaching the main housing to a part of a user's body, comprises an adhesive surface suitable to be adhered on a user's skin, and wherein preferably the adhesive surface is provided on the consumable component's contact surface.

12. A wearable device according to any of the claims, comprising a heart rate sensor and a sweat rate sensor, and wherein the device is adapted to operate as device for monitoring user fatigue.

13. A wearable device according to any of the claims 1 to 11, comprising a sweating sensor, a conductivity sensor and a ion sensor, and wherein the device is adapted to operate as a device for dehydration monitoring in athletes, based on data provided by the sweating sensor, the conductivity sensor and the ion sensor.

14. A wearable device according to any of the claims 1 to 11, comprising: a heart rate sensor, a sweating sensor, a conductivity sensor, and a glucose sensor preferably adapted to detect glucose concentrations below 55 mg/L, and wherein the device is adapted to operate as device for nocturnal hypoglycaemia monitoring based on data provided by the heart rate sensor, the sweating sensor, the conductivity sensor and the glucose sensor.

15. A wearable device according to any of the claims 1 to 11, comprising a heart rate sensor, an accelerometer, a sweat rate sensor, a conductivity sensor, an ions sensor preferably a sodium sensor, and a lactate sensor, and wherein the device is adapted to operate as a device for peritoneal dialysis monitoring based on data provided by the heart rate sensor, the accelerometer, the sweat rate sensor, the conductivity sensor, the ions sensor and the lactate sensor.

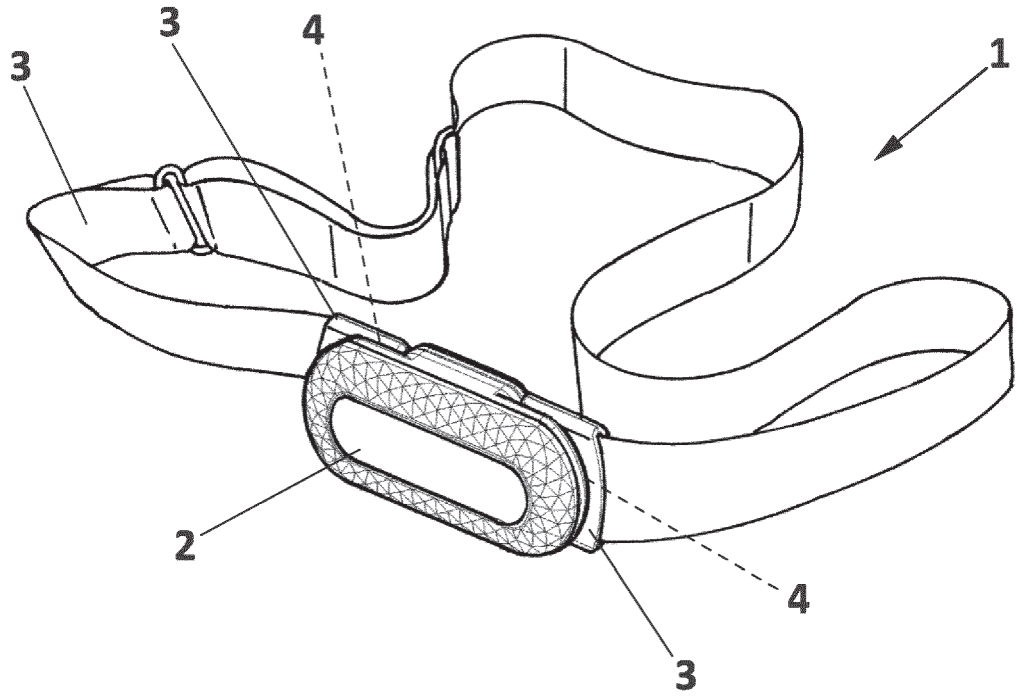

FIG. 1

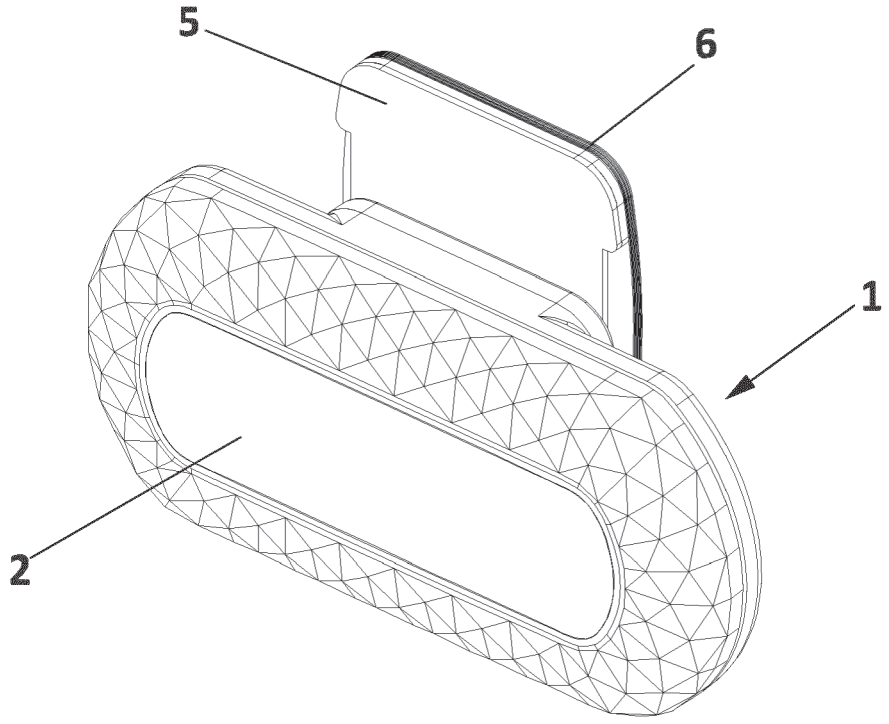

FIG. 2

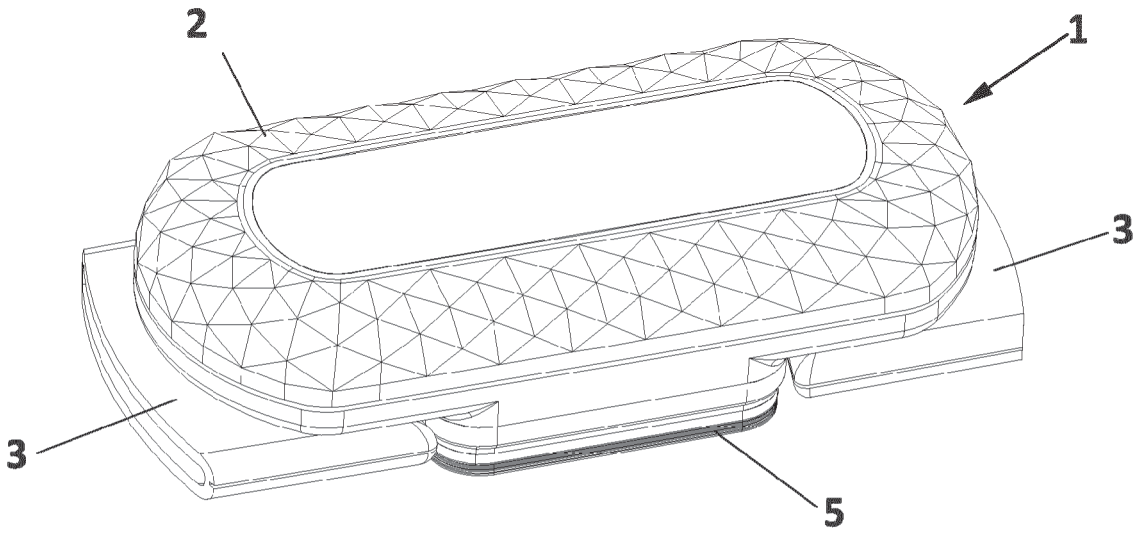

FIG. 3

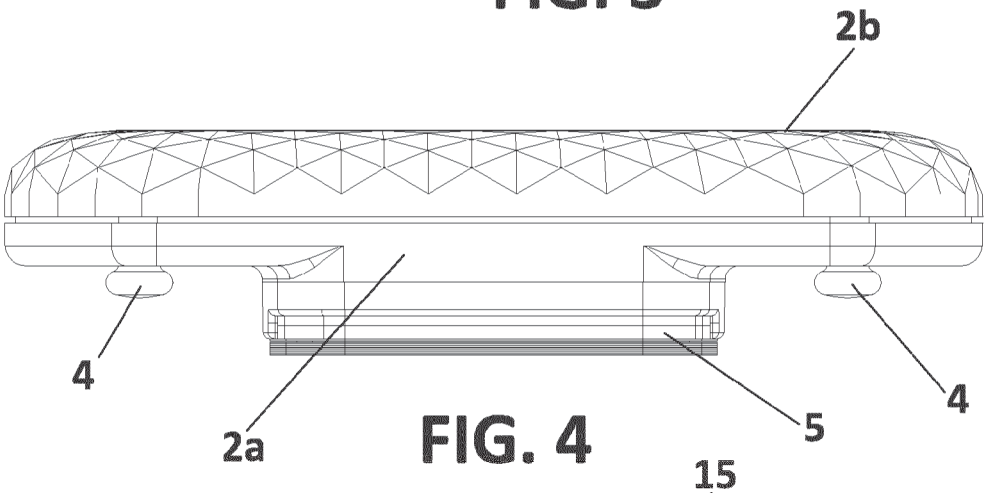

FIG. 4

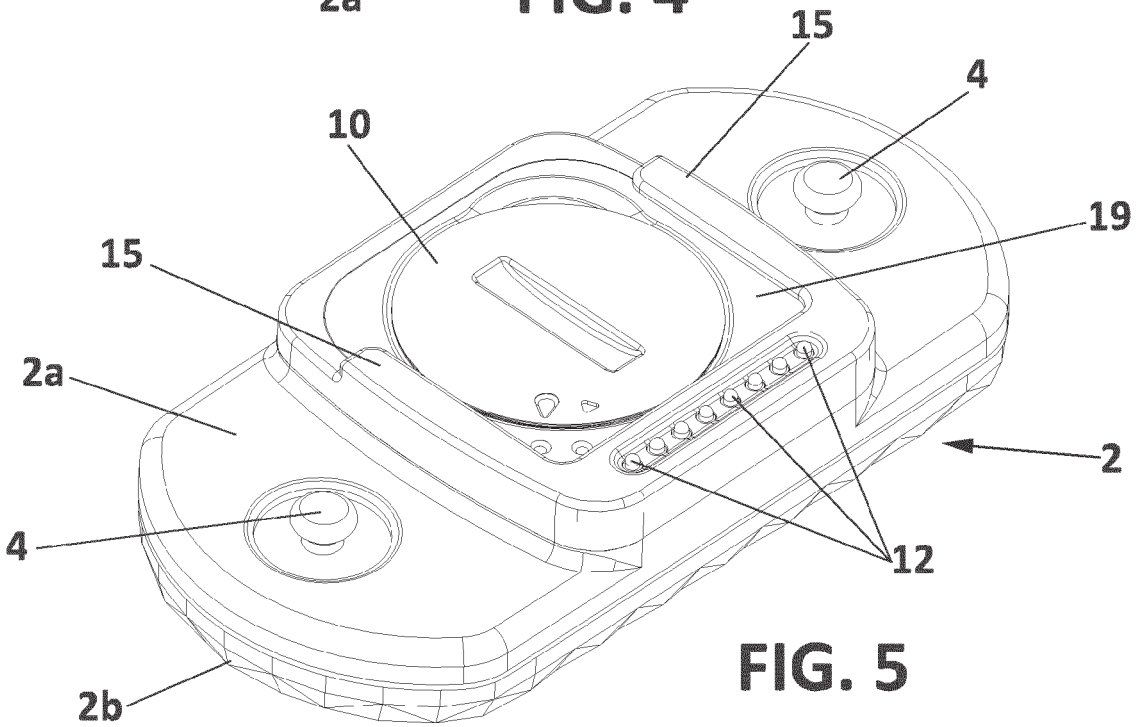

FIG. 5

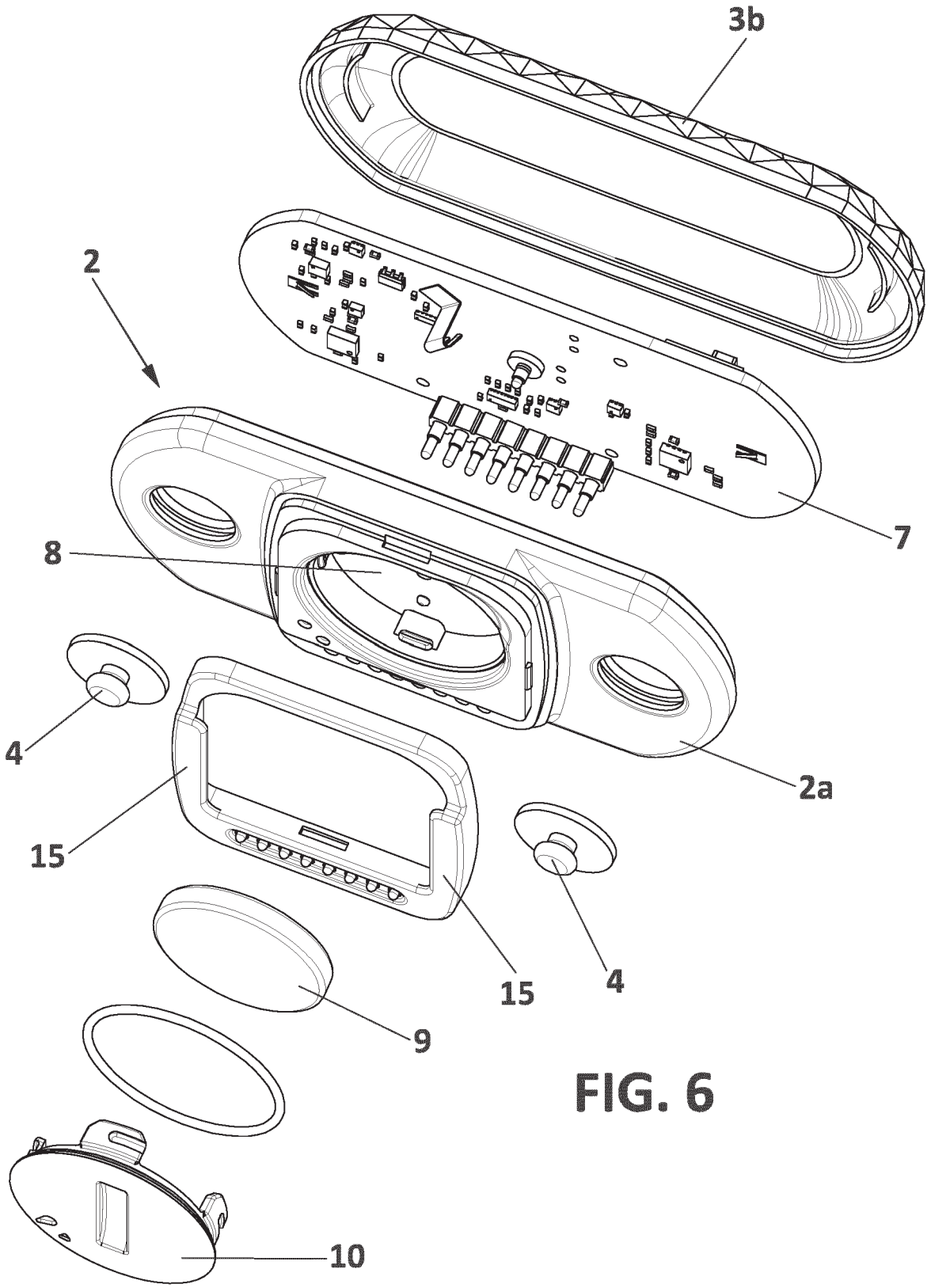

FIG. 6

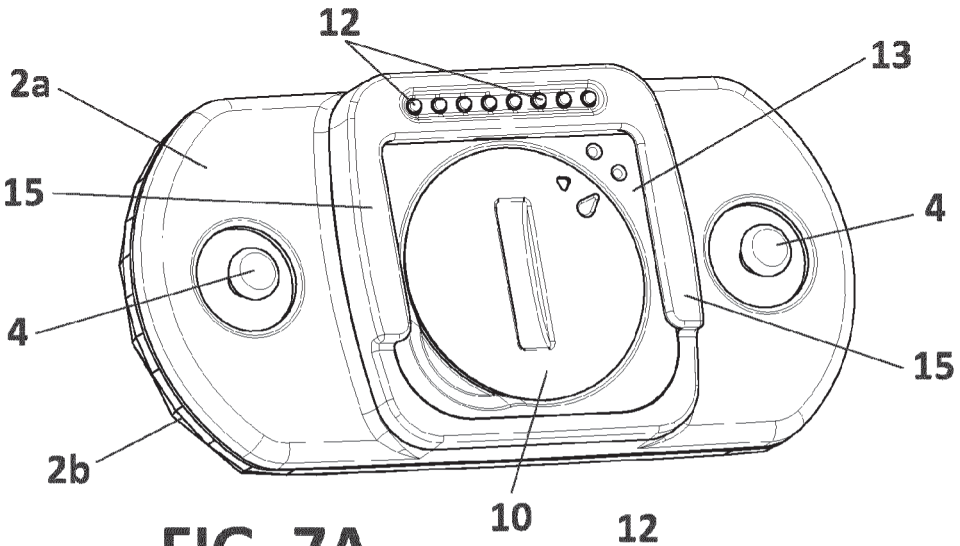

FIG. 7A

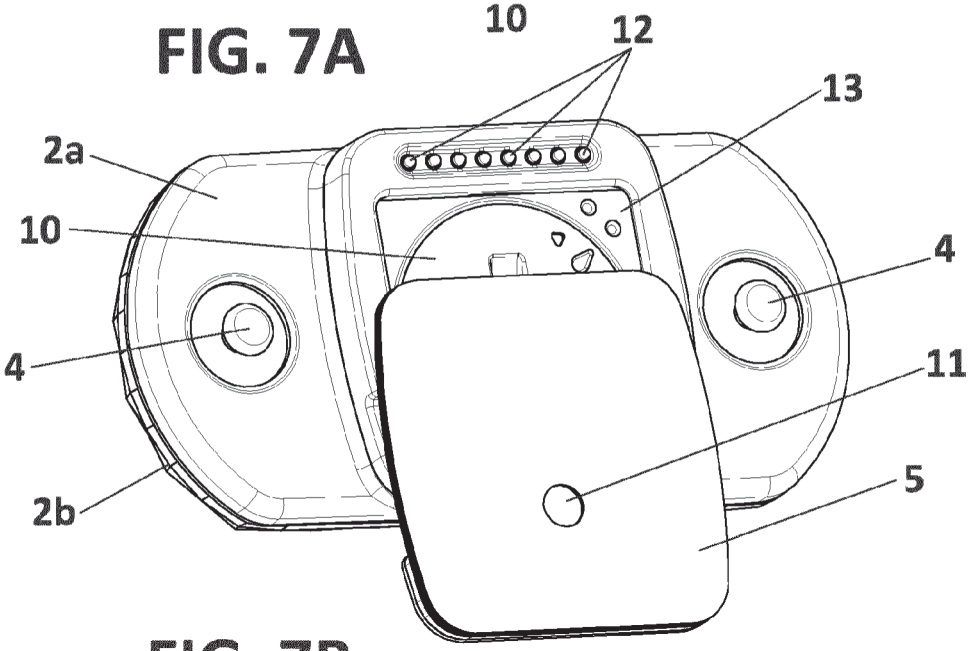

FIG. 7B

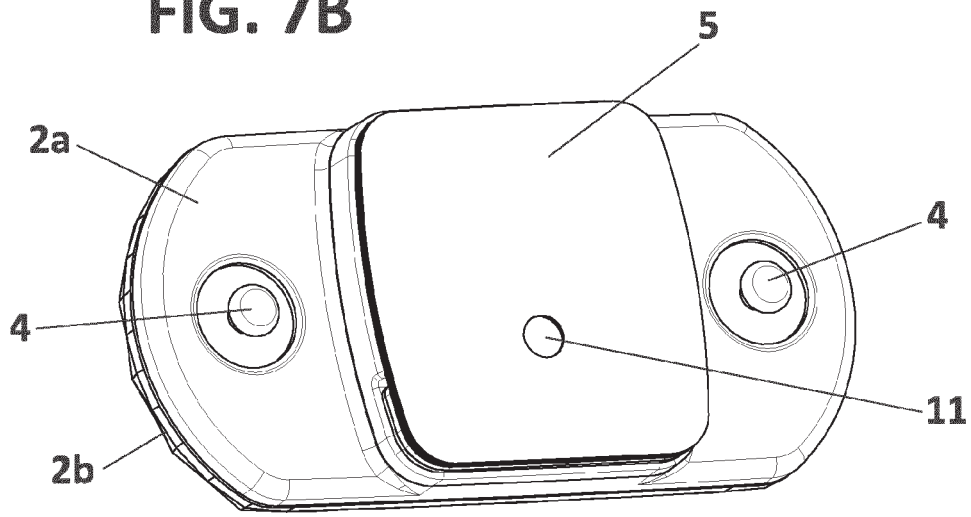

FIG. 7C

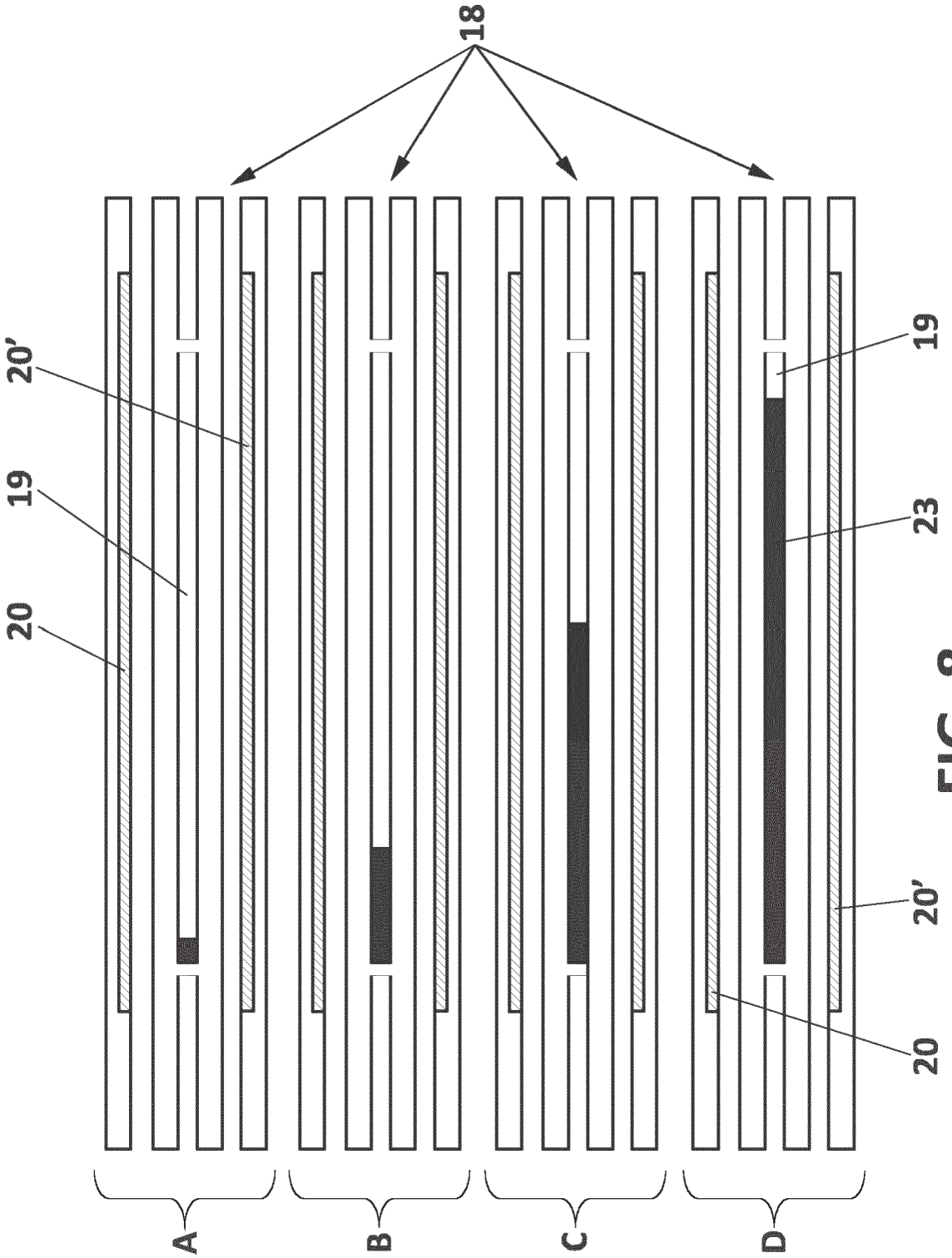

FIG. 8

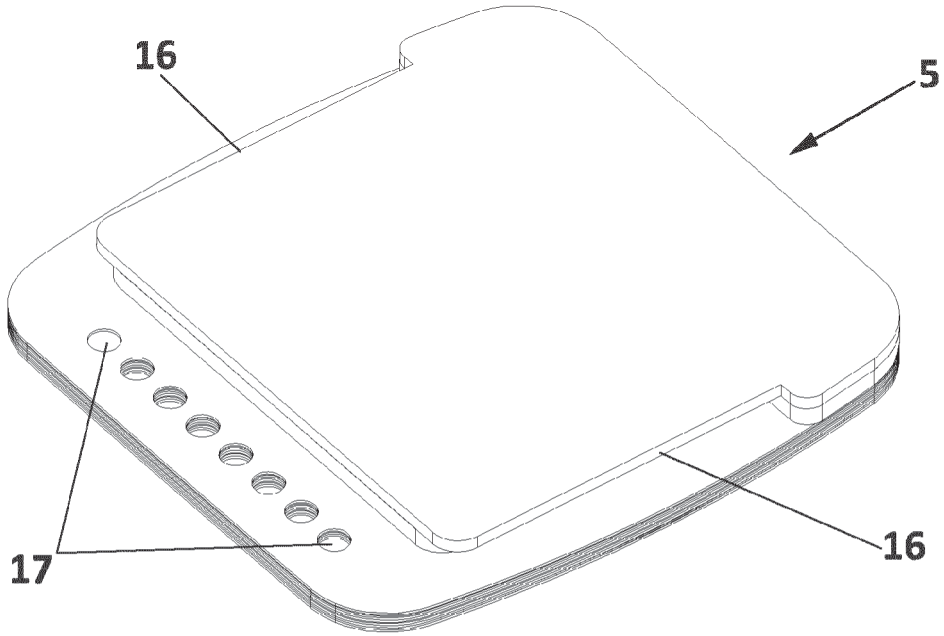

FIG. 9

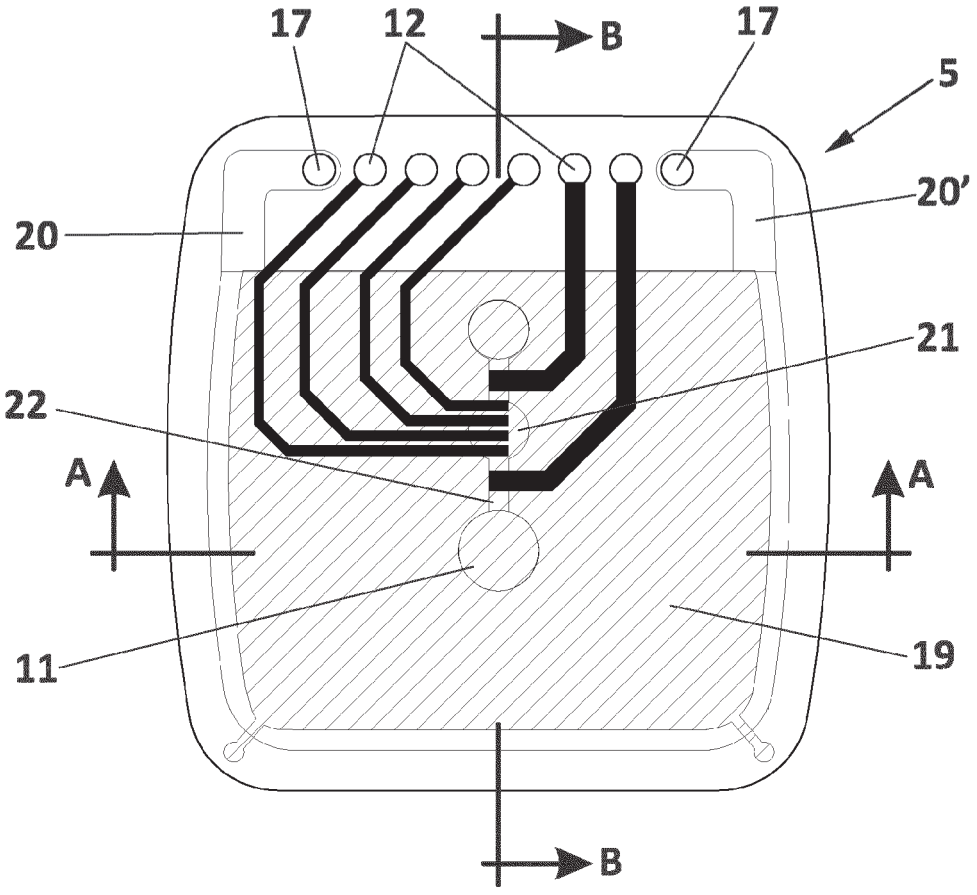

FIG. 10

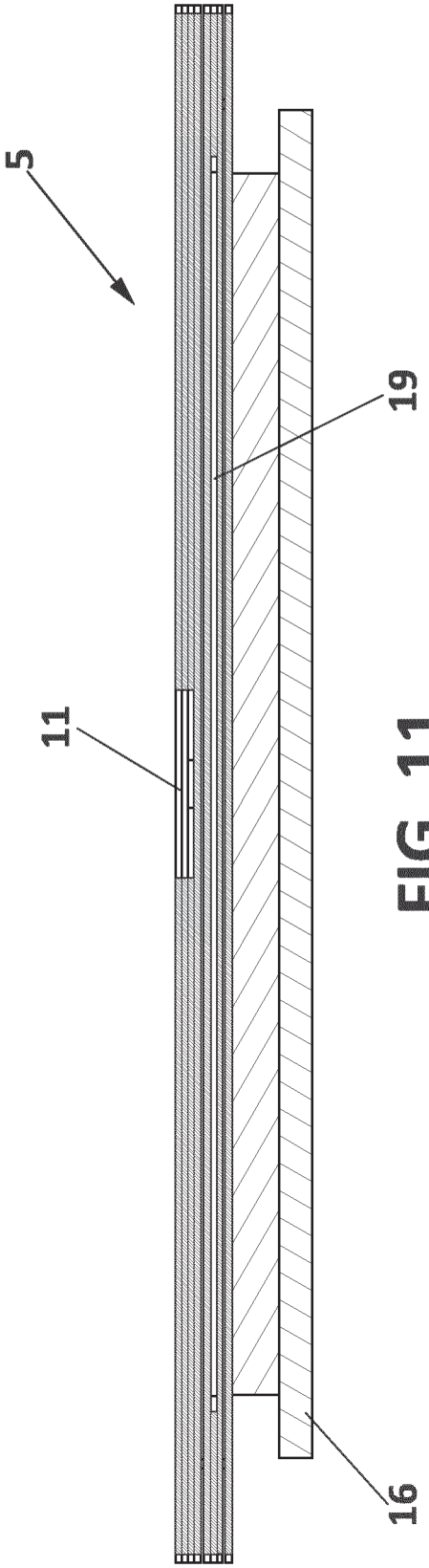

FIG. 11
A-A

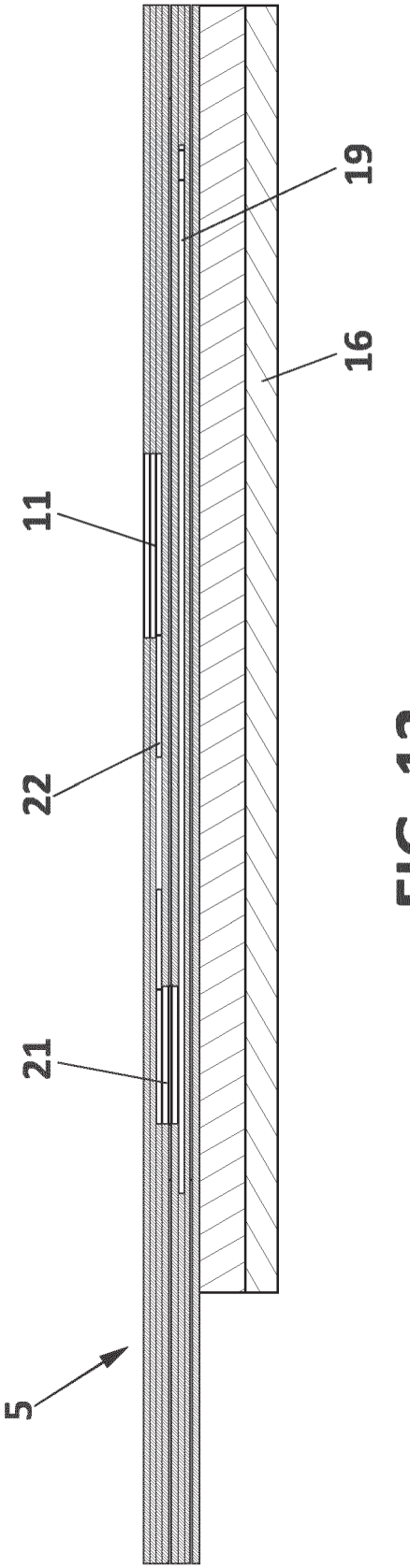

FIG. 12
B-B

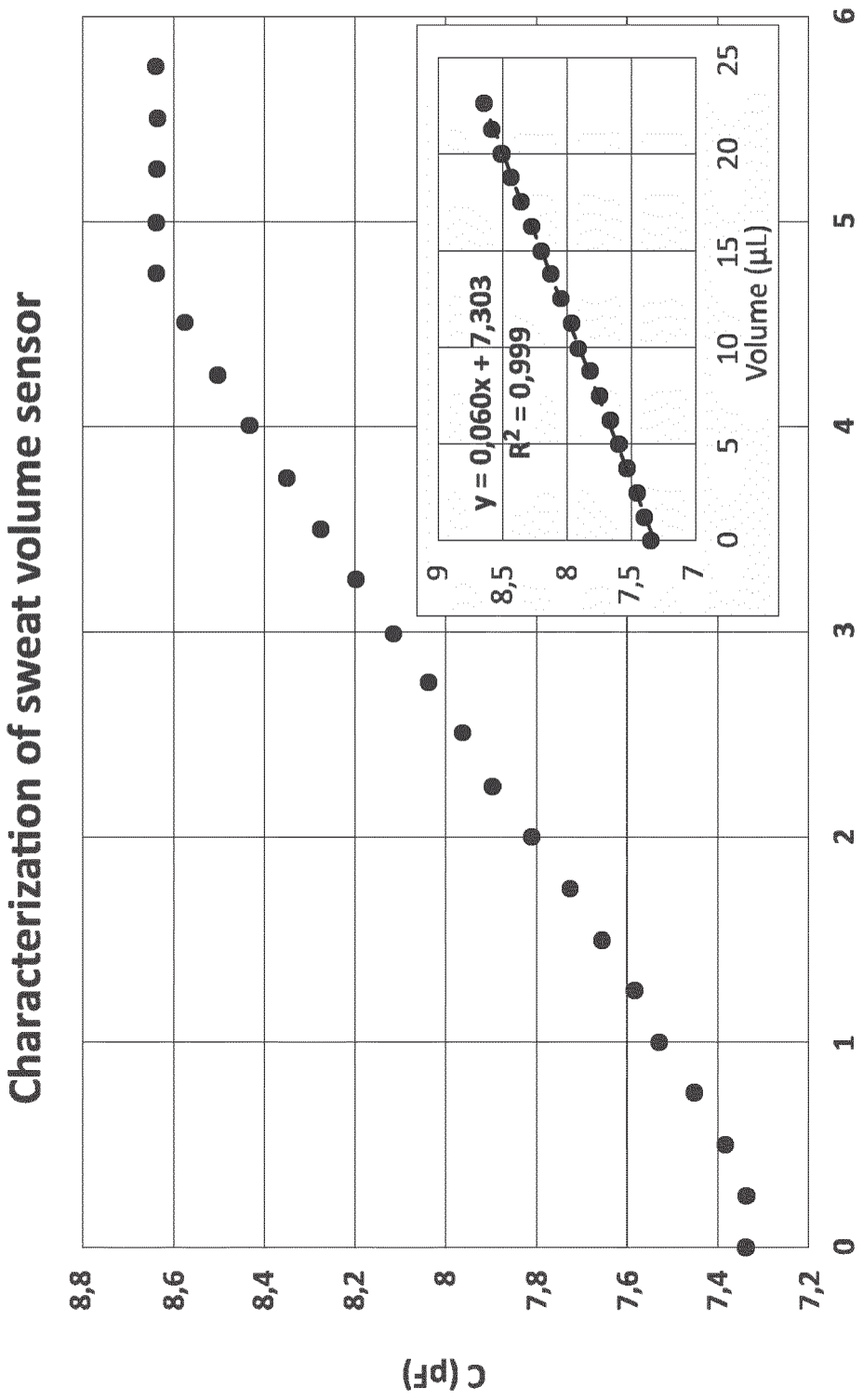
Characterization of sweat volume sensor
C (pF)
Time (min)
8,8
8,6
8,4
8,2
8
7,8
7,6
7,4
7,2
0
1
2
3
4
5
6
y = 0,060x + 7,303
R2 = 0,999
Volume (µL)
9
8,5
8
7,5
7
0
5
10
15
20
25

FIG. 13

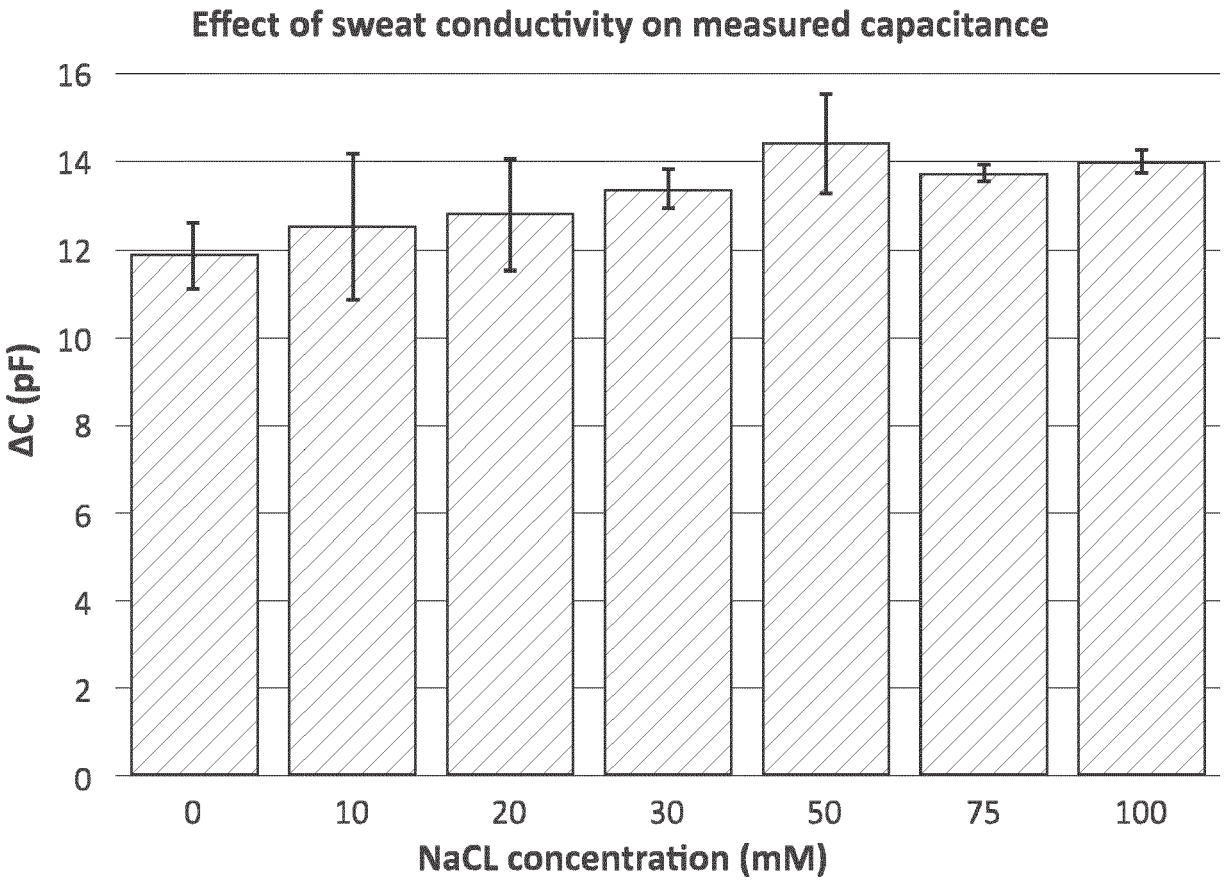
Effect of sweat conductivity on measured capacitance
16
14
12
10
8
6
4
2
0
ΔC (pF)
0
10
20
30
50
75
100
NaCL concentration (mM)

FIG. 14

Europäisches Patentamt
European Patent Office
Office européen des brevets

EUROPEAN SEARCH REPORT

Application Number
EP 21 38 3240

DOCUMENTS CONSIDERED TO BE RELEVANT

Category	Citation of document with indication, where appropriate, of relevant passages	Relevant to claim	CLASSIFICATION OF THE APPLICATION (IPC)
X	JP 2019 129965 A (LIFE KEA GIKEN KK) 8 August 2019 (2019-08-08) * figure 1 * * paragraphs [0019], [0022] - [0025], [0029], [0032], [0040] *	1-15	INV. A61B5/024 A61B5/145 A61B5/00
X	EP 3 364 183 A1 (ECCRINE SYSTEMS INC [US]) 22 August 2018 (2018-08-22) * figures 7, 8A, 8B * * paragraphs [0036], [0037], [0043], [0044], [0052] - [0053] *	1-15	
X	US 2018/020966 A1 (BEGTRUP GAVI [US] ET AL) 25 January 2018 (2018-01-25) * paragraphs [0038], [0039], [0044], [0045], [0075] *	1-15	
X	US 2020/397315 A1 (RAJ MILAN S [US] ET AL) 24 December 2020 (2020-12-24) * paragraphs [0036] - [0039], [0042], [0064] - [0065], [0072], [0091] *	1-15	TECHNICAL FIELDS SEARCHED (IPC)
A	JP 2018 093891 A (FUJITSU LTD) 21 June 2018 (2018-06-21) * figure 3 * * paragraphs [0015] - [0017] *	9-11	A61B
A	WO 2018/067412 A1 (GEN ELECTRIC [US]) 12 April 2018 (2018-04-12) * paragraph [0058] *	9-11	

The present search report has been drawn up for all claims

Place of search	Date of completion of the search	Examiner
The Hague	21 June 2022	Vanderperren, Yves

CATEGORY OF CITED DOCUMENTS

X : particularly relevant if taken alone
Y : particularly relevant if combined with another document of the same category
A : technological background
O : non-written disclosure
P : intermediate document

T : theory or principle underlying the invention
E : earlier patent document, but published on, or after the filing date
D : document cited in the application
L : document cited for other reasons

& : member of the same patent family, corresponding document

EPO FORM 1503 03.82 (P04C01)

ANNEX TO THE EUROPEAN SEARCH REPORT ON EUROPEAN PATENT APPLICATION NO. EP 21 38 3240

This annex lists the patent family members relating to the patent documents cited in the above-mentioned European search report. The members are as contained in the European Patent Office EDP file on
The European Patent Office is in no way liable for these particulars which are merely given for the purpose of information.

21-06-2022

Patent document cited in search report	Publication date	Patent family member(s)	Publication date
JP 2019129965 A	08-08-2019	NONE	
EP 3364183 A1	22-08-2018	CN 108451502 A	28-08-2018
		EP 3364183 A1	22-08-2018
US 2018020966 A1	25-01-2018	CN 110035690 A	19-07-2019
		EP 3487390 A1	29-05-2019
		US 2018020966 A1	25-01-2018
		WO 2018017619 A1	25-01-2018
US 2020397315 A1	24-12-2020	NONE	
JP 2018093891 A	21-06-2018	NONE	
WO 2018067412 A1	12-04-2018	NONE	

EPO FORM P0459

For more details about this annex : see Official Journal of the European Patent Office, No. 12/82